March 2006

Long-Term Impact Analysis of the University of Connecticut's Fenton River Water Supply Wells on the Habitat of the Fenton River

Glenn S. Warner
University of Connecticut Department of Natural Resources Management and Engineering

Fred L. Ogden
University of Connecticut Department of Natural Resources Management and Engineering

Amvrossios C. Bagtzoglou
University of Connecticut Department of Civil and Environmental Engineering

Piotr Parasiewicz
University of Massachusetts, Amherst

Study Report of

Long-Term Impact Analysis of the University of Connecticut's Fenton River Water Supply Wells on the Habitat of the Fenton River

Submitted by:

Glenn S. Warner, Ph.D., P.E.
Associate Professor of Natural Resources Management and Engineering

Fred L. Ogden, Ph.D., P.E., P.H.
Associate Professor of Civil and Environmental Engineering

Amvrossios C. Bagtzoglou, Ph.D.
Associate Professor of Civil and Environmental Engineering

Piotr Parasiewicz, Ph.D.
Assistant Research Professor, University of Massachusetts, Amherst

March 7, 2006

Table of Contents

ACKNOWLEDGEMENTS

The Principal Investigators wish to acknowledge the significant efforts and contributions made to the study by many people. Both undergraduate and graduate students were involved in field data collection and analysis. Undergraduates David Barker (CEE), Keith Mikolinski (CEE) and David Grunwald (NRME) were very helpful in the conduct of field work and data collection. M.S. Students Michael Rogalus III (CEE), Derek Dilaj (CEE), Sandrine Baun (CEE), Scott Bighinatti (NRME), Robbette Schmit (NRME) and Tra Pham (GEOL) assisted greatly with instrumentation, data collection, and analysis. Ph.D. candidates Juan Stella (NRME), Farhad Nadim (CEE) and Rick Jacobson (NRME) performed significant portions of the research work towards completion of their degrees.

We thank Professor Lanbo Liu, Dept. of Civil and Environmental Engineering at the University of Connecticut, who performed the seismic and ground penetrating radar geophysical investigations. The results of those studies provided important data and results that greatly helped in the other parts of the study.

We acknowledge the assistance of Janet Stone, Jeffrey Starn and Remo Mondazzi of the U.S. Geological Survey, Connecticut District, in the installation of instrumentation, data collection, and for assisting with geological and geophysical data analysis and interpretation.

The Technical Advisory Group (TAG) set up to provide guidance and oversight of this project served well. Their input was valuable and improved our project. Members of the TAG included: Ms. Corinne Fitting (CTDEP); Mr. Brian Murphy (CTDEP); Mr. Jeff Smith (CTOPM); Mr. Townsend Barker (USACE); Mr. Greg Padick (Town of Mansfield); Mr. John Manfred (Trout Unlimited); Michael Callahan (Windham Water Works), Mr. Robert Miller (Town of Mansfield); Ms. Denise Burchsted; and Ms. Margaret Miner (Rivers Alliance).

We acknowledge the assistance and support from the Dept. of Architectural and Engineering Services at the University of Connecticut, particularly James Pietrzak, project manager.

The comments received from members of the TAG and other groups were very helpful in improving the draft report.

LIST OF FIGURES

LIST OF TABLES

EXECUTIVE SUMMARY

This study was necessitated by the State of Connecticut, Office of Policy and Management (OPM), as part of their review of the University of Connecticut's (UConn) Environmental Impact Evaluation for the North Campus Master Plan. OPM required that UConn conduct a study to determine whether and how water withdrawals from the University's Fenton River water supply wells affect the fisheries habitat of the Fenton River adjacent to the well field. UConn withdraws water using water supply wells placed in a stratified drift aquifer located along a one-mile section of the Fenton River. The four Fenton River wells are registered by CTDEP for a maximum withdrawal rate of 0.8443 million gallons per day, MGD (1.31 cubic feet per second, cfs) (CTDEP Letter, June 21, 1991). As part of the impact assessment of UConn's water use, we have investigated the relationships between fish habitat and in-stream flow for a section of the Fenton River in the vicinity of the UConn well field. For reference, the study site is shown in Figure 1.1.

1.1 Study Objectives

The specific objectives of this study were to:

- Develop relationships between in-stream flow and habitat in the Fenton River for selected fish species;
- Derive the relation between the magnitude and timing of groundwater withdrawals on the stage and flow of water in the Fenton River principally from Old Turnpike Road to Stone Mill Road using existing data, new data collection, and mathematical simulation modeling; and,
- Mathematically model selected water-management scenarios to optimize water withdrawals while minimizing adverse impacts on stream flow and in-stream habitat.

1.2 Fisheries Habitat

We used the Physical Habitat Simulation System (PHABSIM), which is part of a wider conceptual and analysis framework of the Instream Flow Incremental Methodology (IFIM), combined with extensive channel morphology surveying and fish-capture to model relationships between instream flow and habitat. The IFIM focuses on habitat of streams and rivers to assess the impacts of human influence. The PHABSIM includes modeling of stream hydraulics at selected representative transects over a range of flows, and then incorporating species habitat information (in the form of Habitat Suitability Criteria, HSC) within the hydraulic model. Target fish species included brown trout, brook trout, fallfish, and tessellated darter. HSC for brown trout, brook trout, fallfish and tessellated darter were developed on-site. Field surveys were conducted to map mesohabitats in the study area, and to identify river segments that represent major habitat conditions based on location in the watershed, gradient, and predominant mesohabitats. Representative reaches and transects within reach were selected based on their representation of habitat conditions within each segment. Velocity, depth, substrate, cover, and water surface elevation were measured at transect points during three calibration flows (high, moderate, and low flows), and bed elevations were surveyed.

Standard weighted usable area (WUA) curves and WUA by mesohabitat type curves were produced. Functions describing the relationship between physical habitat and discharge were used to conduct habitat time series and range of variability analyses. Details are presented in Section 5.

Figure 1.1: Aerial view of study site. Monitoring wells are denoted as "MW" or "UC". Wells are denoted as "Pump".

1.3 Surface Water Investigations

Surface water investigations were conducted primarily during the summer months of 2003, 2004 and 2005, and included rainfall collection, stream discharge measurements in the Fenton River and selected tributaries, monitoring of shallow water table levels near the river and statistical determination of the frequency of flow and recession curves. Both 2003 and 2004 had above average rainfall during the summer, and flows during the typical low-flow season (August-September) in both 2003 and 2004 were not as low as required (<5 cfs) for sufficient time periods to make direct measurements of impacts on stream flow due to pumping. The summer of 2005 was abnormally dry and presented the opportunity to perform investigations under extreme low flow in the Fenton River.

The Fenton River in the vicinity of the UConn well field is a complex system. We observed several gaining and losing reaches, where water either flows from groundwater to the stream or vice-versa within the study area. Reaches can switch from gaining to losing depending on recent rainfall. The post-glacial history of sedimentary deposition in the river valley has created what are thought to be preferential flow paths between the surface and subsurface in a number of locations. In general, in the absence of pumping, the study reach of the Fenton River tends to gain flow in the downstream direction, even in times of drought.

Determination of the long-term frequency of low flows in the Fenton River was accomplished by correlating the limited available gauging data from the Fenton River with the long-term gauging data from the nearby Mt. Hope River. Results of these analyses are presented in Section 6. The magnitude of surface and ground water source contributions to instream flow is relevant when compared to the registered pumping capacity of the wells because the Fenton River can have flows less than 1 cubic feet per second (cfs) under drought conditions. During the summer of 2005, the flows in the Fenton River became very low, and the river bed became dry over an approximately 12 day period (5-16 September) in the vicinity of UConn Wells A and B. Fortuitously, the field data collection equipment procured for this project was operated by the investigators beyond the end of the original field data collection period, providing strong evidence of the effect of pumping of the wells on the Fenton River during drought conditions.

The drawdown of groundwater due to wells near streams can cause the groundwater table in the vicinity of the stream to fall below the stream water surface and in some locations, the stream bed. In these cases, water will infiltrate from the stream bed into the groundwater system. This is called “induced infiltration” due to pumping of groundwater. We used three independent means to estimate induced infiltration. These methods included the use of thermistors and nested piezometers, weirs, and the stream loss observations from the summer of 2005. Our results indicate that the published results of Rahn (1971) and Giddings (1966), slightly underestimate the induced infiltration.

Observations from the summer of 2005 significantly reduced the uncertainty in our analysis. Section 6.3 explains why the Fenton River went dry during the period 5-16

September, 2005. The explanation is based on analysis of rainfall, observed stream flow, pumping, and groundwater level data, all of which provide key indications of factors that lead to the drying of the river over an approximately 600 m reach from upstream of Well B to downstream of Well A. These observations are particularly relevant to the objectives of this study. Figure 1.2 shows the locations of the UConn groundwater Wells A, B, C, and D, and the monitoring wells used to observe groundwater levels. The monitoring wells are denoted with "UC" or "MW".

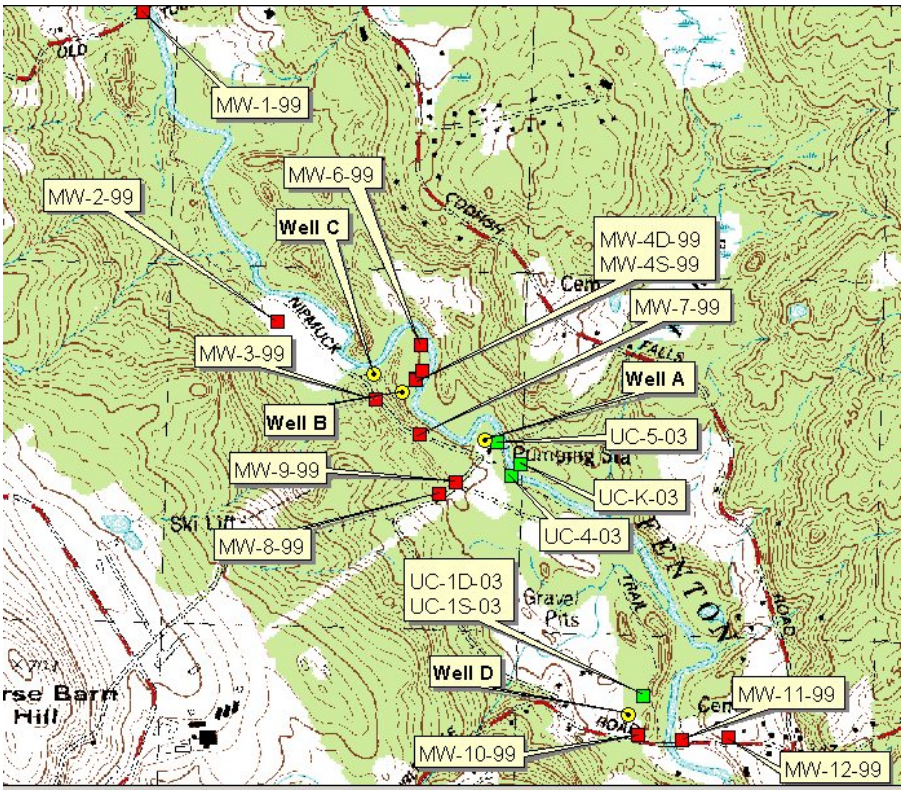

Figure 1.2: Study Site Map Showing Pumping and Monitoring Wells.

1.3.1 Rainfall

Rainfall data used in this study were obtained from the UConn Agronomy Farm, and from a recording rain gage operated by the investigators at the Fenton River well field near Well A. Historical precipitation data were obtained from the National Climatic Data Center, and the climatologic analysis by Miller et al. (2003). The comparison of historic and 2005 rainfall data revealed that the summer period of 2005 was one of the driest on record (Section 6). In particular, the total recorded rainfall during July and August, 2005 at the well field was less than 0.1 inch.

1.3.2 Water Table Levels

Water table levels near the Fenton River were recorded using Minitroll® water level loggers manufactured by In-Situ, Inc. Minitroll® water level loggers are pressure-transducers, with built-in programmable controllers for collecting data at user-specified

intervals. The loggers were placed in monitoring wells, and the distance to the logger and water level were measured. The loggers are connected to the surface by a vented cable with an electronic connection allowing programming and offloading of data without disturbing the logger itself. The vented cables provided atmospheric pressure to the pressure transducer, eliminating the need for post-processing to remove the effects of changes in barometric pressure.

1.3.3 Streamflow

Streamflow measurements were made using a number of different methods depending on the site and amount of flow in the Fenton River. A water level logger was installed in a housing at the Old Turnpike bridge and operated throughout the project. The stage data were coupled with discharges measurements to develop rating curves for different flow conditions and periods of time. The rating curve varied from one period to another due to changes in the control immediately downstream of the Old Turnpike bridge.

We determined, with the concurrence of the Technical Advisory Group that flows less than five cubic feet per second (cfs) were required in the Fenton River to make meaningful measurements of induced infiltration in the Fenton River near the well field. The summer of 2003 was dominated by higher than normal flows, with no extensive periods of flow less than five cfs during the August-September period when flows are climatologically at their lowest.

We used an acoustic-doppler current profiler (ADCP) to measure flows for intermediate flows between 5 and 30 cfs that were quite common during the summer of 2004 at Old Turnpike Road and various other sites along the Fenton, including sites immediately upstream and downstream of the well field. Our objective was to use repeated observations to reduce measurement error, allowing discrimination of the effect of well field pumping on induced infiltration. However, the 2004 results obtained with the ADCP were inconclusive due to the natural variation of flow and high flows during that season. During the summer of 2004, we built two weirs on the Fenton River, upstream and downstream of Well A as a direct measurement of difference in flow at those locations. However, decaying tropical storms at seven to 10 day intervals brought regular rains that increased the Fenton River flows, and destroyed our constructed weirs. The Fenton River experienced only one two-day period of flow less than five cfs when both of weirs were in place.

During the very low flow period in August and September, 2005, flow measurements at various locations were made using a Marsh-McBirney electromagnetic flow meter mounted on a top-setting wading rod. The depths in the river were typically too shallow for use of the ADCP during this period.

1.4 Groundwater Observations and Aquifer Tests

As part of this study, we conducted a series of aquifer tests on the Fenton River water supply wells, both separately and simultaneously as infrastructure and permit constraints allowed. Beginning in March 2004, we performed a series of tests to measure the response of the local groundwater level during pumping of each well in the Fenton well field. Several of these tests lasted for more than two weeks. Electronic pressure transducers were placed in observation wells at varying distances from pumping wells to observe changes in groundwater table elevation over time in response to pumping. Due to instrumentation limitations and other logistical constraints only four monitoring wells' records for the March 2004 pumping test were utilized. A set of nested piezometers and thermistors were installed by the U.S. Geological Survey (USGS) in the bed of the Fenton River near Well B to observe vertical flows in the streambed and estimate streambed conductivity. Data collected during aquifer tests were used to calibrate a mathematical model (MODFLOW-2000) of groundwater flow, which was subsequently validated against the historical data of Rahn (1971) and Giddings (1966).

1.5 Hydrogeophysical Investigations

Geologic characterization of the well field and surrounding area consisted of soil borings, bedrock outcrop mapping, and the use of both seismic and ground penetrating radar (GPR) geophysical techniques. Three new bedrock wells and nine new observation wells were installed. Three soil borings were made and completed as overburden monitoring wells in the glacial till along three transects. The interpretation of well borings was aided by the USGS. The geophysical investigations allowed us to generate the most realistic three-dimensional representation of the stratigraphy and structure of the Fenton River well field aquifer to date. Details of the hydrogeophysical investigations are presented in Section 7.

Geophysical data revealed that there is a relatively narrow constriction in the bedrock surface near Well A, between Wells B/C and D, that partially separates the stratified drift aquifer. The existence of this narrow section in the bedrock surface provides an indication that the effects of pumping from the aquifer upriver and downriver from the bedrock constriction might be partially independent lending some credence to the "egg-carton" compartmentalization of the aquifer hypothesis. This hypothesis was tested in the selected management scenarios.

1.6 Mathematical Modeling

A conceptual model of flow in the vicinity of the Fenton River well field that captures the possible interactions between the underlying bedrock layers and the surficial geologic units was developed. This model attempts to describe the complex and temporally variable interactions between the upland areas that are covered by either thick till or till and the stratified drift, which feeds water into or gets fed water from the Fenton River. Based on this conceptual model a mathematical model and associated numerical model was developed for the site. The numerical model employed a graphical user interface developed by the USGS embedded in the Argus-ONE numerical environment.

The geographical information system layers pertaining to the Fenton River watershed were linked to the standard-practice MODFLOW-2000 numerical code, which is the numerical engine used in this study.

The mathematical model of groundwater flow was calibrated using all available data, which included improved geophysical estimates, groundwater levels during pumping tests, and estimated streambed conductance. The Fenton River was incorporated in the model as a head source with an impeding layer, which effectively couples the ground water-flow model with surface-water processes. After model calibration, the simulated drawdown results were in reasonably good agreement (average residuals in the range of 0.1 to 0.3 ft) with the measured levels for the wells. The numerical model using detailed average values of daily stream flow and recharge produced results that are very comparable to the 1966 measurements reported in Rahn (1971) and Giddings (1966), thereby further lending credence to our model.

The calibrated and validated numerical model was used to calculate water budget estimates in order to quantify the complex interactions between the geologic units in the vicinity of the Fenton River. When averaged over the simulation domain, the August 8th (representative of drought conditions) water budget rates indicate that there exists negative recharge over both the till and stratified drift. Near the Fenton River the second bedrock layer contributes water to the first bedrock layer and this, in turn, to the stratified drift. Moreover, the stratified drift is also receiving water from the upland areas (till) and the Fenton River is a minimally losing stream. For the November 26th (representative of normal conditions) water budget, the situation changes for the upland areas in terms of the interactions between the till and the bedrock layers. However, the stratified drift is now replenished by water from only the upland areas (till) with minimal contribution from the bedrock. Furthermore, and most importantly, the Fenton River is now a gaining stream being replenished from the stratified drift. Calibration and validation results are discussed in Section 8.

1.7 Scenario Testing

MODFLOW-2000 was used to simulate the effect of pumping on stage and discharge in the Fenton River under several management scenarios, to reveal the effect of pumping on streamflow and fisheries habitat. The simulation domain used in MODFLOW-2000 included upland glacial till areas that are believed to continue to contribute recharge to the stratified drift aquifer in times of drought.

Ground water withdrawals can be managed to minimize impacts on streamflow and fish habitat. Streamflow has a delayed response to ground water withdrawals. The timing and rates of withdrawals with respect to periods of ground water recharge and periods that are critical for fish populations can be managed to minimize impacts. Exhaustive evaluation of management options was beyond the scope of the project. However, we have tested selected management scenarios that show potential for minimizing the effect of pumping on the fish habitat in the Fenton River. Our results indicate that there exists an almost perfect linear dependence of streamflow loss as a

function of the total daily pumping. It was also concluded that there exists very little difference between scenarios that spread the same total pumping over longer durations during the day. Moreover, as more pumping is switched from Wells A and B to Wells D and C, which reach their registered capacity the effects in the vicinity of Well A are reduced with minimal changes being effected due to re-distribution of pumping between Wells B and C. Finally, it appears that the best management scenarios call for relocation of Well A by moving it either 250 feet in the South direction (i.e., without requiring a new permit) or approximately halfway between the original location of Well A and D (on university property). It should be noted, however, that no formal optimization analysis has been conducted in regards to the placement of Well A as such an analysis was beyond the scope of this study.

Given the natural tendency of the Fenton River to reach flows during dry periods (droughts) that approach the magnitude as UConn's permitted pumping rate, there will be times when no management scenario will mitigate the effect of pumping on fish habitat. During those times, pumping will have to be severely curtailed or stopped until flows in the river increase. Scenario comparison and evaluation is discussed in Section 9.

1.8 Summary of Conclusions and Recommendations

An exhaustive search for optimal management strategies was beyond the scope of this project. However, we tested a number of infrastructure improvements and plausible management options. Those improvements and management options considered included: 1) increasing the capacity of well D; 2) increasing the capacity of well A and moving it to a new location farther from the Fenton River and towards the parts of the aquifer where the stratified drift has the greatest thickness; 3) increase the capacity of well D and pump wells B, C, and D only during times of low river flow; and 4) reduce pumping from the well field on a daily basis as flows fall below six cfs. Of these four primary options, the fourth option was found to be most effective.

Studies of the fish habitat for the four species considered (brown trout, brook trout, tessellated darter, and fallfish) reveal that at flows greater than approximately ten cfs as measured at Old Turnpike Road, we cannot discern the effect of well field pumping on the quantity of fish habitat in the vicinity of the well field. The habitat starts to become noticeably reduced when the Fenton River flow is somewhat less than seven cfs as measured at Old Turnpike Road. The degree of habitat reduction increases as flows decrease further to four cfs as measured at Old Turnpike Road. When the flow in the Fenton River decreases to three cfs, habitat is quite significantly reduced by pumping of the well field.

Although, habitat values naturally decrease with decreasing discharge below these thresholds, the thresholds represent ecological bottlenecks at which anthropogenic effects should be avoided. Consequently, we recommend direct application of fixed flow rules supported by continuous monitoring of river discharge at Old Turnpike road. As discharge establishes a decreasing trend approaching seven cfs, preparations should be

made to reduce reliance on the Fenton River well field. As flows approach six cfs measured at Old Turnpike Road management rules must be applied.

Within the context of our understanding of the current physical limitations of the Fenton River well field infrastructure, and the clearly identified need for increased flexibility in operating the well field to preserve fish habitat during times of low flow in the Fenton River, our specific recommendations are to:

1. Install a continuously-operating, telemetered stream flow gaging station on the Fenton River in the vicinity of Old Turnpike road to manage pumping of the Fenton River well field on a daily basis.
2. Repair or replace Well D so that it can run continuously and pump at its maximum capacity.
3. Replace Well A with a well of similar capacity farther from the river and in a deeper part of the stratified drift aquifer to the south or southeast of the present well location.
4. Install up-to-date electronic speed controls or duty-cycle controllers on all well motors.
5. Upgrade motor controls to enable more flexible operation of each well, and the entire well field.
6. Calibrate and maintain flow meters on the discharge line of each well pump.
7. Install a chemical disinfection system that follows best established practices to maintain the correct quantity of disinfectant over a wide range of pump flow rates from individual wells in order to add flexibility in pumping rates from each well and combination of wells.
8. Reduce the daily volume of pumping to 633,000 gpd if the flow in the Fenton River at Old Turnpike Road is less than 6, but greater than or equal to 5 cfs.
9. Reduce the daily volume of pumping to 422,000 gpd if the flow in the Fenton River at Old Turnpike Road is less than 5, but greater than or equal to 4 cfs.
10. Reduce the daily volume of pumping to 211,000 gpd if the flow in the Fenton River at Old Turnpike Road is less than 4, but greater than or equal to 3 cfs.
11. Do not pump the Fenton River well field if the flow in the Fenton River is less than 3 cfs.
12. Pumping of all Fenton River wells should stop if the flow in the river continues below 6 cfs for more than 15 consecutive days, or below 5 cfs for more than 5 consecutive days, even though the lower thresholds for reduced pumping are not met, to avoid increasing the frequency of occurrence of fish habitat reduction due to pumping.

With regard to recommendations 8 through 12, the results presented in Section 6 (Hydrologic Assessment) can be used for future analysis of detailed pumping strategies, and to evaluate the frequency at which flow reductions will occur under those strategies. As discussed in Section 6, there will be extensive periods when pumping reductions are not necessary, and in some wet years, will not be necessary at all. The re-starting of pumping after cessation based on the criteria in Recommendations 8 through 11 is partially addressed in Recommendation 12. The decision for re-starting pumping when

flow returns to above 6 cfs should be based on the amount of flow and the expected time of recession back to the 6 cfs threshold based on the equations in Section 6.5.3 and Figure 6.22. As indicated in Section 6, the recession can be much faster following small runoff events and not reflect a true sustained baseflow condition where flow would persist above 6 cfs. As the Time Series Analysis in Section 5 demonstrates, the duration and frequency of low flow events can have a substantial effect on the resilience of the aquatic community. The triggers for resuming withdrawals from the well field are therefore an important consideration in the overall operating plan. The recession times, combined with the daily monitoring of discharge levels in the Fenton River, provide valuable information that can be incorporated into plans for implementation of water conservation measures. As more data are collected from a gaging station at Old Turnpike, the recession curve should be updated to provide a greater assurance of the response of the stream under different hydrologic conditions.

2.0 INTRODUCTION

Part of a satisfactory finding by the State of Connecticut, Office of Policy and Management (OPM) of the University of Connecticut's (UConn) Environmental Impact Evaluation for the North Campus Master Plan, requires that UConn conduct a study to determine whether and how water withdrawals from the University's Fenton River water supply wells affect the aquatic habitat of the Fenton River. UConn withdraws water using water supply wells placed in a stratified drift aquifer located along a one-mile section of the Fenton River. The four Fenton River wells are registered by CTDEP for a maximum withdrawal rate of 0.8443 million gallons per day, MGD (1.31 cubic feet per second, cfs) (CTDEP Letter, June 21, 1991). As part of the impact assessment of UConn's water use, we have investigated the relationships between fish habitat and instream flow for a section of the Fenton River from Old Turnpike Road to Mansfield Hollow Lake. This report details the findings of our multi-disciplinary study.

This report is organized as follows. Section 3 describes UConn's Fenton River well field. Section 4 lists what is known from past studies about the hydrologic, hydrogeologic, and habitat characteristics of the study area. Section 5 describes the methods and results of the present fish habitat study. Section 6 describes the surface hydrologic investigations and the analyses of hydrologic data used to estimate low-flow intensity-duration-frequency curves and recession curves. Section 7 describes the hydrogeological investigations performed in the course of this study. Section 8 describes the MODFLOW-2000 calibration. Selected management scenarios are presented in Section 9. Section 10 contains the bibliography. Several appendices are included that provide further details of methods and some of the data. Much more of the data and model inputs/outputs are to be provided on a CD for future reference and potential investigations.

3.0 UCONN'S FENTON RIVER WATER SUPPLY WELLS

UConn withdraws water through water-supply wells near the Fenton and Willimantic Rivers. The university operated eight water-supply wells to serve the university with potable water. Four wells are located along the Fenton River and four are located along the Willimantic River. (University of Connecticut Water Supply Plan, October 1999). This project is concerned with the Fenton River well field only. According to UConn's Water Supply Plan, the four wells located along the Fenton River have the following characteristics:

Table 3.1 Characteristics of Fenton River field wells.

Well A: Dug Well-Caisson Type	Installed 1926	28' deep	24" O.D. Casing	Screen length unknown
Well B: Gravel Packed	Installed 1949	70' deep	12" O.D. Casing	21.5' Screen Length
Well C: Gravel Packed	Installed 1949	63' deep	12" O.D. Casing	21.5' Screen Length
Well D: Gravel Packed	Installed 1959	59' deep	12" O.D. Casing	15' Screen Length

From 1994 through 1998, the annual withdrawal of water from the Fenton River wells varied as follows: 1994 –75 MG (million gallons), 1995 – 84 MG, 1996 – 85 MG, 1997 – 63 MG and 1998 – 63 MG. The rate of water withdrawal from the Fenton River wells is quite variable on a monthly basis. In 1998, for example, the lowest monthly withdrawal rate was 0.03 million gallons per month in June and the highest monthly withdrawal rate was 13.48 million gallons per month in October. During 1994 through 1998, the highest monthly withdrawal rate was at 19.87 million gallons per month (0.641 MGD) in August 1995.

Data collected during Level A mapping show that the rate of water withdrawal from the aquifer can be approximately equal to the rate of ground water inflow to the Fenton River near the well field; thus, the wells can potentially have significant impact on low flows in the river. Aquifer tests were reported as part of UConn's Level A Mapping in 1999. During that time, flow in the Fenton River at Stone Mill Road was 18.5 cfs, which represents a flow equaled or exceeded 58 percent of the time. The well field was shut down on November 12, 1999 and the pump test was commenced on November 16, 1999 at a pumping rate from Well B alone of 517 gpm (1.15 cfs). The test was terminated on November 19, 1999. Flow measurements were made at several locations on November 12, 16 and 19, 1999. Flows in the Fenton River were impacted by the prior use of the well field (prior to November 12, 1999) and by the aquifer test, somewhat confounding interpretation of the results. Nevertheless, the difference in flow in the Fenton River between Old Turnpike Road (upstream of wells) and Stone Mill Road (downstream of wells) on November 12, 16 and 19, 1999 was 2.1 cfs, 3.5 cfs and 1.4 cfs, respectively. Also during this period, contributions to surface-water flow from Mason Brook, Fishers Brook and Roberts Brook were 1.4 cfs, 1.49 cfs and 1.57 cfs, on

November 12, 16 and 19, 1999, respectively. In a simplistic analysis, water withdrawn from the aquifer can be assumed to represent the amount by which streamflow is decreased. Given the Well B pumping rate of 1.15 cfs, one can readily examine the relevance of flow contribution from all surface water and ground water sources in the area between Old Turnpike Road and Stone Mill Road.

Wells near streams do not take all their water directly from the stream. Rather, groundwater withdrawals are proportioned between decreases in alluvial aquifer storage and the interception of ground water flows that would ultimately reach the river. The interception of flows that would have reached the river in the absence of pumping do not represent a loss to the stream, rather interception represents a "lack of gain" in the stream.

4.0 FENTON RIVER NEAR UCONN WELL FIELD

4.1 Hydrologic Characteristics

The Fenton River is located in the Natchaug River Watershed, which is part of the Thames River Basin (Rahn, 1968). Runoff in the Thames River Basin is estimated to average approximately 22.5 inches per year (1.64 cfs/mi^2), while the average annual rainfall is about 44 inches. (Department of the Army, August 1982). The Fenton River Watershed is about 34.36 square miles in area above the Mansfield Hollow Reservoir; therefore, the annual direct runoff from the Fenton River into Mansfield Hollow Lake is approximately 56.35 cfs (36.41 MGD).

The drainage area of the Fenton River at Stone Mill Road is 23.8 mi^2. The streamflow in the Fenton River at Stone Mill Road that is exceeded 10 percent, 50 percent, and 90 percent of the time is 96 cfs (62.0 MGD), 24 cfs (15.5 MGD) and 3.3 cfs (2.13 MGD), respectively. In UConn's Level A Mapping study, the 180-day drought simulation utilized 0.7 cfs in the Fenton River at Stone Mill Road. This streamflow was the 7-day low flow equaled or exceeded that occurs once every 10 years (7Q10) for the Fenton River at Stone Mill Road. From a historical record perspective in September of 1963, in the middle of one of the worst droughts in history, streamflow on the Fenton River at Gurleyville was 0.5 cfs. Streamflow at the upstream gage at Old Turnpike Road was 0.91 cfs, indicating that about forty five percent of the streamflow was lost either by pumping from the Fenton River well field or discharge from the river into the subsurface.

In August 1966, Rahn (1968) conducted a study on the effects of water withdrawls from the UConn wellfield on the flow in the Fenton River. Pump tests conducted using UConn's water supply Well B during an exceptionally low flow period in August 1966 resulted in the loss of surface water flow in the Fenton River in the well field area and for approximately one-half mile downstream. During this time surface water flow in the Fenton River was between 0.419 cfs and 0.450 cfs, approximately 1000 feet upstream from Well B. Portions of this work were also documented by Giddings (1966) in a UConn Masters thesis. Giddings additionally reported that there was no surface water flow past the UConn Water supply wells in the Fenton River in August 1965.

There have been no continuous monitoring stream gauges located on the Fenton River, prior to the UConn study funded by the Willimantic Water Works. The United States Geologic Survey (USGS) maintains a continuous stream gauge on the Mount Hope River at Warrenville, which is accessible on a real-time basis. The Mount Hope River drainage area at Warrenville is 28.6 mi^2 and represents the closest streamflow data to the Fenton River. The lowest recorded 7Q10 in the Mount Hope River at Warrenville was 0.40 cfs on August 8, 1957. The USGS made same-day measurements at 10 sites in the Fenton River basin during 1963, one of the worst droughts in history. In September 1963, streamflow on the Fenton River at Gurleyville was 0.50 cfs.

4.2 Hydrogeologic Characteristics

The Fenton River water-supply wells are located in the floodplain of the Fenton River. The dominant unconsolidated materials in the Fenton River valley are coarse-grained stratified glacial deposits. Prior investigations by Giddings (1966), Rahn (1968), USGS and LBG (2001) along the Fenton River Valley clearly indicate the presence of low-permeability layers of silt and very fine sand (glacial lacustrine deposits) in the areas of Well B and Well C. These deposits vary from a few feet to more than ten feet thick. Uplands in the Fenton River watershed consist primarily of glacial till deposits. Hilltops and hillsides along Horsebarn Hill extend down toward the stratified drift and consist of thick glacial (drumlin) till. The till deposits generally vary in thickness from a few feet in shallow bedrock areas to twenty to thirty feet, but can be greater in drumlin areas. Bedrock under the unconsolidated deposits consists of metamorphosed bedrock of Devonian or earlier age. Three types of bedrock units have been identified in the area to be investigated in the project (LBG 2001)--Hebron Gneiss, Brimfield Schist and the upper member of the Bigelow Brook Formation.

4.3 Fish Habitat Characteristics

In July 1994, a fisheries survey was conducted by the Fisheries Division of the Connecticut Department of Environmental Protection 75 m upstream from the University well field (Hagstrom et al. 1996). The most abundant species listed in descending order of abundance included blacknose dace *Rhinichthys atratulus*, white sucker *Catostomus commersoni*, fallfish *Semotilus corporalis*, and tessellated darter *Etheostoma olmstedi*. Wild brook trout *Salvelinus fontinalis* and brown trout *Salmo trutta* were also documented. Fish species included in our in-stream flow study include a native recreationally important species (brook trout and brown trout) and two non-game fluvial specialists (fallfish and tessellated darter).

The physical habitat of the Fenton River throughout the proposed study site changes from upstream to downstream. Upstream near the pump houses, the river is dominated by riffle/run/pool sequences and substrates are dominated by cobble, gravel, and occasional boulders. The frequency of riffles declines downstream to the confluence at Mansfield Hollow Reservoir. Downstream sections are dominated by pools and runs and substrates of sand and gravel. The most downstream reach consists of primarily pool habitat.

5.0 FISH HABITAT ANALYSIS

5.1 Fisheries and Habitats of the Fenton River

Water extraction, whether from ground or surface sources, has been shown to affect the quantity, quality and distribution of physical habitats necessary for the reproduction, growth and survival of aquatic biota. Several techniques have been developed to quantify the interactions (Annear, et al., 2004). As part of its directive, the State of Connecticut Office of Policy and Management required that the University conduct studies within the framework of the Instream Flow Incremental Methodology (IFIM) as developed by the U.S. Fish and Wildlife Service (Bovee, 1986). These studies were to incorporate the habitat response quantification protocols of Physical Habitat Simulation Modeling (PHABSIM) (Milhous, et al., 1989).

PHABSIM is a collection of mathematical models. Individually, the models are used to project the relative importance of various physical phenomenon to aquatic biota (e.g., Habitat Suitability Criteria), and changes in hydraulic characteristics (e.g., cell specific depth, velocity and associated channel index values) as a function of changes in stream discharge. These outputs are subsequently combined to quantify changes in habitat abundance and distribution for aquatic biota.

Habitat suitability criteria (HSC) used in PHABSIM applications are measurements of fish habitat suitability quantified as depth, velocity, and substrate, cover and related physical features combined into a single channel index value. HSC have been developed and applied in several instream flow studies; however, transferability of HSC among rivers and within regions has been known to be problematic. Several factors, including inter- and intra-specific competition (Fausch and White, 1986), habitat availability, and food abundance, can influence river-specific habitat selection patterns resulting in poor transferability of HSC among rivers and regions (Moyle and Baltz, 1985; Bovee, 1986; Bozek and Rahel, 1992; Baker and Coon, 1997; Freeman et al., 1997; Strakosh et al., 2003). Application of HSC among dissimilar systems (e.g., western HSC applied to eastern rivers) could have detrimental outcomes by predicting incorrect flow regimes (Thomas and Bovee, 1993; Groshens and Orth, 1994). Baker and Coon (1997) noted that even slight differences in species HSC input for PHABSIM could result in an inaccurate model. Strakosh et al. (2003) found that transferability of brown trout HSC from established sources to the West Branch Farmington River, Connecticut was poor. Therefore, development of site-specific HSC is highly recommended (Moyle and Baltz, 1985; Bozek and Rahel, 1992; Groshens and Orth, 1994; Newcomb et al., 1995; Glozier et al., 1997).

Modeling of hydraulic characteristics within the PHABSIM protocols is based on one-dimensional modeling principals. Physical variables of depth, velocity and channel index are measured at intervals (cells) across representative transects, under differing flow conditions. These data are in turn used in hydraulic simulation models to project changes in water depth and velocity in each cell, in association with the channel index variables for those cells as a continuous response over the range of flow conditions under

investigation. The number and location of representative transects, as well as the number of cells per transect, are critical to the confidence intervals associated with extrapolation to whole-river assessments (Williams, 1996) as errors associated with individuals measurements are extrapolated across broad areas.

Wherein PHABSIM is a collection of mathematical models, IFIM is a collection of iterative quantitative and qualitative analyses of human use needs (e.g., consumptive water withdrawal), ecological consequences, and management alternatives intended to maximize meeting needs with minimization (or avoidance) of ecological harm.

The Department of Natural Resources Management and Engineering conducted studies within the PHABSIM protocols to quantify the relationship between stream discharge and aquatic habitat for selected fish species and life stages. The specific objectives of these studies included:

1. To develop relationships between instream flow and habitat in the Fenton River for selected fish species;
2. To develop the relation – using existing data, new data collection, and mathematical simulation modeling – between the magnitude and timing of ground water withdrawals and stage and discharge in the Fenton River, principally from Old Turnpike Road to Stone Mill Road; and
3. To mathematically model selected water-management scenarios to optimize water withdrawals while minimizing adverse impacts on stream flow and instream habitat.

5.2 Methods

5.2.1 Reach Delineation

Spatial distribution and aerial extent of mesohabitats were mapped between July 8 and July 19, 2003. The survey was between River Mile 0.0 (RM 0.0), the point at which the river transitions from fluvial to impoundment at Mansfield Hollow Reservoir (figure 5.1), and Old Turnpike Road (RM 5.47). The mesohabitats were drawn as polygons in ArcPad 6.0.3 on a Hewlett-Packard iPAQ h1945 handheld computer mated with a Bluetooth GPS receiver, with digital photo overlays and ArcView Templates for data entry.

Each mesohabitat polygon was further characterized by depth and mean column velocity at seven randomly located positions using a Dipping Bar (Jens 1968), substrate distribution according to the Austrian Standard ÖNORM 6232 (1995) (table 5.1), degree of embeddedness (loose, embedded or compacted), and presence (absent, present, or abundant) of physical attributes of canopy cover, undercut banks, woody debris, overhanging vegetation, submerged vegetation, boulders, riprapped banks, shallow margin, and riparian land use (forested, field, pasture, roadway, residential, or urbanized).

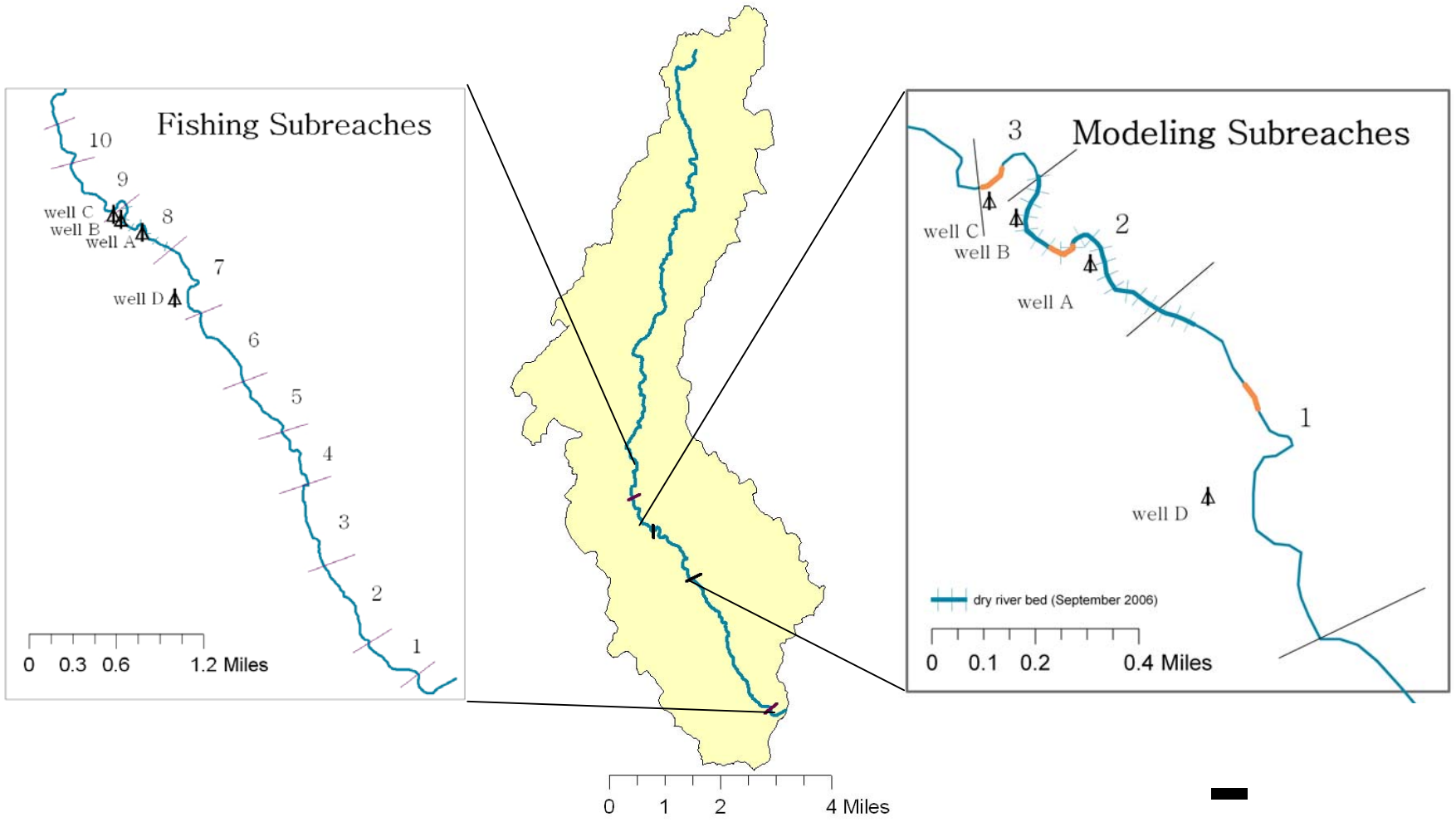

Figure 5.1. Map of the Fenton River study area, fishing sub-reaches and modeling sub-reaches.

Table 5.1. Dominant substrate characteristics (types) (ÖN M6232).

	Type	Grain Size (cm)	Description
Abiotic Types	Megalithal	>40	Boulders to bedrock
	Macrolithal	> 20 to 40	Course blocks and head-sized cobbles
	Mesolithal	> 6.3 to 20	Fist to hand sized cobbles
	Microlithal	> 3 to 6.3	Coarse gravel (size of pigeon egg to a child's fist
	Akal	> 0.2 to 2	Fine to medium size gravel
	Psammal	0.065 to 2	Sand
	Pelal	< 0.065	Silt, loam and clay
Biotic Types	Detritus		Deposits of particulate organic matter (e.g., fallen leaves, and fine particulate organic matter
	Xylal		Tree trunks, branches, roots
	Sapropel		Sludge
	Phytal		Submerged plants, floating stands or mats, aggregations of filamentous algae, or combinations of the above
	Debris		Organic or inorganic matter deposited with the splash zone area by wave motion and changing water levels (e.g., mussel shells, snail shells)

5.2.2 Fishing Reaches

Ten sub-reaches were delineated for purposes of fish collections (figure 5.1) to provide coverage of the entire study area, while ensuring an equal distribution of fishing effort across the array of mesohabitats identified. Two fishing sub-reaches were established upstream of the modeling reach (upstream of river mile 4.26), two within the modeling reach, and six downstream of the modeling reach, between RM 0.0 and Chaffeeville Road RM 3.14.

5.2.3 Modeling Reach

The modeling reach extended 1.12 miles from RM 3.14 (200 yards downstream of Old Stone Mill Road) upstream to RM 4.26 (the lower extreme of the Meadow). Although the cone of depression for Well A is expected to extend into the Meadow, the Meadow was omitted for the fisheries habitat modeling exercise because of the physical characteristics of the channel (very deep and slow, with extensive undercut banks). The hydraulic characteristics of these channel forms would not be expected to change over the range of flows of concern (less than 80 percent duration flow); hence including them would dampen the expression of hydraulic effects of the well field on the remainder of the modeling reach.

The modeling reach was subsequently divided into three sub-reaches (modeling sub-reaches 1, 2 and 3). Subdivisions were based on the distribution of mesohabitats and their respective locations with the area affected by the wellfield. Sub-reach 1 extended 0.64 miles from RM 3.14 to RM 3.78, sub-reach 2 extended 0.35 miles from 3.78 to 4.13, and sub-reach 3 extended 0.13 miles from RM 4.13 to 4.26.

5.2.4 Fish Collections

Fish collections were conducted during mid-day hours (9 AM to 5 PM) on clear to overcast days over the period July 25 through August 22, 2003. All fish collections were made using a grid electrofishing technique (Bain et al., 1985). The grids consisted of two 6-meter electrodes separated by two 1-meter PVC spacers and were coupled with a Honda EX1000 generator and 15 Amp Coffelt VVP-2C transformer. Grids were pre-positioned parallel to the stream channel in groups of five, with the area left undisturbed for at least 25 minutes prior to sampling.

All fish were collected, identified, measured to total length (TL) and returned to the river to recover. Selected samples were retained and transported to the Department of Environmental Protection, Eastern District Headquarters, Marlborough, CT for confirmation of identifications by State fisheries biologists.

The location of each grid was entered into a georeferenced data layer in ArcPad, superimposed over the aerial photo and mesohabitat polygons collected previously. Depth and mean column velocity (Dipping Bar), and substrate type and degree of embeddedness data were collected at the four corners of each grid. In addition, presence of physical attributes of canopy cover, undercut banks, woody debris, overhanging vegetation, submerged vegetation, boulders, riprapped banks, shallow margin, and riparian land use associated with each grid was recorded.

5.2.5 Habitat Suitability Criteria Development

Univariate habitat suitability criteria for depth and mean column velocity were developed for juvenile, adult and composite life stages of fallfish (*Semotilus corporalis*), brook trout (*Salvelinus fontinalis*) and brown trout (*Salmo trutta*). Depth and mean column velocity associated with each fish captured (as measured at the sampled grid) was divided into discrete ranges resulting in a continuous suitability-index curve (SI curve). The suitability index was calculated by dividing the number of individuals of a single species captured in a given range by the total number of individuals of the same species caught. The resulting curves were compared across life stages to assess the degree of life stage separation in depth and current velocity preference. In each intra-species comparison it was noted that juveniles and adults shared depth and velocity utilization, differing from the results reported by Raleigh et al. (1986).

In that the number of individuals by species (table 5.2), relative to the number of grids (n=523) was low for the distinct age classes, and the similarity in the depth and velocity preferences between juvenile and adult life stages of the three species exhibiting

multi-modal size distributions, we concluded that the greater strength attributed to the logistic regression modeling efforts by virtue of the larger sample size of the composite age classes out-weighted the advantages of age specific HSC development. Similarly, a review of the size distributed of tessellated darter (*Etheostoma olmstedi*) reveals no distinct size at age differentiation. Consequently, we developed a single composite age class HSC for this species as well. Univariate habitat suitability criteria for depth and velocity for tessellated darter were calculated similarity as those for brook trout, brown trout and fallfish. For each species, the curves were corrected based on plausibility (correspondence of interpretation with literature data).

Multivariate suitability curves for channel index for the composite age classes were computed by applying logistic regression (SPSS, version 13.0) to substrate, embeddedness, cover and other physical features associated with the location point of each fish collected. A step-wise, forward logistic model (Tabachnick and Fidell, 2001) was applied to determine the attributes that correlate well with species presence and abundance. The model uses likelihood ratios to determine which parameters should be included in the following regression formula:

$$\mathbf{R=e^{-z}}$$

where:

- e = natural log base
- z = $b_1 \cdot x_1 + b_2 \cdot x_2 + \ldots\ldots + b_n \cdot x_n + a$
- $x_{1..n}$ = significant physical variables
- $b_{1..n}$ = regression coefficients
- a = constant

For each sampled grid, the probability of fish presence was calculated using computed regression equations and the following formula:

$$\mathbf{p = \frac{e^z}{(1+e^z)}}$$

This probability value was used as a surrogate for channel index.

5.2.6 Fallfish Nest Habitat Suitability Criteria Development

Surveys of the entire study reach (RM 0.0 to RM 5.47) were conducted in late spring 2004 and mid-spring 2005. Once identified, nest sites were marked and the position noted on reference maps for subsequent data collection. A ten-by-ten grid was superimposed over the riverine area at each nest location, with the nest centered in the grid. Depth, mean column velocity, substrate type and embeddedness within a 0.5-meter radius, canopy shading, distance from nearest bank, and temperature data collected at the nest site and at 3 random points within the grid overlay.

Univariate habitat suitability criteria for depth and mean column velocity were generated similarly to those for fishes. Multivariate suitability curves for fallfish nest location were similarly constructed as for fishes, except that the analysis was limited to the physical features (including temperature and distance to nearest bank) as outlined above.

5.2.7 Hydraulic Surveys

Physical and hydraulic surveys were conducted between July 6, 2004 and April 26, 2005. One site was established in each of the three modeling sub-reaches for conducting the hydraulic simulations following the representative reach approach of Bovee (1986). Eleven to nineteen cross sections were established at each site (Appendix A.2) for a total of 42. Cross sections were established based on the mapped mesohabitat information, characterizing all major mesohabitat types (e.g., riffle, run, glide and pool). Upstream and downstream weighting factors were established following the Mesohabitat-Typing approach as described by Bovee (1994), which assigns cell length corresponding to the cumulative length of the mesohabitat of the type represented by the cross section.

Cross sections were subdivided into vertical cells. The cells were defined using topographic principles that adequately characterize the hydraulic conditions (Parasiewicz, 1996). Spatial orientation of each transect and vertical cell, including elevation, was recorded in the Connecticut State Plane (1983) coordinate system using a Leica TCR 307® total station. Substrate type and degree of embeddedness was recorded at each vertical cell during the topographic survey.

Depth and mean column velocity were collected at each transect and cell at three discharges in modeling sub-reaches 1 and 2 and at two discharges in modeling sub-reach 3 using a topset wading rod and electromagnetic current meter (Marsh-McBirney Flow Mate 2000®). Water surface elevation data were collected at three fixed locations (bricks embedded in the substrate; near left and right banks and in the center of the channel) at five discharges in each modeling sub-reach. Canopy cover at each transect was determined from hemispherical images captured with a Niko Coolpix 5000® digital camera fitted with a Nikor FC-E8 0.21X® fisheye converter at approximately 1.5 meters above the substrate at the midpoint of each transect. Images were subsequently analyzed using Gap Light Analyzer, version 2.0 (Simon Fraser University, Burnaby, British Columbia, CANADA).

5.2.8 Hydraulic Modeling

One-dimensional hydraulic models were used to compute depth and mean column velocity in each cross section (PHABSIM for Windows, version 1.20) (Bovee, 1982). Water surface elevations were simulated using the Stage Discharge, Step-Backwater, and Step-Backwater with initial condition established with the Stage Discharge models (Waddle, 2001). Mean column velocities were simulated using the VELSIM model

(Milhous, et al., 1989). Calibration of water surface elevation simulations were performed following the guidance of Waddle (2001) (see appendix A.3).

Quantification of habitat change with discharge (observed and simulated) was performed using the HABTAE model (Waddle, 2001). Habitat suitability at each cell was calculated as the combined suitability of depth, mean column velocity and channel index. Cell specific habitat suitabilities were summed for each cross section and expanded by the associated upstream and downstream weighting factors to produce cross section specific weighted usable area (WUA). Cross section specific WUA were summed to generate the Weighted Usable Area for each site, representing the respective modeling sub-reach.

5.2.9 Time Series and Continuous Under-Threshold Analysis

An analysis of temporal and spatial habitat variability was conducted to assess alternate well operating protocols to avoid or minimize observable adverse impacts on aquatic biota of the Fenton River. To analyze the duration and magnitude of habitat variations, modified continuous under-threshold habitat-duration curves (UCUT-curves) (Capra et al., 1995, Parasiewicz in print) were constructed.

A single set of UCUT-curves was generated from the simulated flow-time series (see Section 6) and the relative value weighted usable area curves for each species by converting daily flow values for each year, converting the flows to thresholds, and merging the results of all the individual years onto one graph. The constant increments between the thresholds were selected on an iterative basis by creating a number of graphs representing the changes of frequency of occurrence of habitat events.

The analysis of the durations of habitat events under the thresholds led to the establishment of common, critical and rare habitat events as a basis for future recommendations consisting of allowable duration of habitat deficits before pump-shut-downs.

5.2.10 Simulation of Critical Events

The occurrence of low flows and subsequent de-watering of the Fenton River adjacent to well A in September 2005 provided an opportunity to investigate the effects of wellfield operation during extreme conditions on aquatic habitat as well as potential mitigation measures. The natural flow time series for this period were approximated for the Old Turnpike location from observations at the Mt. Hope gauge. Based on computed relationships between pumping and induced recharge we simulated flow conditions at modeling sub-reach 2. The flow time series were transformed into habitat time series to investigate the impact on habitat. The scenarios were selected to simulate habitat levels at natural flow conditions. Because of the drying event, special attention has been given to modeling sub-reach 2 and the usable area curves from this location were used to determine the flows corresponding with habitat thresholds.

5.3 Results

5.3.1 Fish data

A total of 523 plots were fished during the fish data collections resulting in capture of 3,402 fish from 17 species. Table 5.2 presents the number of fish captured by species, figure and 5.2 displays the proportions of the targeted species relative to blacknose dace and other species combined in the community. The overall fish abundance is 1.08 fish per square meter.

Table 5.2. Number of fish captured (all age classes combined) in the Fenton River (bold indicates species used in subsequent modeling exercises).

Fish	Number of Individuals
Brown trout (*Salmo trutta*)	**431**
Fallfish (*Semotilus corporalis*)	**248**
Tessellated darter (*Etheostoma olmstedi*)	**133**
Brook trout (*Salvelinus fontinalis*)	**23**
Blacknose dace (*Rhinichthys atratulus*)	1551
Bluegill (*Lepomis macrochirus*)	278
Pumpkinseed (*Lepomis gibbosus*)	189
White sucker (*Catostomus commersoni*)	241
Common shiner (*Luxilus cornutus*)	132
Largemouth bass (*Micropterus salmoides*)	104
Golden shiner (*Notemigonus crysoleucas*)	34
Northern pike (*Esox lucius*)	10
Yellow perch (*Perca flavescens*)	7
Green sunfish (*Lepomis* cyanellus)	6
Chain pickerel (*Esox niger*)	5
Smallmouth bass (*Micropterus dolomieu*)	1
Yellow bullhead (*Ameiurus natalis*)	1
TOTAL	**3402**

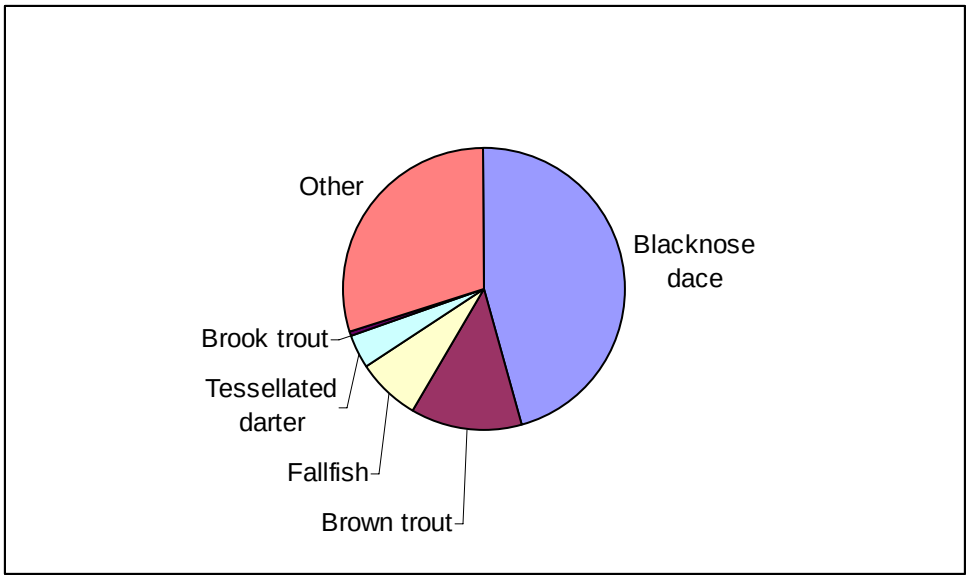

Figure 5.2. Proportions of targeted species relative to blacknose dace and other species collected combined).

Age structure of species used in subsequent modeling exercises was assessed by review of the size distribution of all collected individuals (figure 5.2). Although degree of gonadal development was not assessed for any of the fishes studied, assumptions of recruitment to reproductive age were inferred from review of the size distribution and literature describing length at age for each species.

Brown trout (n=431) exhibited a bi-modal size distribution with one mode (<160 mm TL; n=357) representing juveniles, and another (>160 mm TL; n=70) representing adults. Conversely, brook trout (n=23) exhibited a tri-modal size distribution with one mode (<100 mm TL; n=6) representing juveniles, and two modes (120-170 mm and >180 mm TL; n=16) representing adults. Caution should be used interpreting these data however, as the number of individuals in each size class are low. Regardless, these distinctions seem reasonable in light of recruitment to reproductive age observed throughout their range.

The modality of the age structure of fallfish (n=248) is less well defined. Regardless, it may be most reasonable to distinguish juveniles as those less than 110 mm TL (n=138), and adults as those greater than 110 mm TL (n=110). There is no modality pattern tessellated darter size distribution and all individuals were considered collectively as a single age class.

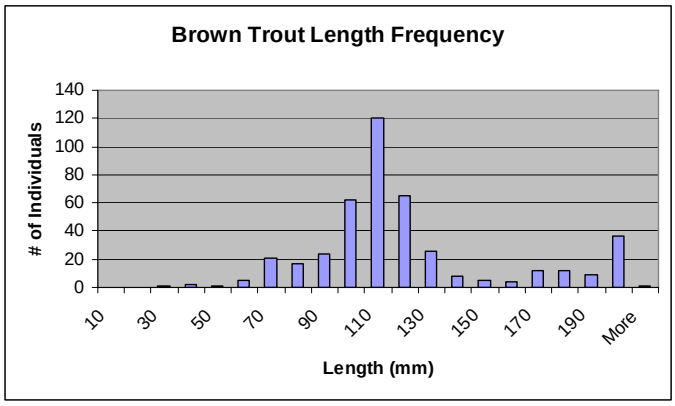

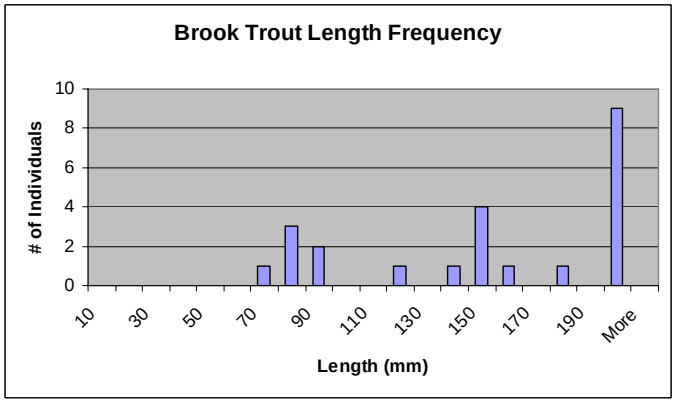

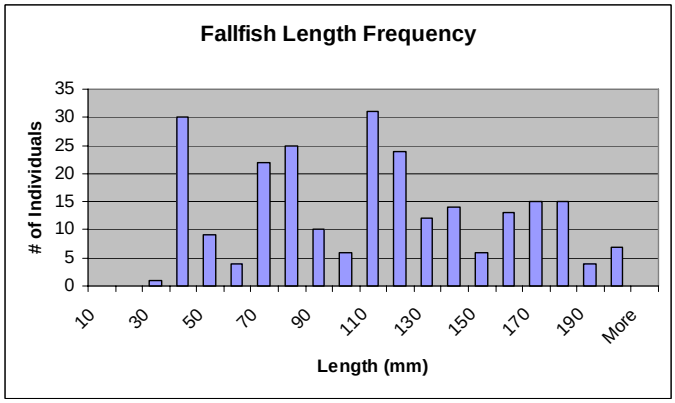

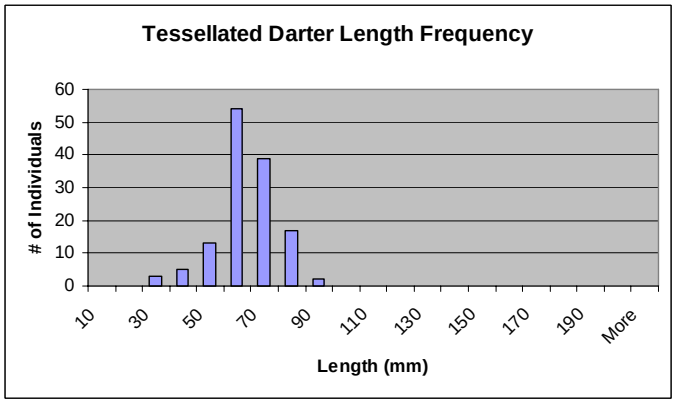

Figure 5.3. Size distributions of brown trout, brook trout, fallfish and tessellated darter.

5.3.2 Habitat Suitability Criteria

Analyses leading to the generation of suitability curves for brown trout, tessellated darter and fallfish were conducted exclusively with data collected during the fisheries survey conducted on the Fenton River in 2003 as part of this study. However, the number of brook trout captured in the Fenton River was not sufficient to for establishing of any habitat suitability criteria (Bovee 1986). Consequently, analyses leading to generation of suitability curves for brook trout were conducted using data from the Fenton River survey supplemented with data from a study of similar design conducted on the Stony Clove River, New York. In July and August 2002 we sampled 456 grids in five similar streams in Catskil Mountains, NY. 269 grids were sampled in the Stony Clove Creek, 107 grids on the Upper Round Out, a stream approximately 35 miles from the Stony Clove, placing approximately 24 grids in each of four different stretches. Additional 80 grids were collected in tributaries of the Beaver Kill, located approximately 55 miles from the Stony Clove. We placed between 16 and 24 grids in each of the four tributaries: Trout Brook, Spring Brook, Stewart Brook and Willowemoc. This data set created solid representation of habitat utilized by brook trout less affected by local habitat availability.

Brook trout – The depth suitability index (SI) (figure 5.4a) for brook trout began at 0.0 at 0.0 ft, increased to 0.1 at to 0.7 ft, before increasing rapidly to 1.0 at 1.0 ft and remained a 1.0 through 2.6 ft, before falling. A strict application of the univariate procedure for depth SI at depths above 3 ft would indicate that brook trout avoid greater depths. This is in conflict with reported habitat use by brook trout (and brown trout) (Smith, 1985) and is believed to be a consequence of depth limitations of the grid electrofishing technique. Consequently, after reviewing the depth distributions through the Fenton River study reach and considering the depth preferences reported in the literature, we corrected the depth SI to reflect optimal habitat utilization at all depths equal to or greater than 1.0 ft. The velocity SI began at 0.1 at 0.0 ft/sec, increased to 1.0 at 1.0 ft/sec, before falling to 0.0 at 2.0 ft/ sec. The regression model of channel index for brook trout presence has a predictive power of 87 percent (table 5.3). Physical features associated with the presence of brook trout are canopy shading (B=0.58), and megalithal (B=0.99) and macrolithal (B=1.10) substrates. Physical features associated with the absence of brook trout are riprap (B=-0.85), overhanging vegetation (B=-0.44), woody debris (B=-0.46), and a constant term (B=-50).

Brown trout – The depth SI (figure 5.4a) for brown trout began at 0.0 at 0.0 ft, increased to 1.0 at 1.0 ft and remained a 1.0 through 2.2 ft, before falling. Similar to brook trout, we concluded that the fall in depth SI at depths above 2.3 ft was inconsistent with published habitat utilization values and adjusted the depth SI to 1.0 for all depths equal to or greater than 1.0 ft. The velocity SI began at 0.1 at 0.0 ft/sec, increased to 1.0 at 1.3 ft/sec, before falling precipitously to 0.1 at 1.6 ft/ sec and 0.0 at 2.0 ft. The regression model of channel index for brown trout presence has a predictive power of 63 percent (table 5.3). Woody debris (B=0.19) was the sole physical feature associated with the presence of brown trout. Physical features associated with the absence of brown trout

are submerged vegetation (B=-0.96), canopy shading (B=-0.37), and akal substrates (B=-1.2).

Tessellated darter – The depth SI (figure 5.4b) for tessellated darter began at 0.0 at 0.0 ft, remained at 0.0 to 0.16 ft, and then increased to 1.0 at 0.8 ft. The depth SI remained at 1.0 to 1.15 ft before falling to 0.0 at 1.8 ft. The velocity SI began at 0.0 at 0.0 ft/sec, increased to 1.0 at 0.8 ft/sec, before falling to 0.0 at 1.8 ft/ sec. The regression model of channel index for tessellated darter presence has a predictive power of 83 percent (table 5.3). No physical features were associated with the presences of tessellated darter. Physical features associated with the absence of tessellated darter are canopy shading (B=-0.65), woody debris (B=-0.31), and psammal substrates (B=-2.1).

Fallfish – The depth SI (figure 5.4b) for fallfish began at 0.0 at 0.0 ft, remained at 0.0 to 0.3 ft, then increased to 1.0 at 1.3 ft before falling to 0.0 at 2.6 ft. The velocity SI began at 0.3 at 0.0 ft/sec, increased to 1.0 at 1.0 ft/sec, before falling to 0.0 at 2.3 ft/ sec. The regression model of channel index for fallfish presence has a predictive power of 85 percent (table 5.3). No physical features were associated with the presences of fallfish. Physical features associated with the absence of fallfish are megalithal (B=-0.42), canopy shading (B=-0.60), and woody debris (B=-0.39).

Fallfish Nests – The 2004 fallfish nest survey was conducted late in the spawning season (as reported in the literature) under the assumption that the survey team would have the greatest likelihood of finding the maximum number of nest locations. However, only one confirmed and five probable fallfish nests were located in during 2004 survey. It was concluded that periods of high discharge associated with late spring rainfalls likely obliterated nests that were constructed early in the spawning season. Given only one confirmed nest location, and the uncertainty that the others sites supported fallfish nest, it was decided to suspend the fallfish nest data collection phase until the 2005 spawning season. Three surveys were conducted in mid to late May, 2005. No fallfish nests were located during those surveys. A review of temperature data from long term data loggers installed in the river in the summer of 2004 revealed that river temperatures had remained unseasonably low throughout the late May, rising above the threshold temperature for fallfish spawning (Smith, 1985) for short periods on only two days. From this it was concluded that the fallfish spawning season was delayed and surveys will recommence when water temperatures rise above 14.4 degrees C.

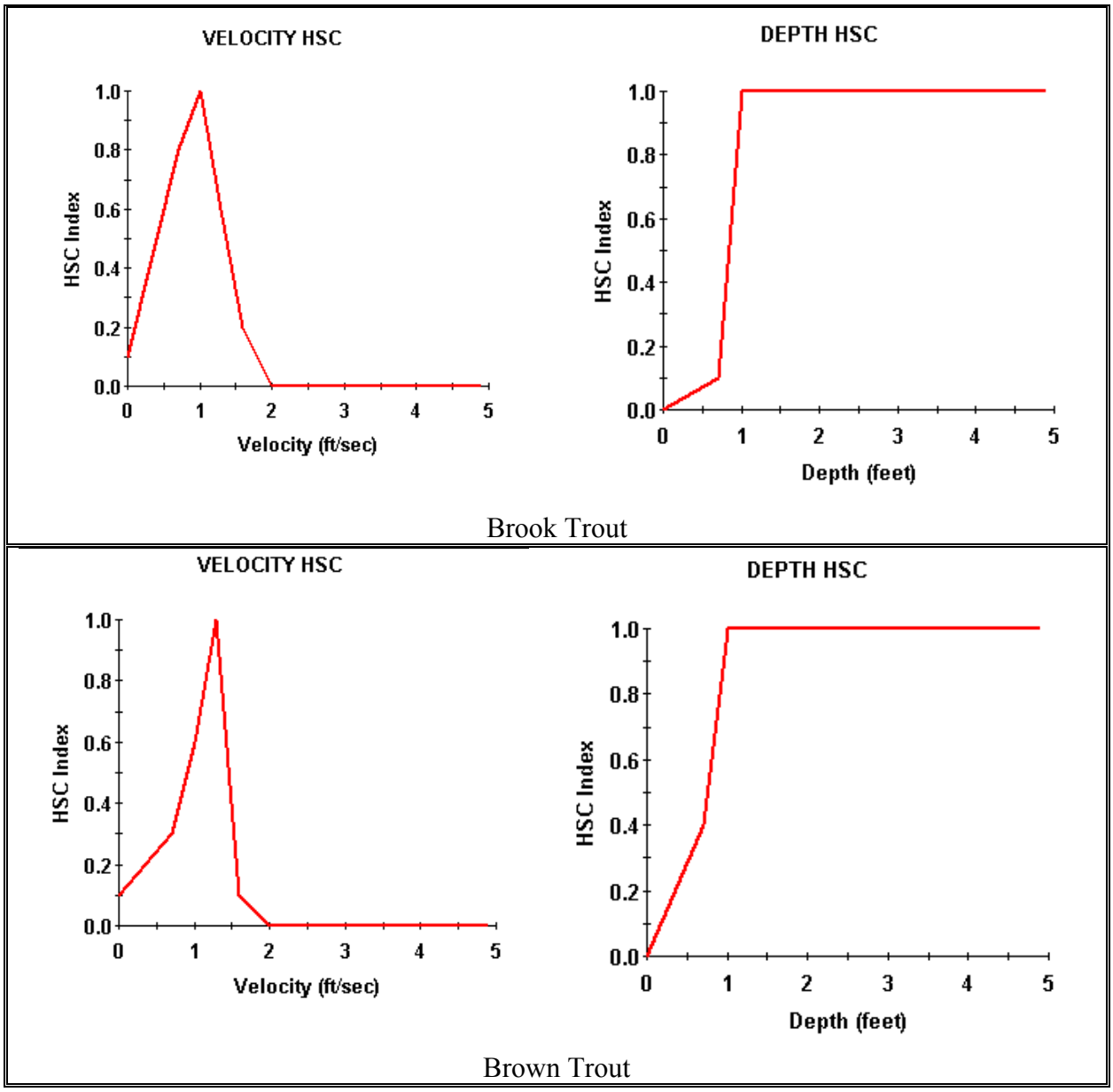

Figure 5.4a. Depth and mean column velocity habitat suitability curves for brook trout and brown trout.

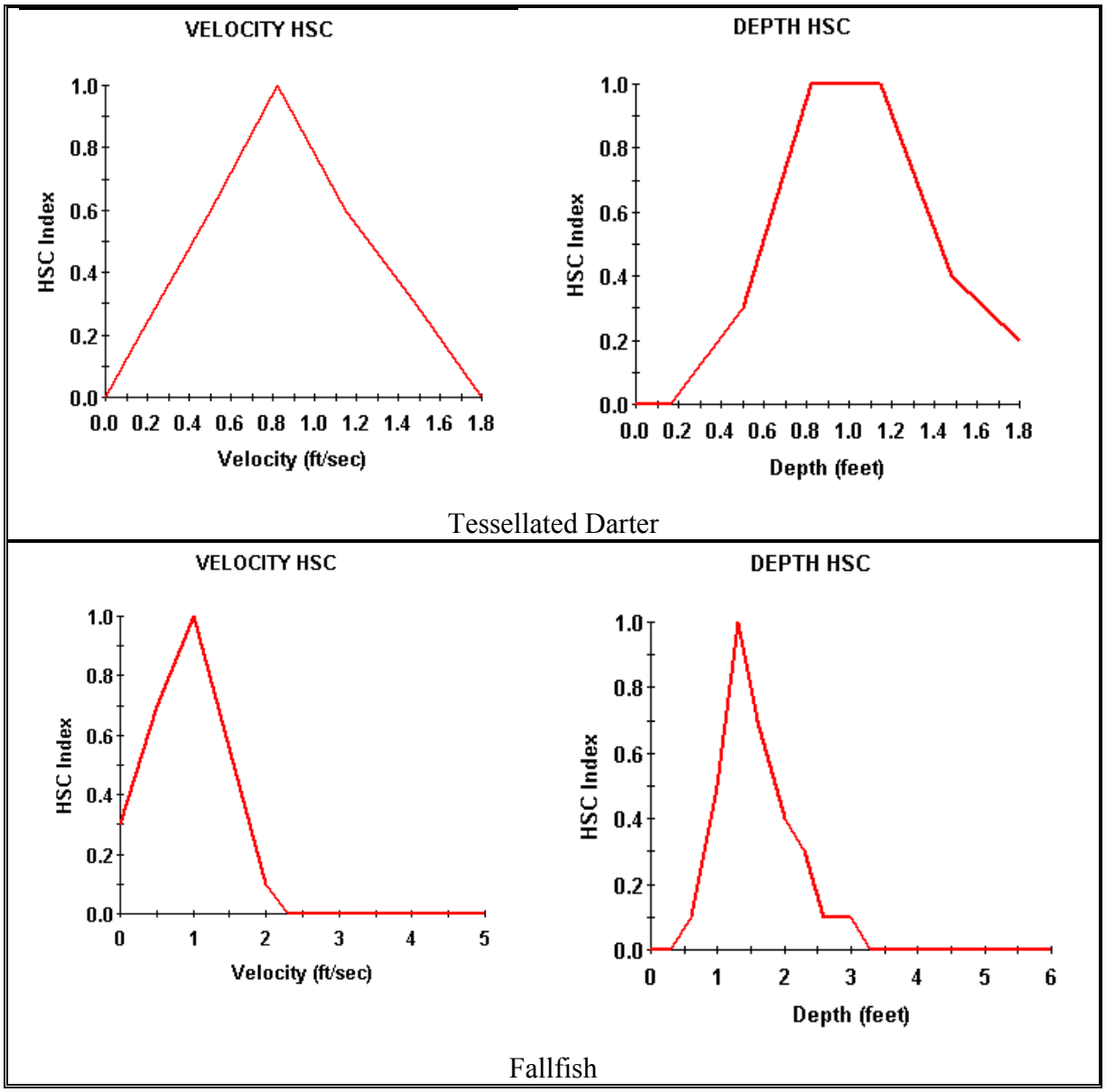

Figure 5.4b. Depth and mean column velocity habitat suitability curves for tessellated darter and fallfish.

Table 5.3. Logistic regression B coefficients for channel index SIs for brook trout, brown trout, tessellated darter and fallfish.

Variables in the Equation: Tessellated Darter							
Predictive value		B	S.E.	Wald	df	Sig.	Exp(B)
83%	Canopy_Shading	-0.646	0.12081	28.58997	1	8.94E-08	0.524155
	Woody_Debris	-0.313	0.114568	7.449651	1	0.006345	0.731467
	Psammal	-2.144	0.728579	8.661507	1	0.00325	0.117157
Variables in the Equation: Fallfish							
		B	S.E.	Wald	df	Sig.	Exp(B)
85%	Boulders	-0.420	0.135696	9.601851	1	0.001944	0.656731
	Canopy_Shading	-0.599	0.128783	21.63907	1	3.29E-06	0.549321
	Woody_Debris	-0.389	0.131257	8.803666	1	0.003006	0.677429
Variables in the Equation: Brown Trout							
		B	S.E.	Wald	df	Sig.	Exp(B)
63%	Submerged_Vegetation	-0.958	0.209419	20.93696	1	4.75E-06	0.383569
	Canopy_Shading	-0.367	0.100927	13.23518	1	0.000275	0.692688
	Woody_Debris	0.194	0.09664	4.012377	1	0.045167	1.213586
	Akal	-1.167	0.509988	5.234947	1	0.022137	0.311345
Variables in the Equation: Brook Trout							
		B	S.E.	Wald	df	Sig.	Exp(B)
87%	Riprap	-0.848	0.31595	7.206253	1	0.007265	0.428206
	Overhanging_Vegitation	-0.436	0.135188	10.39029	1	0.001267	0.64677
	Canopy_Shading	0.575	0.153792	13.99856	1	0.000183	1.777857
	Woody_Debris	-0.465	0.127847	13.21737	1	0.000277	0.628262
	MegaLithal	0.986	0.329595	8.941741	1	0.002787	2.679364
	MacroLithal	1.097	0.25481	18.52086	1	1.68E-05	2.993958
	Constant	-2.497	0.28927	74.53458	1	5.96E-18	0.082302

5.3.3 Mesohabitat Distribution

Although the discrete proportions and rank order were different, the three dominant mesohabitat types of the study area were the same as those found in each of the modeling sub-reaches (figure 5.5). This information was used to select the study areas and to position the study sites and cross sections to optimize the effectiveness of using the representative reach analysis in developing weighted usable area response curves.

5.3.4 Weighted Usable Area Curves

Flows in the Fenton River during the summer of 2004 were unusually high (see Section 6). Consequently, the lowest discharge observed while conducting hydraulic surveys in modeling sub-reach 3 in the summer of 2004 was 6.4 cfs. This constrained the plausible lower limit of the simulation range to 2.0 cfs. The upper simulation range (109.3 cfs) coincided with the highest discharge during which hydraulic measurements were obtained.

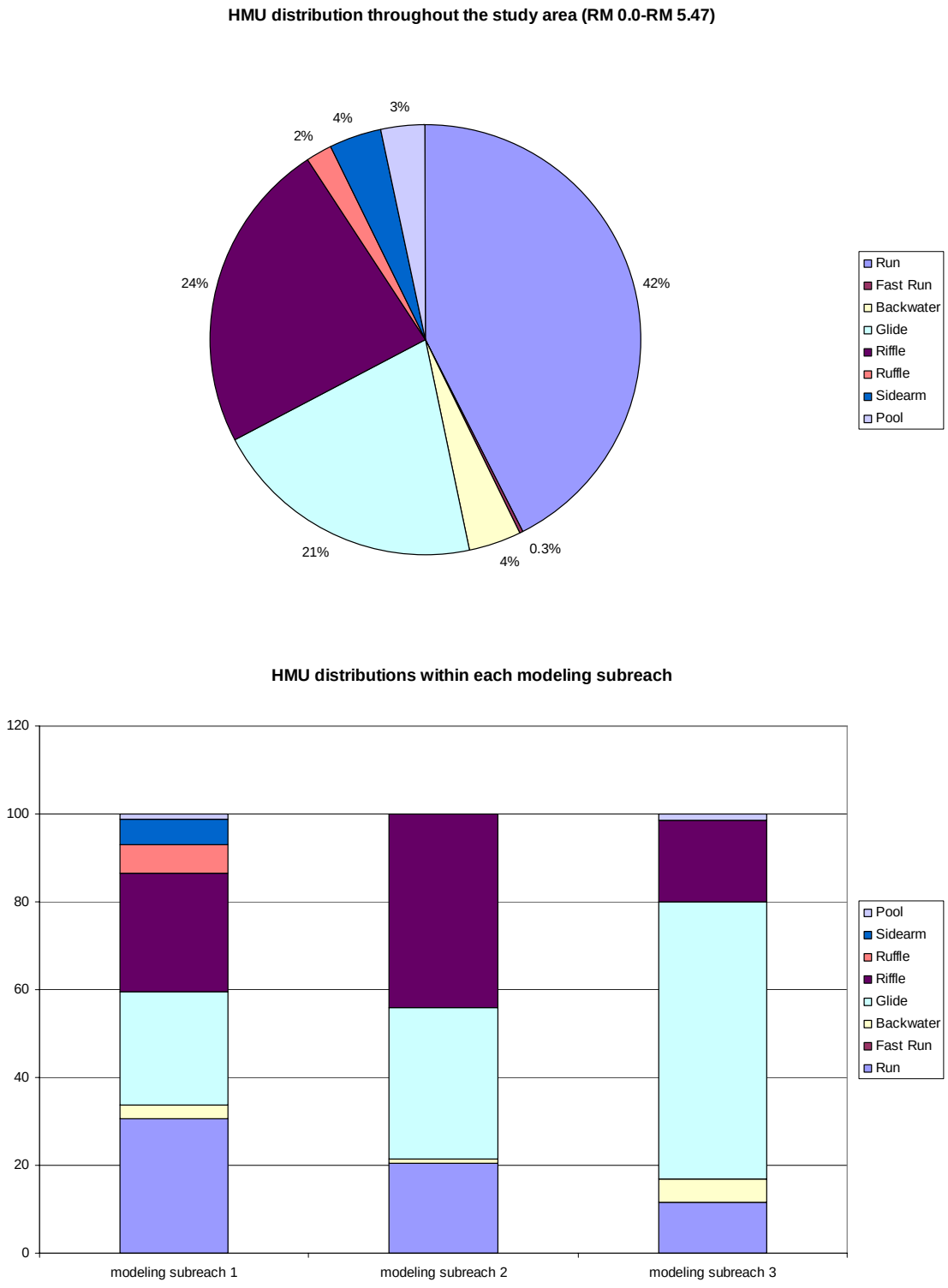

Figure 5.5. Distribution of hydromorphologic units (HMU) over the entire study area and within the three modeling sub-reaches.

Representative observed and simulated water surface elevation and velocity plots reflecting the rigor of the calibration step in the hydraulic modeling is presented for sub-reaches 1, 2 and 3 (see appendices A.3.1, A.3.2 and A.3.3, and A.4.1, A.4.2 and A.4.3)

Weighted usable area as a function of discharge was similar in each modeling sub-reach (see appendices A.5.1a and b, A.5.2a and b and A.5.3a and b). The weighted area for each modeling sub-reach was applied to the representative sub-reach lengths to obtain sub-reach specific usable area as functions of discharge. These values were subsequently summed and converted to percentages of maximum usable area to obtain the cumulative usable area to discharge relationships (figure 5.6) for the entire modeling reach.

Over the range of simulations flows, all species followed remarkably similar patterns, rising from extremely low usable area values at the lowest flows modeled to maximum values at 25 to 50 cfs, before gradually falling (figure 5.6). Maximum usable area for brook trout (17,772 sq ft) was the lowest of all species observed and coincided with a discharge of 50 cfs. Brown trout and fallfish shared very similar overall trends in usable area, with maximum values of 20,051 sq ft at 50 cfs and 20,217 sq ft at 50 cfs, respectively. Maximum usable area of 18,890 sq ft for tessellated darted was reached at a substantially lower discharge of 25 cfs.

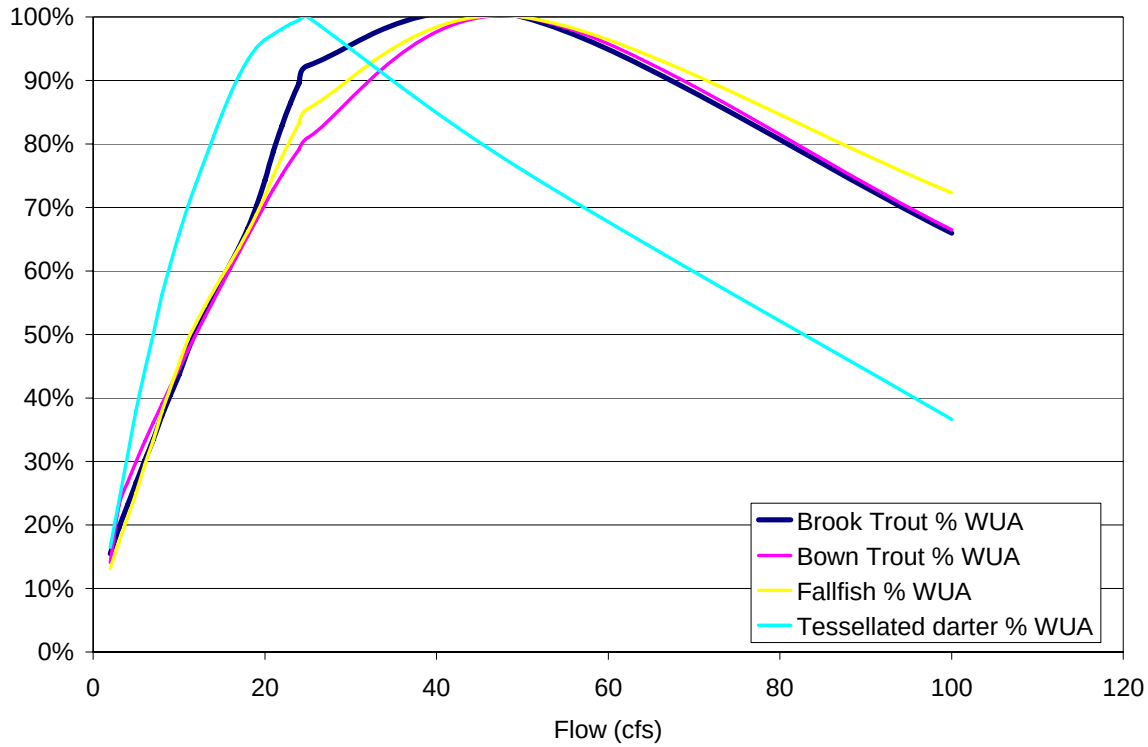

Figure 5.6. Usable area curves for all species over the full range of simulation discharges (2.0 to 109.4 cfs).

Of greatest interest in the assessment of the effects of the University of Connecticut well field is the habitat response at the lower range of flows. To make this assessment, projections of usable area were constrained to simulated discharges of 2.0 to 10.0 cfs. This range was selected based on the conclusion that the maximum well field effect on stream flow was approximately 0.8 cfs in the vicinity of well A (see Sections 6 and 9), which fell within the measurement error for discharge above 10 cfs.

To assess the consistency of species specific habitat response to changing discharge over this constrained range of discharge we conducted an analysis of the weighted usable area curves for the selected species from modeling sub-reach 3. It is notable that the response curve over this range of flows at all modeling sub-reaches approached a straight line (figure 5.7) with flows decreasing rapidly with stream flow. We removed the variability in the simulation results that occur as a function of measurement, simulation and extrapolation error, by application of the General Linear Model (Tabachnick and Fidell, 2001).

Linear regression was performed between discharge over the simulation range of 2 to 10 cfs as the dependent variable and Weighted Usable Area for the four fishes as the independent variables. Analysis was performed using SAS Regression and SAS Univariate Distribution and Normality for tests of assumptions (SAS Institute, version 9.0.3). Results of evaluation of assumptions revealed that the data were normally distributed and that transformations were not warranted.

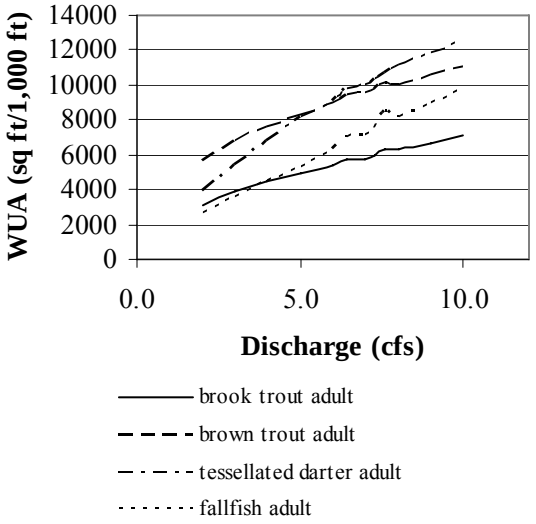

Figure 5.7. Weighted usable area response curve for all species over a restricted range of discharge (2.0 to 10.0 cfs).

Table 5.4. Regression coefficients for weighted usable area (sq ft/1,000 ft; the dependent variable) with discharge (the independent variable) over the range of 2.0 to 10.0 cfs for selected species.

Species	Intercept	Slope Coefficient
Tessellated darter	2330	1080 a†
Fallfish	810	926 b
Brown trout	4830	658 c
Brook trout	2400	489 d

† Values for the slope coefficient followed by the same letter are not significantly different according to the Tukey's Honestly Significant Difference (HSD) Test (α=0.05).

The R^2, t and p values, and the intercept and slope parameter estimates for each species are presented in table 5.4. R^2 for the regression was significantly different from zero for all species and the models described between 97 and 99 percent of the variability

in the data are displayed in table 5.4. A supplemental analysis of homogeneity of the regression coefficients revealed that the slope coefficients for all species were significantly different from one another.

There is an exponential increase in the proportion of weighted usable area decline as discharge decreases from 10.0 cfs to 2.0 cfs for all species (figure 5.8). The decline is most notable in shallow dwelling species, fallfish followed by tessellated darter reaching a maximal rate of decline of 18 and 14 percent, respectively. Alternately, the rate of decline remains comparatively constant for brook trout and only slightly more pronounced in brown trout with maximal declines of approximately 8 and 6 percent at the lowest simulated flow.

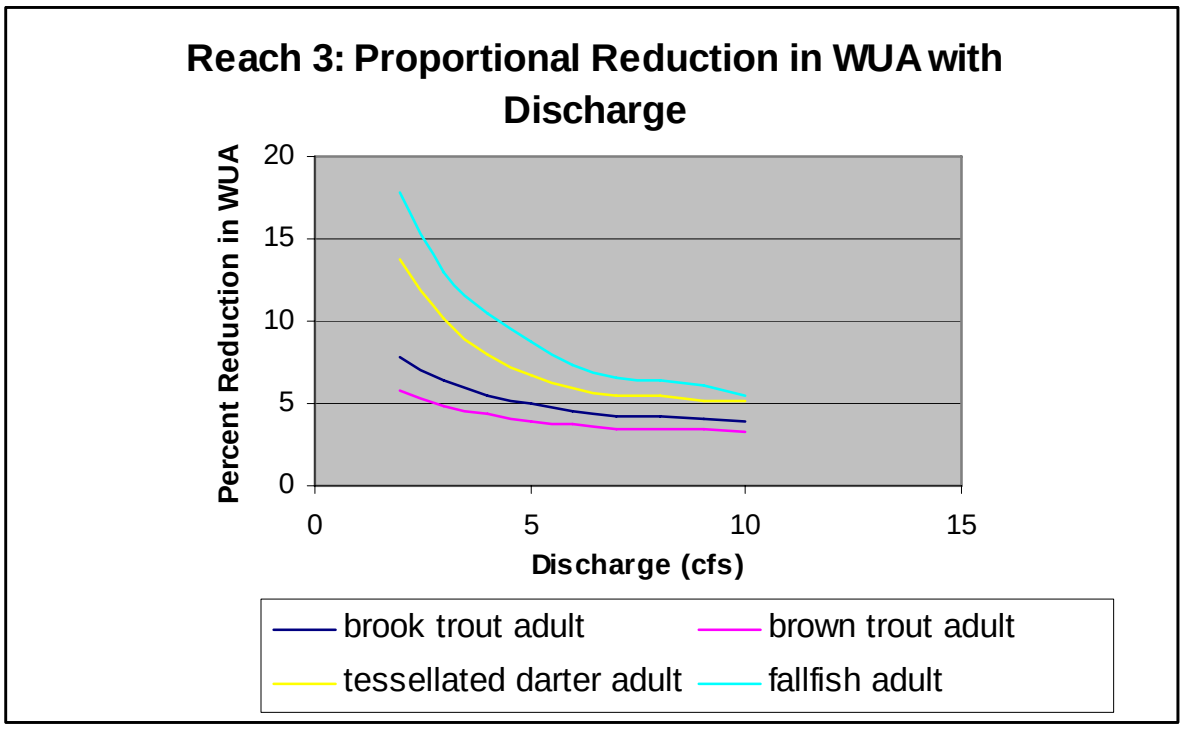

Figure 5.8. Modeling Sub-Reach 3: Proportional reduction in WUA with discharge.

5.3.5 Time Series and Continuous Under Threshold Analysis

Brown trout – Continuous Under Threshold (UCUT) curves for brown trout in the summer season are displayed in figure 5.9. Each curve represents the frequency and duration that habitat stayed under specific levels. Habitat frequency and duration increase gradually beginning with 3 percent of maximum weighted usable area (corresponding to zero discharge) to approximately 15 percent of maximum weighted usable area. No substantive increase in the frequency of events is observed until 15 percent of maximum weighted usable area wherein frequency increases to 25 percent of the period of record. Such events do not last longer than 17 days. Because assuming that brown trout has sufficient habitat under no flow is unreasonable expectation, we arbitrarily select 15% as

a rare habitat threshold. It corresponds with approximately 2.1 cfs flow. Increasing the threshold from 20 percent (2.6 cfs) to 35 percent (7 cfs) of maximum weighted usable area dramatically increases the frequency of habitat events, as indicated by the inflection points on corresponding curves. The events providing less or equal to 35 percent of maximum weighted usable area occur over 73 percent of the period of record. Increasing the threshold to 40 percent of maximum weighted usable area raises the frequency of occurrence by only 4%. Further increases of the habitat threshold do not substantially change the frequency of occurrence. Therefore 35 percent of maximum weighted usable area (7 cfs) was selected as a threshold separating common and unusual summer habitat levels and 20% (2.5 cfs) separating critical levels. The duration of unusual habitat levels is from 15 to 40 days.

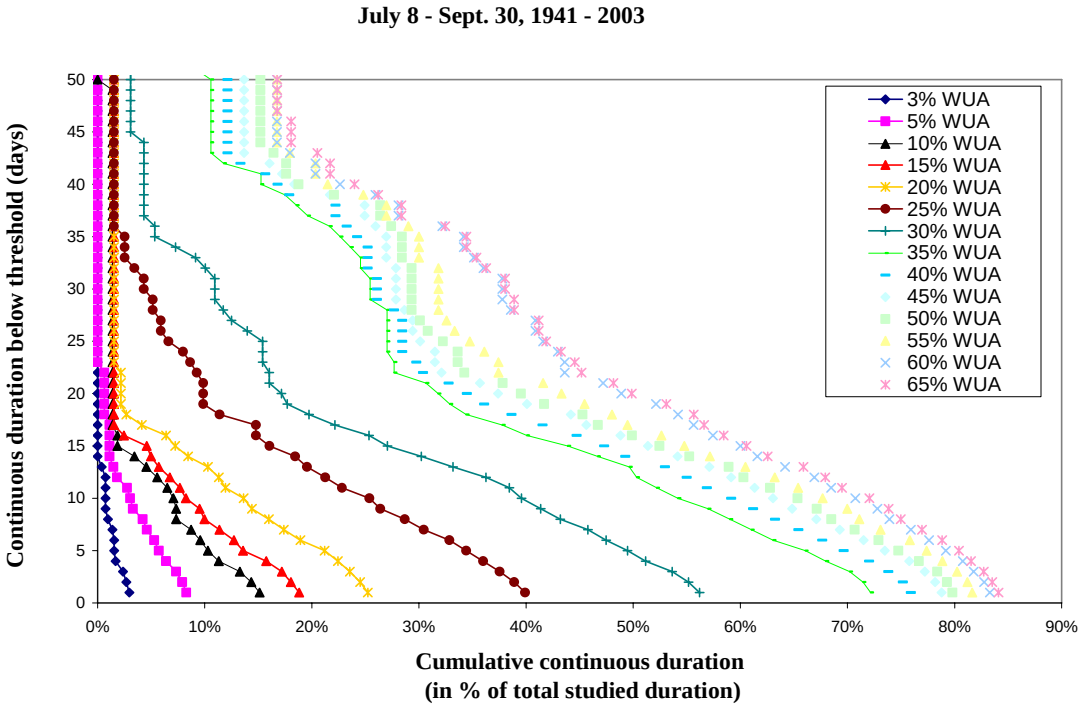

Figure 5.9. Selected habitat UCUT curves for brown trout. Common habitat threshold is in green, critical in yellow and rare in red.

Brook trout - UCUT curves developed for brook trout in the summer season are displayed in figure 5.10. Each curve represents the frequency and duration habitat stayed under specific levels. Discharges during which less than 12 percent of maximum weighted usable area occurred were infrequent (8 percent of the entire period). Such events do not last longer than 10 days and events longer than 5 days comprise fewer than 4 percent of the flow record. This threshold corresponds with approximately 1.5 cfs flow. The 15% threshold (2 cfs) indicates events two times as common (18% of time) with longest common duration of 15 days. Increase of the threshold level to 35% (7.5 cfs) dramatically increases the frequency of habitat events. Commonly the habitat does not

stay under 35% level for much longer than 40 days as indicated by inflection points on corresponding curve. The events providing less or equal to 35% of WUA make in total 78% of entire period of record. Increase of threshold to 40% of total WUA (9 cfs) raises the frequency of occurrence by only 1%. Further increases of habitat threshold are not changing the frequency of occurrence very dramatically. Therefore 35% of WUA can be selected as a threshold separating common and unusual summer habitat levels.

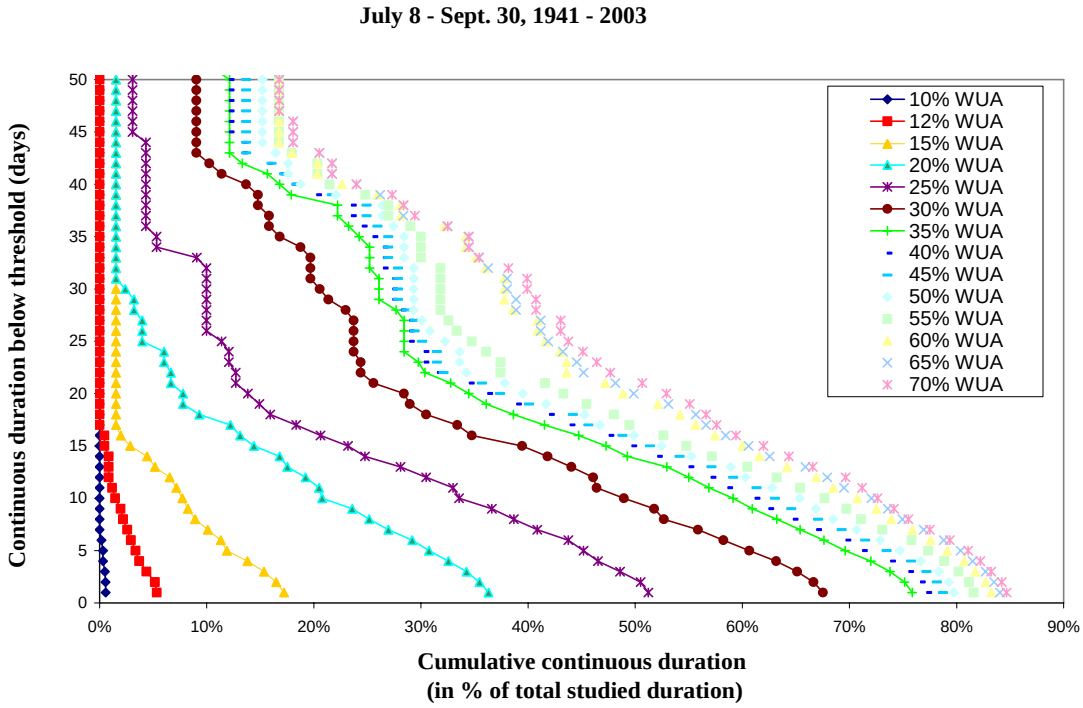

Figure 5.10. Selected habitat UCUT curves for brook trout. Common habitat threshold is in green, critical in yellow and rare in red.

Tessellated darter - UCUT curves were developed for tessellated darter in the summer season (figure 5.11). Each curve represents the frequency and duration of how long the habitat stayed under a specific levels. Less than 10% of highest possible WUA is highly unusual (6% of the entire period). Such events do not last longer than 5 days and events longer than 5 days make less than 2% of cases. This threshold corresponds with approximately 1.1 cfs flow. The 15% threshold (1.8 cfs) indicates events four times as common (25% of time). Sequential increases in thresholds from 20% (2.5 cfs) through 45 % (6.3 cfs) dramatically increase the frequency of habitat events. Commonly the habitat does not stay under 45% level for much longer than 40 days what is indicated by inflection points on corresponding curves. The events providing less or equal to 45% of WUA make in total 75% of entire period of record. Increase of threshold to 50% of total WUA raises the frequency of occurrence by only 5%. Further increases of habitat threshold are not changing the frequency of occurrence very dramatically. Therefore 45%

of WUA can be selected as a threshold separating common and unusual summer habitat levels.

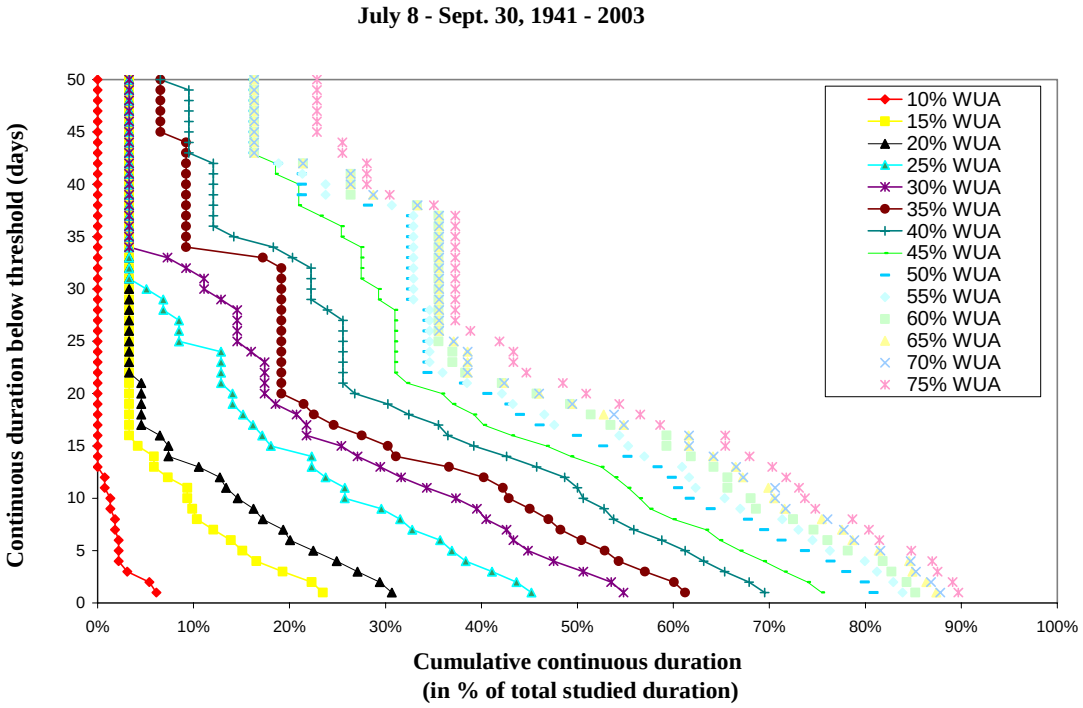

Figure 5.11. Selected habitat UCUT curves for tessellated darter. Common habitat threshold is in green, critical in yellow and rare in red.

Fallfish - UCUT curves developed for fallfish in the summer season are displayed in figure 5.12. Each curve represents the frequency and duration of how long the habitat stayed under a specific levels. The situation with available habitat less than 10% of WUA are very infrequent (10% of the entire period). Such events do not last longer than 5 days and events longer than 10 days make less than 2% of cases. This threshold corresponds with approximately 1.5 cfs flow. The 15% threshold (2.5 cfs) indicates events three times as common (27% of time). Sequential increases in thresholds from 20% (4 cfs) through 35 % (7.5 cfs) dramatically increase the frequency of habitat events. Commonly the habitat does not stay under each mentioned level for much longer than 15 to 20 days respectively as indicated by inflection points on corresponding curves. The events providing less or equal to 35% of WUA make in total 78% of entire period of record. Increase of threshold to 40% of total WUA (8.5 cfs) raises the total frequency of occurrence by only 2%. Further increases of habitat threshold are not changing the frequency of occurrence very dramatically. Therefore 25% of WUA can be selected as a threshold separating common and unusual summer habitat levels.

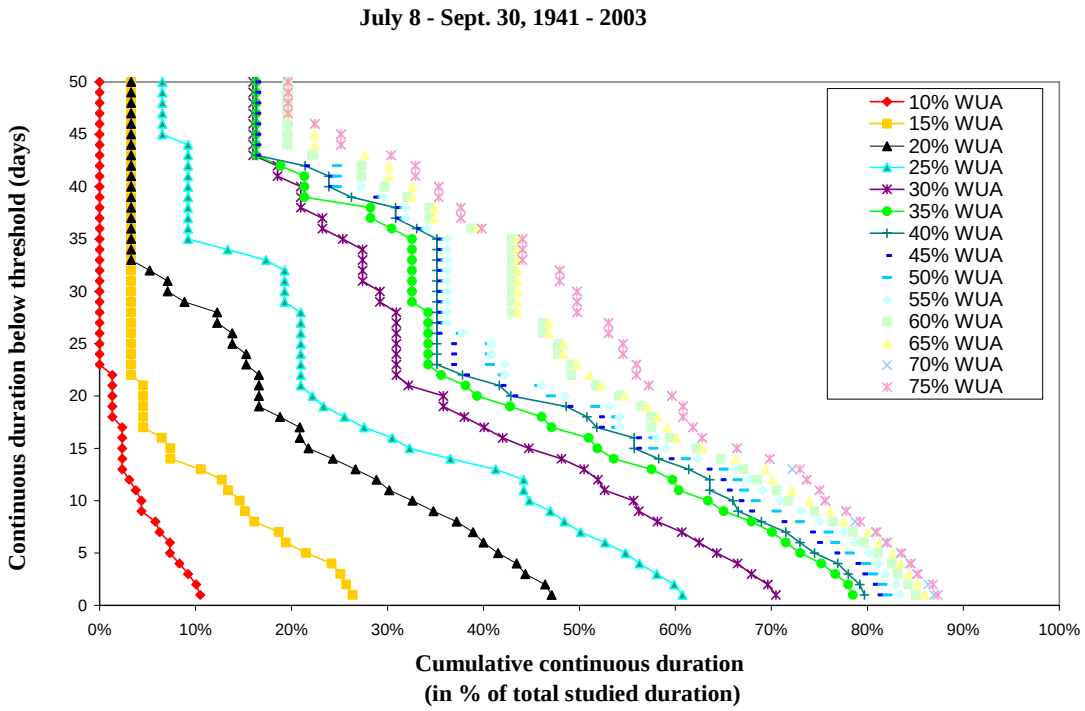

Figure 5.12. Selected habitat UCUT curves for fallfish. Common habitat threshold is in green, critical in yellow and rare in red.

5.3.6. Simulation of Critical Events.

As mentioned above special attention is given to the drought event in the area of the Modeling Sub-Reach 2 that occurred in September 2005. Figure 5.13 represents flow and habitat time series from Spring and Summer 2005 as it would be in the entire study area naturally and the figure 5.14 documents the impact on the Modeling Sub-Reach 2. As visible on the graphs pumping at the level of 844,000 gal/day not only completely depleted the habitat, but also reduced the magnitude and duration of short pulsing events, which would provide relief to stressed fauna.

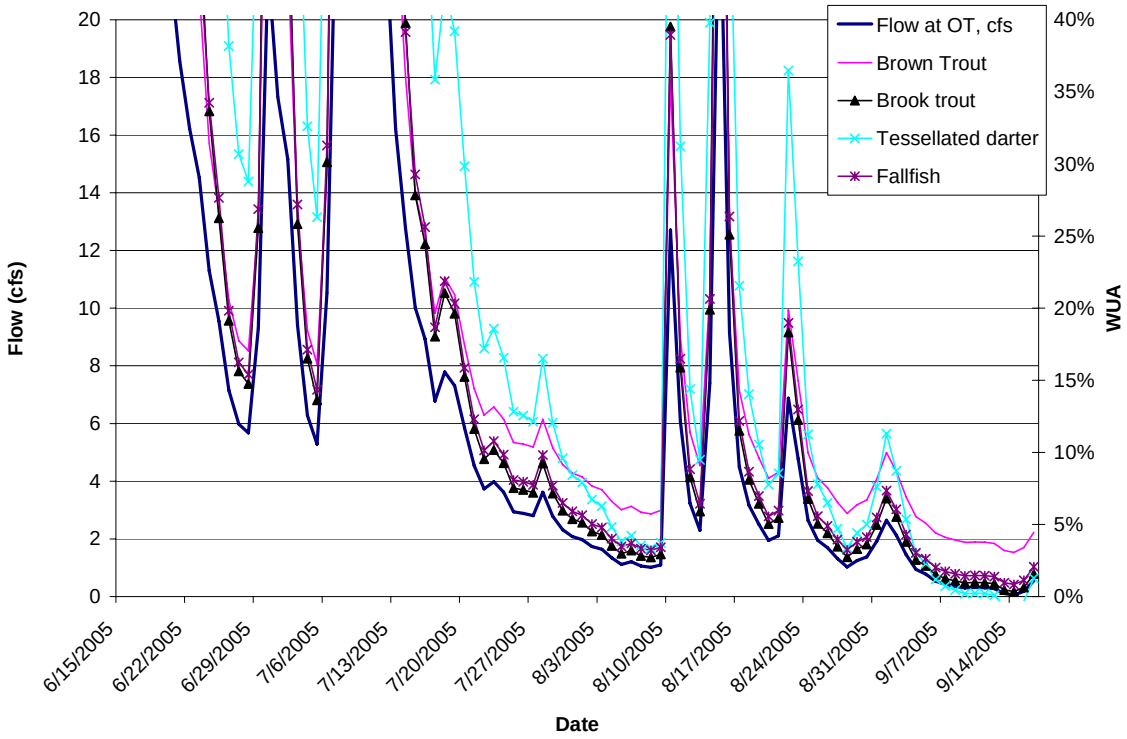

Figure 5.13. Flow and habitat time series as it would occur at modeling sub-reach 2 without pumping (OT- Old Turnpike Road).

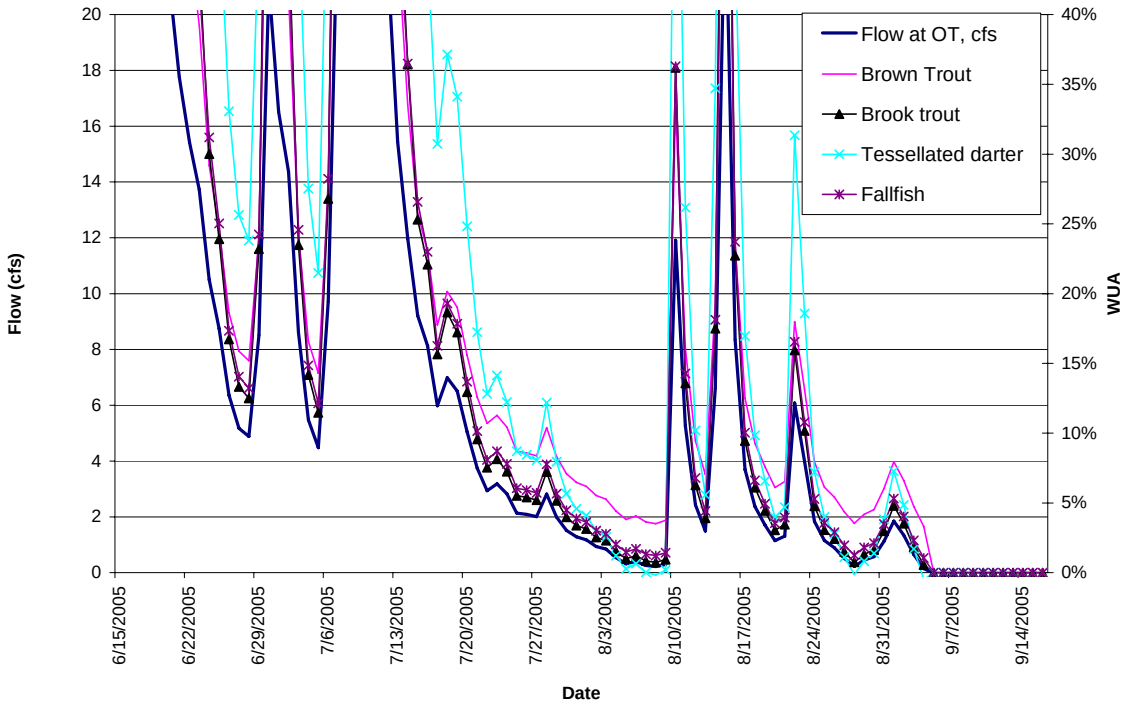

Figure 5.14. Flow and habitat time series as it did occur at modeling sub-reach 2 with pumping (OT- Old Turnpike Road).

5.4 Discussion

Although an investigation of the existing fish community is beyond the scope of this study the preliminary analysis leads to the conclusion that although the fish community is comprised of approximately 60 percent fluvial specialist and fluvial dependent species, the large proportion of bluegill and pumpkinseed is indicative of a disturbed condition. Furthermore the observed fish abundance of 1.08 fish square meter is substantially below streams of similar size and type within the region. The comparatively low numbers of brook trout and high proportion of non-native species (45%) also requires attention. From these observations we conclude that the fish population of the Fenton River is adversely impacted by anthropogenic forces, including water extraction.

In spite of the apparent similarities in the weighted usable area response curves among the species, it is notable that the slope coefficients for the decline in weighted usable area in the restricted discharge range were significantly different from one another. This confirms that each species responds uniquely to changes in habitat as affected by instream flow, and the relative importance of developing habitat suitability criteria, and subsequently weighted usable area for each.

The inflection points in the falling limb of the weighted usable area curves appear to be approximately 10 to 20 cfs. This begins to manifest itself as lower water surface elevations (lower depths) and slower mean column velocities. These findings highlight

the importance of focusing attention on the lowest flow range, that range where the effects of water extraction can be observed.

Although it is informative to describe how habitat changes with discharge at moderate to high discharges, it is also clear that the effects of withdrawals from the well field are limited to periods of naturally low discharge. However, once a low discharge event occurs, withdrawals from the well field can have substantial direct effects on habitat as reflected in water depth, mean column velocity and associated channel index values.

It may seem counter-intuitive that the more precipitous declines in proportional weighted usable area are exhibited by fallfish and tessellated darter as opposed to brook trout and brown trout. However, the majority of mesohabitats throughout the study area are comprised of riffles, runs and glides, each a comparatively shallow water habitat. As discharge falls, these areas begin to drain transitioning from shallow to very shallow or marginally deep to shallow water. It is reasonable to expect that trout, whether brook or brown, are seeking refuge in pool habitats.

The time series analysis indicates a similar order of magnitude of common thresholds for all investigated species. Interestingly, thresholds for brook trout, tessellated darter and fallfish are readily apparent. Corresponding thresholds for brown trout were comparatively difficult to discern. This could be a consequence of brown trout not being native to the Fenton River, and therefore a poor match of biological and physical templates. As a result, duration thresholds selected for brown trout are presented below for discussion but are not incorporated in subsequent assessments of the threshold values for the fish community. Values for habitat event length (longest) and the corresponding discharges are presented in table 5.5. For all species the habitat levels corresponding with flows lower than 1.5 to 2.1 cfs appear to be critical. Such conditions may appear approximately every 5-10 years for at least one day. Such events longer than 15 days can be classified as highly unusual and should not happen more often than once in approximately fifty years. At this level of flow reduction, even by 0.3 to 1.2 cfs may have dramatic adverse effects on aquatic fauna as a function of the frequency with which such events occur (e.g., <1.5 cfs with durations of 5-10 days are of catastrophic magnitude). The common low habitat conditions for brook trout begin at approximately 7.5 cfs, with a recurrence interval of 1.5 years. The corresponding common low habitat conditions for fallfish and tessellated darter are 7.3 cfs and 6.3 cfs, respectively with 1.5 year recurrence frequencies. It should be noted that available habitat fluctuates naturally, but that fluctuations between critical and common levels for up to 40 days are of short duration.

Table 5.5. Threshold levels selected as rare, critical and common for all four species.

	Brown trout	Brook trout	Tesselated darter	Fallfish
Common habitat (WUA)	35%	35%	45%	35%
Common flow (cfs)	7	7.5	6.3	7.3
Maximum common duration (days)	42	40	40	40
Critical habitat (WUA)	20%	15%	15%	15%
Critical flow (cfs)	2.6	2	1.8	2.5
Maximum critical duration (days)	17	15	17	15
Rare habitat (WUA)	15%	12%	10%	10%
Rare flow at (cfs)	2.1	1.3	1.1	1.4
Maximum duration of minimum (days)	17	10	5	5

Considering that the recent events dramatically damaged the fauna in Fenton River, the success of mitigation and recovery efforts will be dictated by management of flow levels critical to modeling sub-reach 2. As visible at the comparisons with other rating curves, modeling sub-reach 2 requires higher flows to obtain the habitat levels prescribed by the thresholds. Therefore we recommend flow thresholds developed from the rating curves from the modeling sub-reach 2 (table 5.6.) The last column depicts the conservative values selected for management recommendations. We took the highest of necessary flow levels computed for native fauna and the corresponding allowable duration. Our recommendation is that if any of the prescribed flow levels in modeling sub-reach 2 will not be reached for the allowable period of time, the pumping will be suspended until flows rebound.

Table 5.6. Threshold levels selected as rare, critical and common for all four species and selected community levels with corresponding flows for modeling sub-reach 2.

	Brown trout	Brook trout	Tessellated darter	Fallfish	Community
Common habitat (WUA)	35%	35%	45%	35%	
Common flow at reach 2(cfs)	12	11	8.5	11	11
Maximum common duration (days)	42	40	40	40	40
Critical habitat (WUA)	20%	15%	15%	15%	
Critical flow at reach 2 (cfs)	7	6	3.5	6	6
Maximum critical duration (days)	17	15	17	15	15
Rare habitat (WUA)	15%	12%	10%	10%	
Rare flow at reach 2 (cfs)	1	5	2.5	4	5
Maximum duration of minimum (days)	17	10	5	5	5

To investigate developed criteria we simulated the implementation of these rules by applying them to the September 2005 time series. As depicted in Figure 5.15, application of the recommendations during the critical drought conditions of 2005 would have avoided reductions in habitat values below the established thresholds or for longer durations than would have occurred naturally.

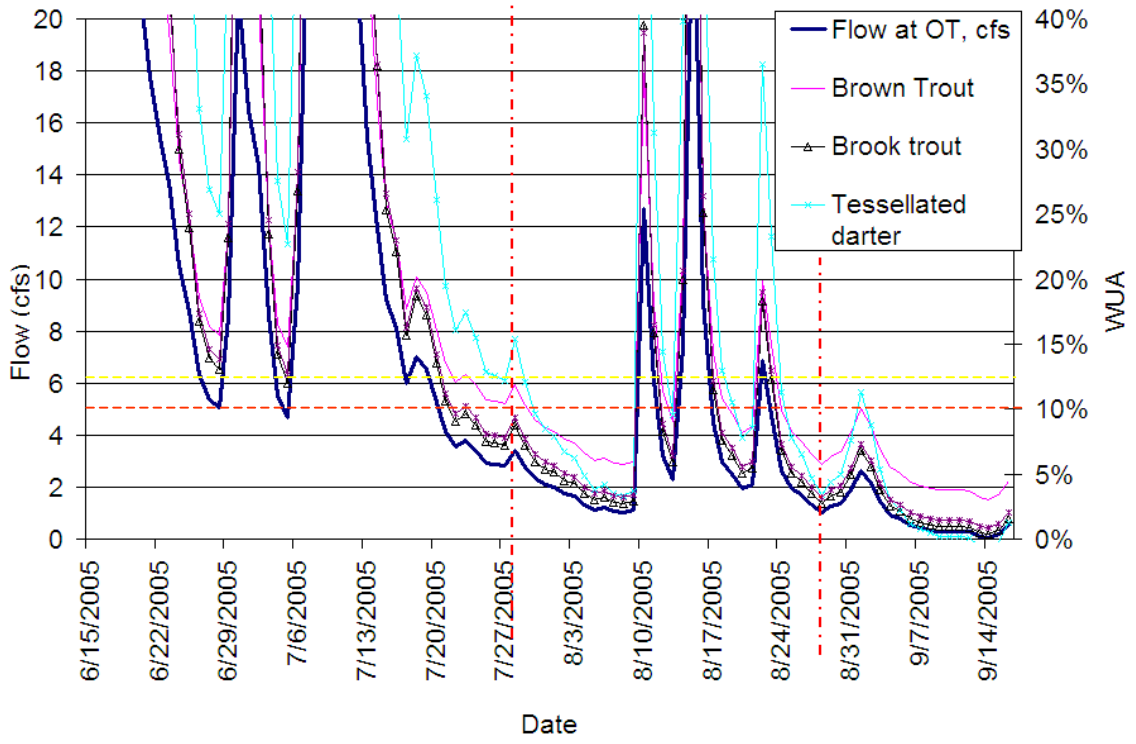

Figure 5.15. Simulated habitat time series with application of developed rules (OT- Old Turnpike Road). The horizontal dashed lines indicate critical (yellow) and rare (red) habitat for brook trout. The vertical dashed lines indicate the day when pumping should be ceased (5 days after approaching the threshold) until the next threshold exceedence for at least two days.

5.5 Conclusions of Fisheries Habitat Analysis

The key conclusion is that during low flow conditions with approximately 5 years recurrence interval pumping that reduces flow in the river by 0.8 cfs or more in the vicinity of well A would impact fish fauna. This impact is exacerbated if the fish population is already under stress by repeated or extended low flows or other factors. As mentioned above, from our observations we conclude that anthropogenic forces, including water withdrawal, may adversely impact the fish population of the Fenton River. This conclusion is reinforced by observations during the drought conditions of late summer 2005. Therefore, maintenance of targeted recurrence intervals and continuous durations of low flows is particularly important. This can be accomplished by developing a pump operation scheme that reduces pumping from the well field when discharge falls below 6 cfs over 15 consecutive days, and discontinuing pumping when flows fall under 5 cfs at Old Turnpike over 5 consecutive days. Alternately, a more complex withdrawal strategy linked to duration of low flow event (i.e. the longer and more frequent the low flow the less water can be pumped or from different pumps) could be instituted. The design and implementation of such a strategy would require continuous monitoring of aquatic fauna and habitat, faunal response, and adaptive management based on the criteria presented in Table 5.6. Because of uncertainty of the status of fish population and its response, continuous monitoring and validation should complement the development strategy.

6.0 HYDROLOGIC ASSESSMENT

Surface water investigations were conducted primarily during the summer months of 2003, 2004 and 2005, and included rainfall collection, stream discharge measurements in the Fenton River and selected tributaries, monitoring of shallow water table levels near the river and statistical determination of the frequency of flow and recession curves.

6.1 Stream Temperature Measurements

The temperature of the surface water in the Fenton River was measured at numerous positions along the river from Old Turnpike to below Gurleyville Road. The temperature data were used for two purposes: 1) to assess whether there were areas of concentrated, localized ground water contribution having a different temperature from surface flow in the stream, and 2) to establish the surface temperature base condition for application of the heat pulse flowmeter to assess the induced infiltration as explained in Section 7.1.3.3 of this report. The results showed some longitudinal variation of temperature along the river, but all rapid temperature variations were judged to be due to small tributary flow rather than localized ground water input. The instrumentation, location of temperature loggers and results are shown in Appendix D. The results for the heat pulse analysis for determination of induced infiltration rate is shown in Section 7.1.8.

6.2 Streamflow Measurements 2003-2004

Streamflow measurements were made using a number of different methods depending on the site and amount of flow in the Fenton River. A water level logger was installed in a housing at the Old Turnpike bridge and operated throughout the project. The stage data were coupled with discharges measurements to develop rating curves for different flow conditions and periods of time. The rating curve varied from one period to another due to changes in rearrangement of boulders in the river which modified the control immediately downstream of the Old Turnpike bridge.

We determined, with the concurrence of the Technical Advisory Group that flows less than five cubic feet per second (cfs) were required in the Fenton River to make meaningful measurements of induced infiltration in the Fenton River near the well field. The summer of 2003 was dominated by higher than normal flows, with no extensive periods of flow less than five cfs during the August-September period when flows are climatologically at their lowest.

We used an acoustic-doppler current profiler (ADCP) to measure flows for intermediate flows between 5 and 30 cfs that were quite common during the summer of 2004 at Old Turnpike Road and various other sites along the Fenton, including sites immediately upstream and downstream of the well field. Appendix B provides further details of the ADCP and other equipment used, stream locations and some sample data obtained with this technique. Our objective was to use repeated observations to reduce

measurement error, allowing discrimination of the effect of well field pumping on induced infiltration. However, the 2004 results for well pumping obtained with the ADCP were inconclusive due to the natural variation of flow and high flows during that season. The use of the ADCP was very helpful in determining a better rating curve for the Fenton River at Old Turnpike Road over an intermediate range of flows.

During the summer of 2004, we built two weirs on the Fenton River, upstream and downstream of Well A (Figure 6.1), as a direct measurement of difference in flow at those locations. However, decaying tropical storms at seven to 10 day intervals brought regular rains that increased the Fenton River flows, and destroyed our constructed weirs. Figures 6.2 and 6.3 show the weirs located upstream and downstream of Well A the first week of September, 2004, before they were destroyed by high flows. The Fenton River experienced only one two-day period of flow less than five cfs when both of weirs were in place as shown in Figure 6.4.

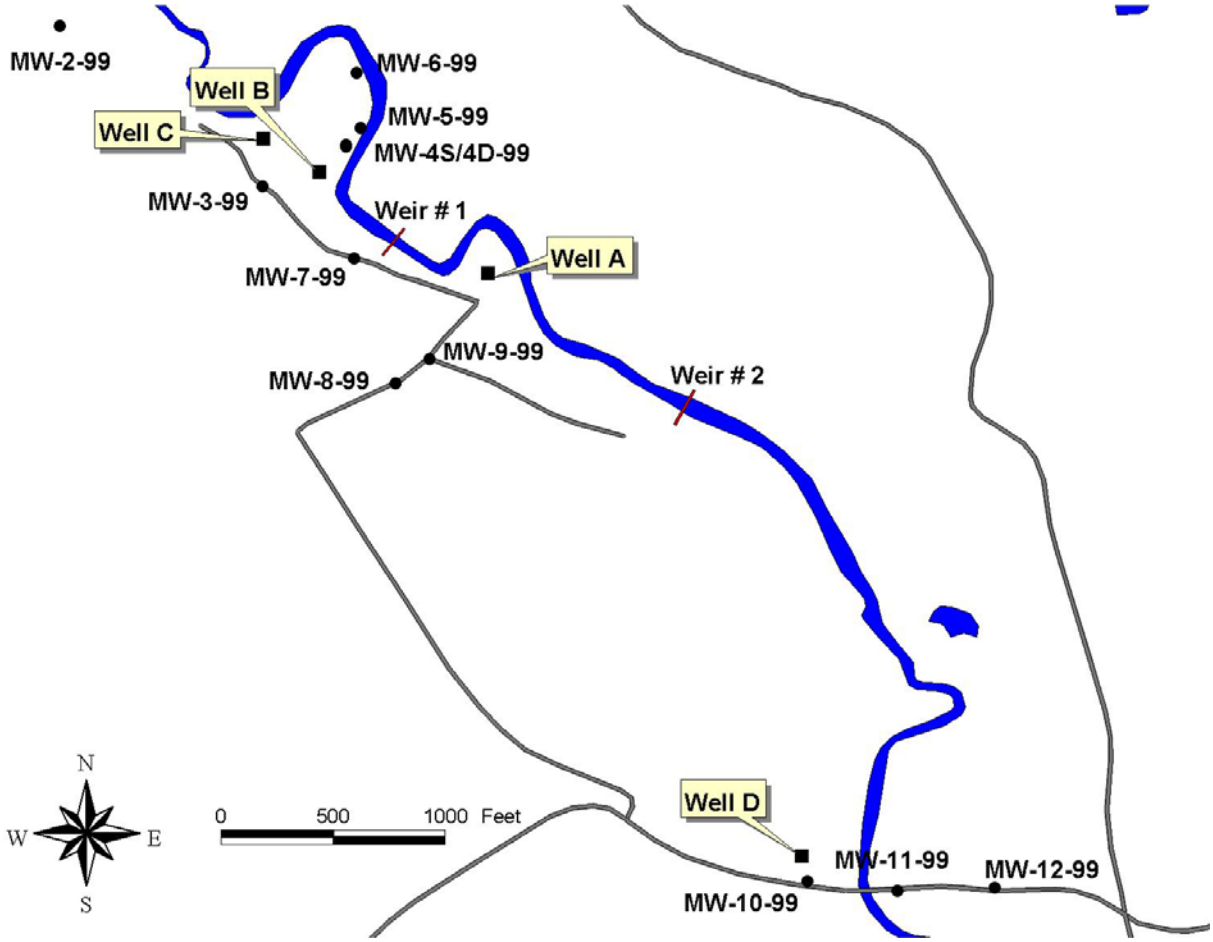

Figure 6.1 Map of Weir locations on Fenton River, Summer 2004

Figure 6.2. Weir No. 1 across Fenton River, Upstream Well A, September 3, 2004.

Figure 6.3. Weir No. 2 across Fenton River, Downstream Well A, September 7, 2004.

Figure 6.4 provides the observed hydrograph on the Mount Hope River at the USGS gage for the period of late August to early September, 2004. The historical median flow for each day is shown as well as the 5 cfs threshold needed for the low flow study. Figure 6.5 provides the measured flow at each weir, the difference in flow loss from the upstream and downstream weirs, and the heavy rainfall (blue line) that began on September 8, 2004. The time during which Well A was being pumped is also shown.

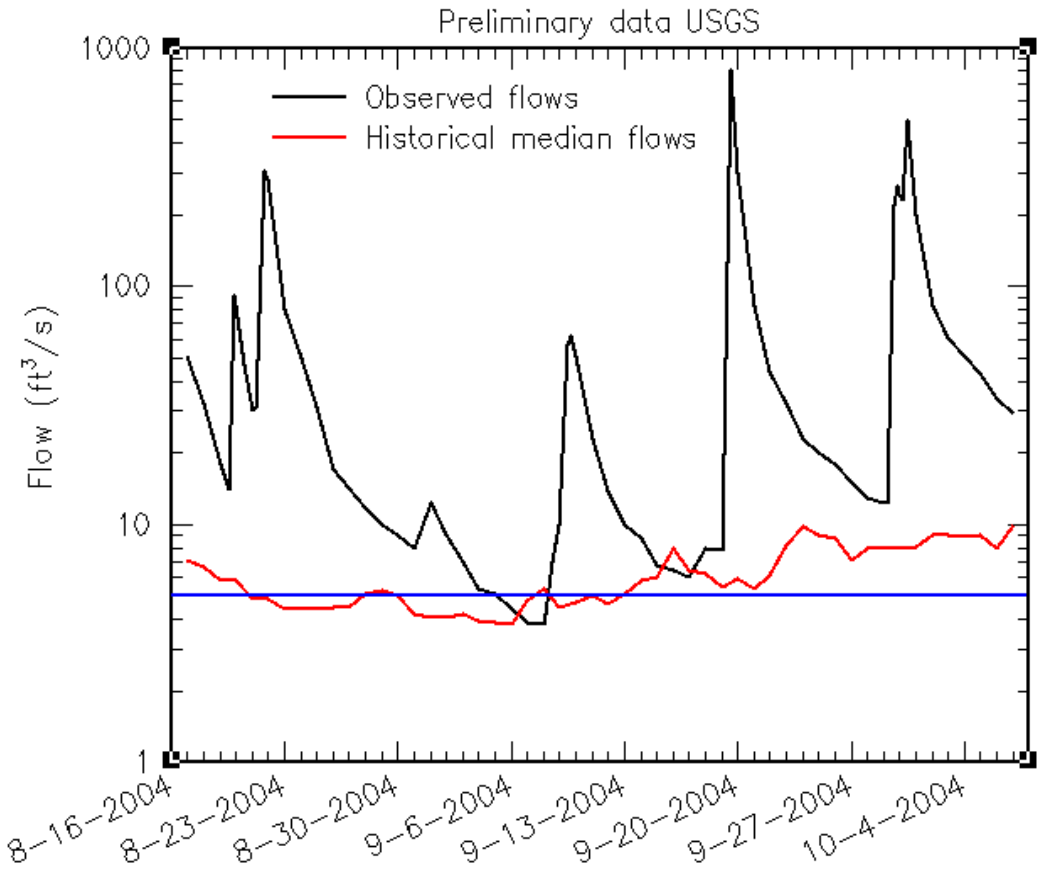

Figure 6.4 Observed flows (black line) in the Mount Hope River, August 16 – October 8, 2004, plotted together with historical median flows (red line) for those same dates. The blue line is at five cfs for reference. Note the absence of low flows less than five cfs during this period, except for a brief four day period beginning September 5.

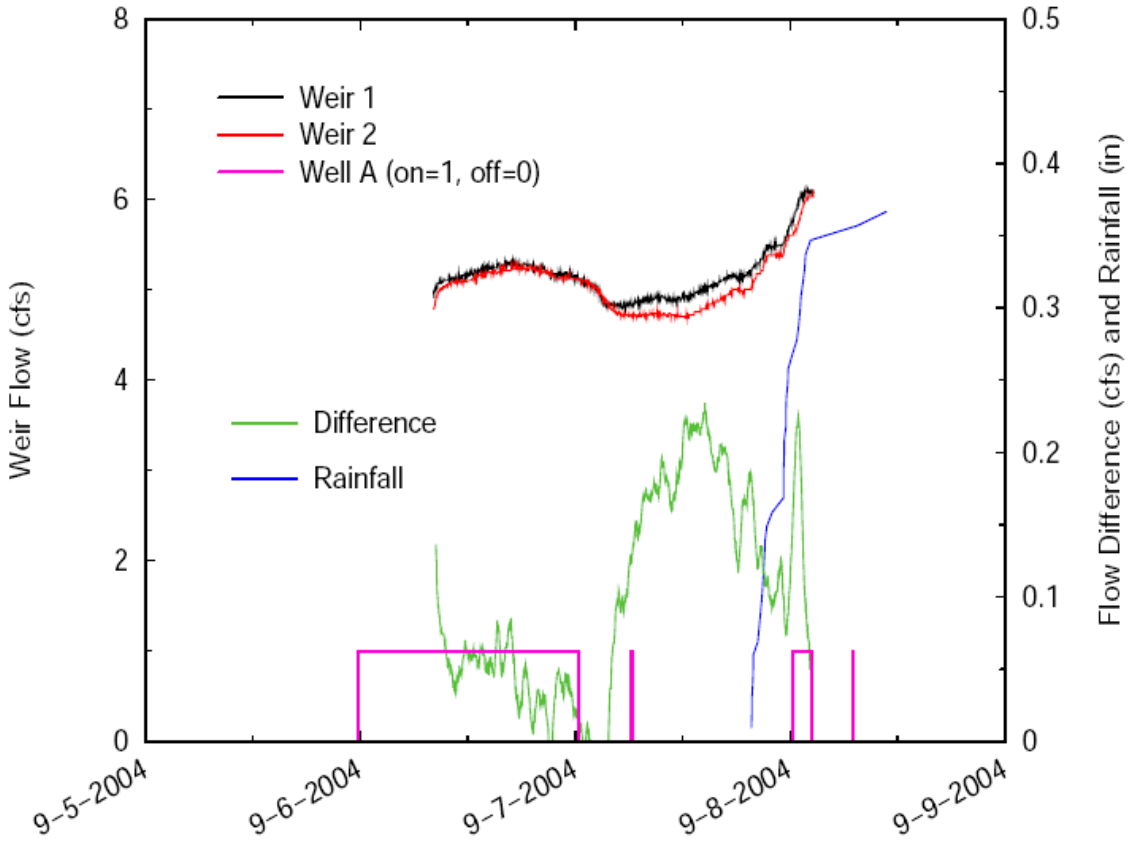

Figure 6.5. Flows in the Fenton River at weir 1 (upstream) and 2 (downstream), September 5-9, 2004. Rainfall (blue line) began on Sep. 8, 2004. The difference between the upstream and downstream weir flows is shown by the green line, and uses the right-hand scale. The time of pumping of Well A is shown by the purple line at the bottom of figure.

6.3 Hydrologic Observations During August-September, 2005

Observations from the summer of 2005 significantly reduced the uncertainty in our analysis of streambed infiltration. The following sections use data to explain why the Fenton River went dry during the period 5-16 September, 2005. The explanation we propose is based on analysis of rainfall, streamflow, pumping, and groundwater level data, all of which provide key indications of factors that lead to the drying of the river over an approximately 600 m reach from upstream of well B to downstream of well A. These observations are particularly relevant to the objectives of this study. Figure 1.2 shows the locations of the UConn groundwater wells A, B, C, and D, and the monitoring wells used to observe groundwater levels. The monitoring wells are denoted with "UC" or "MW".

Rainfall data were obtained from the UConn Agronomy Farm and from a recording rain gage operated by the investigators at the Fenton River well field, as well as from historical data from the National Climatic Data Center, and climatologic analysis by

Miller et al. (2003). Streamflow measurements during the very low flow period in August and September, 2005, were made using a Marsh-McBirney electromagnetic flow meter mounted on a top-setting wading rod. Groundwater levels were recorded using water level loggers manufactured by In-Situ, Inc.

The drawdown of groundwater due to wells near streams can cause the groundwater table in the vicinity of the stream to fall below the stream water surface and in some locations, the stream bed. In these cases, water will infiltrate from the stream bed into the groundwater system. This is called "induced infiltration" due to the pumping of groundwater.

6.3.1 Rainfall, Summer 2005

The summer of 2005 represented some of the driest months of July and August on record in much of eastern Connecticut. The USGS "Drought Watch" (http://water.usgs.gov) showed all of eastern Connecticut as "severe hydrologic drought" in early September, 2005. Precipitation at the UConn Agronomy farm for July and August, 2005 was 2.82 and 0.71 inches, respectively. However, at the a rain gage operated by the investigators near Well A (see Figure 1.2), rainfall for those two months was recorded as 0.03 and 0.01 inches during July and August, respectively. Figure 6.6 shows a plot of cumulative rainfall recorded at the Well A rain gage from Sept. 2004-Sept. 2005.

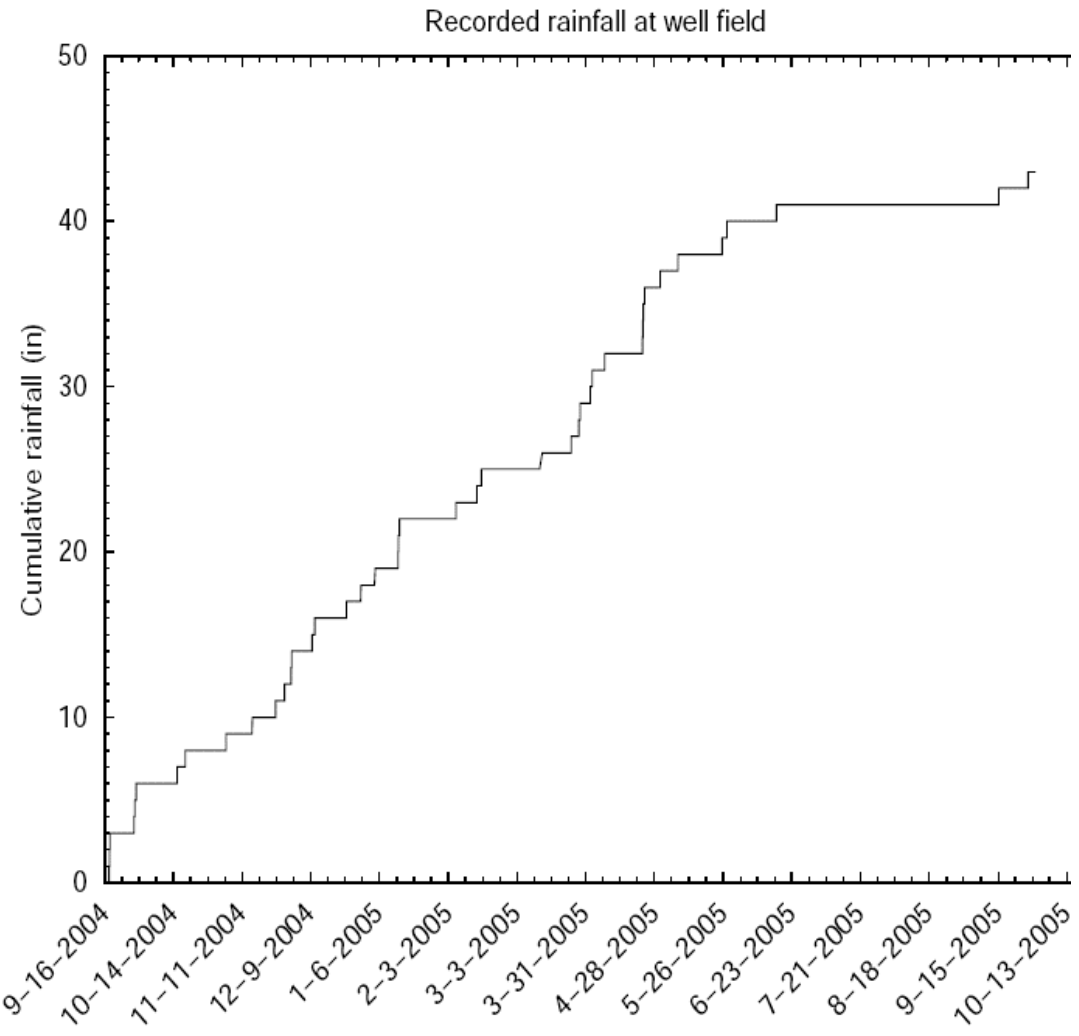

Figure 6.6. Cumulative Rainfall (inches) Near Well A, 16 September, 2004- 22 September, 2005.

As the rainfall data in Figure 6.6 show, virtually no rain fell at the well field during July and August, 2005. How do these observed monthly rainfall totals compare against historical values? Figure 6.7. compares monthly rainfall from April-September 2005 in a historical context to rainfall at Storrs, Connecticut, between 1889 and 2002 over the same months (NOAA, 2005), and 1966, when Rahn (1968) observed the drying of the Fenton River.

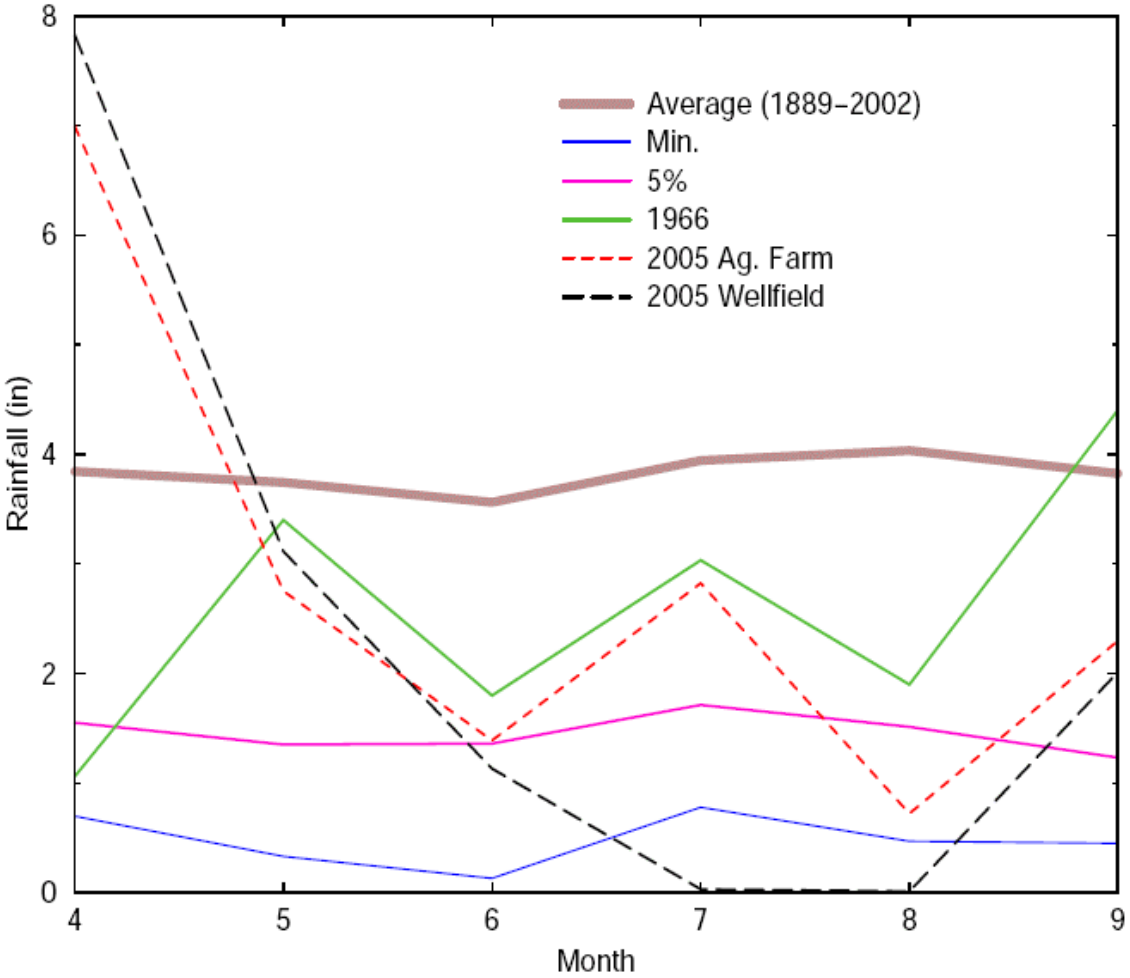

Figure 6.7. Comparison of Summer 2005 Rainfall vs. Climatological Values and 1966 Rainfall.

As Figure 6.7 shows, the recorded rainfall at the Well A rain gage are considerably below the minimum monthly rainfall observed between 1889-2002 (NOAA, 2005) for both July and August, 2005. The recorded rainfall at the Agronomy Farm differs from the Well A data due to the spatial variability of summertime convective rainfall.

6.3.2 Groundwater Levels, Summer 2005

Rahn (1971) hypothesized that the groundwater table falls below the bed of the Fenton River in the vicinity of well B, which was pumped in 1966 at a rate of approximately 1,000,000 gallons per day, which is in excess of the currently permitted 844,000 gallons per day rate. We designed an experiment during the summer of 2005 to test this hypothesis during times of low flow.

With reference to Figure 1.2, groundwater level recorders were placed in each of the monitoring wells near the river. The elevation of the top of each monitoring well was surveyed, as was the elevation of the river bed nearest to the well. Figure 6.8 shows a

summary of observed groundwater table elevations at three of the monitoring wells near pumping wells, relative to the nearby river bed elevation..

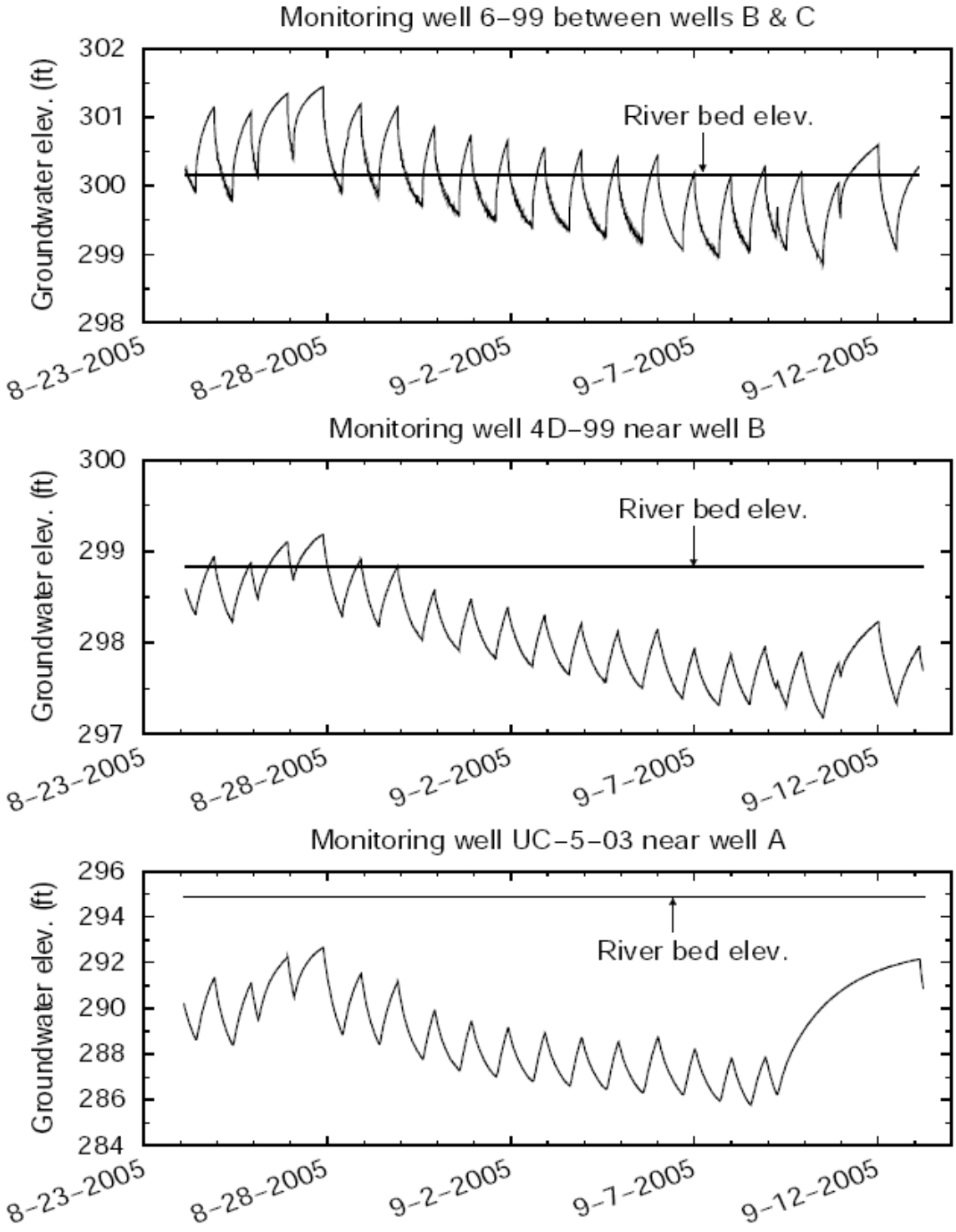

Figure 6.8. Groundwater Levels Near Fenton River During Summer of 2005. Note, Fenton River was dry between wells B and A from September 5-16..

The wells shown in Figure 6.8 were selected because of their proximity to the river and the portion of the Fenton River that went dry. These wells are MW-6-99 (between wells B and C), MW-4D-99 (near well B), and UC-5-03 (near well A).

The data shown in Figure 6.8 indicate that Rahn's hypothesis is true, and that the vertical distance from the river bed to the groundwater table varies in both space (with distance from the well) and time (according to pumping schedules). Between wells B and C, the groundwater table varied from 1 ft above the river bed to 1.2 ft below. Near well B, the groundwater table was as much as 1.7 ft below the river bed on Sept. 10, 2005. Near well A, the groundwater table was routinely 5 to 8 ft. below the river bed. Analysis of data from September through November, 2004, which was a considerably wetter period, also revealed that the groundwater table near well A can be up to 7 ft. below the river bed even when the river is flowing. Notice on the bottom graph in Figure 6.16, that pumping was stopped at Well A from 9 Sept. through 13 Sept., and the groundwater level rose from nearly nine feet below the river bed to about 3 ft of the river bed, over this five day period. During this time, the river was dry near well A. This rise in groundwater table is due solely to "infilling" of the cone of depression in the groundwater table around well A by groundwater from the aquifer. Notice also that this infilling process occurs over a short period of time, indicating a relatively short system memory, on the order of days, not weeks.

6.3.3 Streamflow, Summer 2005

During the very low flow period in August and September, 2005, flow measurements at various locations were made using a Marsh-McBirney electromagnetic flow meter mounted on a top-setting wading rod. The depths in the river were typically too shallow for use of the ADCP during this period. Streamflow measurements at five locations reveal changes in discharge along the longitudinal profile of the Fenton river on different dates. Figure 6.9 shows longitudinal profiles of flow in the Fenton river from data collected on August 8, August 11, August 26, and September 8, 2005. The data in Figure 6.9 show that there is a general, consistent loss of water during low flow periods between the head of the meadow and Well A during the summer of 2005. Downstream from well A, the river consistently gains flow. The loss of flow in the Fenton River between the head of the meadow and the vicinity of Well A varied from 0.38 to 0.89 cfs (244,000 to 570,000 gpd), with an average of 0.62 cfs (400,000 gpd). This loss cannot be solely attributed to pumping because of other exchanges between the aquifer and stream, as evidenced by the gain in flow between Old Turnpike Road and the head of the meadow seen on August 26.

During periods of low flow with no recharge, the data suggest that the river bed conductance integrated over the entire river from Old Turnpike Road to near well A is approximately 0.6 cfs (400,000 gpd), which is 47% of the 1.31 cfs (844,000 gpd) pumped from the well field daily. If the flow in the Fenton River reaches or falls below approximately 1.0 cfs, the river may go dry near wells A and B, where the cone of depression is below the river bed and induced infiltration is maximum, if pumping persists. Note with reference to Figure 6.9, that on September 8 with the flow at Old Turnpike Road of 0.39 cfs, the Fenton River was dry near well A.

The reason that 100% of the well withdrawals do not come from the river is due to several aspects of the coupled groundwater/surface water system. First, there is an impeding layer in the stream bed that reduces the flow of water from the river to the groundwater table. Second, there is likely some flow from deep bedrock fractures upward into the stratified drift aquifer. Third, there is a considerable amount of storage in the stratified drift aquifer itself. Finally, there is some down-slope flow from upland till areas, even in times of drought, that partially replenishes the groundwater in the stratified drift aquifer.

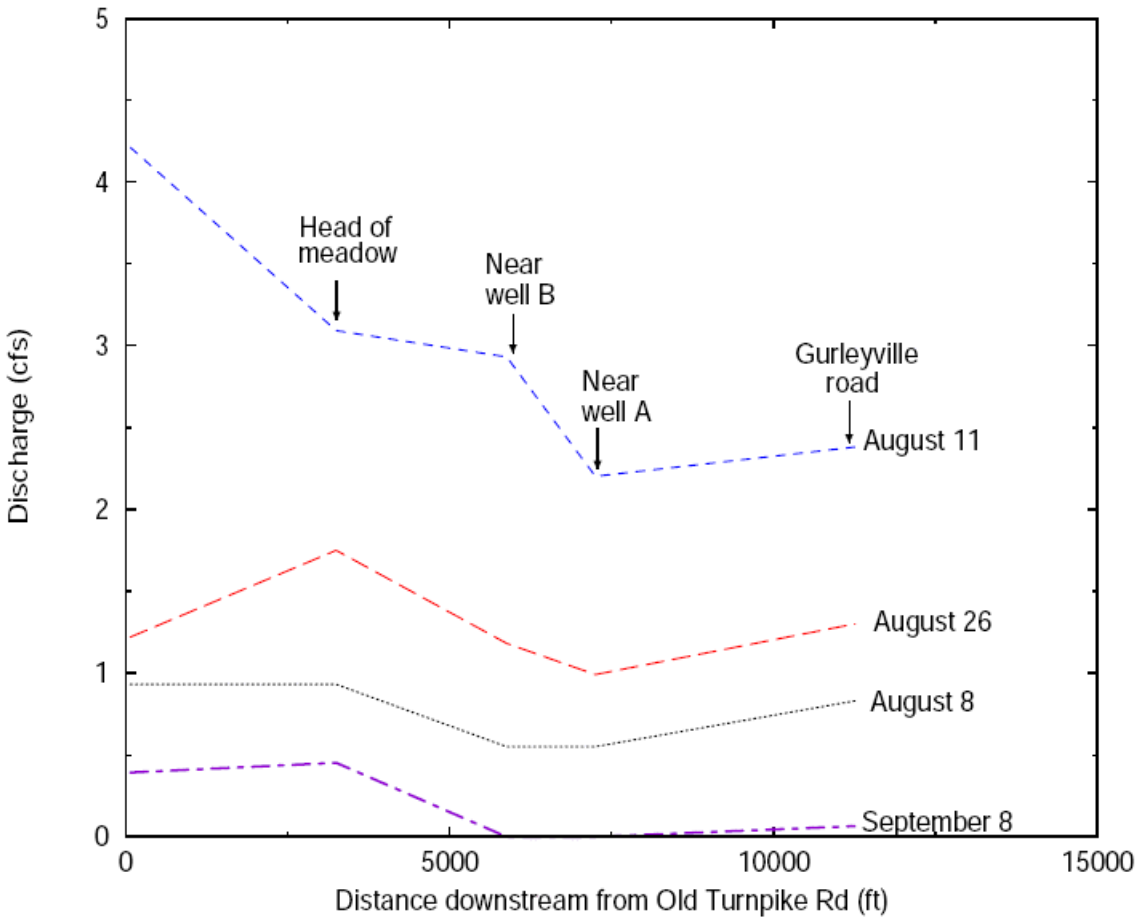

Figure 6.9 Longitudinal Profiles of Discharge in the Fenton River on Different Dates during the late Summer of 2005.

The Fenton River did not become dry in the vicinity of wells C or D (see Figure 1.2). Well C is near the meadow, which contains a significant amount of stratified drift. Furthermore, the channel upstream of well C is quite deep, and the channel bed is likely finer in texture due to lower velocities in that region. The cone of depression in the groundwater near Well C most likely contributed to induced infiltration, but not in a significant enough manner to cause the river to go dry near well C.

Well D was used relatively infrequently during the summer of 2005. It is thought that this well has a partially-plugged screen, and it is used as a backup to primary production wells A, B, and C. When activated, well D does not pump continuously. Rather, it cycles on and off automatically due to the frequent occurrence of low water within the casing caused by the partially plugged well screen.

During the period from 5-16 September, flow in the Fenton River re-emerged approximately 200 m downstream from well A. The point of re-emergence remained relatively constant during the entire period when the river upstream was dry. This is likely due to the limited radius of influence of well A, and the slope of the valley (from well A towards well D), both of which will combine to reduce the downstream extent of the influence of well A. Furthermore, as the data in Figure 6.9 show, there is a natural tendency of the Fenton River downstream from well A to be a gaining stream, even in times of drought. In addition to ground water inflow, there were small lateral inflows from both Fisher's and Robert's Brooks which enter between the flow re-emergent point and Gurleyville Road.

Streamflow became re-established in the Fenton River near well A at approximately 1:30 a.m. on Friday, 16 September. A thunderstorm dropped about 2 inches of rainfall in the upper Fenton River watershed early on Thursday, 15 September. The subsequent runoff reached the well field sometime before 11:00 p.m. on 15 September. Observations of the advancing flow across the dry stream bed near well A in the early morning hours of 16 September revealed that the flow advanced as surface water, not groundwater. That is to say, the surface water advanced across the stream bed and over obstacles, rather than seeping into the stream bed and emerging beneath obstacles. This provides additional strong observational evidence of existence of an impeding layer in the stream bed that limits induced infiltration.

6.3.4 Conclusions- Direct Observations of Induced Infiltration

From the observations taken during 5-16 September, 2005, we draw the following conclusions:

- The Fenton River went dry over an approximately 600 m long reach in the vicinity of Wells A & B during the period 5-16 September, because of the combined effects of drought and pumping of the UConn Fenton River well field. Had there been no drought, or no pumping, the river would not have gone dry
.
- Had there been no pumping, the flow in the Fenton River near well A from September 8-16, 2005, would have likely been less than 1.0 cfs due solely to the effect of drought.

- The average induced stream bed infiltration from the head of the meadow to the vicinity of well A (Fig. 1.6) was approximately 0.6 cfs (388,000 gpd). The pumping rate during this time was 844,000 gpd. during an extended summertime period with no rainfall.

6.4 Determination of Low-Flow Discharge Frequencies for the Fenton River

Two hydrologic assessments were performed for the Fenton River: the first to answer the question "How often do specific discharges (Q) occur on the Fenton River in the study area ?" and the second to answer the question, "How quickly does the flow recede in the river under summer low flow conditions ?". The first question is one of frequency and the second one of persistence of flow.

6.4.1 Using Long Term Records from the Mount Hope River

The frequency or exceedence level of flow in the Fenton is needed to assess the probability of a given discharge occurring. Flow in Connecticut streams is very seasonal so exceedence levels need to be determined for specific periods of the year in order to address the potential impact of pumping at various times of the year. However, a long-term continuous record is needed to perform frequency analysis, usually 30 years or longer. Since a long-term continuous gage does not exist on the Fenton River, flow statistics were determined from the long term United States Geological Survey (USGS) gaging station (#01121000) on the Mount Hope near Warrenville. This gage has continuous records from 1940 and provides a surrogate for the Fenton River. The drainage areas of the two rivers are similar (Mount Hope = 28.6 mi^2 , while the Fenton at Old Turnpike = 19.6 mi^2 and Fenton at Gurleyville = 23.0 mi^2), as are the land uses and geology. The rainfall and evapotranspiration (ET) are assumed to be similar over the long term. Short term differences in rainfall due to local storms can be checked using existing rain gages that were installed in each watershed. A synthetic flow duration curve and hydrograph were developed for the Fenton River based on the Mount Hope data as illustrated below. Statistics are first developed for the Mount Hope and transferred through correlation to the Fenton. This approach does not assume that the flows are equal or even equal on a per area basis for the two rivers. Instead, the assumption is made that the flows on the two rivers are occurring at the same exceedence level due to the proximity of the basins and similarity in climate and land use.

6.4.1.1 Development of Flow Statistics on Mount Hope River

The large seasonal variation of flow in the Mount Hope River is shown in Fig. 6.10 in the form of boxplots by weekly intervals. The flow is lowest in August and September, as is the typical variation (shown by the height of the box). Extremes (or outliers) are not shown so the extreme floods, such as the '55 hurricane, that occasionally occur in late summer/early fall are not shown.

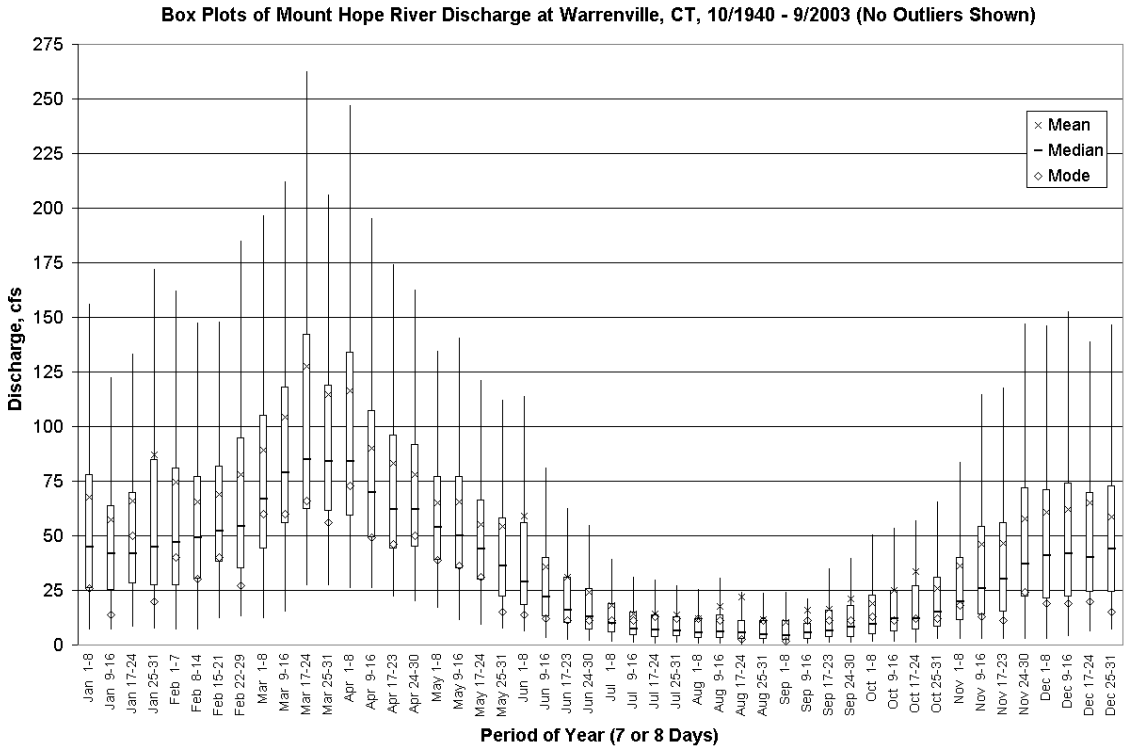

Figure 6.10. Weekly Breakdown of Discharge at Mount Hope River, Warrenville, CT

6.4.1.2 Construction of Flow Duration Curves (FDC)

Another way of showing the variation of flow is a Flow Duration Curve (FDC) in which the discharge (usually average daily) in cubic feet per second (cfs) is plotted against the exceedence probability, i.e. the percent of time that a particular discharge is equaled or exceeded. The usual way to construct an FDC is to use all of the daily flows over the entire period of record. This is referred to as the "annual" FDC. However, the analysis of the Mount Hope data on a seasonal basis shows that there are large differences (Figure 6.11). For example, the discharge for the 99% exceedence is 0.7 cfs when using the July-to-September period and about 1.2 cfs for the annual-based period. In other words, the discharge is less than or equal to 1.2 cfs only 1 % of the time when all days from Oct. 1940 to Sep. 2003 are used, but 0.7 cfs when only the days in July through September of those years are used. Shortening the period used will highlight when the driest and wettest flows occur as shown in Figure 6.12 for biweekly periods for the Mount Hope River. Caution is advised in using values beyond about the 99 to 99.5 % exceedence level due to the 60 year record which may not have captured the most extreme drought events.

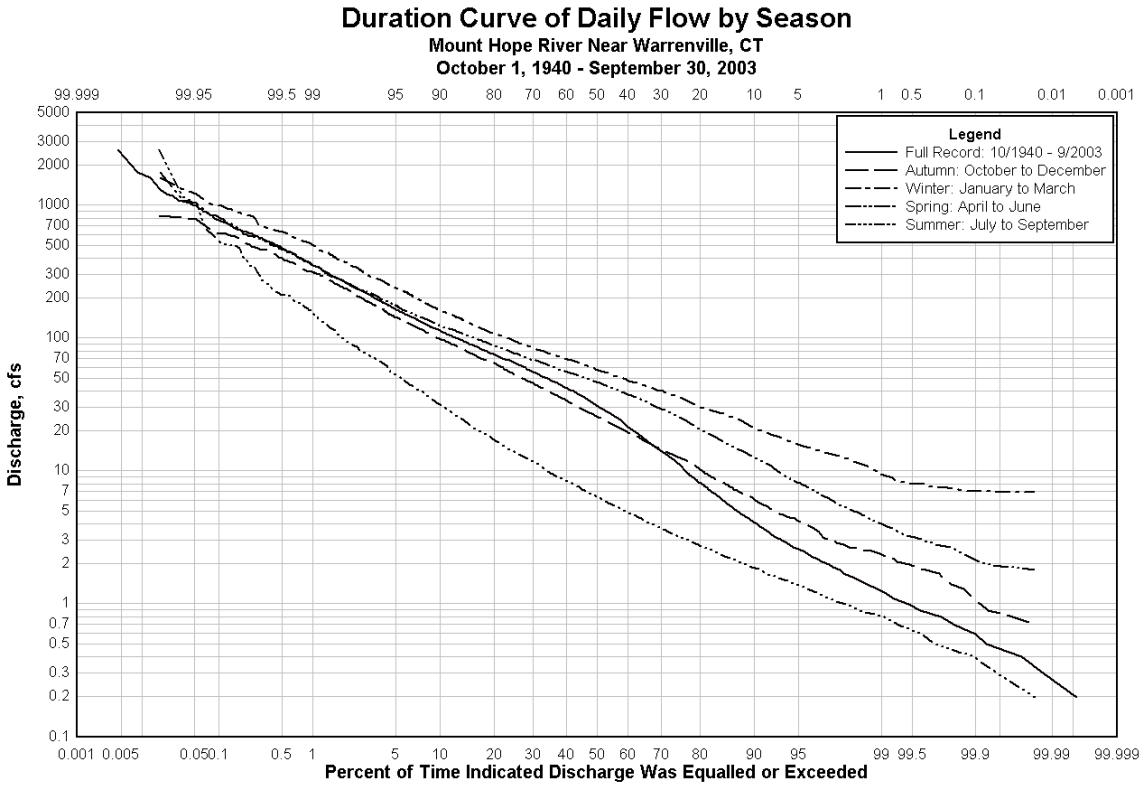

Figure 6.11. Monthly Flow Duration Curves by Daily Data for Mount Hope River

One problem with traditional FDC approaches is that the daily flows are not independent, but are serially correlated. For example, the flow on August 15 is highly dependent on the flow on August 14. It is risky therefore to assign a probability of occurrence of flow based on the traditional FDC. The serial correlation can be avoided by treating flow on a given day as independent of the flow on that day for other years. A new FDC can be constructed from the means or medians of that day of the year, thereby providing a probability basis for the occurrence of flow on that day. Confidence intervals can also be assigned as the estimate of the mean or median flow using this approach. Figure 6.13 illustrates the variation in expected flow levels on the Mount Hope for the June 30 to October 31 period of the year. Polynomials are fitted through the highly variable daily flows as a smoothing function for each exceedence level. The X values in the equations are the Julian day of the year (Jan. 1 = 1, Dec 31 = 365).

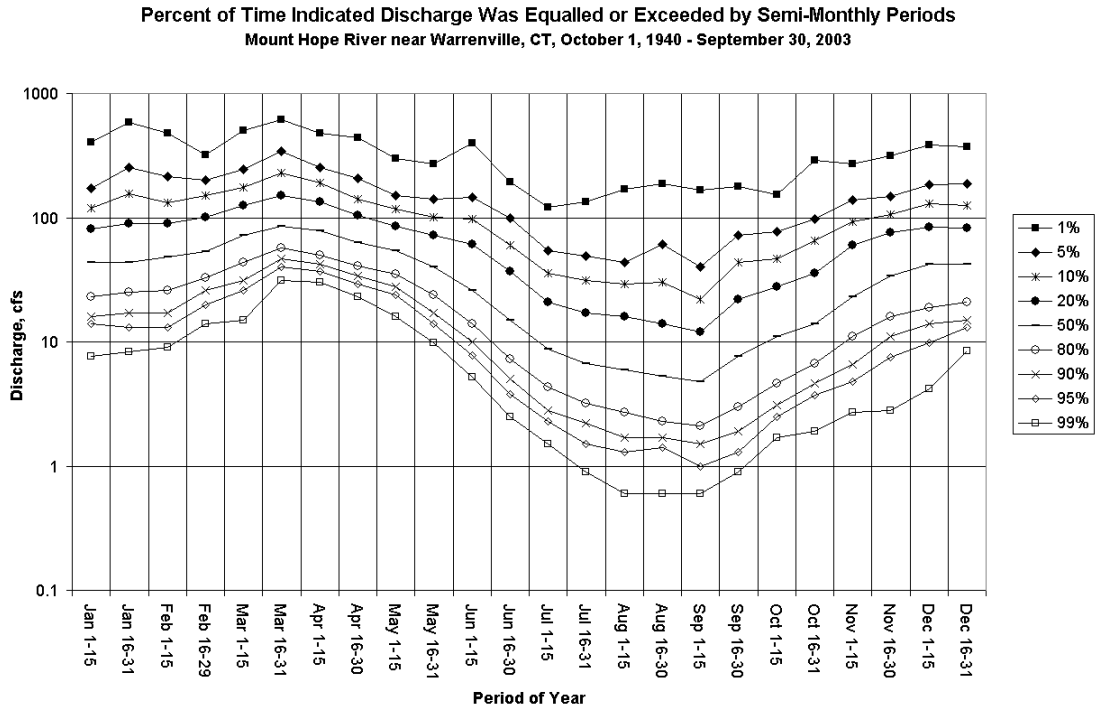

Figure 6.12. Semi-Monthly Percent Duration Graph for Mount Hope River

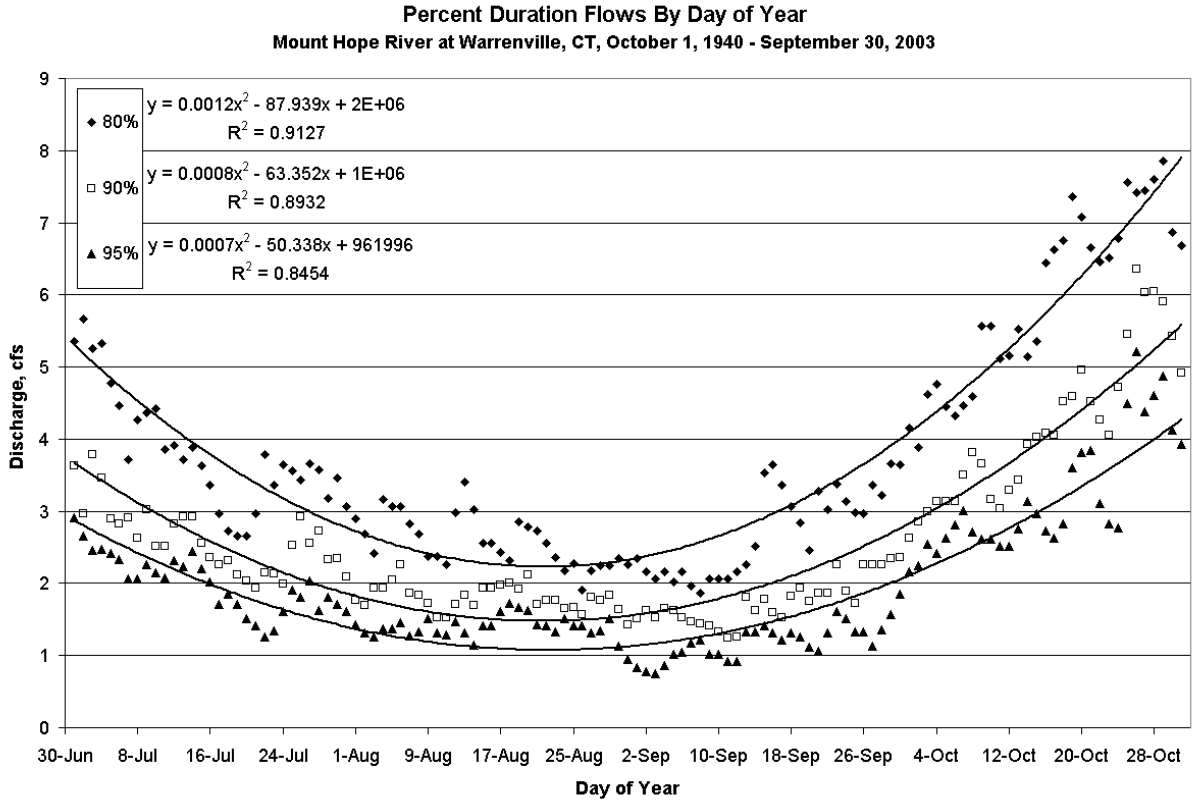

Figure 6.13. Percent Duration Flows By Day of Year with Associated Trendlines

6.4.1.3 Correlation of Fenton Low Flow Discharge to Mount Hope

Searcy (1959) presents methods for estimating a long-term FDC at a site that uses either a short-term, continuous flow record or spot base flow measurements. Both methods use an "index" station, e.g. Mount Hope, to establish the FDC at the short-term station, e.g. the Fenton River. Both stations should be on unregulated streams with no significant changes to the watershed over the period of record used. Additional recommendations (Searcy 1959) for a successful extension are:

1. The two gauging stations should be within 50 miles of each other.
2. The two gauging stations should have the same likelihood of receiving rain. They do not necessarily need to have concurrent rains. Thus, a station in the rain shadow of a mountain could not be used to adjust the record of a station on the other side.
3. A station on the same stream as the short-term station is usually a better index-station than one in another watershed
4. The index station and the short-term station must have enough concurrent records to establish a useable relation.

Where spot base flow measurements are used to develop a correlation, the discharges at both the gauged and ungaged sites should be made well after any significant rain, and each individual measurement should be separated by a rainfall event such that each measurement is independent (Searcy 1959). In the northeastern US, these points would ideally be taken in the late spring to late fall period to avoid the impact of snowmelt on the base flow discharges of the watersheds. Use of a short-term continuous record has the advantage of correlating flows over a larger range which then can used to develop a synthetic hydrograph that includes high flows.

We applied both short-term extension and the spot base flow measurement approaches for developing an FDC for the Fenton from the Mount Hope River records. The short-term record for the Fenton was developed from continuous water level measurements from 2001 to 2003 taken at Old Turnpike Road. The pressure transducer failed for much of 2004 so we were unable to use that year's data. The rating curve for the Fenton at Old Turnpike was developed from periodic stage-discharge measurements. Overall its accuracy is "fair" for lower discharges, but "poor" at higher discharges since few high flow events could be measured during the period. A portion of the lower discharge portion was affected by a rock "dam" constructed downstream of the measurement point by unknown parties.

6.4.1.4 Development of Fenton Synthetic FDC using short-term continuous record

In order to compare gauging station records in a given area with each other, they must represent or be adjusted to concurrent periods. This adjustment is necessary such that differences in the records are due to climatic and watershed characteristics and not because the records are based on different periods. Also, FDCs based on short periods are

insufficient for predicting the future pattern of flow, but they can be made more reliable by extending them to represent a longer period (Searcy 1959).

As described by Searcy (1959), the continuous record from 2001 to 2003 at Old Turnpike was used to develop a short term FDC on the Fenton. A short term FDC for the Mount Hope was developed for the same dates. The relationship between the short-term and long-term FDCs on the Mount Hope was then used to extend the short-term Fenton FDC to a long-term FDC for the Fenton. It is important to note that the calculation of discharge in this manner is only accurate for the range of data covered by the breadth of the trendline. Searcy (1959) notes that 1) the trendline should not be extended to discharges much lower than those measured at the ungaged site unless one has extensive knowledge of the geology of the two drainage basins, and 2) the relation breaks down for higher flows. A comparison of the FDCs created by the extension method is shown in Figure 6.14. The relationship between the two rivers is fairly consistent in the middle part of the curve, but diverges at the upper end as expected.

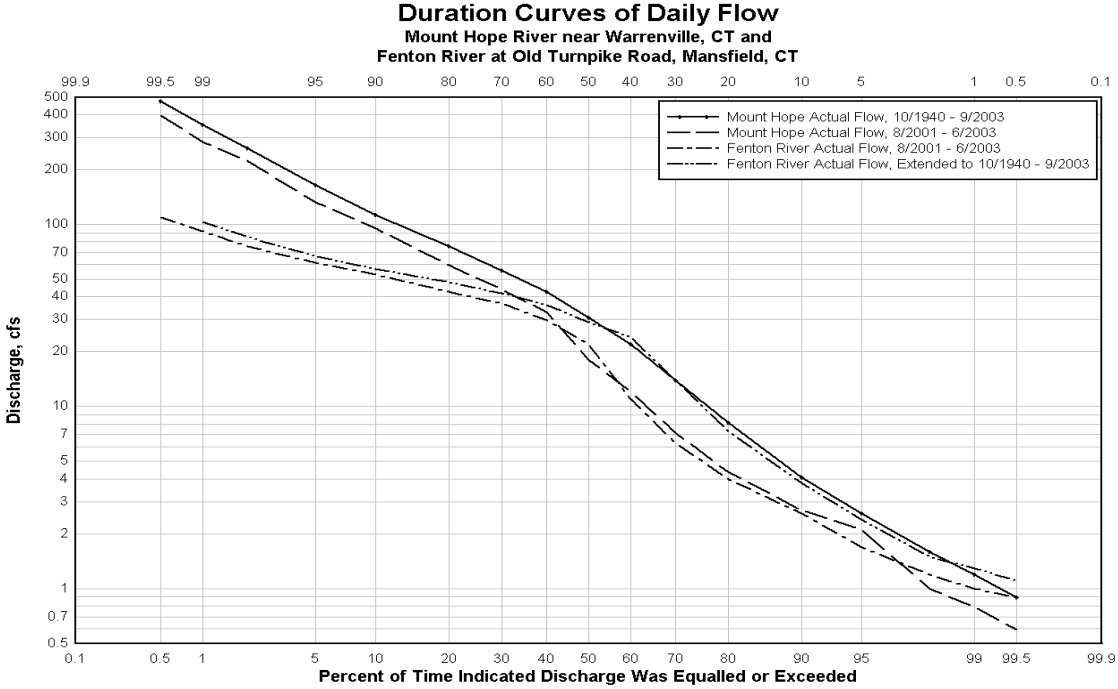

Figure 6.14. Flow Duration Curves of Mean Daily Flow for Mount Hope and Fenton Rivers based on short-term record on Fenton River 8/2001 and 6/2003.

6.4.2 Construction of Synthetic Hydrograph for Fenton River

A logical extension of the synthetic FDC for the Fenton River is development of a synthetic hydrograph. The discharges for the Fenton at 17 selected exceedence levels are shown in Table 6.1. These points were then plotted on logarithmic paper against the corresponding discharges for the Mount Hope (Figure 6.15).

Table 6.1. Discharge of Equal Percent Exceedence on Mt. Hope and Fenton Rivers

Percent Exceedence	Mt. Hope Flow, cfs, 8/2001 to 6/2003	Old Turnpike Flow, cfs, 8/2001 to 6/2003	Mount Hope Flow, cfs, 1940 to 2003	Old Turnpike Flow, cfs, extended to 1941-2003
0.5	445	116	474	**[1]
1	356	103	354	103
2	273	86	263	84
5	159	66	165	67
10	106	55	113	57
20	70	46	76	48
30	50	40	56	42
40	38	33	43	36
50	26	21	31	26
60	14	7.3	22	16
70	7.3	5.0	14	7.3
80	4.5	3.2	8.2	5.3
90	2.8	2.3	4.1	3.0
95	2.3	1.5	2.6	2.0
98	0.94	1.1	1.6	1.3
99	0.72	0.95	1.2	1.2
99.5	0.47	0.87	0.91	1.1

[1]Unable to calculate data point, as it is outside the boundary of correlation.

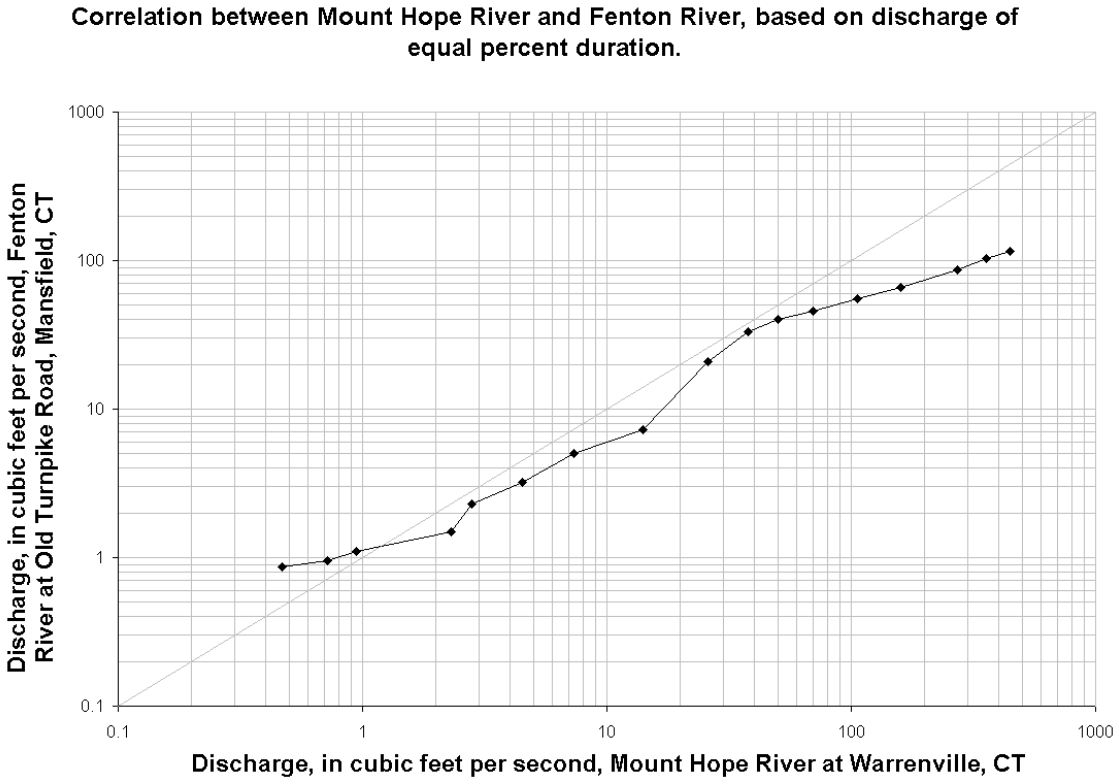

Figure 6.15. Correlation Between Mount Hope and Fenton Rivers, Based on points in Table 6.1.

Values for the synthetic Fenton hydrograph are created from the recorded mean daily flow on the Mount Hope by interpolating between points in Fig. 6.6. The predicted hydrograph is shown along with the observed hydrograph for the Fenton for August, 2001 to June, 2003 in Fig. 6.16.

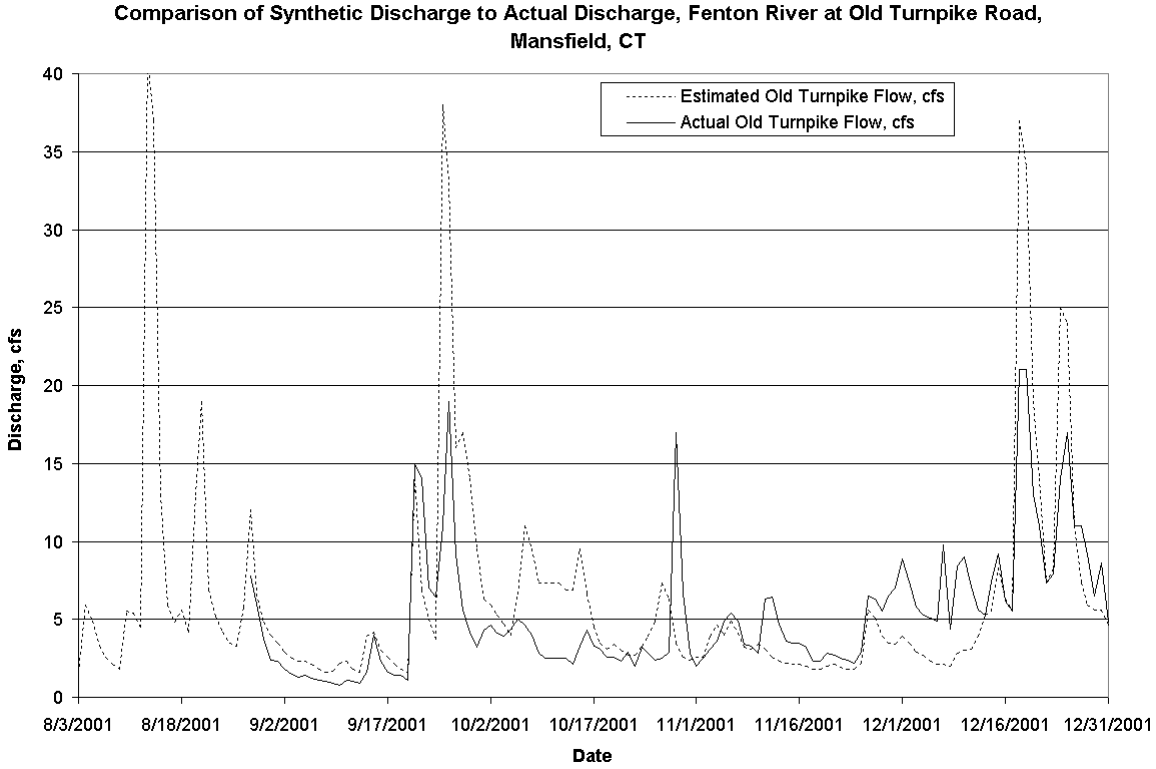

Figure 6.17. Comparison of Synthetic Hydrograph to Actual Hydrograph for Fenton River at Old Turnpike Road, Mansfield, CT

The observed and synthetic hydrographs compare well, especially at the lower discharges. The larger differences at higher flows are thought to be due to the extrapolation of the rating curve for the Fenton River at the high end of the observed flows. The recession parts of the curves, in general, are acceptable for the purposes of this study. The resulting synthetic hydrograph for an extended period can be used to assess the frequencies and durations of potential reductions in flow in the Fenton due to pumping.

6.4.3 Development of Fenton Synthetic FDC using spot base flow method

Since we are interested in the low flow end of the FDC for purposes of impacts of pumping on flow in the Fenton, use of the spot base flow method is appropriate. Flow on the Fenton was correlated to the Mount Hope by selecting pairs of discharge points on the Fenton and Mount Hope. Measurements at Old Turnpike Road on the Fenton taken with the ADCP were used for the primary correlation. A total of 24 measurements were taken during the June through October period in 2004 at Old Turnpike. The ranges of discharges measured were from about 4 to 169 cfs on the Fenton and about 4 to 322 cfs on the Mount Hope. Higher discharges were eliminated from the correlation in order to

relate low flows only. In addition, one apparent outlier (11, 26) was not included in the regression. The results with the remaining 17 points are shown in Fig. 6.8 for all discharges below 30 cfs on the Mount Hope except the outlier. (Interestingly, when the higher flows were included, an $R^2 = 0.97$ was obtained. However, the one very high discharge of 322 cfs on the Mount Hope had tremendous leverage. Therefore the relationship shown in Fig. 6.17 is thought to better represent the low flow relationship.

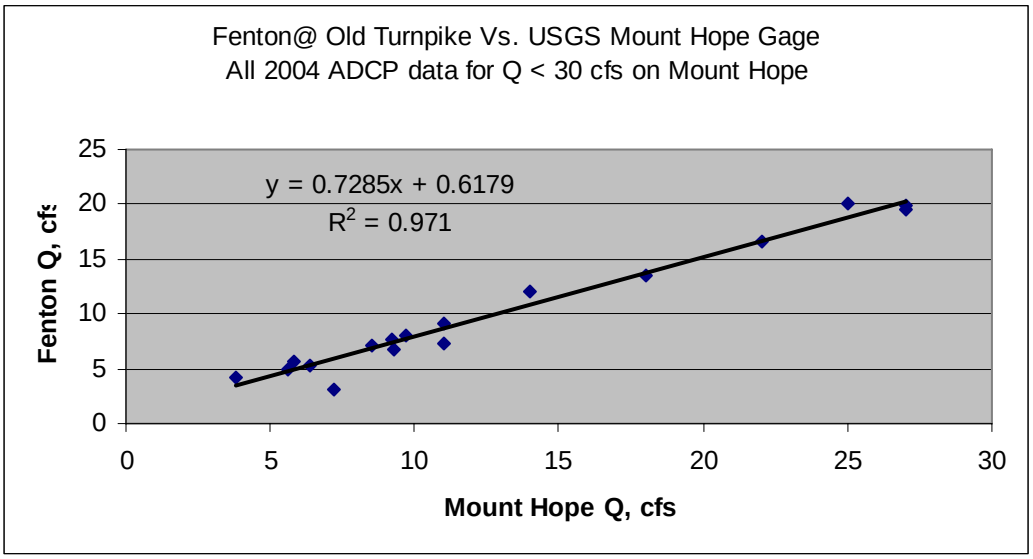

Figure 6.17 Fenton River at Old Turnpike vs. Mount Hope River at Warrenville for low flow measurements by ADCP during Summer 2004.

6.4.4 Comparison of Two Methods

The results of the two methods, extension of short-term continuous record and the spot base flow measurements, are both shown in Table 6.2. The values agree quite well at low flows, e.g. 90% and higher exceedences. High flows cannot be compared since the base flow spot measurement method purposely excludes higher flows. There is a shift in the middle frequencies which is probably due to the fact that the base flow spot measurement approach used the FDC from June to November since that was the period when measurements were taken, while the extended FDC for 1941-2003 shown in Table 6.2 is based on the annual-based FDC.

Caution is advised in application of the correlations given between the Fenton and Mount Hope for any given year or specific time. Differences in recent rainfall amounts in the two watersheds can lead to a much higher flow for short periods of time on one river compared to the other. Greater confidence in application of the correlations exist where rainfall amounts document no major recent rainfall in either watershed.

Table 6.2 Comparison of Two Methods of determining Percent Exceedence Discharge on Fenton River at Old Turnpike

Percent Exceedence %	Based on FDC extended to 1941-2003 from Table 6.1 cfs	Based on Regression in Fig. 6.8 for low flow, cfs
1	103	**NA**
2	84	**NA**
5	67	**NA**
10	57	**NA**
20	48	**NA**
30	42	**16.6**
40	36	**12.3**
50	26	**8.6**
60	16	**7.3**
70	7.3	**5.0**
80	5.3	**3.6**
90	3.0	**2.6**
95	2.0	**2.0**
99	1.2	**1.3**
99.5	1.1	**1.2**

NA = Not Applicable, Out of regression range.

6.4.5 Comparison for Fenton River at Gurleyville

A correlation was also performed between the flow in the Fenton River at Gurleyville, CT and the Mount Hope River. The spot measurements used came from two sources: some USGS miscellaneous measurements taken on the Fenton from 1962 to 1973 and some 2004 measurements with ADCP. Gurleyville Road is near the downstream end of the project and just below Well D, the most-downstream water supply wells. The results are shown in Fig. 6.18 and also exhibit a linear relationship, but with somewhat more scatter. The FDC at Gurleyville is potentially impacted by the pumping wells at low flows which confounds interpretation and use of the relationship with the Mount Hope for development of a synthetic FDC or hydrograph.

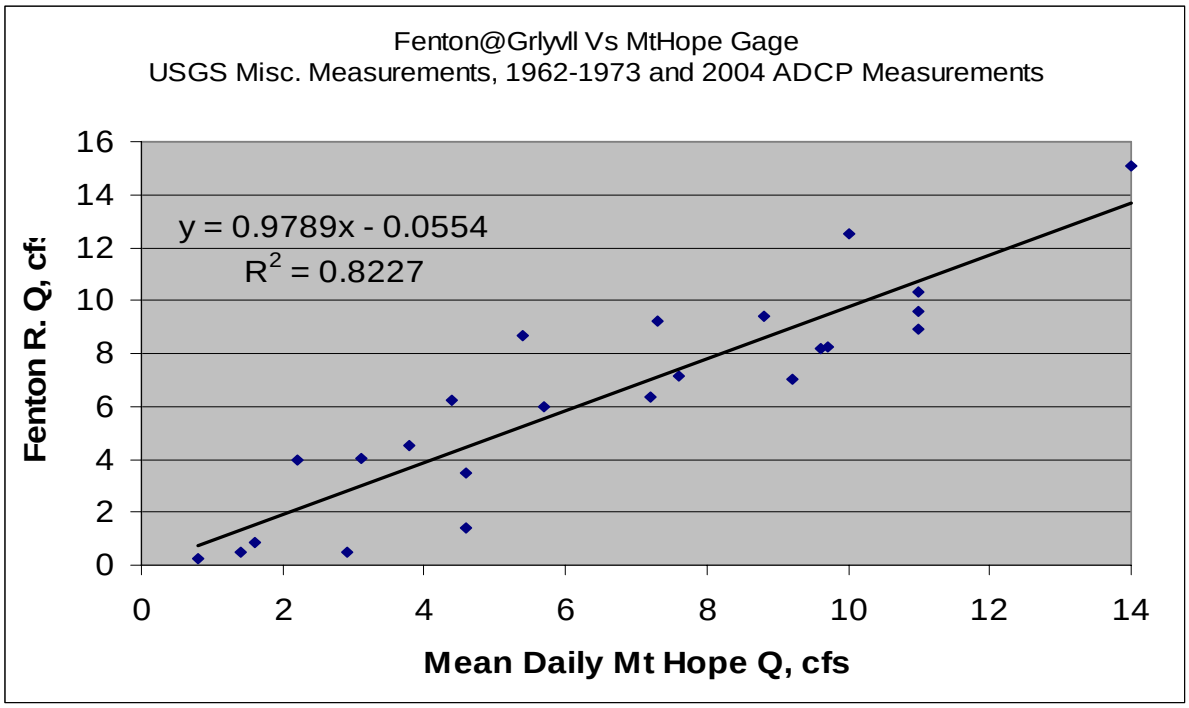

Figure 6.18 Low Flows in the Fenton River at Gurleyville Predicted from Low Flows in the Mount Hope River.

6.4.6 Discussion of Frequency Analysis

Analysis of existing hydrologic data from the USGS Mount Hope River gaging station near Warrenville, CT, in conjunction with Fenton River flows measured as part of this project has shown that low flow measurements on the Mount Hope River can be used to predict low flows in the Fenton River with some confidence.

The expected exceedence level of 6 cfs in the Fenton River based on a correlation with the Mount Hope FDCs is about 50 % when the July to September period is used, i.e. 6 cfs is expected to occur about 1 out of 2 years on average. In contrast, the exceedence levels for 6 cfs for April-June and October-December are about 97 and 90 %, respectively. The Mount Hope records have not shown 6 cfs occurring during the January to March period. The exceedence values for 3 cfs are about 78% for July-Sep, 97% for Oct-Dec., and over 99.5% in April-June on the Mount Hope. By correlation, the Fenton values are about the same.

6.5 Development of Recession Curves for the Fenton River

6.5.1 Introduction

Recession curves or constants are used to predict the future baseflow level in a river for a given current flow. Usually the constants are developed for non-rainfall or very low rainfall periods to avoid event runoff. The constants can be used to predict how

quickly the flow will reach a certain critical discharge, e.g. "Given a flow of X cfs today, how many days until the flow is "Y' cfs.

The hydrograph used for the recession analysis was developed for the Fenton River at Old Turnpike Road in Mansfield using a continuous stage recording and a rating curve. The hydrograph covered the period of May through September 2005. The stage was measured with a Minitroll pressure transducer placed in a pipe that was attached to the upper, left (facing downstream) bridge over the Fenton on Old Turnpike. The pipe extended horizontally below the water level at all observed flows. Stage was recorded at 5 minute intervals. Discharge in the Fenton was determined for various stages using either an Acoustic Doppler Current Profiler (ADCP) or a velocity-cross sectional area approach using a Marsh-McBirney flow meter. The ADCP was used at intermediate levels, while the Marsh-McBirney was used at very low flow levels during the drought periods of late summer 2005. A rating curve, discharge versus stage, was developed from coincident flow measurements and stages. The rating curve was divided into two regions: one for low flows and one for intermediate flows. The rating curve is shown in Fig. 6.19 along with the equations and corresponding R^2 for each region. The Fenton hydrograph is shown in Fig. 6.20, along with provisional data for the same period for the Mount Hope River at the USGS station (#01121000). The Fenton and adjacent Mount Hope watersheds are similar in shape and land use and should have similar shaped hydrographs. The Mount Hope watershed is slightly larger, and should have a slightly larger flow. The somewhat lower flow (provisional) in the Mount Hope versus the Fenton River shown in Figure 6.20 is attributed to different rainfall during July-September, 2005. All of eastern Connecticut was experiencing a "severe hydrologic drought" during the first week of September, 2005 as determined by streamflow at USGS gages.

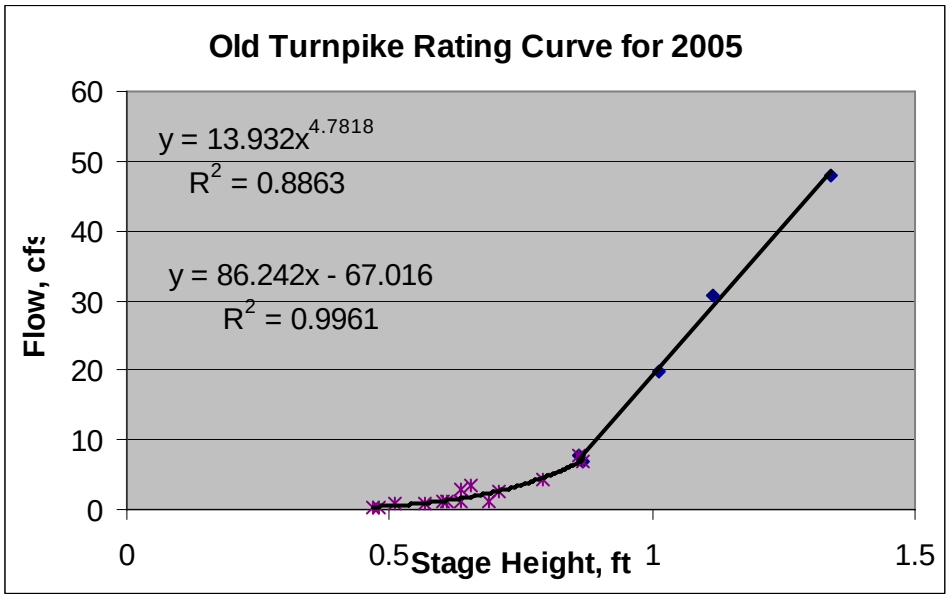

Figure 6.19. Rating curve for Fenton River for summer 2005

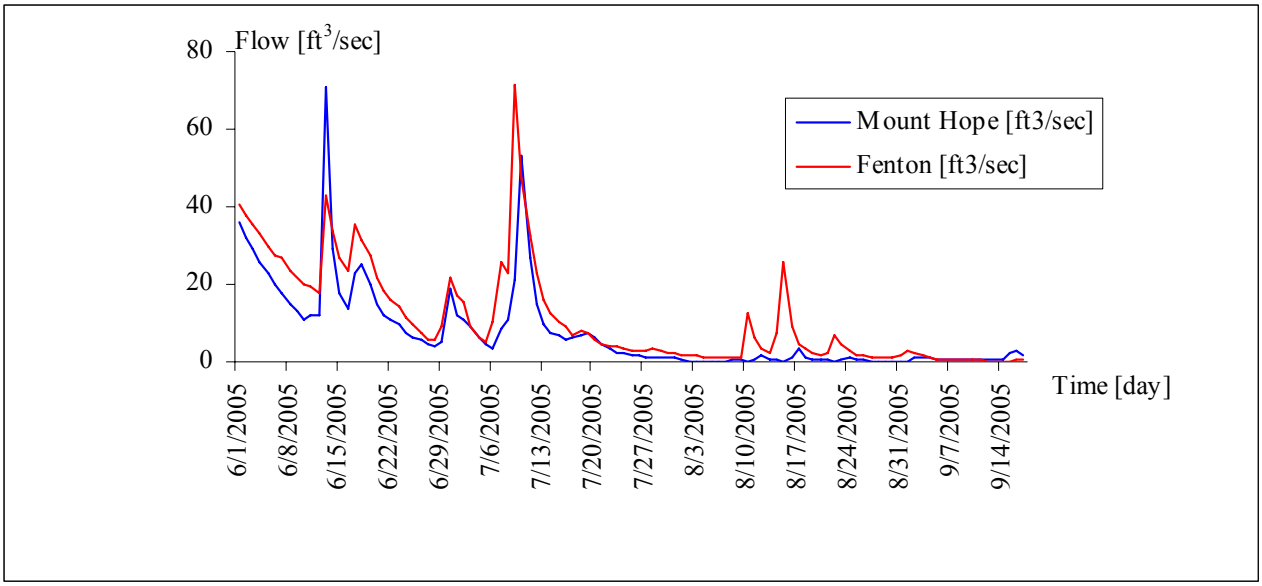

Figure 6.20. Hydrographs for Fenton and Mount Hope Rivers, summer 2005
Note: Mount Hope data from USGS are provisional and subject to revision.

6.5.2 Selection of recession periods

Periods of decreasing flow were selected from the summer 2005 Fenton hydrograph. Only the portion of recessions at least 2 or 3 days (depending on size of event) after a peak from a runoff event was included to avoid surface runoff recession phenomena as much as possible. Five recessions were initially extracted for further analysis, ranging from 3 to 20 days in length. A composite graph of the five recessions (Fig. 6.21) was developed by shifting the recessions along the "Time" axis by finding coincident points of recession. This approach is typically used to develop a Master Recession Curve. After review, three of the recessions were dropped from the analysis: Number 5 was considered out of the range of interest (below about 3 cfs); Number 4 was considered too short; and Number 2, after further analysis of Fig. 6.20, was thought to be due to a small runoff event rather than baseflow.

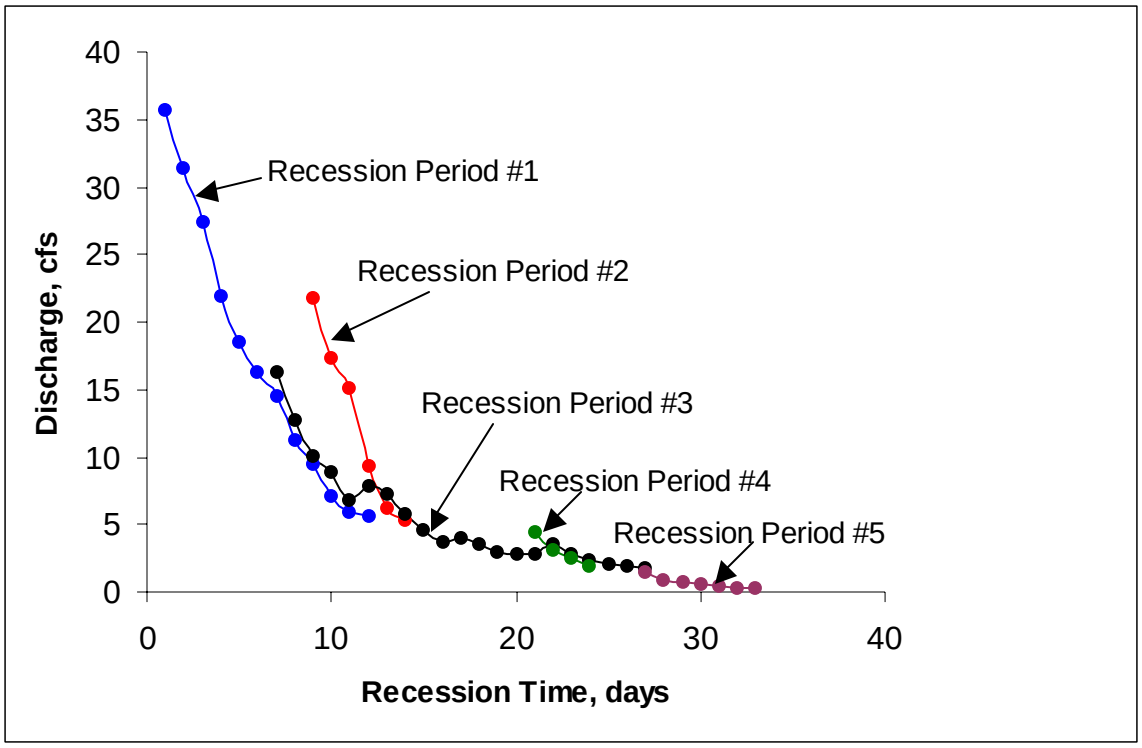

Figure 6.21. Composite recession curves for Fenton River, summer 2005

6.5.3 Development of prediction recession curves and constants

Several approaches were tested to obtain the best prediction of the discharge within a given number of days for the remaining recessions in Fig. 6.12. These approaches include: visually fitting a line to minima in the observed composite recession curve, and regression analyses. The visually fitted approach was attempted on both semi-log and arithmetic plots, while both power-based and exponential equations were attempted in a regression between days of recession and the mean daily flow for the non-recharge periods in 2005. The regression approach provides a smoothing mechanism, while the fitted line through minima provides a lower boundary for the predicted flows. However, the fitted line is more subjective than the regression approach.

Typically, recessions exhibit an exponential decay process resulting in a straight line on a semi-log plot of discharge versus time. The regression analysis did show that an exponential equation in general had a higher R^2 and a better 1:1 line on a simulated versus observed discharge plot, when compared to a power curve. However, the exponential decay curve did not capture the full extent of the recession well over the range of the composite curve shown in Fig. 6.21.

The fitted line approach was applied to selected segments of the curve as shown in Fig. 6.22. Recession curves often exhibit changes in slope with decreasing flow, which is attributed to changes in stream flow contributions from surface runoff, interflow and ground water. A semi-log plot was also investigated, but linear segments were judged to

be a good fit to the two segments of interest: from about 20 to 6.5 cfs, and from 6.5 to about 3 cfs. The break point of 6.5 cfs provides a common point for the two lines. The two segments can be used to help develop management strategies for operation of the wells.

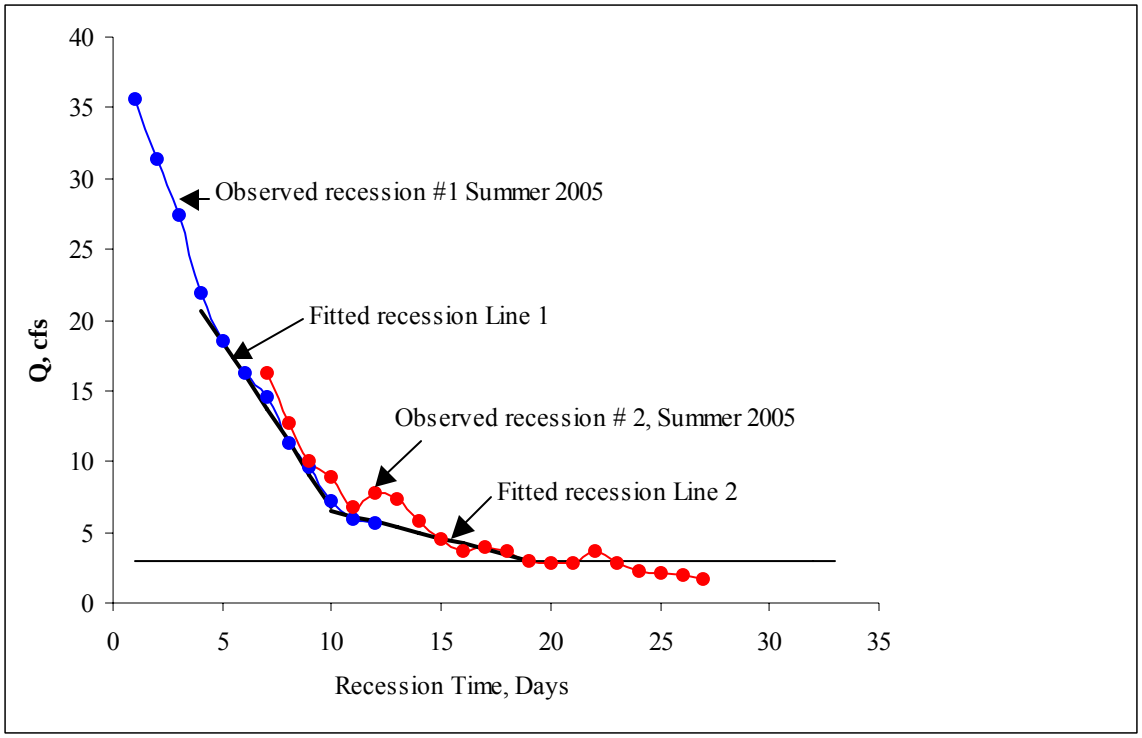

Figure 6.22. Composite observed recessions, Summer 2005 and fitted linear segments.

The equations for the lines exhibited are:

For Line 1: $Q_t = Q_0 - 2.33$ Days where Q_0 and Q_t are in cfs

And $6.5 < Q_0 <= 21$, $0 <$ Days < 6.

For Line 2: $Q_t = Q_0 - 0.39$ Days where Q_0 and Q_t are in cfs

And $3.0 < Q_0 <= 6.5$, $0 <$ Days < 8

The equations should be used with caution to verify that both the initial Q and the number of recession days are within the ranges specified. Also, care should be taken to assure that the initial value of Q is not near the peak of a small runoff event. As shown by Recession #2 in Fig. 6.21, the flow can drop much faster when the recession is due to surface runoff as compared to sustained baseflow.

6.5.4 Discussion and Conclusions of Recession Analysis

The recession lines or equations can be used to predict the expected flow in the Fenton River at Old Turnpike for a given number of days without any recharge or surface runoff for summer conditions. The flow drops rapidly from around 20 cfs to 6.5 cfs, and then more slowly from 6.5 to 3.0 cfs. It only takes about 6 days to drop from 20 to 6.5 cfs, while it takes about 8 days to drop from 6.5 to 3.0 cfs. The recession analysis was

developed from one summer of data. As more data are collected from a gaging station at Old Turnpike, the above lines/equations should be verified and modified as needed. With several years of data, a master recession curve could be developed that includes a greater assurance of the response of the stream under different hydrologic conditions.

6.6 Summary and Conclusions of Hydrologic Assessment

Both 2003 and 2004 had above average rainfall during the summer, and flows during the typical low-flow season (August-September) in both 2003 and 2004 were not as low as required (<5 cfs) for sufficient time periods to make direct measurements of impacts on stream flow due to pumping. The summer of 2005 was abnormally dry and presented the opportunity to perform investigations under extreme low flow in the Fenton River.

The Fenton River in the vicinity of the UConn well field is a complex system. We observed several gaining and losing reaches, where water either flows from groundwater to the stream or vice-versa within the study area. Reaches can switch from gaining to losing depending on recent rainfall. The post-glacial history of sedimentary deposition in the river valley has created what are thought to be preferential flow paths between the surface and subsurface in a number of locations. In general, in the absence of pumping, the study reach of the Fenton River tends to gain flow in the downstream direction, even in times of drought.

The magnitude of surface and ground water source contributions to instream flow is relevant when compared to the registered pumping capacity of the wells because the Fenton River can have flows less than 1 cubic feet per second (cfs) under drought conditions. During the summer of 2005, the flows in the Fenton River became very low, and the river bed became dry over an approximately 12 day period (5-16 September) in the vicinity of UConn wells A & B. Fortuitously, the field data collection equipment procured for this project was operated by the investigators beyond the end of the original field data collection period, providing strong evidence of the effect of pumping of the wells on the Fenton River during drought conditions.

The drawdown of groundwater due to wells near streams can cause the groundwater table in the vicinity of the stream to fall below the stream water surface and in some locations, the stream bed. In these cases, water will infiltrate from the stream bed into the groundwater system. This is called “induced infiltration” due to pumping of groundwater. We used three independent means to estimate induced infiltration. These methods including nested piezometers, weirs, and the stream loss observations from the summer of 2005. Our results indicate that the published results of Rahn (1971), slightly underestimate the induced infiltration.

Observations from the summer of 2005 significantly reduced the uncertainty in our analysis. Section 6.3 explains why the Fenton River went dry during the period 5-16 September, 2005. The explanation is based on analysis of rainfall, streamflow, pumping, and groundwater level data, all of which provide key indications of factors that lead to the

drying of the river over an approximately 600 m reach from upstream of well B to downstream of well A. These observations are particularly relevant to the objectives of this study. Figure 1.2 shows the locations of the UConn groundwater wells A, B, C, and D, and the monitoring wells used to observe groundwater levels. The monitoring wells are denoted with "UC" or "MW".

Determination of the long-term frequency of low flows in the Fenton River was accomplished by correlating the limited available gauging data from the Fenton River with the long-term gauging data from the nearby Mt. Hope River. The use Flow Duration Curves (FDC) based on seasonal or even biweekly periods is recommended over use of the annual-based FDC (period of record). The exceedence level for a discharge of 6 cfs is about 50% based on the summer-based FDC, and the corresponding level for 3 cfs is about 80%. The recession lines or equations can be used to predict the expected flow in the Fenton River at Old Turnpike for a given number of days without any recharge or surface runoff for summer conditions. The flow drops rapidly from around 20 cfs to 6.5 cfs, and then more slowly from 6.5 to 3.0 cfs. It only takes about 6 days to drop from 20 to 6.5 cfs, while it takes about 8 days to drop from 6.5 to 3.0 cfs. The recession analysis was developed from one summer of data. As more data are collected from a gaging station at Old Turnpike, the above lines/equations should be verified and modified as needed. With several years of data, a master recession curve could be developed that includes a greater assurance of the response of the stream under different hydrologic conditions.

7.0 HYDROGEOLOGIC ASSESSMENT

The goal of this portion of the study was to form a better understanding of the geology of the Fenton River well field aquifer. Core samples were collected from the aquifer, and the subsurface was analyzed using an array of geophysical techniques. Nested piezometers were installed in the bed of the Fenton River to collect data useful for determining the hydraulic conductivity of the stream bed.

Geophysical investigations using seismic refraction and ground penetrating radar (GPR) were conducted at the Fenton River Well field area for the purpose of:

- Determining depth-velocity structure of the subsurface at the study site in order to locate water table levels, delineate bedrock topography and stratigraphically characterize the lithology of the area;
- Applying different data analysis methods to the same set of seismic refraction data to produce an integrated stratigraphic model; and
- Developing accurate spatial geophysical inputs to the mathematical model of groundwater flow.

7.1 Subsurface Core Sampling

The two newly installed bedrock wells near production wells B and C were logged using conventional and advanced borehole-geophysical methods in August and September 2003. The third borehole, which was installed on the hill near the abandoned ski lift was not logged due to site accessibility issues. Borehole-geophysical methods provide information about the physical and chemical properties of rock and fluids in the subsurface and provide important information on subsurface structures including the lithology, the rock fabric, and the location, orientation, and hydraulic properties of fractures. The conventional geophysical-logging methods included caliper, gamma, fluid temperature, and fluid resistivity. Advanced logging methods included optical and acoustic imaging of the borehole wall and heat-pulse flowmeter.

7.1.1 Borehole Drilling and Monitoring Well Installation

Three boreholes were drilled and bedrock-monitoring wells were installed by U. S. Geological Survey personnel from May 2 through May 9 2003 as part of the Fenton River study to access the long-term impact of the University Of Connecticut's (UConn) Fenton River water supply wells on the habitat of the Fenton River. Rotary drilling with a 5-inch diameter tri-cone bit was used to penetrate the unconsolidated overburden material and approximately 3 ft into competent bedrock. A biodegradable drilling fluid, which is designed to break down after approximately 48 hours, was used when drilling through the overburden in order to hold the borehole open. Steel 4-in diameter casing was set through the overburden and into the rock. The steel casing, which had a drive shoe affixed to its lower end, was set into the pre-drilled borehole. Sections of casing, approximately 21 ft in length, were threaded together and lowered into the borehole until the drive shoe

reached the bottom of the hole. A mixture of cement and bentonite grout was poured into the annular space around the casing in order to seal the casing and isolate the water in the unconsolidated glacial materials from the water in the bedrock. The entire length of casing was lifted approximately 2 ft and then dropped into place to ensure that the grout filled the annular space. The casing was hammered into the rock to assure a tight fit. The grout was left to set undisturbed overnight. A diamond-impregnated carbide bit was used the following day with a rotary-coring tool to cut into the rock. A wire-line system was used to recover 5-ft sections of bedrock cores during the drilling process. The wire-line method allows the drill rod to remain in the borehole, while the core barrel is pulled up the borehole through the drill rod on a wire line. This method saves time and also reduces the possibility of the borehole collapsing. The finished borehole is defined as the open hole from the bottom of the casing to the depth drilled.

7.1.2 Conventional Borehole Geophysical Methods

Conventional geophysical-logging methods are used to determine rock properties, infer locations where water enters or exits boreholes, and identify variations in dissolved solids in the fluids within a borehole and in the rock adjacent to the borehole.

7.1.2.1 Caliper Logging

Caliper logging is used to generate a continuous profile of the borehole diameter with depth. The caliper tool is pulled up the borehole allowing three spring-loaded arms to open as they pass borehole enlargements. Enlargements in the borehole diameter generally are related to fractures, but also can be caused by changes in the lithology or borehole construction.

7.1.2.2 Gamma Logging

Gamma logging measures the natural-gamma radioactivity of the formation surrounding the borehole (Keys, 1990). The most significant naturally occurring sources of gamma radiation are potassium-40 and daughter products of uranium and thorium decay series. Gamma emissions can commonly be correlated with rock type or with fracture infilling. Potassium-40 is abundant in some feldspars and mica, and geochemical processes can concentrate uranium and thorium. Deviations in the gamma log indicate changes in lithology or the presence of altered zones or mineralized fractures. The probe is able to detect gamma radiation through plastic and steel casing. Because the gamma log does not have a unique lithologic response, interpretation must be correlated with other information such as drilling logs and other geophysical logs.

7.1.2.3 Fluid-Temperature Logging

Fluid-temperature logging is used to identify where water enters or exits the borehole (Williams and Conger, 1990). In the absence of fluid flow in the borehole, the temperature gradually increases with the geothermal gradient, about 1° F per 100 ft of depth (Keys, 1990). Deviations from the expected geothermal gradient indicate potential

transmissive zones in the borehole. Changes in the fluid temperature indicate water-producing and (or) water-receiving zones.

7.1.2.4 Fluid-Resistivity Logging

Fluid-resistivity logging measures the electrical resistivity of the fluid in the borehole (Williams and Conger, 1990). Changes in the electrical resistivity indicate differences in the concentration of the total dissolved solids in the fluid in the borehole. These differences typically indicate sources of water that have contrasting chemistry and have come from different transmissive zones. Specific conductance is the reciprocal of the fluid resistivity.

7.1.3 Advanced Borehole-Geophysical Methods

Advanced borehole geophysical logs are used to aid in the identification of the lithology of the boreholes and in determination of the location and orientation of foliation and laminations in the bedrock and of fractures intersected by the boreholes. The advanced methods included optical and acoustic imaging of the borehole wall, and heat-pulse flowmeter (under ambient and pumping conditions).

7.1.3.1 Optical-Televiewer Logging

Optical-televiewer (OTV) logging records a continuous, magnetically oriented, and digitized 360° color image of the borehole wall (Williams and Johnson, 2000). The images permit the direct inspection of the borehole for fractures, changes in lithology, water level, bottom of casing, and borehole enlargements. Optical images can be collected above or below the water surface, provided the water is sufficiently clear for viewing the borehole wall. Fracture characteristics such as the presence of iron oxidation or fracture infilling can be visually confirmed. The digital image of a borehole can be viewed as an unrolled, flattened image that shows the depth along the vertical axis and the magnetic direction along the horizontal axis. The x-axis represents a 360° scan of the borehole wall from south through west, north, east and south again. The depth in feet is shown along the y-axis. The sinusoidal curves on the flattened image represent planar surfaces. Thus, planar features such as fractures, foliation, and lithologic contacts, can be identified directly on the images. Because the image is oriented to Magnetic North, the strike and dip can be determined.

7.1.3.2 Acoustic-Televiewer Logging

The acoustic televiewer (ATV) produces a high-resolution, magnetically oriented, digital image that is used to determine the location and orientation of fractures that intersect the borehole (Williams and Johnson, 2000). The ATV tool emits a narrow acoustic beam that rotates 360° and is focused at the borehole wall. The acoustic wave moves through fluid in the borehole and is reflected off of the borehole wall and recorded by the tool. The log records the amplitude and travel time of the reflected signal, which can be displayed as a flattened 360° view of the borehole wall. A fracture that intersects the borehole causes scattering of the acoustic wave and appears as a high contrast, low

amplitude line on the acoustic amplitude log. On the acoustic travel time log, a fracture is indicated by an increase in the one-way travel time of the wave, due to an increase in borehole diameter. The OTV and ATV measure different properties so not all features are seen by both imaging tools. Characteristics such as oxidation, precipitation, or fracture infilling, may be seen only by the OTV. The ATV image may show an increase in borehole diameter where a fracture cannot be confirmed in the OTV image. The best interpretation is with a side-by-side presentation of images collected from both tools.

7.1.3.3 Heat-Pulse Flowmeter Logging

Heat-pulse flowmeter logging measures the direction and rate of vertical flow in a borehole. Used in conjunction with other geophysical logs, individual fractures or fracture zones where water enters or exits the borehole can be identified. Under ambient conditions, differences in hydraulic head between two transmissive fractures produce vertical flow in the borehole. Water enters the borehole at the fracture zone with the higher head and flows toward and out of the fracture with the lower head. If the heads in transmissive zones are the same, no vertical flow will occur in the borehole. Therefore, flowmeter logging also is conducted under low-rate (0.25 to 1 gal/min) pumping conditions to identify transmissive zones with similar ambient heads that would not be identified without stressing the aquifer. The flowmeter used in this investigation uses a heat-pulse tracer that moves upward or downward in the presence of vertical flow. The measurements were collected at discrete locations, usually above and below fractures. The heat-pulse flowmeter can measure flows as small as 0.01 +/- 0.005 gal/min (Hess and Paillet, 1990). The water levels were recorded during pumping and heat-pulse flowmeter measurements were made after the borehole reached a quasi-steady state in which the amount of water coming out of storage was less than the measurement resolution of the tool.

7.1.4 Borehole MS 82 (hilltop)

Location and construction. Borehole MS 82 is located west of the Fenton River on a terrace near the abandoned ski lift shed. MS 82 has a total of 21 ft of 4-in diameter steel casing set approximately 3 ft into competent bedrock. Below the casing, the hole is open to the bedrock to a depth of 113.3 ft below the top of casing. The ambient water level was 6.79 ft below the top of casing on May 9, 2003. All measurements are referenced to the top of casing, which is 1.1 ft above land surface.

7.1.5 Borehole MS 83 (near production well B)

Location and construction. Borehole MS 83 is located approximately 30 ft northeast of the pump house containing UConn production well B. MS 83 has a total of 63 ft of 4-in diameter steel casing. Below the casing, the hole is open to the bedrock to a depth of 125.2 ft below the top of casing. The ambient water level was 7.41 ft below the top of casing on July 1, 2003. All measurements are referenced to the top of casing, which is 1.7 ft above land surface.

Lithologic characterization. Borehole MS 83 intersects gray medium-grained schist and gneiss. Foliation is fairly uniform and nearly horizontal over the length of the well, dipping very gently to the northwest. The transmissive fracture at approximately 97.4 feet trends to the east-northeast and dips gently to the northwest.

Hydraulic characterization. Under ambient (unstressed) conditions, no flow was detected in borehole MS 83 with the heat-pulse flowmeter tool. Under low-rate pumping conditions of approximately 0.25 gal/min, the majority of water is produced from a fracture at 97.4 ft. A small amount, less than 10 percent, is produced from fractures at 94 ft. It was not known if production well B was pumping at the time of the flowmeter work. The effect, if any, from pumping well B on the flowmeter measurements is not known at this time.

7.1.6 Borehole MS 84 (near production well C)

Location and construction. Borehole MS 84 is located approximately 30 ft northwest of the pump house containing UConn production well C. MS 84 has a total of 63 ft of 4-in diameter steel casing. Below the casing, the hole is open to the bedrock to a depth of 112 ft below the top of casing. The ambient water level was 7.46 ft below the top of casing on July 2, 2003. All measurements are referenced to the top of casing, which is 1.5 ft above land surface.

Lithologic characterization. Borehole MS 84 intersects gray medium-grained schist and gneiss. Foliation is fairly uniform and nearly horizontal over the length of the well, trending to the south-southwest

Hydraulic characterization. Under ambient conditions, no flow was detected in borehole MS 84 with the heat-pulse flowmeter tool. Under low-rate pumping conditions of approximately 0.33 gal/min all the water enters the well from a fracture zone between 63.5 and 68 feet below top of casing. The water-producing zone consists of several nearly horizontal fractures. Half of the water is produced from fractures at 67 to 68 ft and half is produced from fractures at 64 to 66 ft. It was not known if production well C was pumping at the time of the flowmeter work. The effect, if any, from pumping well C on the flowmeter measurements is not known at this time.

Table 7.1: Geologic logs of bedrock monitoring wells installed by USGS.

Well Identifier	Depth Interval (feet below land surface)	Description of Material/Drilling
MS 82	0 to 16.3	Till
	16.3 to 113.3	Bedrock, gray Gneiss and Schist
MS 83	0 to 11	Sand and Gravel – crunchy drilling, rig was bouncing and jerking
	11 to 20	Sand – steady, smoother drilling
	20 to 58	Sand and Gravel – crunchy drilling, rig was bouncing and jerking
	58 to 125.2	BEDROCK, GRAY GNEISS AND SCHIST
MS 84	0 to 60	Sand and Gravel – crunchy drilling, rig was bouncing and jerking
	60 to 112	Bedrock, gray Gneiss and Schist

7.1.7 Characterization of Geoprobe Test Borings

Continuous cores were collected in nine test borings (UCSB-1, UCSB-2, UCSB-3, UCSB-4, UCSB-5, UCSB-6, UCSB-7, UCSB-7B, and UCSB-8) by the Environmental Research Institute located at the University of Connecticut using a Geoprobe rig. The continuous cores, collected in 4-foot sections, did not always yield 100 percent recovery of the 4-foot interval. Geoprobe boring logs and core photos are shown in Appendix E of this report.

7.1.8 Heat transport and ground-water flow

Naturally occurring changes in temperature in a stream environment can be large and rapid, providing a thermal signal that is easy to identify and measure. Differences between temperatures in a stream and surrounding sediments can be analyzed to trace the movement of ground water to and from streams. Variations in streamflow temperature are transmitted into the underlying sediments by heat transfer processes that include conduction and advection. “Heat conduction is the transfer of heat along a temperature gradient by the diffusion of kinetic energy. The rate that heat is transferred by conduction is proportional to the thermal conductivity of the stream sediments. Heat advection refers to the transfer of heat from the movement of water through stream sediments. Its role in heat transfer is directly related to the downward fluid flux, or infiltration rate” (Galloway et al, 2003).

7.1.8.1 Piezometer Installation in the Fenton River

Two piezometers were installed in the Fenton River in the vicinity of production well B on Thursday July 15, 2004 using the Environmental Research Institute (ERI) Geoprobe rig. One piezometer was installed near the center of the stream channel and the second piezometer was installed near the edge of the right bank. The piezometers were installed to a depth of 11 feet below the streambed at each location. Continuous Multi-channel Tubing (CMT®) manufactured by Solinst Canada LTD was used to construct two multi-level piezometers with seven discrete measurement intervals for ground-water level measurements. Type T thermocouple sensors were inserted into four of the seven channels in the CMT tubing at 2, 5, 8, and 11 feet below the streambed. Four channel EL041 thermocouple converters in conjunction with EL005 dataloggers, manufactured by Pico Technology Limited, were used to measure temperature variations. Featuring built-in cold junction compensation, the EL041 thermocouple converter is designed to measure a wide range of temperatures (-270 to 1820°C) with any thermocouple that uses a miniature size thermocouple connector. The configuration of this system is shown in Figure 7. Analysis and results of the data are discussed in Chapter 8, and shown in Figures 8.6 through 8.9, where the data were used to estimate streambed conductivity.

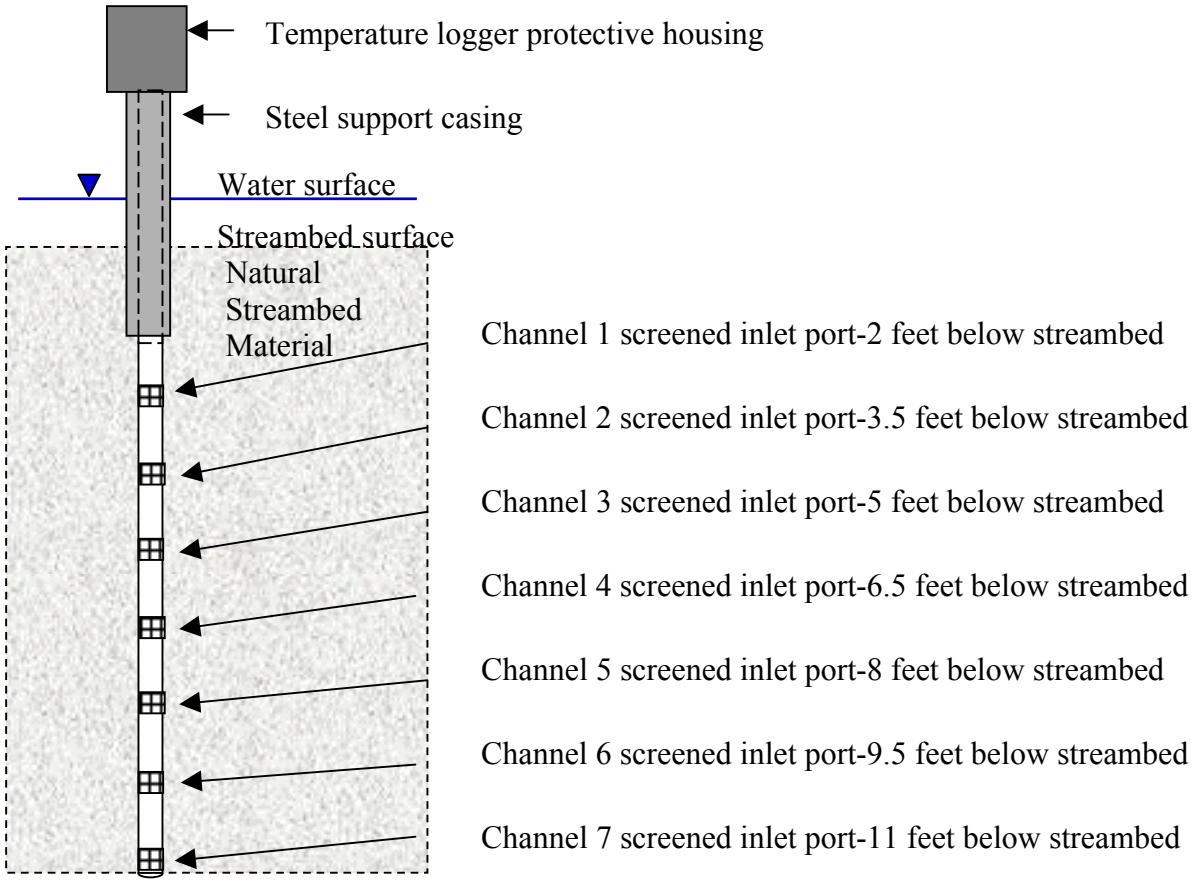

Figure 7.1: Diagram of piezometers installed in Fenton River

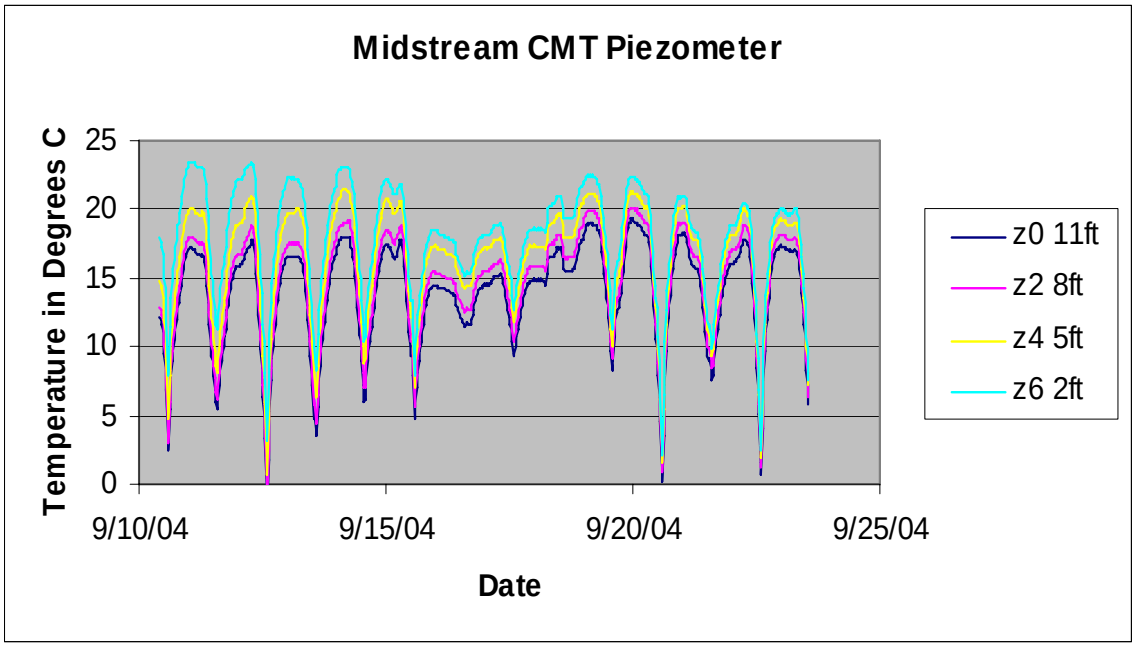

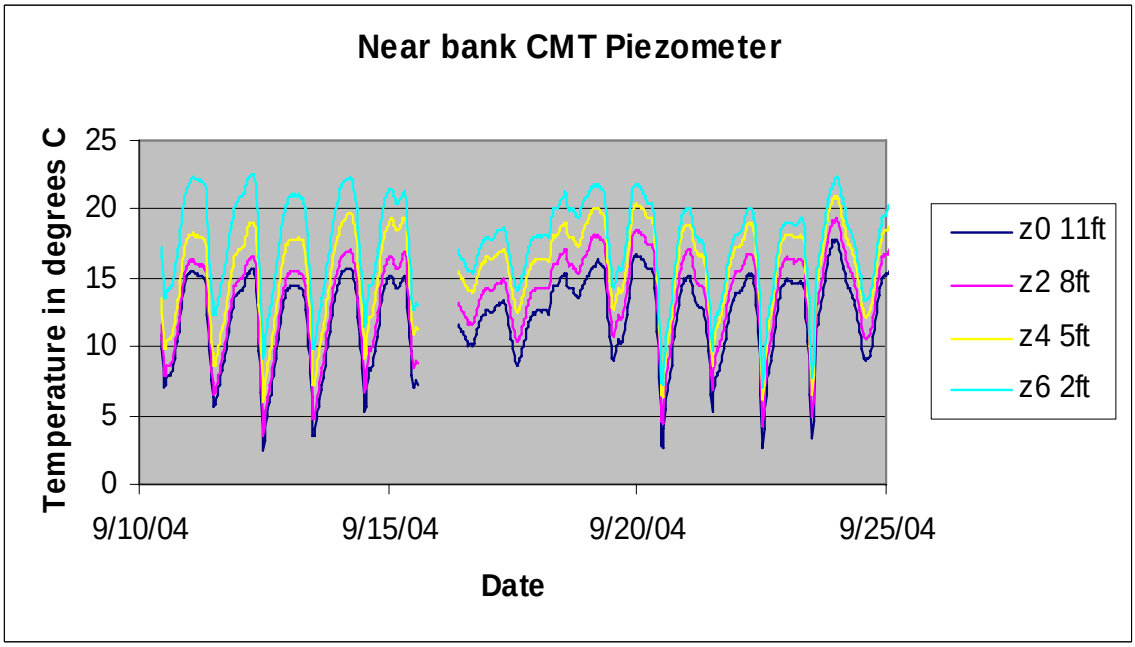

Figure 7.2: Graphs showing streambed temperature profiles for piezometers midstream and near bank installed in Fenton River

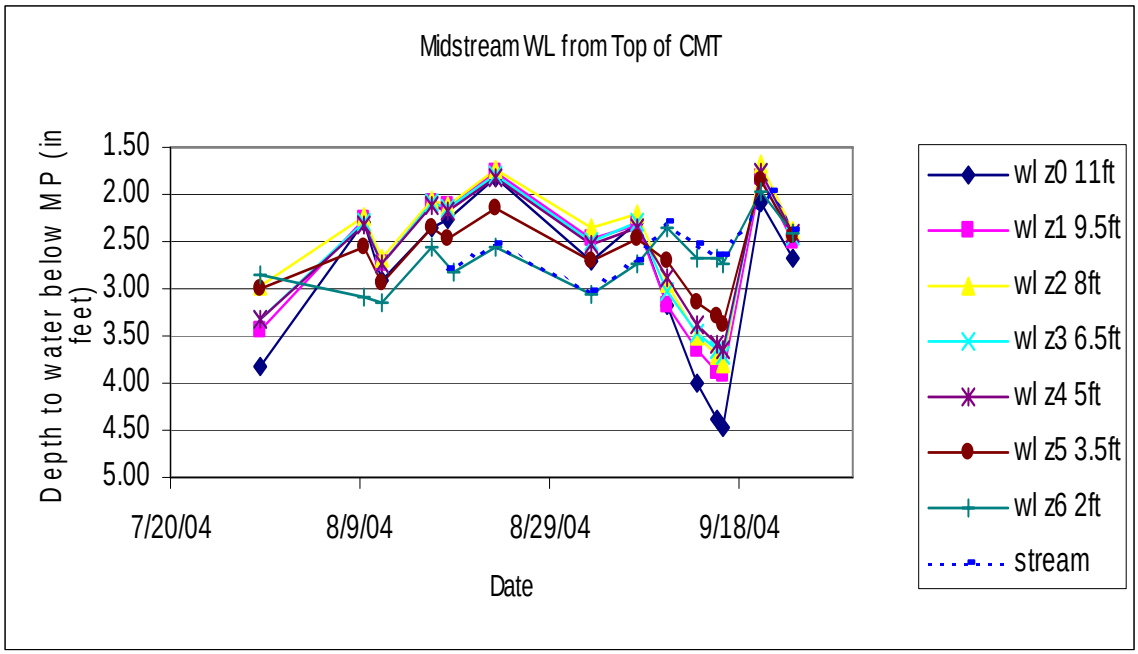

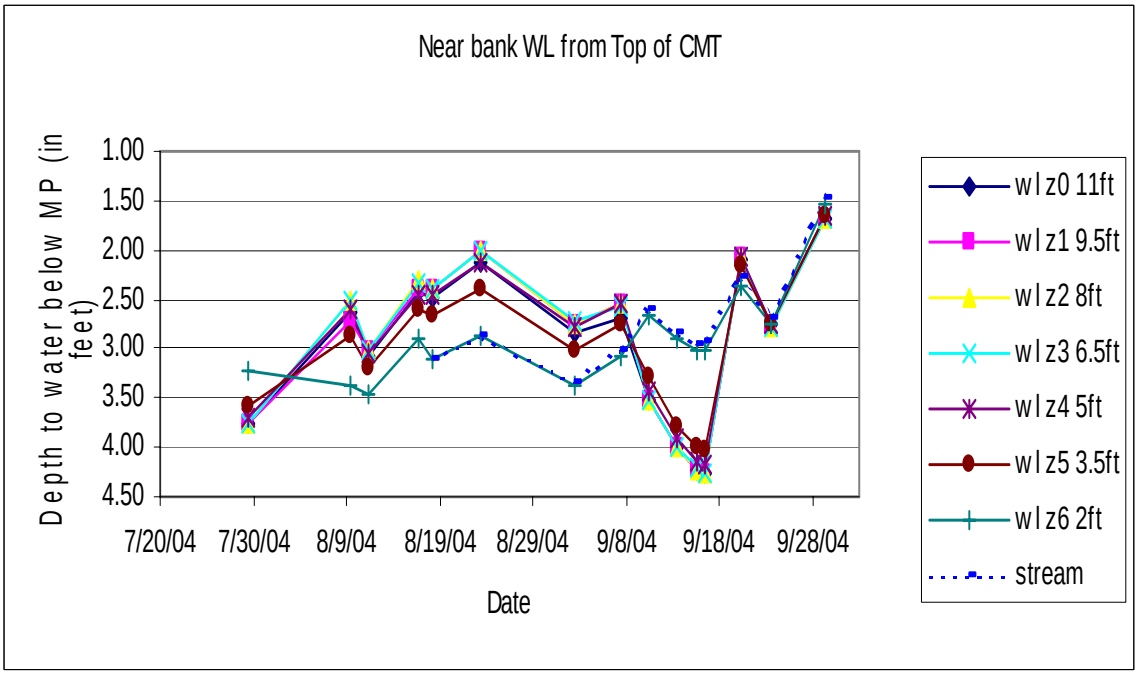

Figure 7.3: Graphs showing differences in water level between stream and shallow groundwater in piezometers midstream and near bank installed in Fenton River.

7.2 Introduction to Seismic Refraction and Ground Penetrating Radar Techniques

7.2.1 Seismic Refraction

Seismic refraction uses arrays of detectors (geophones) and time-recorders (seismographs) to measure the travel time of seismic head waves in the earth. These seismic waves are generated by sources such as sledgehammers, shotguns or explosions, etc. The objective is to use these head waves to map the depth to the refractors in which they travel (Sheriff, 2002). Seismic refraction uses laws of physics that govern the propagation of sound to study compressional sound waves generated by a source to travel down the earth and back up to detectors placed on the surface.

The instruments that are capable of recording the ground motion generated by seismic source are called geophones. The geophones are actually low-frequency transducers that can convert the ground motion into electrical signals which are recorded by a seismograph. At one particular location, the amplitude of ground motion will be recorded against the time of propagation of seismic waves. A plot of this time history of ground motion is referred as a seismogram.

7.2.2 Hydrogeologic Applications of Seismic Techniques

When combined with other tools, such as pumping tests, simulation modeling, test drilling, geologic maps, bore holes, and well logs, seismic refraction can be used to solve a wide range of hydrologic problems. Success in applying seismic refraction techniques to hydrology depends on the hydrogeologic settings in which they are used. Generally speaking, hydrogeologic settings in which layer velocities increase with depth, no thin layer are present, and a significant velocity contrast exists at the interface of layers are ideally suitable for seismic refraction. According to Haeni (1988), seismic refraction techniques have proved to be a great tool in hydrogeological settings where:

1) Unconsolidated unsaturated glacial or alluvial material overlies glacial or alluvial aquifers. Since velocity of sound in unconsolidated, unsaturated sands and gravels ranges from 120 m/s to 500 m/s while velocity of sound in unconsolidated, saturated sands and gravel ranges from 1200 m/s to 1800 m/s, seismic refraction techniques can help to determine depth to water table.

2) Unconsolidated glacial or alluvial material overlies consolidated bedrock. The contrast of velocity of sound in bedrock and saturated material is 3000-6000 m/s compared to 1200-1800 m/s. provided the thickness from the top of the water table to the top of the bedrock (saturated zone) is not too thin, and the velocity contrast is large enough, seismic refraction can be used successfully to delineate the saturated zone.

3) Unconsolidated stratified-drift material overlies significant deposits of dense lodgment glacial till, which in turn overlie crystalline bedrock. The velocity constraint of refraction techniques which requires velocity of sound in each layer to increase with depth is satisfied in this setting. The estimated velocity of sound in unsaturated stratified-drift saturated stratified drift, till and bedrock is about 300 m/s, 1500 m/s, 2200 m/s and 4500 m/s correspondingly. However, in many cases, till has shown to be an almost

undetectable intermediate layer. Thus, significant thickness of till is essential for seismic refraction to work well.

7.2.3 Ground Penetrating Radar

A ground penetrating radar (GPR) survey was first performed by a German geophysicist, Hulsenbeck, who used pulsed radar to investigate the nature of buried feature in 1926 (Reynolds, 1997). By definition, GPR is a means of exploring the shallow subsurface with electromagnetic waves (radar), usually in the 10 to 1000 MHz band. The two-way travel times of reflected radar waves give the depths where changes in electrical properties occur (Sheriff, 2002). A GPR system consists of a transmitting antenna, a receiving antenna, and a control unit. A pulse of radiowave that travels at high speed is generated from the transmitter at a specified frequency of the antenna. It is scanned by the receiver antenna at a fixed rate. The travel time it takes for the pulse to return to the receiver is recorded. As the antenna is moved over the ground, the received signals are displayed as a function of two-way travel time (radargram).

7.3 Geophysical Surveys of Near-Surface Stratigraphy

Geophysical investigations along survey profiles DD', EE', BB', S0, S1, S2, and S3 have been conducted at the Fenton River Project site as part of hydrogeological assessment of the project area (Figures 7.4 and 7.5). Seismic Refraction and Ground Penetrating Radar (GPR) are chosen as the primary tools for conducting the subsurface investigation. For an easier identification of the survey lines, the locations of the seismic and GPR survey profiles are superimposed onto the topography map (Figure 7.4) and aerial photo of study area (Figure 7.5). Due to heavy vegetation and impossible accessibility, geophysical surveys were called off for line FF' (Figures 7.4), which was originally planned.

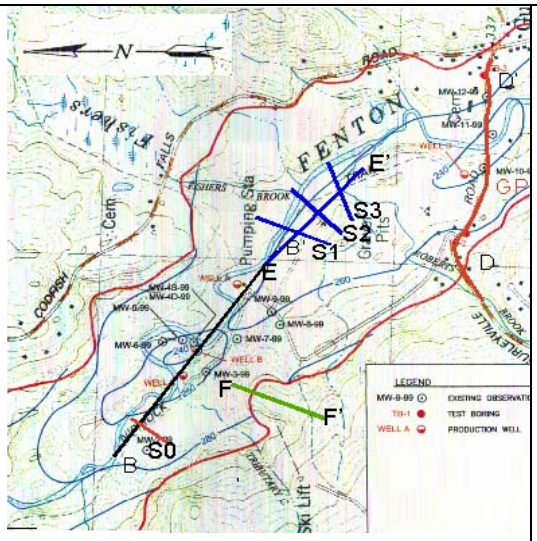

Figure 7.4: Site map of Fenton River project (BB', EE', DD', S0, S1, S2, S3, FF' are proposed GPR/seismic lines).

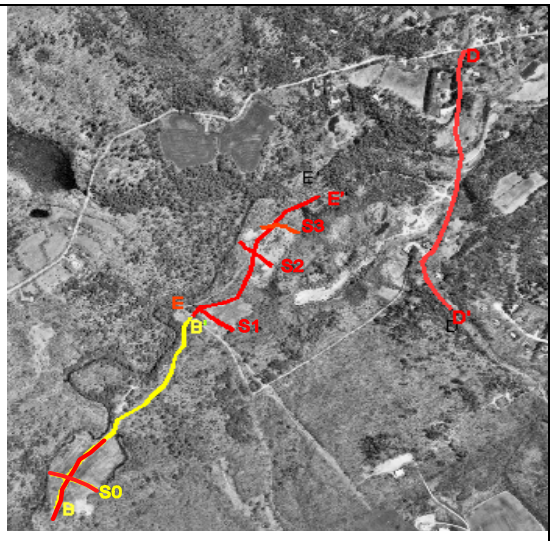

Figure 7.5: Aerial photo map of Fenton River. Red lines indicate both GPR and seismic surveys. Yellow lines only GPR.

7.3.1 Line B-B'

Oriented roughly S52E, line BB' starts at the hilly section where Tributary B goes into Fenton River, cross the entire meadow area along the dirt road, and ends at Well A. Line BB' passes through an area crowded by a number of observation wells and 3 main production wells (Well A, Well B, and Well C). On October 7th, 2004, a GPR survey was performed along BB' using the RAMAC 100 MHz shielded antenna system. The total length of the GPR survey was 869 m. On April 7, 2005, a seismic refraction survey was performed a long the first 300 meters of line BB'. This line starts uphill at the starting point of line BB, going northeast direction toward well C and ends about 100 m before the tributary C cuts the trail. Seismic survey details can be found in Table 7.2a.

7.3.2 Line E-E'

The seismic surveys were conducted from the beginning to middle of summer, 2004. Line EE' is a continuation of line BB'. It starts where line BB' stops, running SE along a small trail through the Gravel Pits and ends where Roberts Brook cuts the trail. Total length of EE' is 487 m. GPR survey for line EE' was implemented on October 7th, 2004 using the RAMAC 100 MHz shielded antenna system. The starting point of GPR line was 2m SW of the starting point of Seismic line, making a GPR profile of 485m long.

7.3.3 Line D-D'

The 959-m long seismic refraction survey along Line DD' was carried out along the SE edge of the Gurleyville Road. The seismic refraction surveys were conducted during the period of October 4th to October 28th, 2004. The survey line starts about 3 meters south of the intersection of Roberts Brook and Gurleyville Road to the uphill direction, and ends at the intersection of Gurleyville Road and Codfish Fall road. There is a break at about 630m from the starting point of the survey line when the line reaches the Fenton River Bridge that is 26 m long. Line DD' connects well TB-2 and TB-3 together while it passes through well D and several observation wells. Details about the survey are given in Table 7.2a.

The GPR survey was carried out using the RAMAC 100 MHz unshielded antenna during October 2002 along the Gurleyville Road. With a total length of about 923 m, the GPR surveys cover almost the total length of DD'. Compared to seismic refraction line, GPR line of DD' starts 7m south of the starting point of the seismic line but ends 43 m south of the ending point of seismic line. GPR data were collected continuously across the Fenton River Bridge. The GPR survey parameters are in Table 7.2b.

7.3.4 Line S0

On November 2, 2002, a seismic refraction surveys was conducted in the meadow area. Line S0 starts 16 m SSE of Geoprobe coring site UCSB07, running down slope a distance of 147 m to link UCSB07 to UCSB05 at the west bank of the Fenton River. On October 7th, 2004, using the RAMAC 100 MHz shielded GPR system, a GPR line of 128

m long was conducted. The line starts near the location of boring UCSB07 and going toward UCSB05 close to the Fenton River.

7.3.5 Lines S1, S2, and S3

During the month July of 2004, a series of seismic refraction surveys was carried out in the vicinity line EE'. Line S1 is one of three proposed cross lines of line EE'. Seismic survey for line S1 starts at 34 m mark of line EE'. It runs SW a distance of 73.5 m and almost perpendicular to EE'. Line S2 is the second cross line of EE'. It starts about 10 m from the west bank of Fenton River and runs 34 m long before it perpendicularly crosses EE' at 272 m mark. The line continues another 40m on the other side of EE', making a total length of 74m. Seismic line S3 starts 10 m from the east side of EE' and cuts EE' at 372 m mark. With the total length of 73.5 m, S3 makes a perpendicular profile with EE. GPR surveys for cross lines S1, S2, and S3 were conducted on October 7th, 2004 using the same system of RAMAC 100 MHz shielded antenna. However, the total lengths of these GPR lines differ from those of corresponding seismic lines. Table 7.2b can be referred to about these differences.

Table 7.2a: Summary of seismic refraction data collection at the Fenton River Well-field.

Line Label	Survey date	Equipment used	Length (m)	Geophone Interval (m)	Shot interval (m)
DD'	4/4 -4/28, 2004	48-ch. StrataView	959	3	12
EE'	5/5 – 7/31,2004	48-ch. StrataView	487	3	6
BB'	4/7, 2005	48-ch. StrataView	300	3	12
S0	11/2, 2002	48-ch. StrataView	147	3	6
S1	7/31, 2004	48-ch. StrataView	73.5	1.5	3
S2	7/19, 2004	48-ch. StrataView	73.5	1.5	3
S3	7/19, 2004	48-ch. StrataView	73.5	1.5	3

Table 7.2b: Summary of GPR data collection at the Fenton River Well-field.

Line Label	Survey date	Equipment used	Length (m)	Antenna Separation (m)	Trace interval (m)
DD'	10/21-10/22, 2002	100 MHz Unshield	923	2	0.5
EE'	10/7, 2004	100 MHz Shield	485	0.5	0.1
BB'	10/7, 2004	100MHz Shield	869	0.5	0.1
S0	10/7, 2004	100 MHz Shield	128.8	0.5	0.1
S1	10/7, 2004	100 MHz Shield	79.7	0.5	0.1
S2	10/7, 2004	100 MHz Shield	82.6	0.5	0.1
S3	10/7, 2004	100 MHz Shield	70.4	0.5	0.1

7.4 Results of Hydrogeophysical Investigations

Data processing for the GPR data is quite standard and straightforward with the use of a commercial software package provided by the GPR manufacturer. The whole purpose is to highlight the subsurface reflectors, which is always, more or less, relates to certain geological and/or hydrogeological interfaces. Nevertheless, the data processing

procedures for the seismic refraction surveys are more computing intensified. However, they all use the first arrival travel time information to reconstruct the subsurface seismic velocity structures. A typical first arrival travel time versus the source-receiver offset is shown in Figure 7.6. We used three parallel data processing procedures: i) the intercept time method; ii) the delay time method using the software of SIPwin; and iii) refraction tomography using the software package of GIT2D. All three methods have given similar results, as shown for individual survey lines in Figures 7.7 to 7.11. The final interpretations for all the survey lines are mostly based on the results of the delay time method (SIPwin).

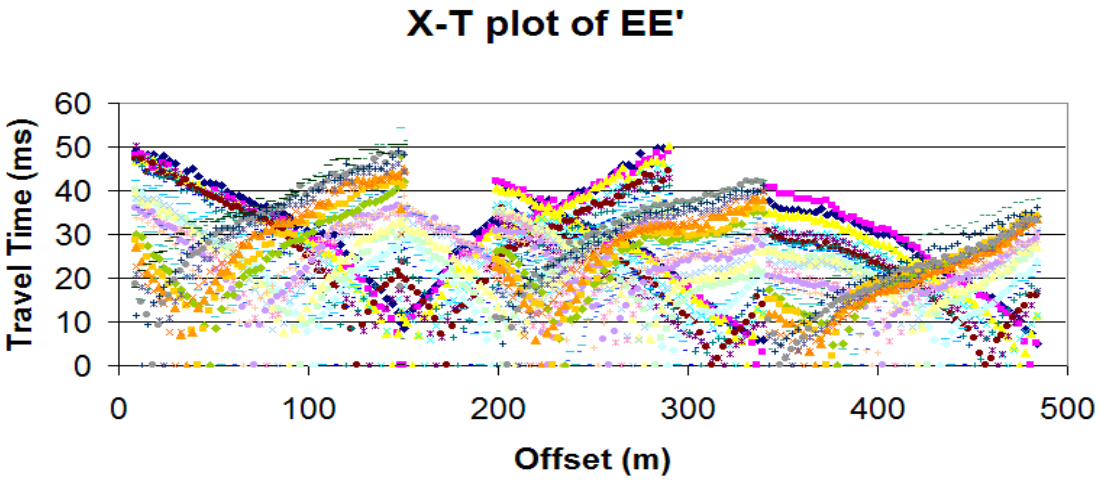

Figure 7.6: The offset-travel time plot for seismic refraction line EE'.

7.4.1 Line B-B'

The subsurface model of line BB' is displayed in Figure 7.7. Figure 7.7a shows the GPR reflection Figure 7.7b shows the water-table and bedrock interface delineated by using SIPwin. The depth-velocity model given by the GIT 2D program for the same set of seismic refraction data can be seen in Figure 7.7c. The interfaces derived from the intercept time method is shown as Figure 7.7d.

The depth-velocity model produced by SIPwin is a two-layer model. Layer 1 has an average thickness of 5 m and seismic waves travel at the average speed of 403 m/s. Velocity of seismic wave in layer 2 averages about 1804 m/s. and its thickness varies laterally. At about 120 m horizontally, the thickness of layer 2 is only about 4m. Layer 2 gets thicker toward the end of the line. This variation in thickness of layer 2 confirms the interpretation of the dipping event seen in GPR profile. The third layer is bedrock which allows the seismic wave to pass through at the speed of about 4112 m/s. Based on the calculated velocities and information on surficial materials of the Fenton River well field, layer 1 can be interpreted as unsaturated stratified drift. Layer 2 can be interpreted to be saturated stratified drift which causes the change in electrical properties of materials found in GPR profile. The interface of first layer and second layer, therefore, is the

location of the water table. Third layer is gneiss or schist unit of the Brimfield Formation (Rodgers, 1985).

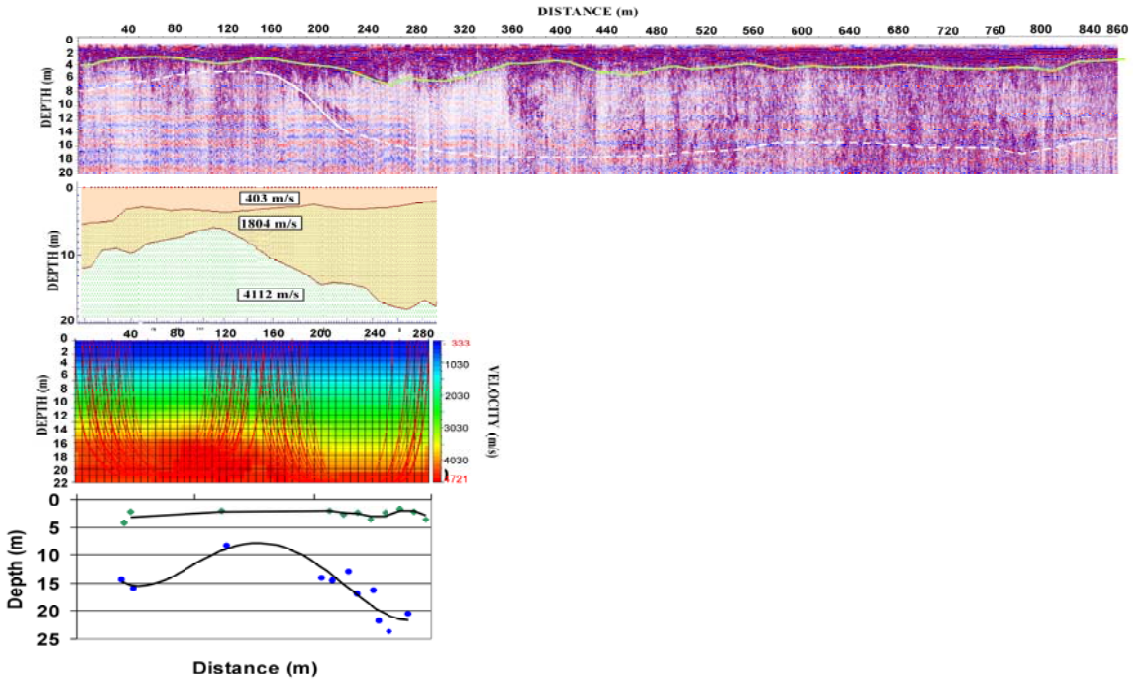

Figure 7.7: GPR data (a), depth-velocity model from SIPwin (b), from GIT2D (c), and from intercept time method (d) for line BB'

7.4.2 Line S0

GPR profile of line S0 suggests a model of almost horizontal layers (Figure 7.8). The water table along line S0 has two distinctive features showing local accumulation of layer 1 at the 20 m mark and 110 m mark. Depth to bedrock can also be sketched out at depth of about 10 m to 12m. Two distinctive features seen in the GPR profile of line S0 are once again marked in the SIPwin model even though they are not as well-defined as in the GPR profile. SIPwin model maps out the water table at a depth of about 2-3 m and bedrock interface at about 10-12 m also. Velocity of about 340 m/s, 1370 m/s and 4400 m/s found in layer 1, layer 2, and layer 3 are typical values for three types of materials mentioned before: unsaturated stratified drifts, saturated stratified drifts, and metamorphic bedrock unit (Bigelow Brook Formation). Since line S0 is a cross line of line BB', a depth check can be done at the intersection point (about the 115 m mark of line BB' and the 75 m mark of line S0). The check shows both lines have similar depth to water table and bedrock at the intersection point.

7.4.3 Line E-E'

A 476-m long GPR depth profile was displayed in Figure 7.9 (a). The energy of the radar wave from the start of the line to about 180 m is generally uniform. This implies a horizontally parallel-layer model. From 180 m to 220 m, there is an accumulation of

layer 1 near the surface to a shallow depth of about 4.5 m. The electrical properties of the materials remain uniform until 280 m. A dipping event is also spotted starting at 350 m. The dipping angle is estimated to be 35° SE.

Seismic refraction data was input into SIPwin program as four different spreads. Length of each spread is specified in data collection part. When put together, all four spreads produce a two-layer model for line EE' (Figure 7.9b). Average thickness of layer one is 2 m. Thickness of layer one maintains 3-3.5 m from the start of the line until it reduces to only 88 cm at about 350 m mark. Velocity of layer 1 ranges from 415 m/s to 692 m/s with and average velocity of 571.5 m/s. This velocity is consistent with the velocity of layer 1 in line BB'. Thus, layer 1 in line EE' is also considered an unsaturated stratified drift layer. The model shows a horizontal layer two at depth of about 13-16 m from the start of the line to about 350 m mark. Its thickness reduces only to about m from 350 m to 360 m making an arc-shaped structure. It is at this location that a dipping event is suspected from the GPR data. When put on the map of bedrock geology, the location coincides with where Black Pond fault separates the Bigelow Brook Formation and the Southbridge Formation. With a velocity in the range of 1947 m/s to 2301 m/s, the materials in layer two can be classified as saturated stratified drift. The special structure found above put the bedrock layer on the left side of the fault to be the Bigelow Brook Formation and the bedrock unit on the right side of the fault to be Southbridge Formation. Because of the similar composition, velocity of seismic wave in these two bedrock units is almost the same and averages 4927 m/s.

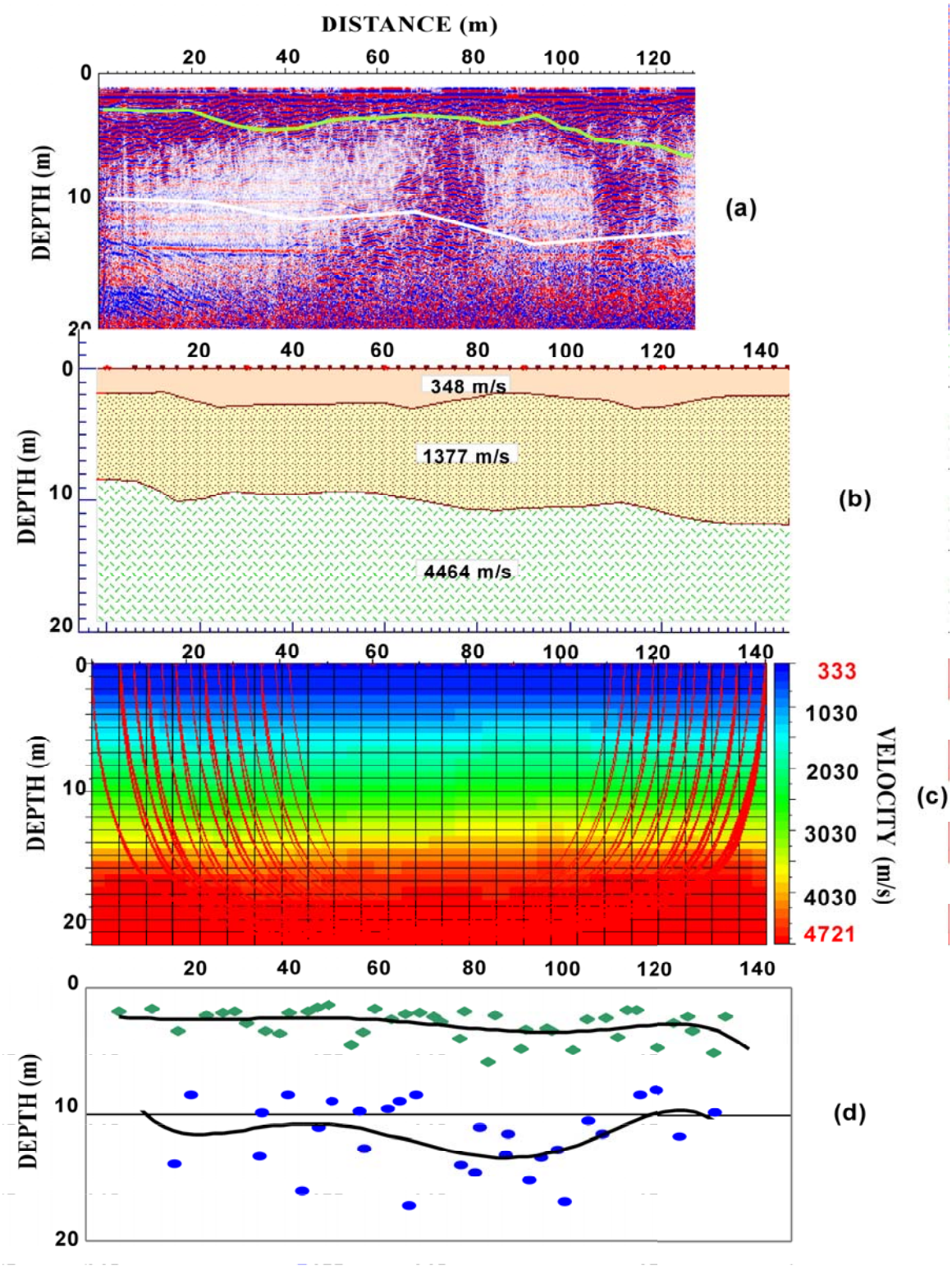

Figure 7.8: GPR profile (a), depth-velocity model from SIPwin (b) depth velocity from GIT2D (c), and depth profile using intercept time method (d) for line S2.

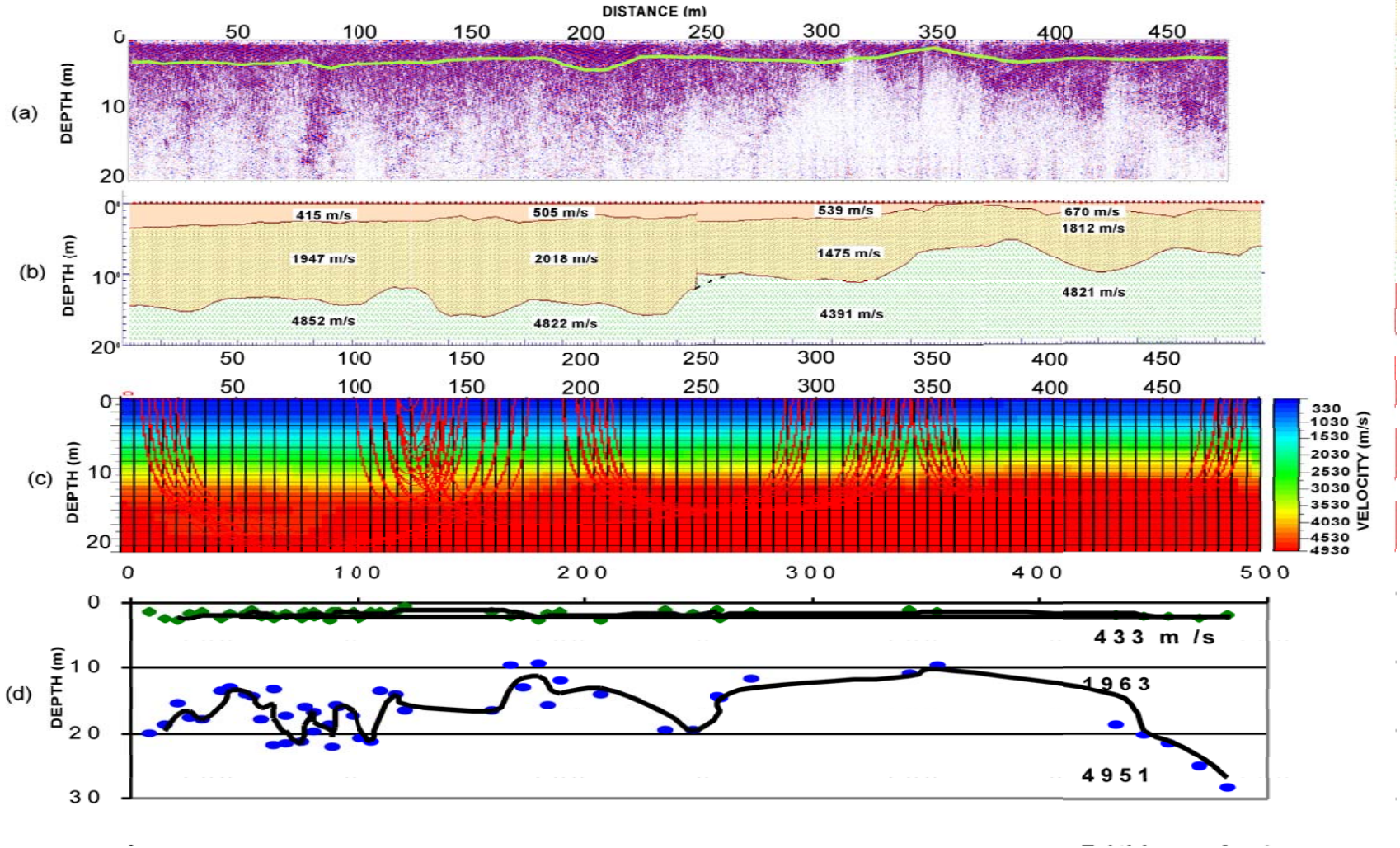

Figure 7.9: GPR profile (a) and depth-velocity model using SIPwin software (b) depth-velocity model using GIT2D software (c) and depth-velocity profile using intercept-time method for line EE'.

7.4.4 Line S1

The GPR data of line S1 in Figure 7.10 (top row, left column) shows mostly horizontal layers of similar property. However, it should be note that there is a change in the electrical properties of the material at 8 m in depth which extends laterally from 20 m to 40 m mark. The SIPwin model in Figure 7.10 (second row, left column) shows an accumulation of stratified drift material about the center of the cross section. Bedrock interface at this location is as deep as 18 m. Seismic wave velocities of unsaturated stratified drift (layer 1); saturated stratified drift (second layer) and bedrock (third layer) are 482 m/s, 1890 m/s and 3931 m/s, respectively. Since line S1 crosses line EE' about 25 m from the start of line EE' near Well UCA, the bedrock unit of line S1 is also the same bedrock unit with that of line EE' at that location or the Bigelow Brook Formation.

7.4.5 Line S2

GPR data in Figure 7.10 (top row, central column) shows a gently dipping layer starting from the beginning of the line at shallow depth of about 4 m. The layer dips more steeply from 20 m mark to 40 m mark. Loss of energy of radar wave can be seen at very shallow depth of about 4-6 m throughout the length of the cross section.

The structure found in the GPR profile turns out to be the dipping layer of stratified drift in the SIPwin model (Figure 7.10, second row, central column). Line S2 cuts line EE' at point A which lies at about the 40 m mark on line S2 and at about the 242 m mark on line EE'. Depth to aquifer at the 40 m mark of line S1 is about 2-3 m which is very close to depth to aquifer of about 2.5m found at the 242 mark of line EE'. Depth to bedrock can also be checked at this intersection. Depth to bedrock found at line S2 is 4 m less than that found at line EE'. Velocities of 484 m/s, 1768 m/s and 5249 m/s are calculated for the seismic wave in layer 1 of unsaturated stratified drift, layer 2 of saturated stratified drift and Bigelow Brook bedrock unit, respectively.

7.4.6 Line S3

The GPR profile of S3 shows a loss of wave energy in the first 30 m and last 20 m of the line (Figure 7.10, top row, right column). The wave energy is attenuated at a very shallow depth of about 5-6m. This depth is consistent with the depth at which the wave is also attenuated at the 342m mark, the intersection point of line S3 and line EE'.

The SIPwin program produces a two-layer model for line S3 (Figure 7.10, second row, right column). The first layer of unsaturated stratified drift has a velocity of 425 m/s and an average thickness of about 2.5 m. The second layer of saturated stratified drift has a velocity of 1624 m/s and its contact with the underlying bedrock unit can be located at depth of about 7-8 m. Line S3 cuts line EE' at its 12 m mark and 342 m mark on line EE'. A check of depth to the water table and bedrock at this intersection point shows a good match.

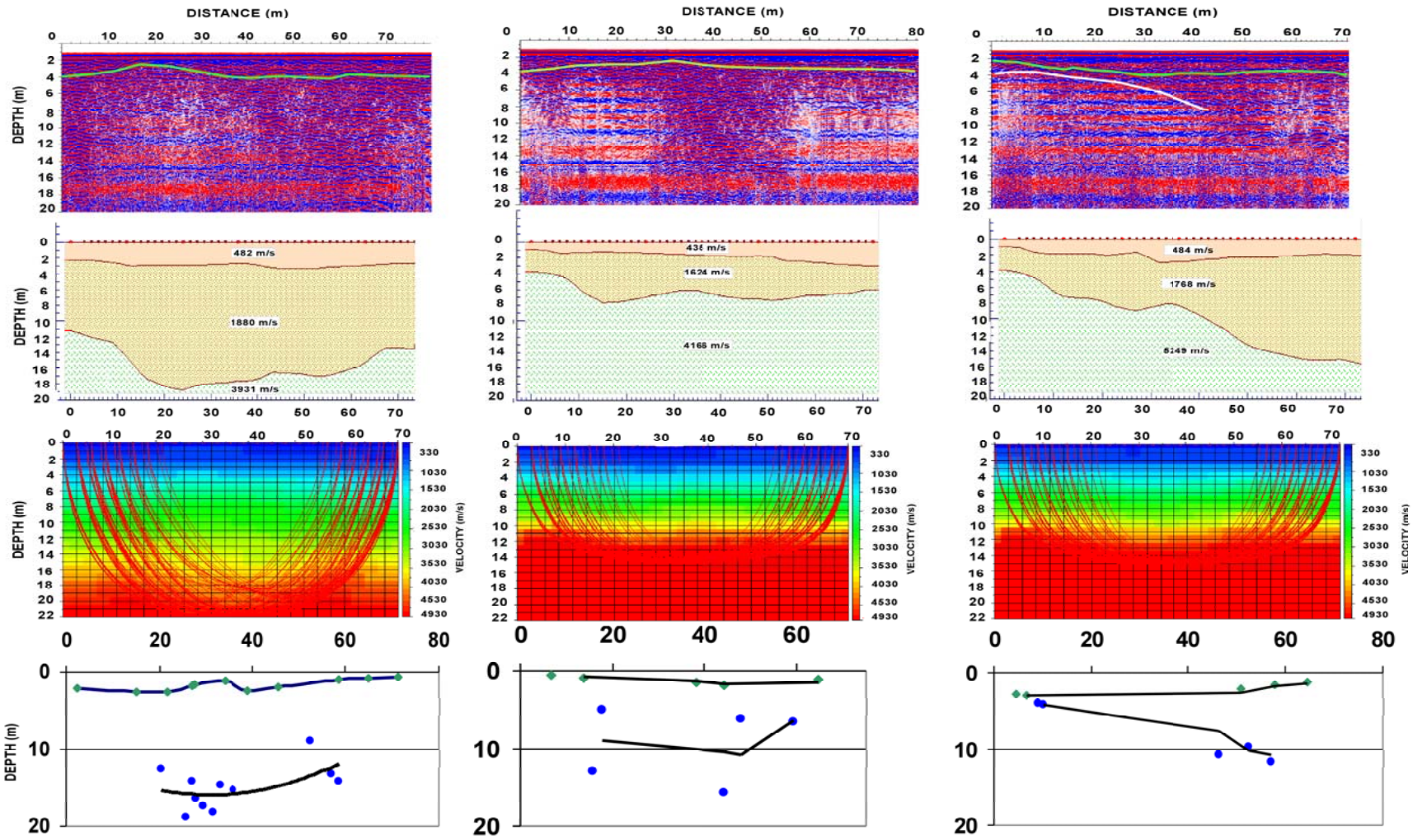

Figure 7.10: GPR profiles (top row) and depth-velocity models using SIPwin software (second row), depth-velocity models using GIT2D software (third row), and depth profiles using intercept time method (bottom row) for line S1, S2 and S3 (from left to right)

7.4.7 Line D-D'

Figure 7.11a shows the GPR profile of a total 916 m in length and 20 m in depth for line DD'. An interval of 20 m from 640 m to 660 m is the location of Fenton River Bridge which perpendicularly cuts line DD'. An overall estimate of the location of the water table or the depth at which the wave energy is lost due to change in the amount of water present in the materials can be easily made throughout the profile. Water table can be expected to be found at as shallow as 3-4 m deep at some location, such as 200 to 240 m interval.

With the input of elevation measurements, the SIPwin program inputs seismic refraction data of six spreads and produces three two-layer models with maximum depth of 70 m (Figure 7.11b). When combined together, the final model shows a thin layer of unsaturated stratified drift at shallow depth of about 4-5 m from the surface. The average velocity of seismic wave in this layer is 594 m/s. Layer 2 of saturated stratified drift starts out as a thin layer of less than 10 m in thickness which then thickens toward the Fenton River Bridge where the thickness reaches about 20m. This value of thickness remains after the bridge until the 740 m mark. To the rest of the line, the thickness of layer 2 averages about 15 m. Since seismic line stops about 39 m before Fenton River Bridge, interpolation of depth to aquifer and bedrock has been made and shown as dash lines. An average velocity of 1727 m/s can be calculated for layer two. Bedrock unit under line DD' is identified as Southbridge Formation through which seismic waves pass with an average velocity of 5293 m/s.

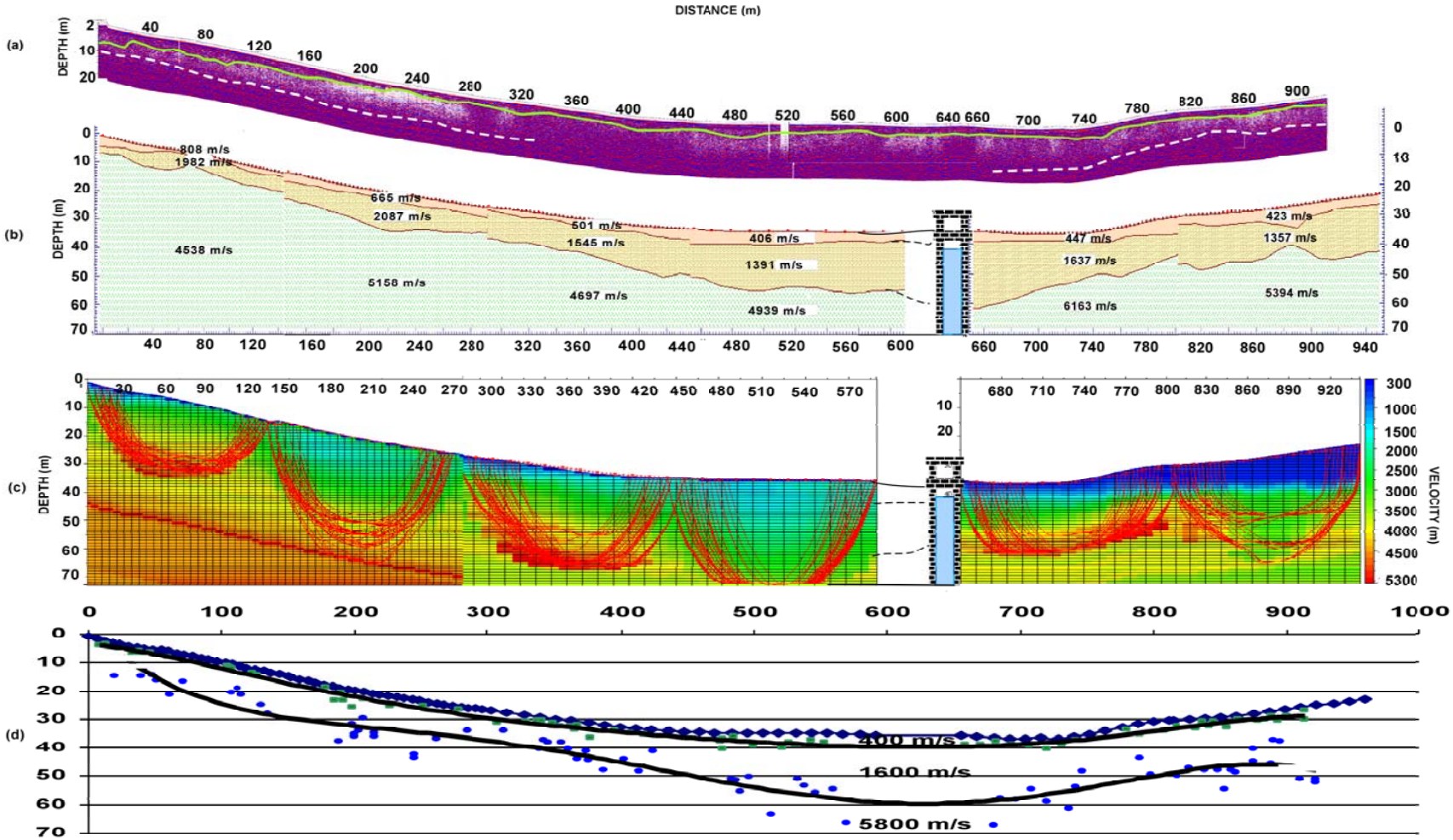

Figure 7.11: GPR profile (a) and depth-velocity model using SIPwin software (b) depth-velocity model using GIT2D software (c) and depth-velocity using intercept time method (d) for line DD'.

7.5 Comparison of Seismic Processing Methods and Results

Table 7.3 summarizes the interpretation of layer velocities and boundaries from the delay time method (SIPwin) that is the most trustworthy method among the 3 approaches. An average velocity of 471, 1751, and 4652 m/s for layer 1, layer 2, and layer 3, respectively. The average depth to the water table ranges from 1 to 4 m. The bedrock interface can be found at depth ranging from 6 m to 16 m.

Table 7.3: Summary of layer velocities, depths to water table and depths to bedrock determined by the delay-time method (SIPwin).

Line	Ave. V1 (m/s)	Ave. V2 (m/s)	Ave. V3 (m/s)	DEPTH Z1(m)		DEPTH Z2(m)	
				Min	Max	Min	Maxi
BB'	403	1804	4112	1.98	5.24	5.96	17.95
S0	348	1377	4864	1.96	3.41	8.95	11.75
EE'	572	2067	4952	0.4	4.75	4.69	16.51
S1	482	1888	3931	2.3	3.4	11.4	18.9
S2	464	1768	5249	1.3	2.96	3.9	17.46
S3	435	1624	4166	1.06	2.69	2.78	11.04
DD'	594	1727	5293	1	8	5	21
AVE.	471	1751	4652	1	4	6	16

All seismic processing method used in this study, the intercept time method, the delay-time method and seismic tomography, are subjective to some level. The subjective process of picking the first arrivals has the effect in all three methods since all methods use first arrivals as input data. In the intercept-time method, the error is also contributed by the process of applying the best fit lines through travel time data to obtain layer velocities. The same source of error can be found in the process of assigning layers in the delay-time method used in the SIPwin program. Among the three methods, seismic tomography used in the GIT2D program is the least subjective method. Nevertheless, the *a priori* initial velocity model still subjectively depends on people's preliminary understanding of the subsurface at the site. Presumably, the inversion results should be robust and are not dictated by the initial model.

7.6 Discussion and Validation

A seismic refraction and ground penetrating radar survey has been conducted to investigate the hydrogeology at the Fenton River Well Field, Storrs, Connecticut. The surveys are part of the hydrogeologic assessment stage of the Fenton River project which studies the long-term impact of the Fenton River water supply wells to the habitat of the Fenton River. The objectives of this report is to discuss the geophysical methods used to collect and process field data in order to locate water table levels, delineate bedrock topography and estimate the lithology at study site. Integrated results were used in ground water modeling for the Fenton River project.

Intercept time method, delay time method and seismic tomography all produced very similar results. However, each method has its own limitations. Intercept time method is the most subjective and time-consuming method. Seismic stratigraphy using the SIPwin program gives a better interpretation of depth to interfaces and structures. Seismic tomography using the GIT2D program can produce a better velocity structure compared to the other two methods, but cannot depict sharp stratigraphic interfaces.

Interpretation of seismic refraction data characterizes the stratigraphy of Fenton River Well field to three layers. The top layer is made of unsaturated stratified drift. Thickness of the top layer averages to about 3-4 m which is fairly uniform at almost every place of the study site. Seismic waves travels at an average speed of less than 1000 m/s. The second layer is composed mostly of saturated stratified drift. The boundary between the top layer and the second layer is considered as the aquifer. Thus, the aquifer of the Fenton River Well field can be located at about 4-5 m from the surface. Thickness of saturated stratified drift and thus, depth to bedrock interface, varies from location to location at study site. Along line BB', bedrock interface is about 6-18 m from the surface. Bedrock topography along line DD' is more varied. Sediments seem to accumulate as thick as 30 m near the Fenton River Bridge. Cross lines S0, S1, S2 and S3 can be used to confirm the results of long line BB' and EE'.

Table 7.4 summarizes the comparison between the depth to aquifer and depth to refusal bedrock given by LBG with our interpretation at the corresponding locations. In general, our determination of depths to aquifer and bedrock has a great similarity to those read from well logs, except for depths to bedrock at well B, well A and TB-3. Our calculation of depth to bedrock at well B is 5.7 m shallower then that given by LBG. This difference can be explained by the offset of locations since this is the interpretation at the assumed location instead of the actual location of well B. As for well A, LBG gives reading of depth to refusal instead of depth to bedrock. Our interpretation of deeper bedrock confirms their estimated depth to bedrock at well A. Depth to bedrock at well TB-3 was calculated 3.4 m deeper than that given by LBG. To explain this difference, the location of TB-3 is at the end of the seismic spread which makes the inversion process of SIPwin difficult and produces spurious bedrock depth in this area. Well MW-2-99 and MW-3-99 were not used by LBG to draw cross section BB' but can be used to validate our interpretation of depth to aquifer and bedrock at the vicinity of these wells. Well MW-3-99 lies exactly on our cross section BB' and its depth to bedrock given by LBG matches very well with our interpretation. The validation of the geophysically-derived stratigraphic model for survey lines BB', S0, and DD' is also shown as Figure 7.12.

Table 7.4: Comparison of depths to the water table and bedrock given by LBG and geophysical surveys at given well locations.

WELL	Depth to water table (m)		Depth to refusal/bedrock (m)	
	LBG	This study	LBG	This study
MW-2- 99	2.7	4.0	5.3	9.2
MW-3- 99	4.3	N/A	17.4	17.5
MW-7-99	4.3	N/A	11.3	16.8
B	2.4	N/A	22.3	16.6
C	1.5	N/A	19.5	17.5
A	2.7	2.4	11.2	14.9
TB2	5.5	2.1	7.9	8.7
D	3.8	3.5	18.0	16.6
MW-10-99	3.2	3.1	8.5	18.0
MW-11-99	2.4	3.5	17.7	15.5
MW-12-99	7.0	4.8	13.1	10.4
TB 3	4.3	5.7	4.7	8.1
UCSB05	N/A	2.68	9.14	11.18
UCSB07	N/A	1.82	9.75	8.95

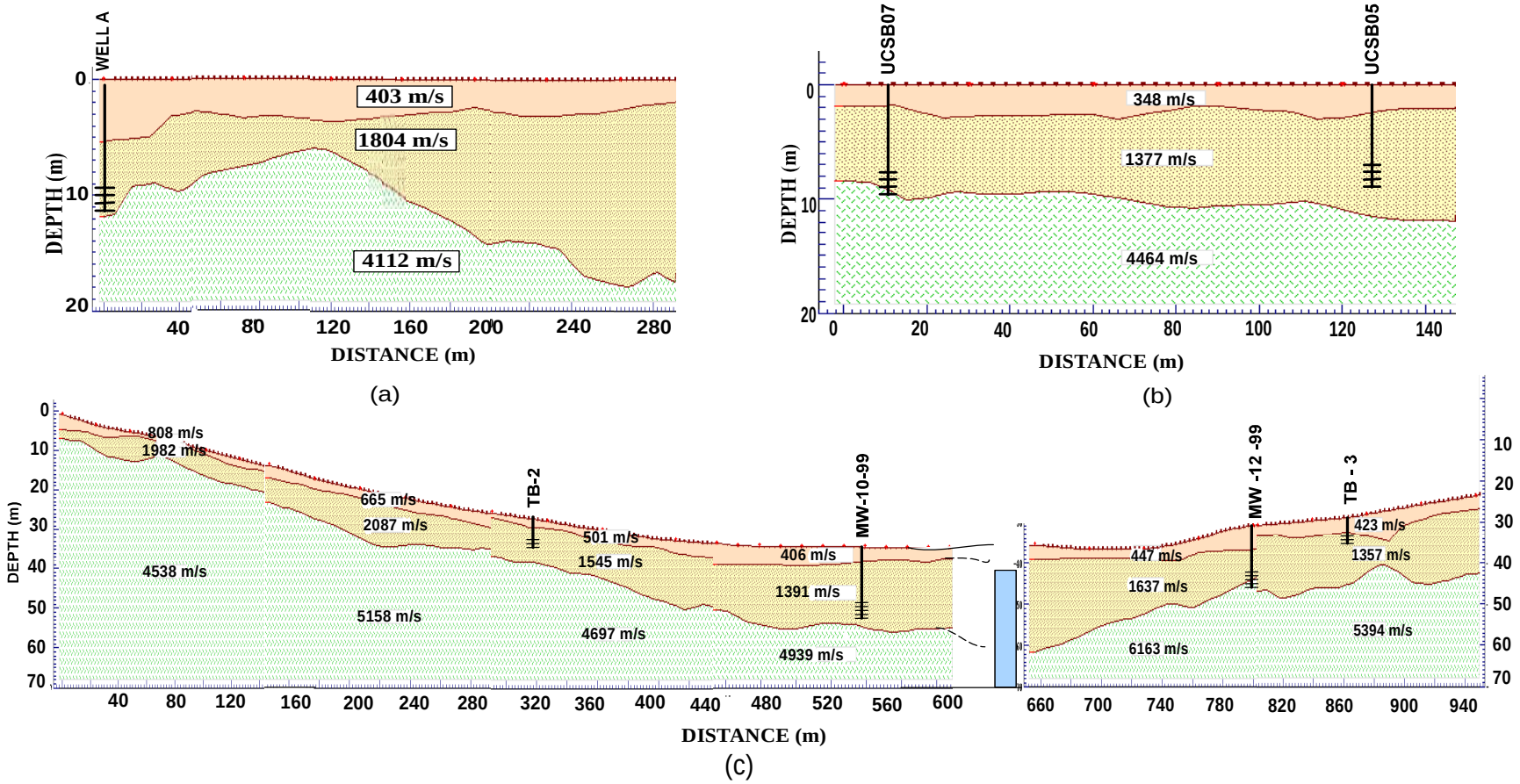

Figure 7.12. Validation of subsurface structure results for the SW most 300 m of line BB' (a), S0 (b), and DD' (c) with drilling information.

7.7 Integration of Geological and Geophysical Survey Results for the Fenton River Drainage Basin

To investigate the hydrogeology of the Fenton River drainage basin, and more specifically characterize the bedrock of the basin in the vicinity of the well-field, three sources of data were used. Prioritizing the sources of geological information in terms of reliability, the most reliable data could be attributed to the physical outcrop of bedrock. After a field survey conducted in the Fenton River well-field, the location of bedrock outcrops were determined on USGS maps. The positions of bedrock outcrop were determined in the field by the University of Connecticut research team using the Pathfinder™ GPS device. The second source of data was the borehole information. Some of the borehole data were taken from newly drilled USGS bedrock boreholes, some were from Level A study conducted by LBG (LBG 2002), and some were from available historical data. The common drawback with using the borehole data in determination of bedrock elevation is that if the drilling device hits a boulder during the soil bore drilling activity, results may mistakenly be interpreted with the actual bedrock. To avoid the problem of misrepresenting bedrock elevations all existing information were thoroughly compared to assure that the bedrock contour was determined with the most possible accuracy. The University of Connecticut Geophysics research team supplied the third source of bedrock elevation data. The bedrock elevations determined with groundwater penetrating radar (GPR) and seismic methods were used qualitatively in creating the bedrock contour maps for the Fenton River well-field.

Bedrock contour maps were incorporated into the model domain by substituting the bedrock elevation data in affected cells with newly estimated bedrock elevations discussed above. The bedrock elevation contours and location of cells replaced in the model domain are shown in Figure 7.13. Based on the new data, the thickness of the till layer was reduced from 50ft to 25 ft uniformly distributed over the upland till layer. To compare the newly generated layer thickness with the initial model assumptions, three cross-sections were provided (transects are identified in Figure 7.13). Figures 7.14, 7.15, and 7.16 show cross-sections A-A', B-B' and C-C'. Cross-sections A-A' and B-B' show the difference between the initial and the calibrated bedrock elevation contours within the model domain. Cross-section C-C' is a East-West cross-section across the simulation domain for all three layers for (a) initial and (b) calibrated simulation domain. Figure 7.17 is a perspective view of the simulation surface topography and the three discrete model layers.

The bedrock delineation data pointed to the fact that the outcropping of the bedrock in the geology of the study site partially divide the stratified drift aquifer at a location close to well A, between wells A and B, as shown in Figure 7.18 lending some credence to the "egg-carton" compartmentalization of the aquifer hypothesis.

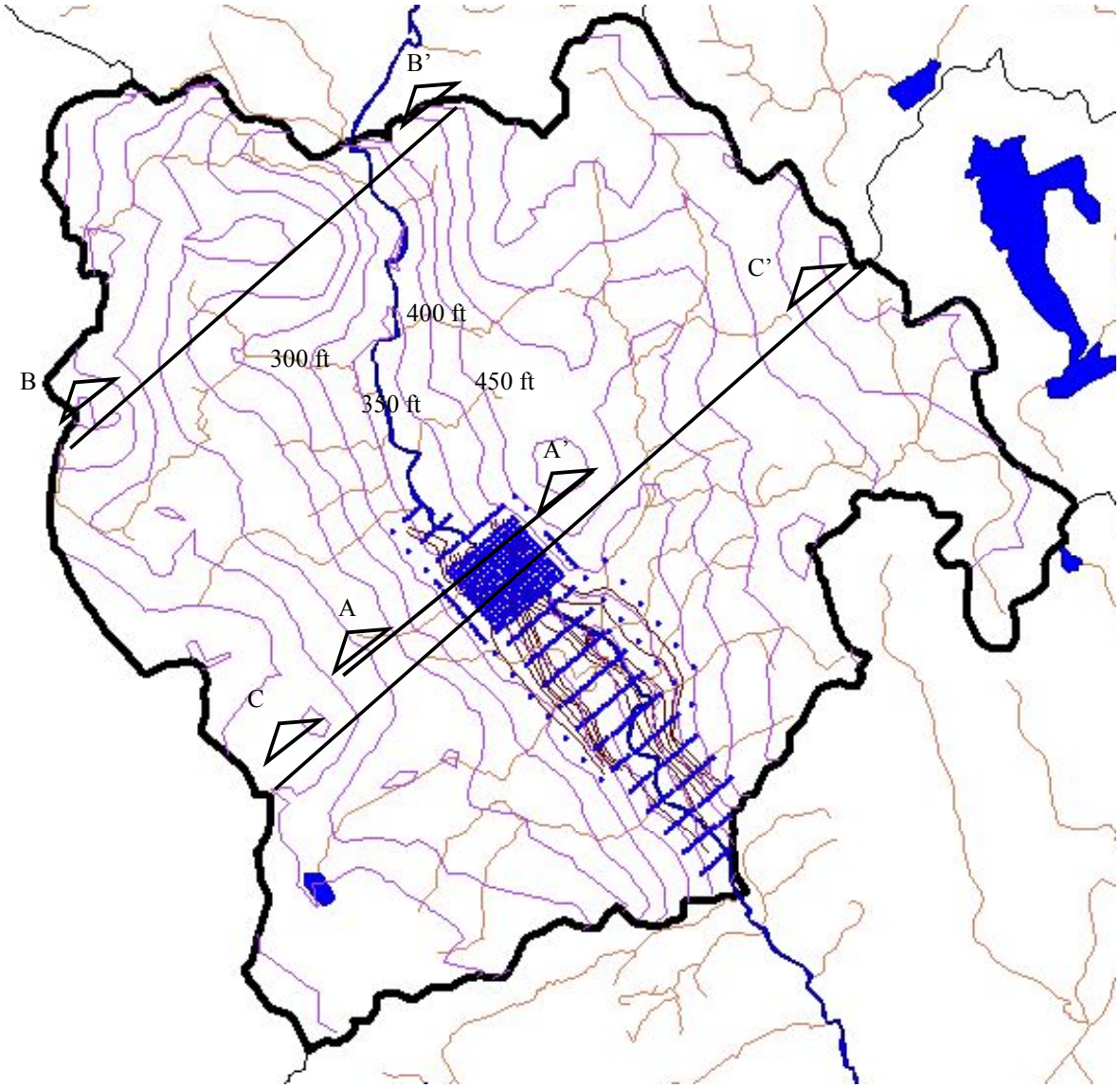

Figure 7.13. Bedrock elevation and topographic surface elevation contours in the model domain. Grid cells affected by the bedrock elevation update are identified as dots. Cross-section transects A-A', B-B', and C-C' are also shown.

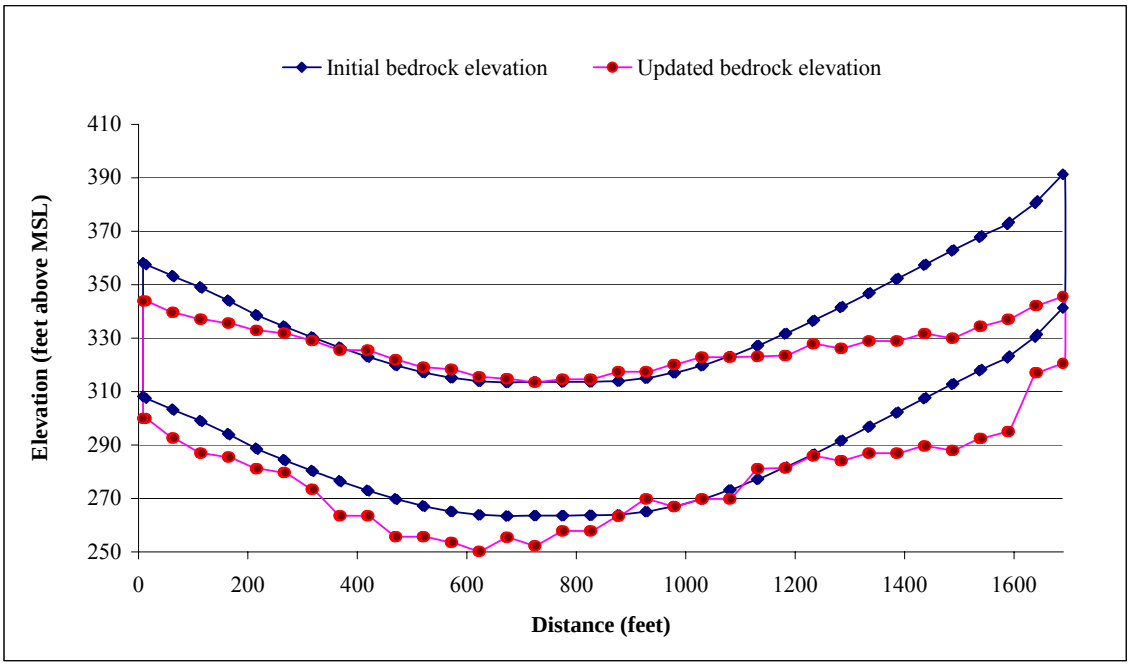

Figure 7.14. Cross Section A-A'. for bedrock layer 1.

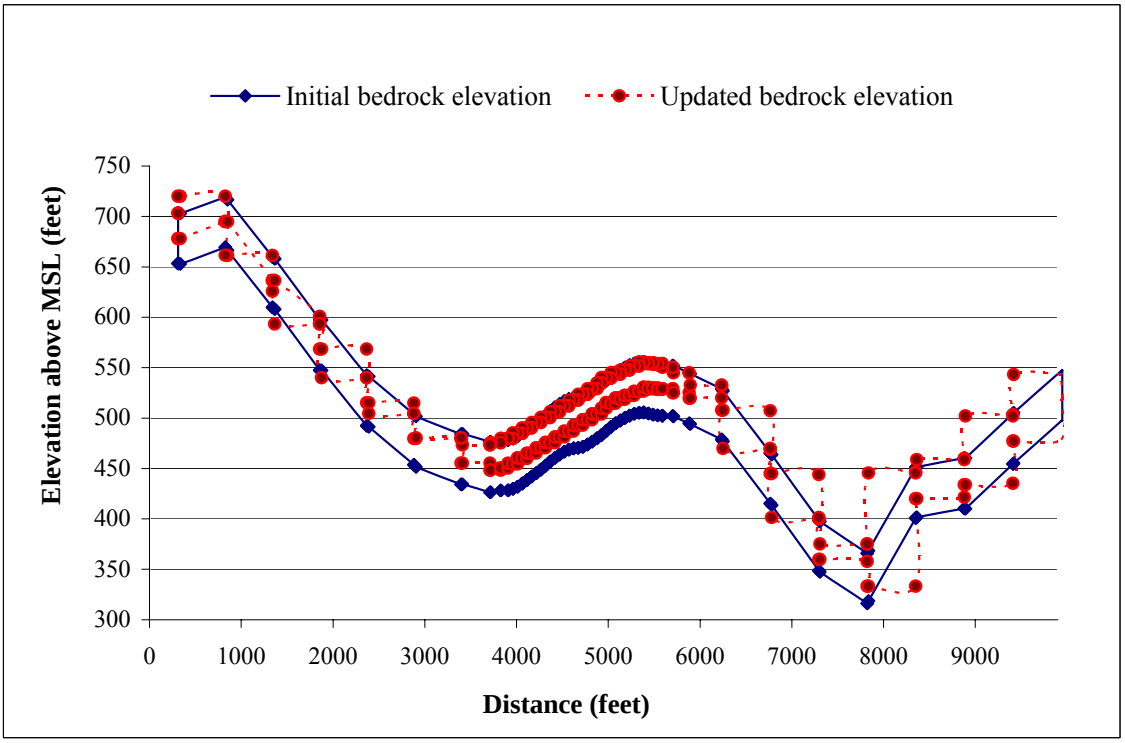

Figure 7.15. Cross Section B-B'. for bedrock layer 1.

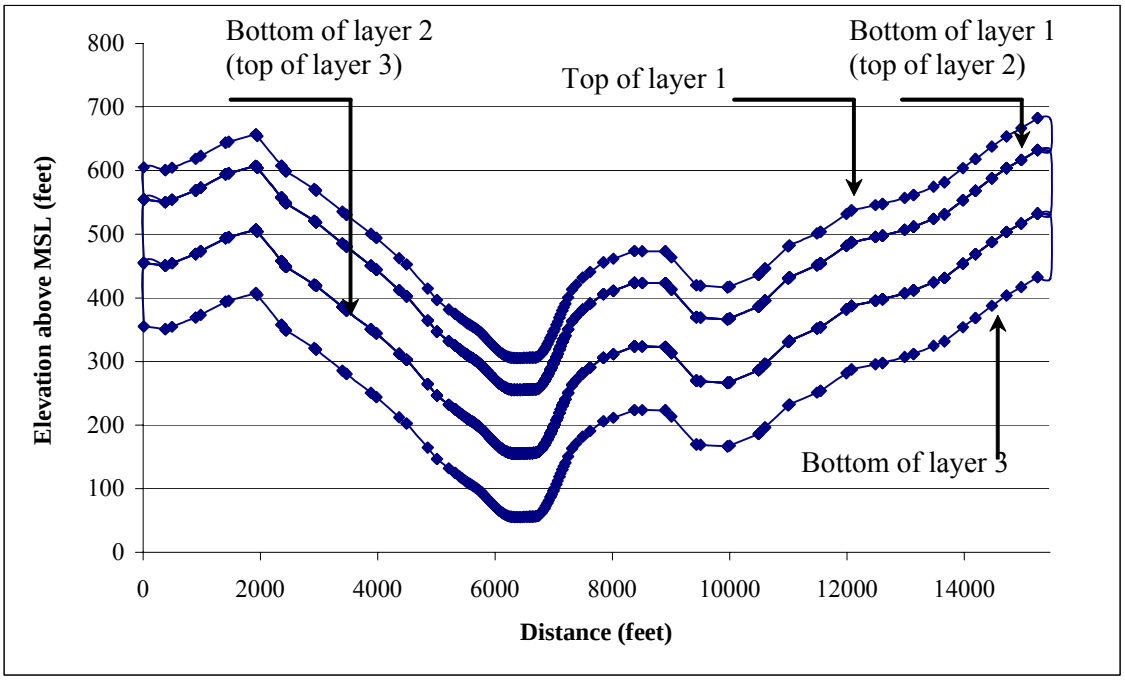

(a)

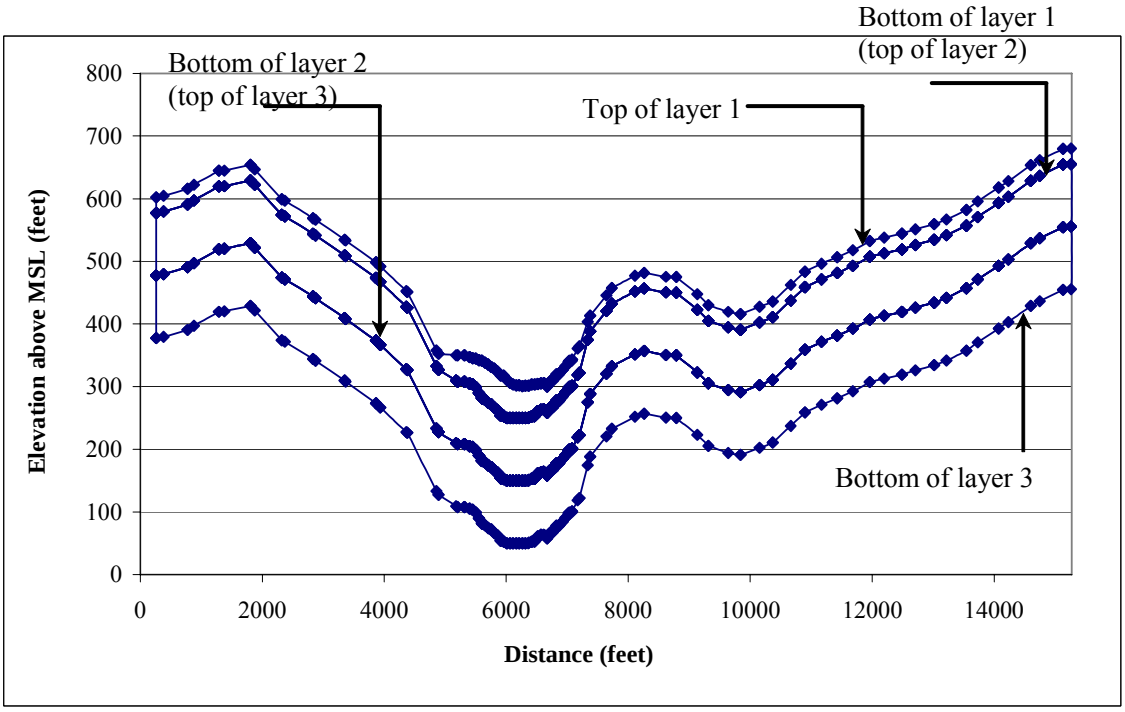

(b)

Figure 7.16. Cross Section C-C', (a) initial and (b) updated simulation layer depths.

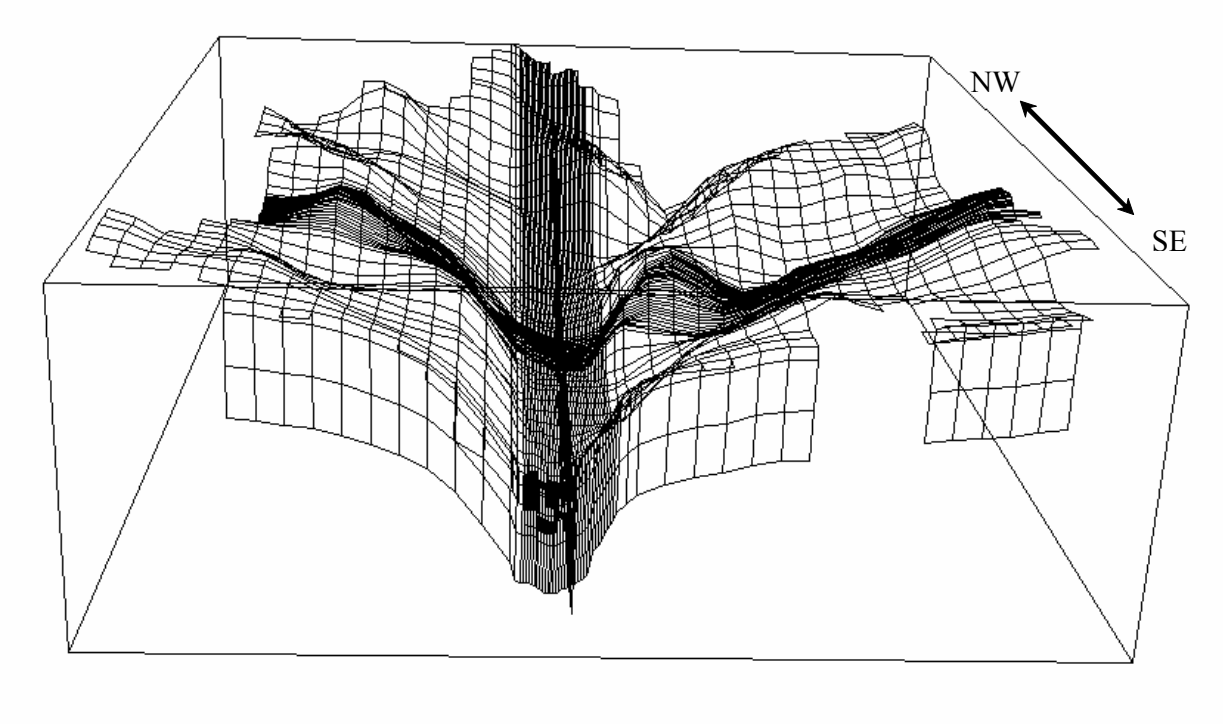

Figure 7.17. Bird's eye view of the model surface topography and the three hydrogeologic layers.

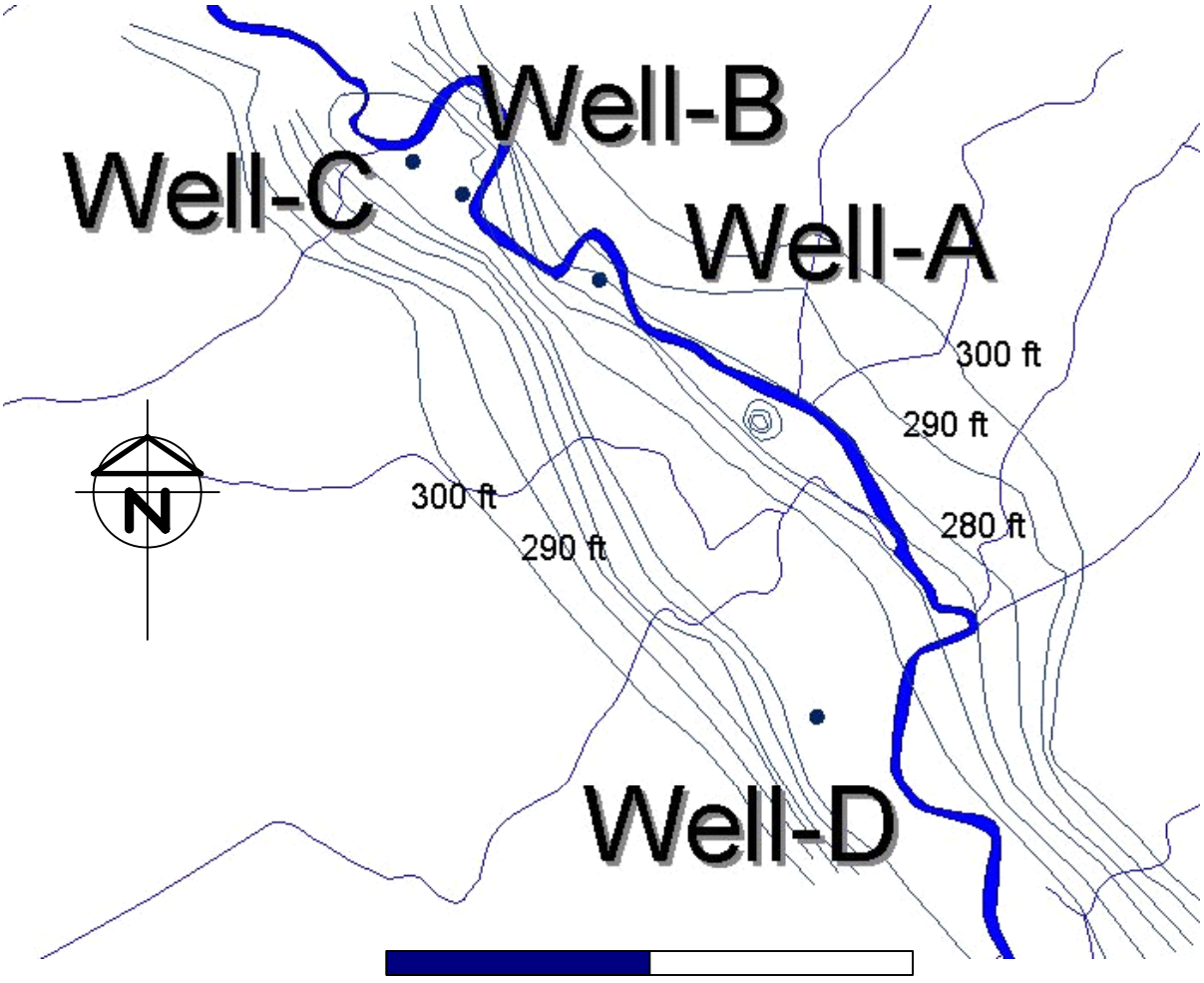

Figure 7.18. Bedrock contours in the vicinity of the pumping wells (contours are plotted with elevation increments of 10 ft).

8.0 MATHEMATICAL MODEL DEVELOPMENT AND CALIBRATION

8.1 Simulation Concept

Our modeling paradigm is based on the "modeling pyramid" (Figure 8.1) , which comprises experimental and field testing protocols, analytical theory, simplified simulations (e.g., closed form solutions and semi-analytical approaches) used for benchmarking, observations used for calibration and validation, and mathematical and associated numerical models. The pyramid's vertex and our modeling paradigm's objective is understanding and approximating reality as closely as possible. In this study, we have employed state-of-the-scientific practice techniques and algorithms for our modeling efforts and these tools have been calibrated and validated using recent experimental testing and historical observations, respectively. It should be recognized, however, that a full and completely accurate representation of reality is a panacea that can never be attained as there will always exist errors and uncertainty with our modeling predictions. Nevertheless, the study team feels reasonably confident that our predictions and management suggestions are accurate, especially since our analysis is based on differential responses, that is how much better one management scenario is compared to the rest, and not on the specific response.

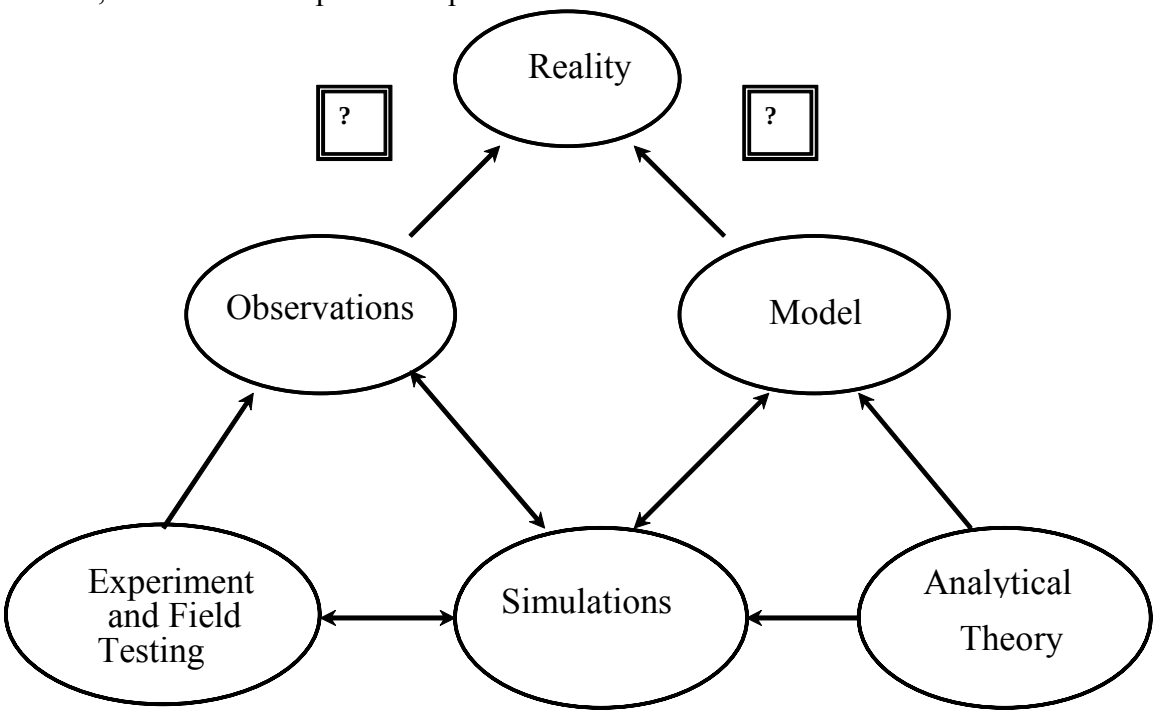

Figure 8.1. Schematic depicting the modeling conceptualization.

8.2 Model Description

In this study, the effect of pumping wells on streambed infiltration during drought periods was simulated with the aid of a computer model. A graphical user interface

(GUI) developed by the United States Geological Survey (USGS) was used to create model input files. The GUI was developed in a numerical environment program called Argus-ONE (ArgusOne, Version 4.2). The geographical information system (GIS) layers pertaining to the Fenton River watershed were linked to MODFLOW-2000 (Harbaugh *et al.*, 2000), which is being used to simulate ground water flow during steady state and transient conditions. The finite-difference grid in MODFLOW-2000 is assumed to be rectangular horizontally, but the grid can be distorted vertically. Time increments in MODFLOW are grouped into periods of constant stress (stress periods) and shorter intervals within the stress periods (time steps). The time-dependent input data can be changed at every stress period.

The equations used by MODFLOW for each finite difference cell are derived based on Darcy's Law and conservation of mass. The derivation gives a partial differential equation, which is used by MODFLOW. The partial-differential equation of groundwater flow used in MODFLOW is:

$$\frac{\partial}{\partial x}(K_{xx}\frac{\partial}{\partial x})+\frac{\partial}{\partial x}(K_{yy}\frac{\partial}{\partial y})+\frac{\partial}{\partial z}(K_{zz}\frac{\partial}{\partial z})-W=S_s\frac{\partial h}{\partial t} \qquad (8.1)$$

where K_{xx}, K_{yy}, and K_{zz} are the values of hydraulic conductivity along the x, y and z coordinate axes; h is the potentiometric head; W is the volumetric flux per unit volume representing sources and/or sinks of water; S_s is the specific storage of the porous material; and t is time. This equation, when combined with appropriate boundary and initial conditions, describes transient three-dimensional ground-water flow in a heterogeneous and anisotropic medium, provided that the principal axes of hydraulic conductivity are aligned with the coordinate directions.

Variable-spaced grid cells were used in the simulations. The far-field grid is 515 × 515 feet, whereas in the well-field area, the grid spacing was refined to pixel dimensions of 125 × 125 feet. The finite difference grid was oriented to follow the axis of the River (Figure 8.2) as much as possible. The eastern boundary of the simulation domain was chosen as the line that divides the Mount Hope and Fenton River watersheds. The western boundary is the line that divides the Fenton River and the Willimantic River watersheds. The northern boundary of the model is located about 0.5 miles north of the Old Turnpike (Route 44) where the aquifer is thin and narrow. The southern boundary of the model is near the intersection of Chafeeville and Stone Mill Roads. Simulation boundaries were initially chosen qualitatively and test simulations were run to determine the zone of influence of the pumping wells through particle tracking. During early simulations, it was found that at steady state, water particles would extend beyond the initial simulation boundaries (Figure 8.3), thus indicating that our simulation boundary had to be extended. Therefore, the model boundaries were extended so that pumping would have minimal (if any) impacts on them (Figures 8.3 and 8.4) within the time horizon of interest in our simulations (less than 50 years).

The model has three vertical layers. Based on available borehole information and maps obtained from USGS, the upper layer was divided into Stratified Drift, Till, and thick Till. Two bedrock layers underlie the upper layer (Figures 7.16, 7.17 and 8.5).

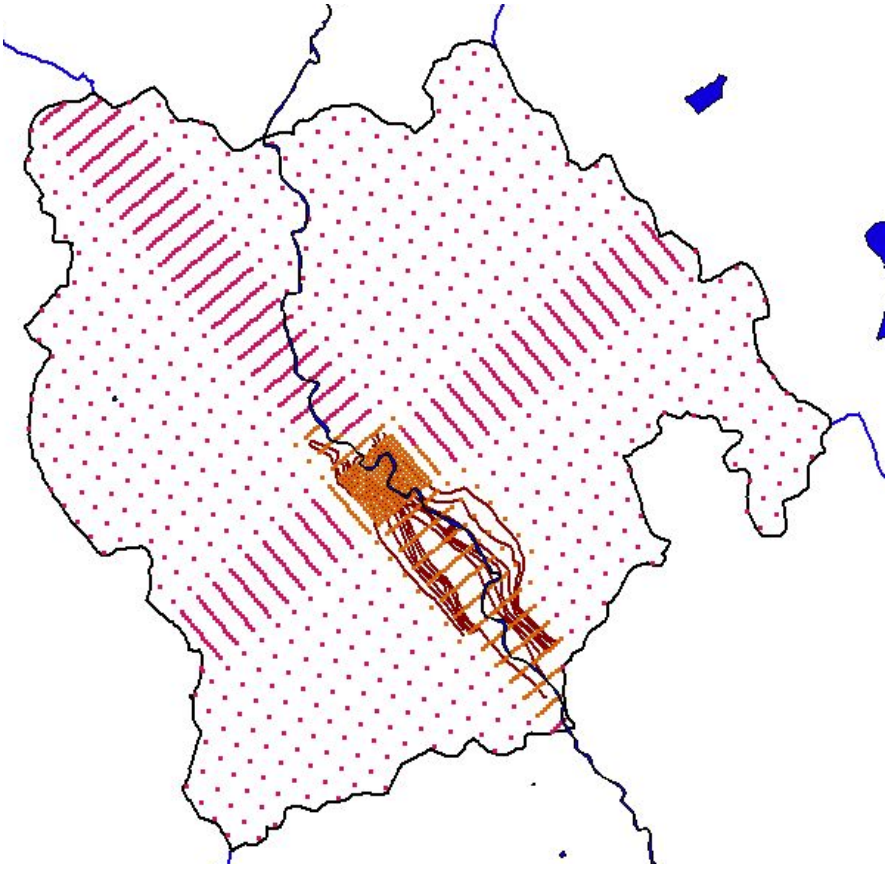

Figure 8.2. Fenton River simulation domain with finite difference grid and bedrock contours in the vicinity of the well-field.

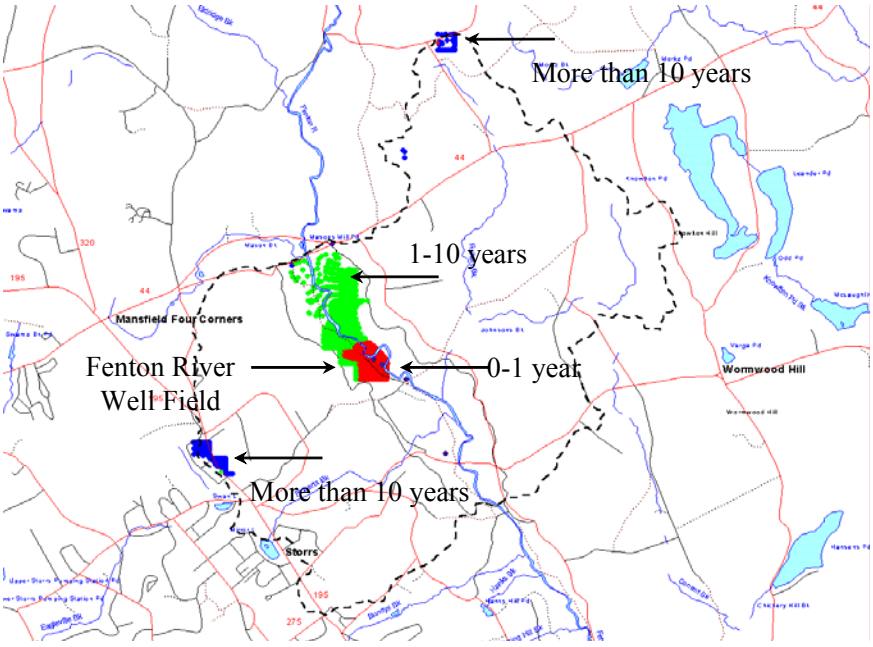

Figure 8.3. Initial simulation domain and zone of pumping influence under steady state flow conditions.

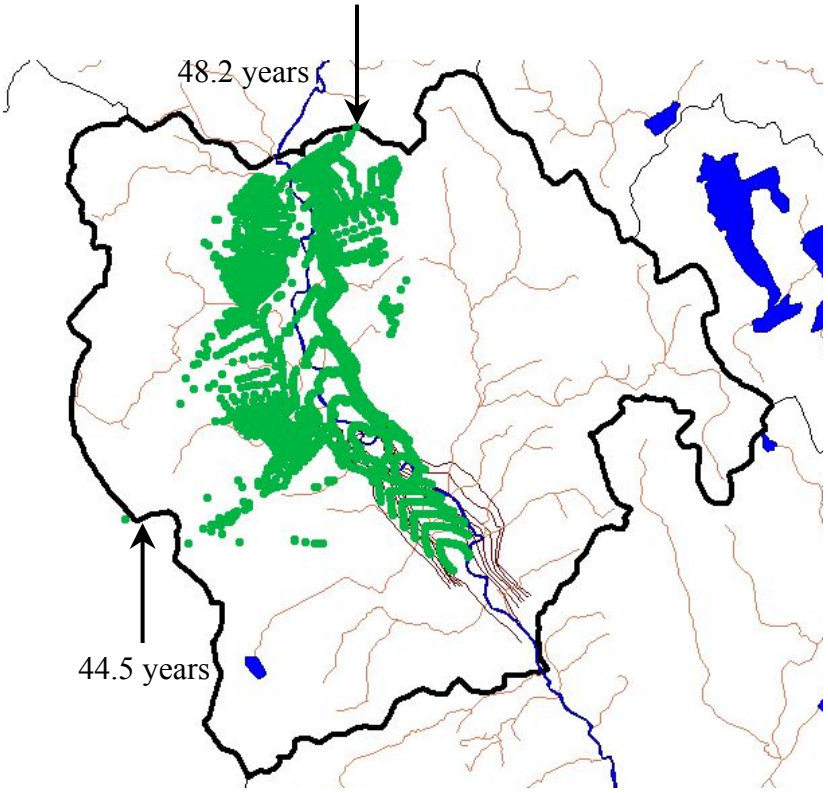

Figure 8.4. Final simulation domain and zone of pumping influence under steady state flow conditions.

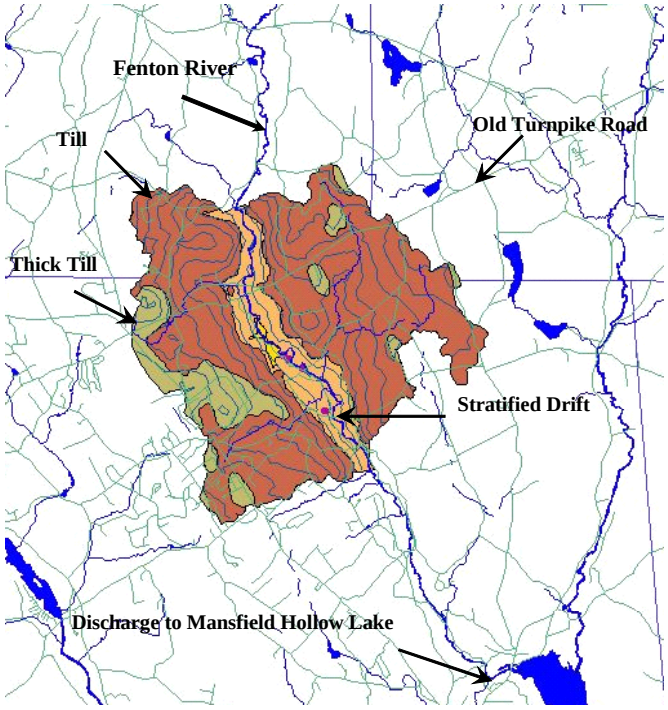

Figure 8.5. Simulation domain and geological unit coverage.

8.3 Model Calibration

Two separate pumping tests were conducted in March and August of 2004 to measure the stream flow loss during pumping and estimate aquifer parameters. During the March pumping test, water levels in six monitoring wells (MW4S-99, MW4D-99, MW5-99, MW6-99, USGS-Bedrock1, and USGS-Bedrock-2) were measured. Automatic water level measuring devices (Minitrols®) were installed in the first four monitoring wells. The USGS-Bedrock1 Well was drilled in Horsebarn Hill (approximately 1200 ft west of the well-field), and the USGS-Bedrock2 Well was placed next to MW5-99. The water levels in the USGS bedrock wells were continuously being measured with the automatic device in the wells by the USGS field team. However, due to low battery the data in the USGS-Bedrock2 Well near the well-field was not recovered and thus could not be used in the parameter estimation procedure. Similarly, due to some mechanical problems, the data from MW4D-99 exhibited inconsistencies and were not used in the parameter estimation process. The August pumping test was disqualified from our analyses since it was plagued by numerous pump shut-offs that essentially invalidated the assumptions of the parameter estimation procedure.

For each monitoring well, point-based, initial aquifer parameter estimation was conducted with the aid of a simulation package called Aquifer-Win32 (ESI, 2003). The software AQTESOLV 3.5 by HydroSOLVE, Inc. was also employed in preliminary scoping calculations.

Both aquifer parameter estimation software implement a variant of the Levenberg-Marquardt non-linear optimization algorithm and ignore the inter-play between different wells and possible spatial distribution of the estimated parameters. The estimated parameters were then used to run the simulations. However, the simulated results showed significant discrepancies from the measured values (Figure 8.6).

Since our calibration and parameter estimation procedure was based on only four monitoring wells spatial distribution of the model residuals cannot be presented in the form of a contour map. However, we will present our model residuals for all 4 monitoring wells as a function of time.

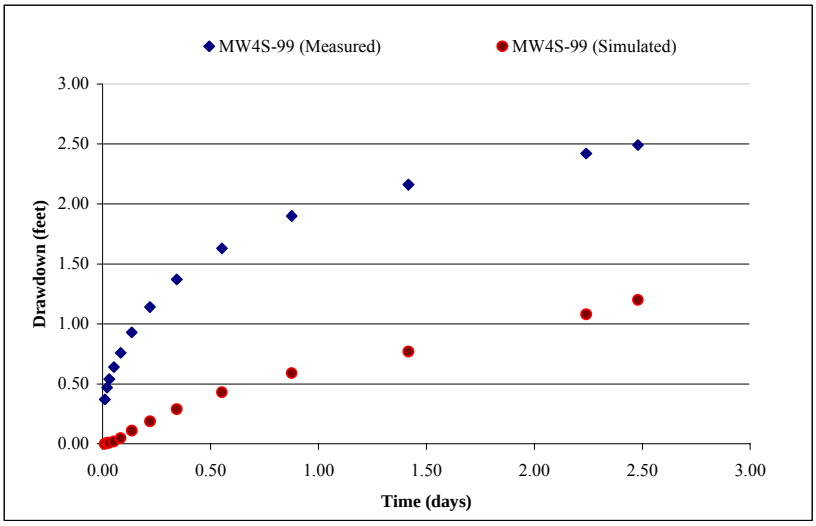

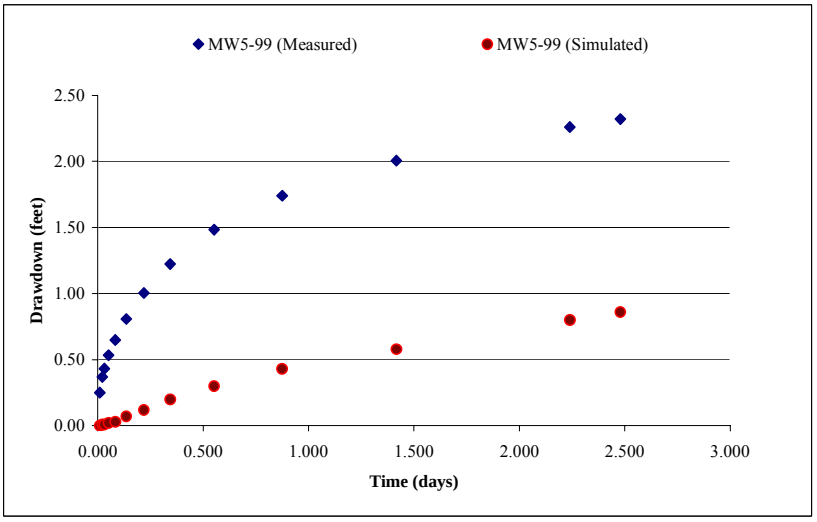

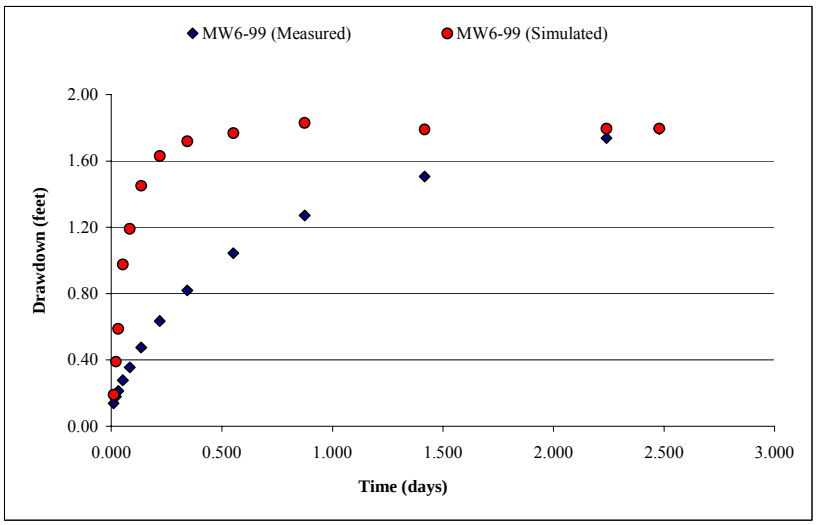

Figure 8.6. Measured vs. simulated drawdown curves using initial point-based calibration data and the pumping test results of March, 2004.

Subsequently, the water level drawdown data in monitoring wells MW4S-99, MW5-99, MW6-99, and USGS-Bedrock1 were provided as input to the parameter estimation package embedded in the Argus-One interface for MODFLOW-2000 and aquifer parameters of the Stratified Drift in the pumping area were estimated (Table 8.1).

Table 8.1. Parameters highlighted in bold letters were estimated with the Parameter Estimation Package and are the final calibration values used in the model.

Parameter	Parameter Description	Value
KxSD	Hydraulic Conductivity (Stratified Drift)	**135.7 (ft/day)**
KxSD(VANI)	Vertical Anisotropy	10
KxT	Hydraulic Conductivity (Till)	**0.1 (ft/day)**
KxT(VANI)	Vertical Anisotropy	10
KxTT	Hydraulic Conductivity (Thick Till)	0.01 (ft/day)
KxTT(VANI)	Vertical Anisotropy	10
KxBed	Hydraulic Conductivity (Bedrock)	**0.01 (ft/day)**
SsBedRock1	Specific Storage (Bedrock Layer 1)	**0.00082**
SyBedRock1	Specific Yield (Bedrock Layer 1)	0.02
SsBedRock2	Specific Storage (Bedrock Layer 2)	**0.000001**
SyBedRock2	Specific Yield (Bedrock Layer 2)	0.002
Recharge (SD)	Recharge to Stratified Drift (normal recharge)	0.0055 (ft/day)
Recharge (Till)	Recharge to Till (normal recharge)	0.00055 (ft/day)
Recharge (SD)	Recharge to Stratified Drift (drought recharge)	0.0026 (ft/day)
Recharge (Till)	Recharge to Till (drought recharge)	0.000275 (ft/day)

The point-based aquifer parameter estimates were used as initial guesses for this phase of the investigation. Recharges to Till, thick Till and the Stratified Drift were also estimated with the same parameter estimation package mentioned above. After model calibration and incorporation of the geophysically updated bedrock contours into the model, the simulated drawdown results were in reasonably good agreement (residuals in the range of 0.2 to 0.5 ft) with the measured levels (Figure 8.7).

Our model predictions are also in reasonably good agreement (residuals less than 0.1 ft) with the observations made at Well USGS-Bedrock1 (Figure 8.8). Note that the plot in Figure 8.8 is in semi-log form due to the very small values in drawdown. This finding is important as our model represents the fractured bedrock through an effective continuum approximation. In the future, the Fenton River numerical model could be enhanced to incorporate more sophisticated fracture bedrock representations, such as the dual continuum approach. UConn is member of a Karst Hydrology consortium of universities and research institutions that has developed a MODFLOW version that can handle this situation. This numerical code is currently in the testing phase.

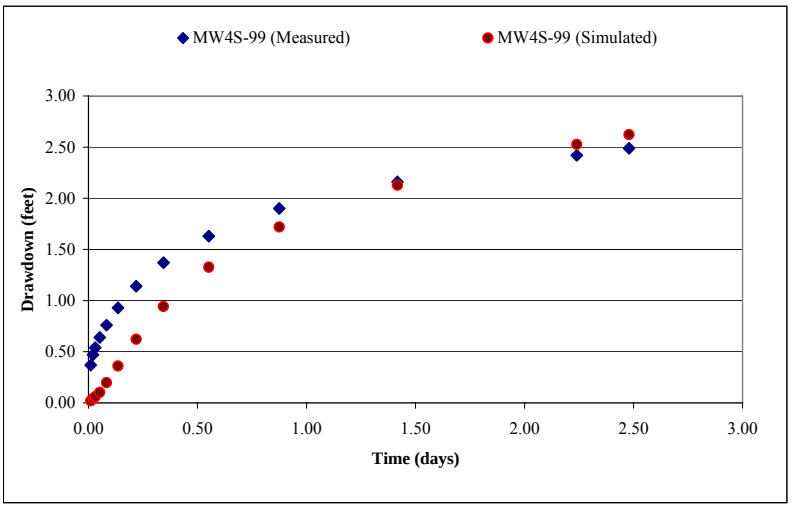

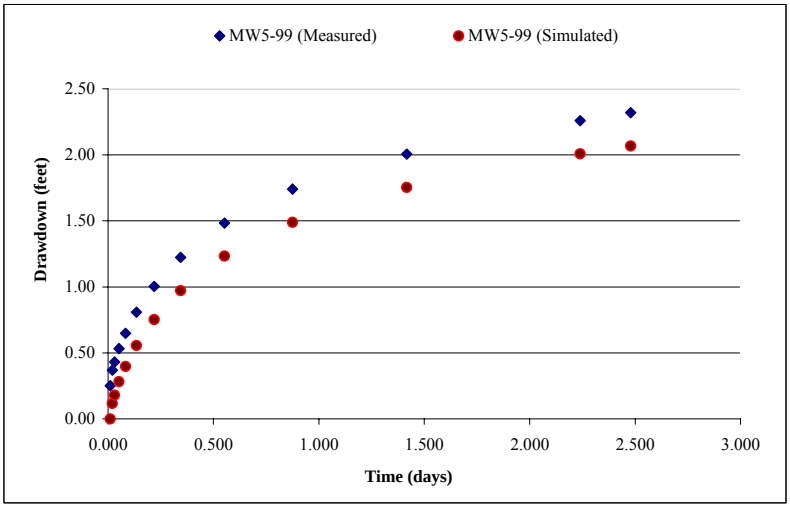

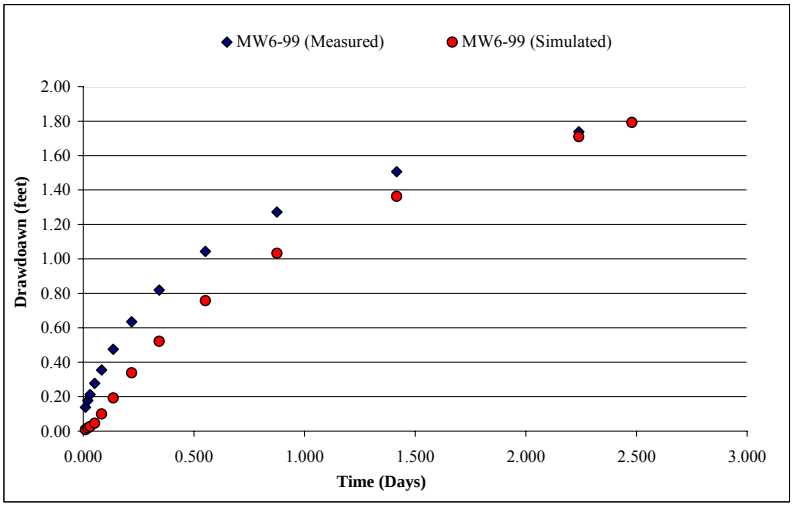

Figure 8.7. Measured vs. simulated drawdown curves using final parameter estimation-based calibration data and the updated bedrock contours for the pumping test results of March, 2004.

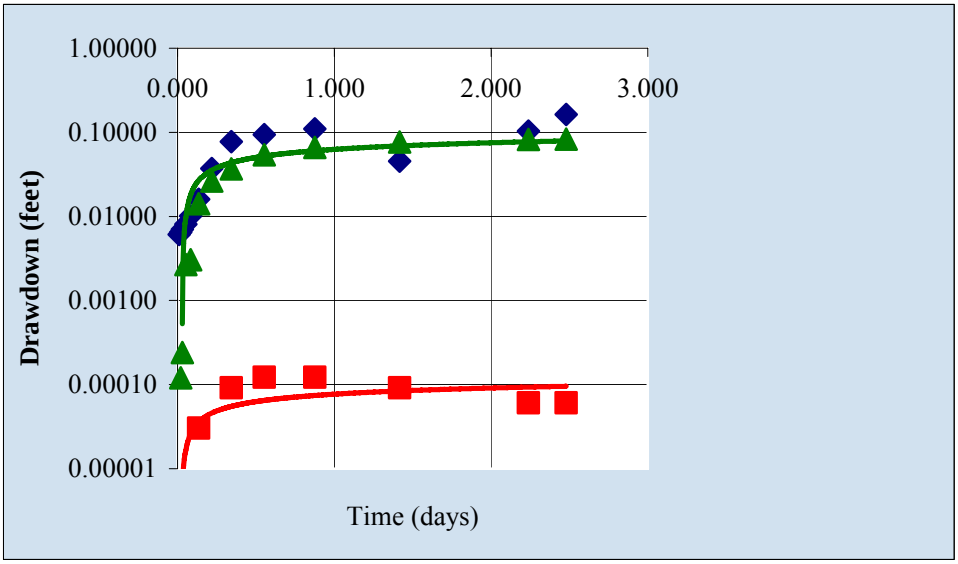

Figure 8.8. Measured (blue diamonds) vs. simulated drawdown curves at Well USGS-Bedrock1 using initial (red squares) and final (green triangles) parameter estimation-based calibration data and the updated bedrock contours for the pumping test results of March 2004.

8.4 Estimation of Streambed Hydraulic Conductivity

8.4.1 Heat transfer and ground-water flow

Changes in temperature in a stream environment can be large and rapid, providing a thermal signal that is easy to identify and measure. Differences between temperatures in a stream and surrounding sediments can be analyzed to trace the movement of ground water to and from streams. In recent years, transfer of heat signals has received substantial attention as a relatively inexpensive and efficient means for estimating hydraulic parameters for streambeds (Constantz et al., 2002; 2003; Constantz and Thomas, 1996; Ronan et al., 1998; Dowman et al., 2003).

Variations in stream flow temperature are transmitted into the underlying sediments by heat transfer processes that include conduction and advection (Galloway et al, 2003). A general equation describing the simultaneous transport of heat and fluid in the earth was presented by Stallman (1963). The equation postulated by Stallman for heat transfer in saturated sediments for one-dimensional (1D) vertical flow (z-direction) is:

$$K_t \frac{\partial^2 T}{\partial z^2} - qC_w \frac{\partial T}{\partial z} = C_s \frac{\partial T}{\partial t} \qquad (8.2)$$

where K_t is the thermal conductivity of the bulk sediments (W/m ^{o}C), T is temperature (^{o}C), q is the liquid water flux (m/s), C_w and C_s are the volumetric heat capacity of water and bulk sediments, respectively (J/m^3 ^{o}C), z is length (m) and t is time (s). Despite

thermo-mechanical dispersion being ignored in this formulation, the equation above has been proven successful in predicting groundwater temperature data before (Constantz et al., 2002).

A numerical code was developed in MATLAB to estimate q via a quasi-Newton optimization algorithm that attempts to minimize the errors between modeled and observed temperature profiles (depth-wise) for selected time snapshots. The objective function can be cast in any form the user desires but routinely either the maximum absolute difference or the root mean square error is employed. The model is based on the 1D finite difference approximation (central in space and implicit in time) of the Stallman equation. The grid size used is 3 feet and the time step is 1 day. Thermal parameters have been estimated based on values reported in the literature as follows: K_t = 1.8 W/m ^oC, $C_w = 4.18\times10^6$ J/m^3 ^oC, $C_s = 7.87\times10^5$ J/m^3 ^oC. q is estimated by Darcy's law

$$q = -K_h \frac{dH}{dz} \tag{8.3}$$

where H is the hydraulic head (m) and K_h (m/s) is the streambed hydraulic conductivity. Once q is estimated, the hydraulic head data obtained in the field provide the gradient and the streambed hydraulic conductivity is calculated from Darcy's law. The data used for this estimation exercise were collected with the help of two piezometer nests measuring both temperature and head at two distinct locations (midstream and at the bank) on the Fenton River near Well B. A daily average temperature was calculated from the raw data and used in subsequent calculations.

8.4.2 Fenton River Temperature Measurements

Two piezometers were installed by USGS in the Fenton River in the vicinity of production Well B on Thursday July 15, 2004. One piezometer was installed near the center of the stream channel and the second was installed near the edge of the right bank. The piezometers were installed to a depth of 11 feet below the streambed at each location. Continuous Multi-channel Tubing (CMT®) manufactured by Solinst Canada LTD was used to construct two multi-level piezometers with seven discrete measurement intervals for ground-water level measurements. Type T thermocouple sensors were inserted into four of the seven channels in the CMT tubing at 2, 5, 8, and 11 feet below the streambed. Four channel EL041 thermocouple converters in conjunction with EL005 data-loggers, manufactured by Pico Technology Limited, were used to measure temperature variations. Featuring built-in cold junction compensation, the EL041 thermocouple converter is designed to measure a wide range of temperatures (-270 to 1820°C) with any thermocouple that uses a miniature size thermocouple connector. A schematic depicting the details of the piezometer nest is shown in Figure 7.1.

Temperature time series as a function of 4 distinct depths for the data collected near midstream and the bank of the Fenton are shown in Figure 7.2. A similar plot is shown in Figure 7.3 for the 7 water levels observed. These data were provided as input in tabular form to the numerical code that performed the optimization-based estimation of the streambed hydraulic conductivity. Finally, surface water temperature loggers were

placed along the Fenton River and the major tributaries to assess temperature changes in the river. The instrument used was the HOBO Temperature Pro by Onset Computer Corporation, Bourne, MA, USA. Again, daily average stream temperature was used as the boundary condition (depth zero) for the model.

8.4.3 Optimization Results

Results from two optimization simulations are presented for the midstream and bank locations near Well B. Figure 8.9 shows the modeled and observed temperature profiles for the midstream location. It can be seen that the profiles are very close with errors in the ±1.2 ^{o}C range. The optimal streambed conductivity was estimated to be 17.7 cm/day (0.58 feet/day). This is in reasonable agreement with Rahn's estimate of 0.22 feet/day.

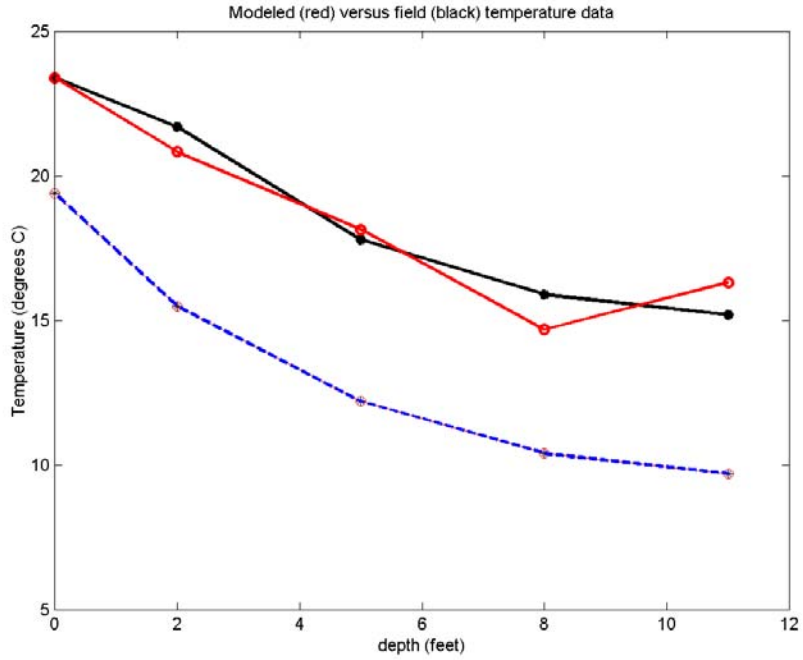

Figure 8.9. Comparison between modeled and observed temperature profiles almost midstream of Fenton River near Well B. Blue curve is the initial condition and red and black curves are the modeled and observed profiles at t=2 days, respectively.

Figure 8.10 shows the modeled and observed temperature profiles for the bank location. It can be seen that the profiles are very close with errors in the ±3 ^{o}C range. The optimal streambed conductivity was estimated to be 5.15 cm/day (0.17 feet/day). This is in excellent agreement with Rahn's estimate of 0.22 feet/day.

These results have also been compared with field observations made during the summer of 2005 campaign season (reported in a different section) and give us confidence for the streambed conductivity used as input in the MODFLOW model. They also point to the fact that in the future and provided that very detailed resolution is needed one could

incorporate spatially variable streambed conductivity values along, and possibly across, river reaches.

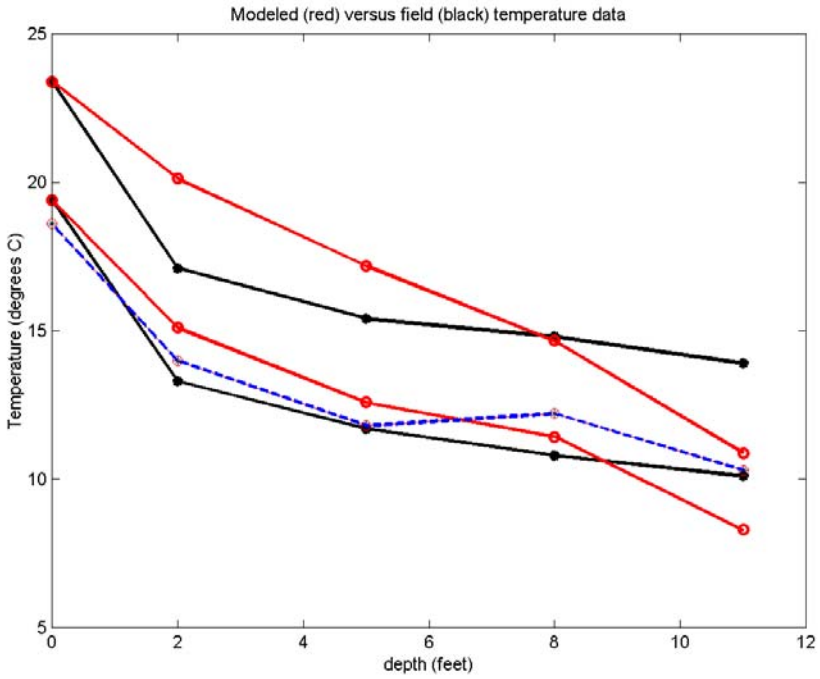

Figure 8.10. Comparison between modeled and observed temperature profiles near the bank of Fenton River near Well B. Blue curve is the initial condition and red and black curves are the modeled and observed profiles at t=2 and 7 days, respectively.

8.5 Model Validation and Sensitivity

The objective of this component of the study is to use the standard-practice groundwater model described in Section 8.2 to investigate selected options for the management of water withdrawals to minimize the impact of groundwater pumping on fish habitat. Before, selected management scenarios were analyzed, however, the calibrated model was validated against historical data and observations made during stressed conditions. Since our measurement period did not coincide with drought conditions, the severe drought conditions of the mid-60s were simulated with the parameters obtained from existing meteorological data and the study conducted by Rahn in 1966 (Rahn, 1971). It should be noted that the majority of the analyses presented in this report were concluded before the Summer of 2005, which was a severe drought. According to a statistical analysis conducted for the Mount Hope River and employing correlations established between the stream flows in the Fenton and Mount Hope Rivers, the summer of 1966 was characterized by a prolonged drought that placed it approximately in the 95% of the historical record. The locations of the weirs used in the study by Rahn are shown in Figure 8.11.

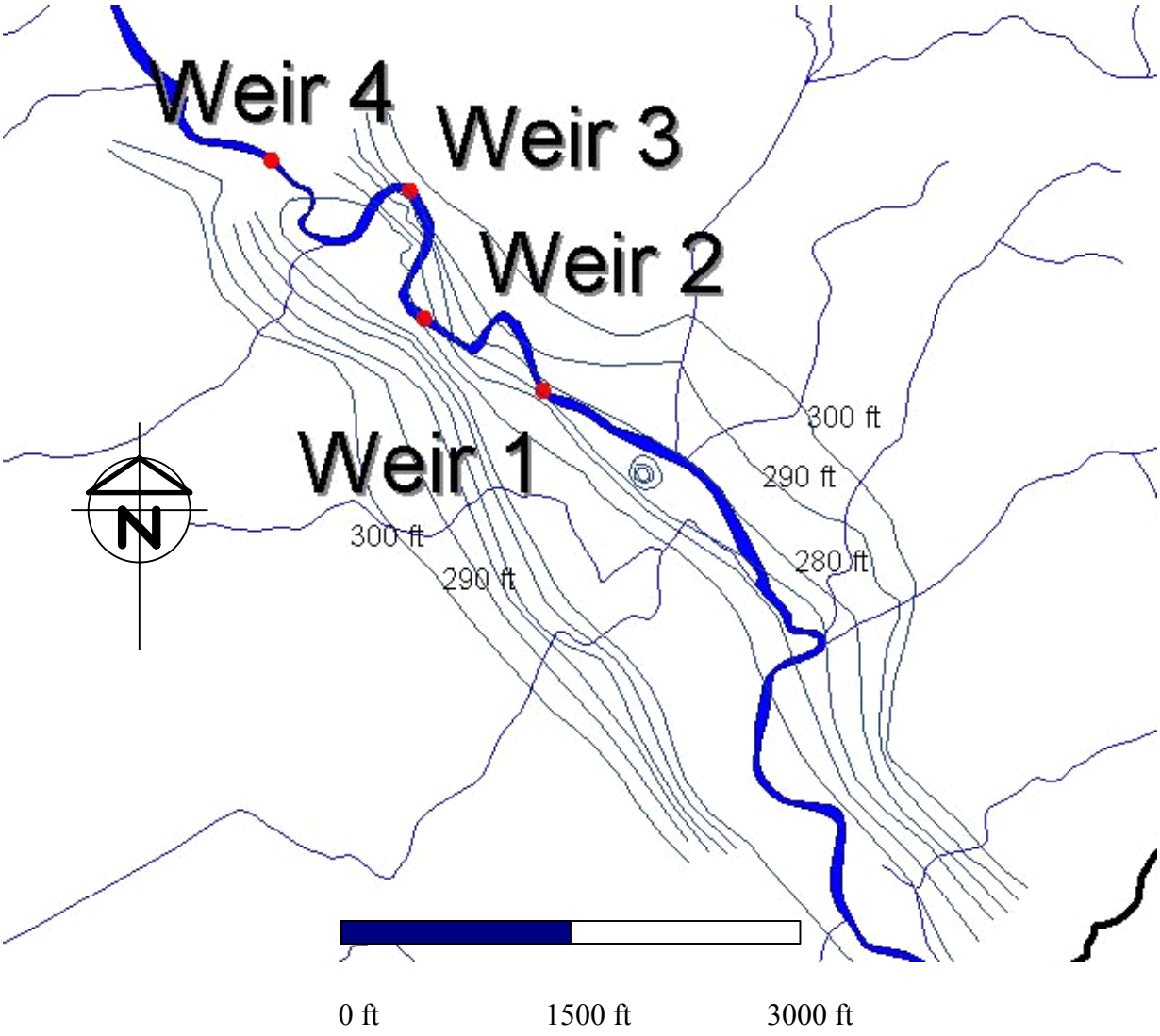

Figure 8.11. Location of weirs in the study conducted by Rahn in 1966.

Simulation results indicated that if the pumps (pumps B and C) located in the northern aquifer kept pumping at normal rates during severe drought periods, the flow in the segment of the Fenton River in the vicinity of pumps B and C would reach critical levels after 30 days of continuous pumping. These results were comparable (albeit slightly higher) with the field measurements of Rahn's study of 1966 (Figure 8.12). The numerical experiment entailed the following: a) Pump B is on for 135 days at a flow rate of 0.9 cfs; b) Pump C starts at day 135 at a flow rate of 0.58 cfs and flow in Pump B increases to 1.02 cfs; c) Both pumps are on for 30 days at total pumping rate of 1.6 cfs; d) All pumps are turned off at day 165 and the stream is allowed to regain its natural flow. Note that Rahn's stream flow measurements at weirs 4, 3, and 2 are slightly lower

than our simulation results by 0.1 cfs at weir 2, 0.12 cfs at weir 3, and 0.18 cfs at weir 4 (Figure 8.12).

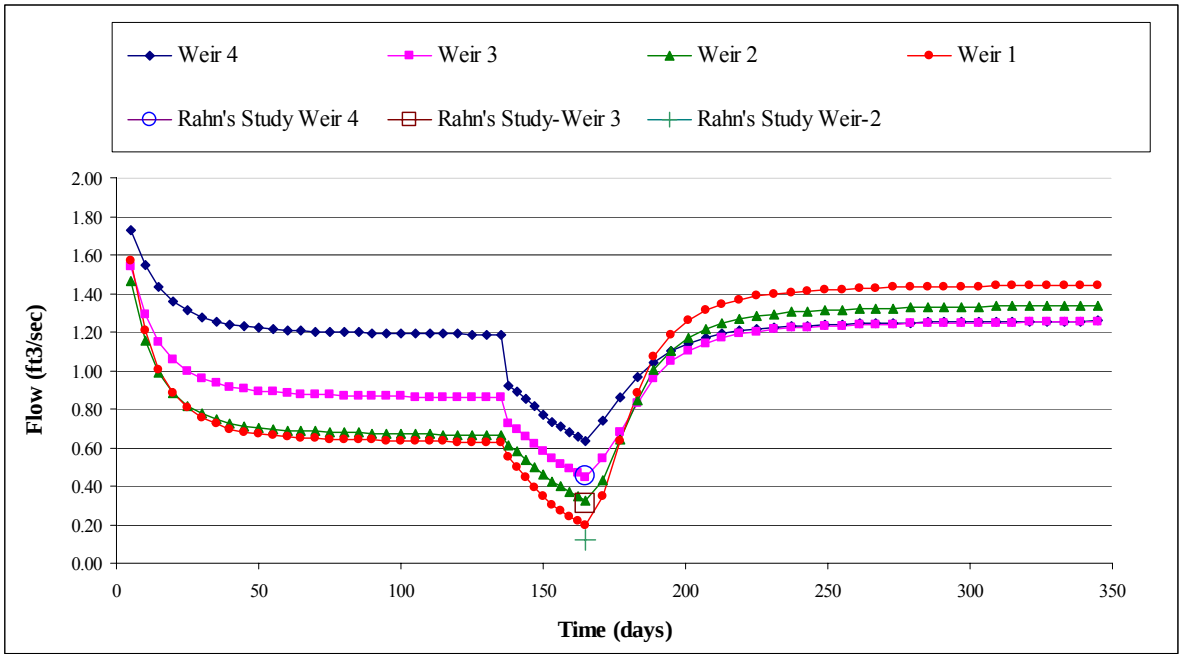

Figure 8.12. Model validation emulating Rahn's study of 1966.

However, this validation exercise was conducted with average monthly recharge of an average drought period, and the stream inflow was taken as a constant value of 2 cfs. In the latest version of the model, detailed average values of daily stream flow and recharge were utilized. Figure 8.13 depicts the recharge as a function of time during 1966 for daily and monthly averaged values. Table 8.2 indicates that the upgraded model produced results that are very comparable to the 1966 measurements conducted by Perry Rahn, thereby further lending credence to our model.

Table 8.2. Simulated vs. measured stream flow at Rahn's weir location.

August-29-1966	***Argus-simulations (cfs)**	****Argus-simulations (cfs)**	**Rahn Measurements (cfs)**
Weir 4	0.42	0.64	0.45
Weir 3	0.23	0.44	0.31
Weir 2	0.12	0.19	0.12

October-14-1966	***Argus-simulations (cfs)**	**Rahn Measurements (cfs)**
Weir 4	2.74	2.18
Weir 3	2.55	2.00
Weir 2	2.42	1.76

* Simulation results using detailed daily recharge and stream inflow.

** Simulation results using average recharge and constant inflow to the stream.

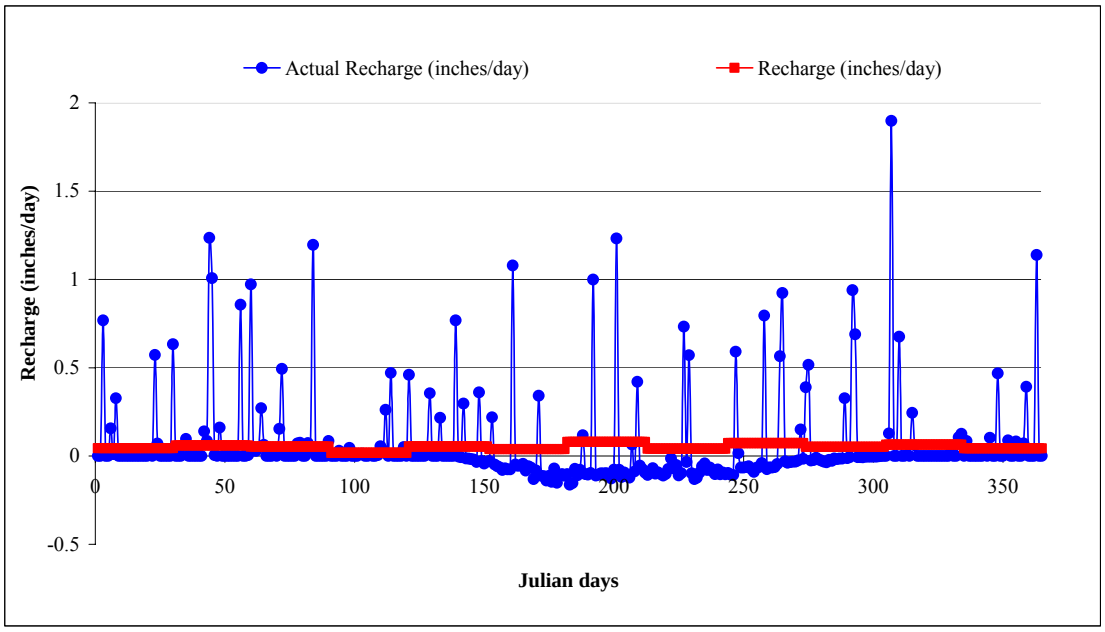

Figure 8.13. Daily vs. monthly average recharge values in 1966 in the Fenton River well-field region.

The drought conditions of the mid-60s and Rahn's pumping scenario were simulated with Well B being on for 135 days at a flow rate of 0.9 cfs, then Well C starts at day 135 at a flow rate of 0.58 cfs and pumping at Well B increases to 1.02 cfs (both pumps are on for 30 days at total pumping rate of 1.6 cfs). As discussed above, during Rahn's study, the flow in Fenton River reached its lowest levels at day 242 (August 30th). Therefore, day 242 was chosen to generate a plot that depicts the stream flow versus the length of the stream downstream from Wells B and C. Simulation results indicated that after 30 days of continuous pumping of Wells B and C, the segment of the River in the vicinity of Well A goes dry (Figure 8.14). It should be mentioned here that during his study, Rahn exceeded the allowable daily pumping limit of 1.31 cfs set forth by the Connecticut Department of Environmental Protection in 1991.

To investigate the sensitivity of the model a number of simulation scenarios were processed and tested for various input parameters. It was found that the model was most sensitive to recharge and streambed hydraulic conductivity values, respectively.

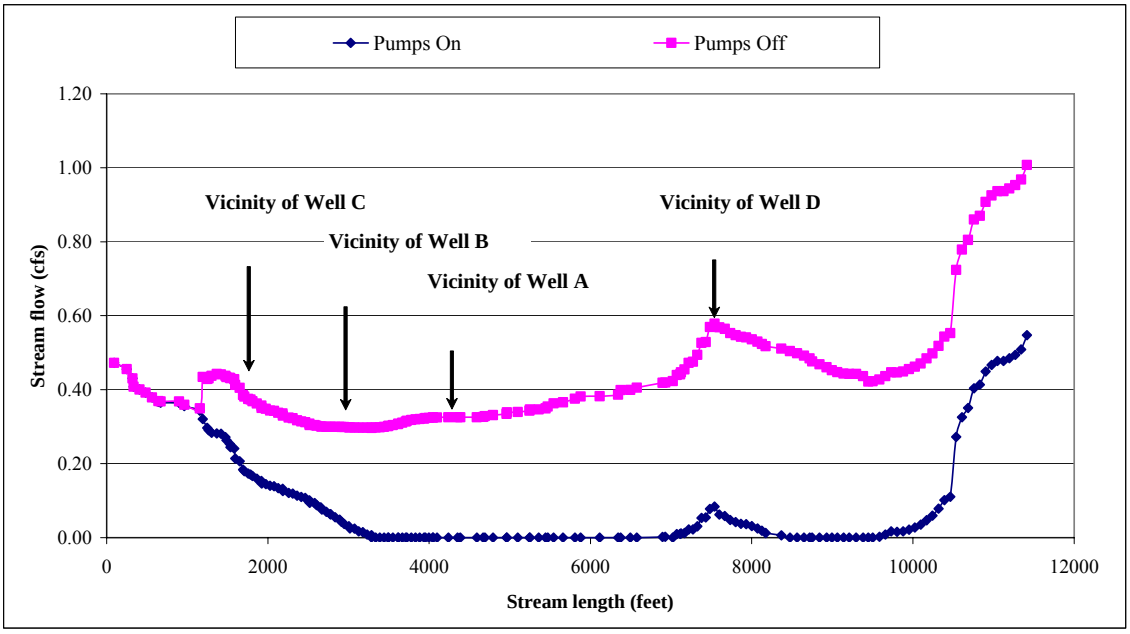

Figure 8.14. Stream flow at day 242 (August 30th) during Rahn's study with pumping rates used by Rahn and stream flow with now pumping taking place.

8.6 Water Budget Components

The water budget analysis package of Argus-One was used to estimate two water budget scenarios. August 8th, 1966 was chosen to represent drought conditions and November 26th was chosen to represent the end of the drought and normal recharge conditions in the Fenton River well-field region. Results of this analysis, for one of the management scenarios tested (described in Section 9 of this report), are shown in Figures 8.15 and 8.16.

When averaged over the simulation domain, the August 8th water budget rates indicate that over the simulation domain there exists negative recharge over both the Till and Stratified Drift. For the majority of the area of interest, water percolates downwards from the Till to the first bedrock layer and from there to the second bedrock layer. However, this reverses near the Fenton River where the second bedrock layer contributes water to the first bedrock layer and this, in turn, to the Stratified Drift. Moreover, the Stratified Drift is also receiving water from the upland areas (Till) and there exists minimal flow interaction between the Stratified Drift and the stream flow with Fenton River acting as a losing stream (Figure 8.15). For the November 26th conditions, the situation changes minimally for the upland areas in terms of the interactions between the Till and the bedrock layers. However, the Stratified Drift is now replenished by water from only the upland areas (Till) with minimal (if any) contribution from the bedrock. Furthermore, and most importantly, the Fenton River is now a gaining stream being replenished from the Stratified Drift (Figure 8.16).

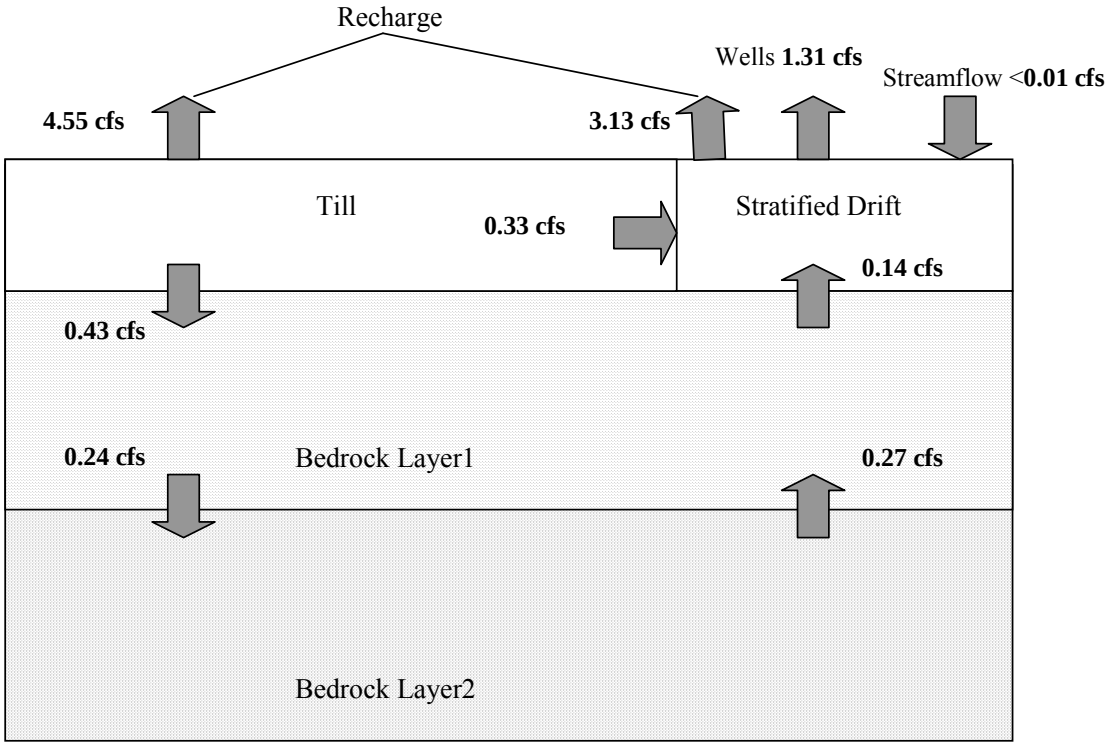

Figure 8.15. Water budget rates estimated for the pumping schedule of scenario 11 (August 8th, 1966 simulation). Rates are averaged over the simulation domain.

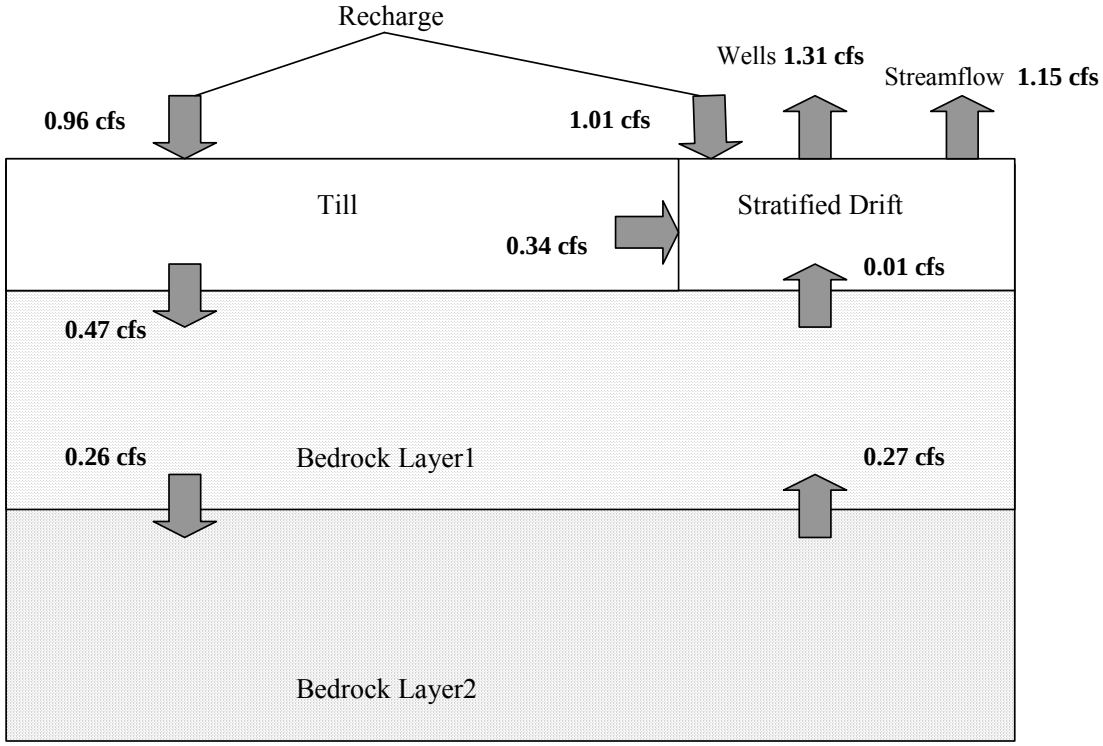

Figure 8.16. Water budget rates estimated for the pumping schedule of scenario 11 (November 26th, 1966 simulation). Rates are averaged over the simulation domain.

8.7 Summary and Discussion

A conceptual model of flow in the vicinity of the Fenton River well-field was developed and describes the possible interactions between the underlying bedrock layers and the surficial geologic units. Moreover, it attempts to describe the complex and temporally variable interactions between the upland areas that are covered by either thick Till or Till and the Stratified Drift, which feeds water into or gets fed water from the Fenton River. Based on this conceptual model a mathematical model and associated numerical model was developed for the site. The numerical model employs a graphical user interface developed by the United States Geological Survey embedded in a numerical environment called Argus-ONE. The geographical information system layers pertaining to the Fenton River watershed were linked to MODFLOW-2000, which is the numerical engine used in this study.

The numerical model was initially calibrated with data obtained from pumping tests, which provided us with point-based aquifer parameter estimates. These were then used as initial guesses for an optimization-based aquifer parameter estimation over the whole simulation domain. Recharges to Till, thick Till and the Stratified Drift were also estimated with the same parameter estimation. Streambed hydraulic conductivity was estimated using thermistors installed in two boreholes, located approximately in the middle and on the bank of the river, and an optimization algorithm. After model calibration and incorporation of the geophysically updated bedrock contours into the model, the simulated drawdown results were in reasonably good agreement (residuals in the range of 0.2 to 0.5 ft) with the measured levels for the Stratified Drift wells. Our model predictions were also in reasonably good agreement (residuals less than 0.1 ft) with the observations made at one bedrock well. The numerical model using detailed average values of daily stream flow and recharge model produced results that are very comparable to the 1966 measurements conducted by Perry Rahn, thereby further lending credence to our model.

The calibrated and validated numerical model was used to calculate water budget estimates in order to quantify the complex interactions between the geologic units in the vicinity of the Fenton River. August 8th, 1966 was chosen to represent drought conditions and November 26th was chosen to represent the end of the drought and normal recharge conditions in the Fenton River well-field region. When averaged over the simulation domain, the August 8th water budget rates indicate that over the simulation domain there exists negative recharge over both the Till and Stratified Drift. Near the Fenton River the second bedrock layer contributes water to the first bedrock layer and this, in turn, to the Stratified Drift. Moreover, the Stratified Drift is also receiving water from the upland areas (Till) and there exists minimal flow interaction between the Stratified Drift and the stream flow with Fenton River acting as a losing stream. For the November 26th conditions, the situation changes minimally for the upland areas in terms of the interactions between the Till and the bedrock layers. However, the Stratified Drift is now replenished by water from only the upland areas (Till) with minimal contribution

from the bedrock. Furthermore, and most importantly, the Fenton River is now a gaining stream being replenished from the Stratified Drift.

9.0 TESTING OF SELECTED WELL FIELD MANAGEMENT SCENARIOS

9.1 Pumping Management Scenarios

Seventeen pumping scenarios (eleven primary and six variants) were proposed to investigate the stream flow loss in the vicinity of wells A, B, C, D, meadows, and Gurleyville Road. These scenarios range from different hours of pumping per day (14, 20, 24 hours), to different total daily pumping (844,000, 633,000, 422,000, 211,000 gpd), to different locations for a replacement of Well A, to imposing limits on the total daily pumping depending on the stream flow. The eleven primary scenarios are listed in Table 9.1. The six secondary scenarios are based on primary scenarios with total daily pumping limited according to the stream flow in the Fenton River (Q_R) as follows:

- $Q_R > 6$ cfs, total amount of water pumped is 844,000 gpd (scenario 12 based on 1)
- 6 cfs $> Q_R > 5$ cfs, total amount of water pumped is 633,000 gpd (scenario 13 based on 7)
- 5 cfs $> Q_R > 4$ cfs, total amount of water pumped is 422,000 gpd (scenario 14 based on 8)
- 4 cfs $> Q_R > 3$ cfs, total amount of water pumped is 211,000 gpd (scenario 15 based on 9)
- 3 cfs $> Q_R$, pumping stops (scenarios 16 and 17 based on 10 and 11, respectively)

Table 9.1. Pumping scenarios tested in this study

Scenario	Hours pumped/day	Pump A	Pump B	Pump C	Pump D	Total daily pumping (gpd)
1	14	225	400	180	200	844,000
2	20	157	280	126	140	844,000
3	24	131	233	105	117	844,000
4	14	160	284	128	142	600,000
5	14	107	190	85	95	400,000
6	14	53	95	43	47	200,000
7	14	163	259	229	354	844,000
8	14	101	160	390	354	844,000
9	14	0	261	390	354	844,000
*10	14	300	186	165	354	844,000
**11	14	300	186	165	354	844,000

All pump flow rates are in gpm

* This implies that well A has moved to a new location (A') within 250 ft of its original setting in the south direction.

** This implies that well A has moved to a new location (A") half-way between Wells A and D in the southeast direction.

9.2 Description of Index Used to Assess Management Scenario Efficacy

In order to assess the relative merit of one pumping management scenario over the others, an index was developed as follows. Each pumping scenario results are compared to the reference case when there is no pumping at different locations along the Fenton River (see Figure 9.1 for an example from Scenario 1 near Well A). The two curves are subtracted from each other and a set of stream flow loss (ΔQ) curves are plotted for selected locations of interest along the river. Figure 9.2 depicts the evolution of this ΔQ with time for selected locations up to the point in time when the river goes dry. The maximal ΔQ value for this scenario is the index that characterizes it and allows one to compare it with respect to the others. Clearly, in this scenario the maximal ΔQ is 1.22 cfs near the Well D. However, we are mostly interested in what

happens near the vicinity of Well A for several reasons. First, and foremost, it is where the Fenton River is known to have gone dry in the past (Rahn 1971, Giddings 1966) and as recently as the summer of 2005. Second, the model used in this study has been calibrated using pumping tests at Well B. Therefore, there exists higher degree of certainty for hydraulic parameters inferred from the calibration near this location. Conversely, towards the south part of the model (Well D and Gurleyville Rd.) the uncertainty about the hydraulic parameters is greater. Finally, all models are known to experience undesirable boundary effects that tend to "corrupt" the solution.

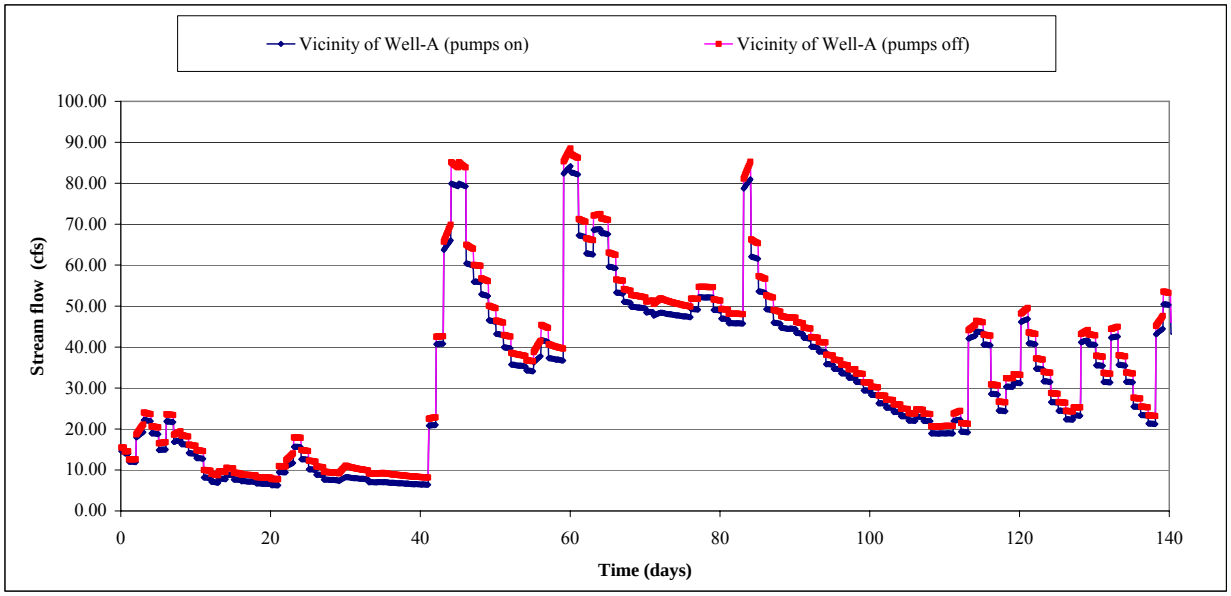

Figure 9.1: Stream flow in the vicinity of pumping Well A (Scenario 1).

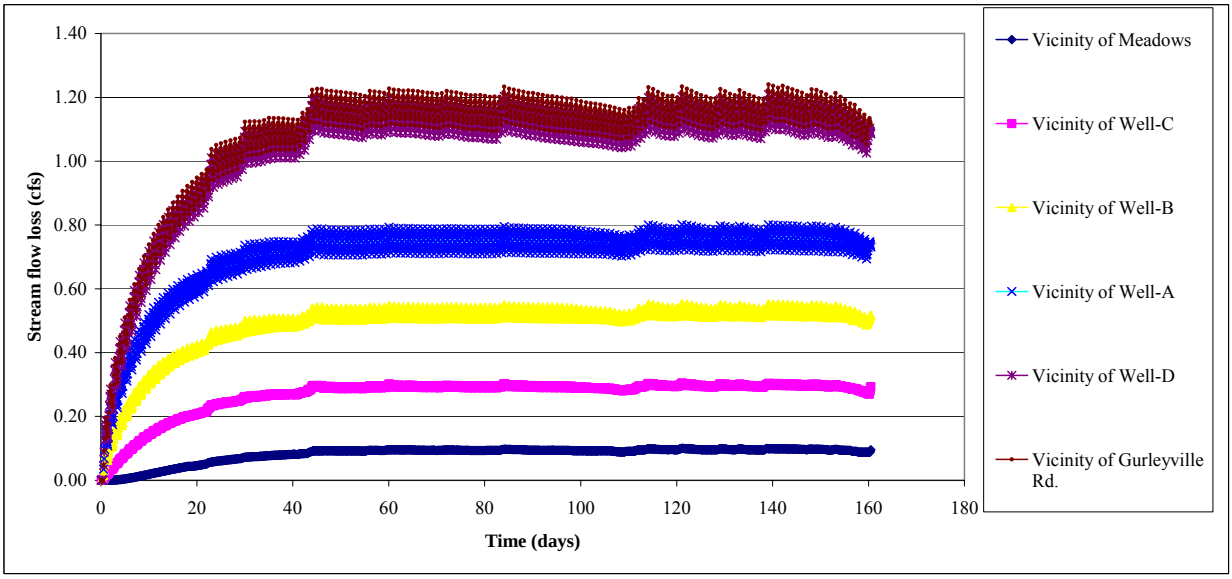

Figure 9.2: Stream flow loss in the vicinity of pumping wells (Scenario 1). Note that graphs for Well D and Gurleyville Rd. are indistinguishable from each other.

To test whether Well D is close enough to the south-east simulation boundary and is affected by its location, the following numerical experiment was conducted. Well D was "moved" from its present location (4,800 ft away from the boundary) to two other virtual locations, one 730 ft away from the simulation boundary and the other at the grid cell adjacent to the boundary, while its pumping rate remains constant. Since the boundary is a no-flow boundary, it is expected that the drawdown experienced at Well D will increase as it is moved closer to the boundary as there will be less replenishment of water from the aquifer. Figure 9.3 presents the temporal variation of the drawdown in Well D as it is moved closer to the simulation boundary. The maximum drawdown is 27.1 ft when Well D is adjacent to the boundary, whereas this decreases to 23.2 ft when Well D is located 730 ft away from the boundary. However, in its present location Well D experiences a drawdown of only 7.5 ft, which indicates that it is located at a sufficient distance from the boundary to warrant any concerns as to the model's reliability in that location. Nevertheless, our management analysis will concentrate on the vicinity of Well A for the reasons discussed above.

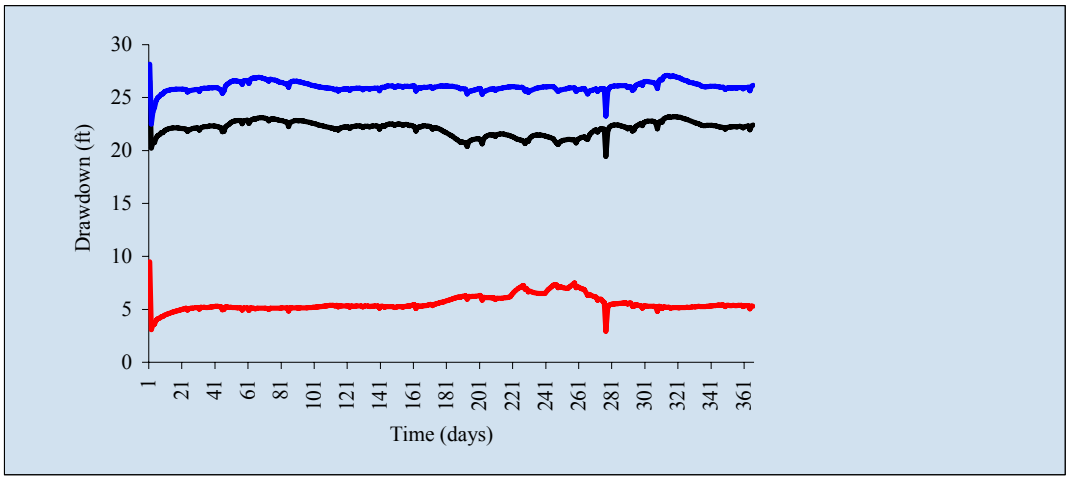

Figure 9.3: Drawdown in Well D as it is moved closer to the simulation boundary (red: present location; black: 730 ft away from boundary; blue: adjacent to the boundary).

The maximal ΔQ also varies in space. Plots of this index along the river reaches allow one to identify areas where one needs to be more careful with the management activities or where one can afford the luxury of being able to pump more water. Figure 9.4 shows stream flow results from a variety of scenarios at a specific point in time. Figure 9.5 presents the ΔQ along the river reaches for these scenarios. One can observe, for example, that Scenario 11 provides us with a reasonably low ΔQ between 4,000 and 7,000 feet along the Fenton River reach. This could indicate a potential zone where some more water can be extracted without the introduction of adverse effects on the river and its habitat.

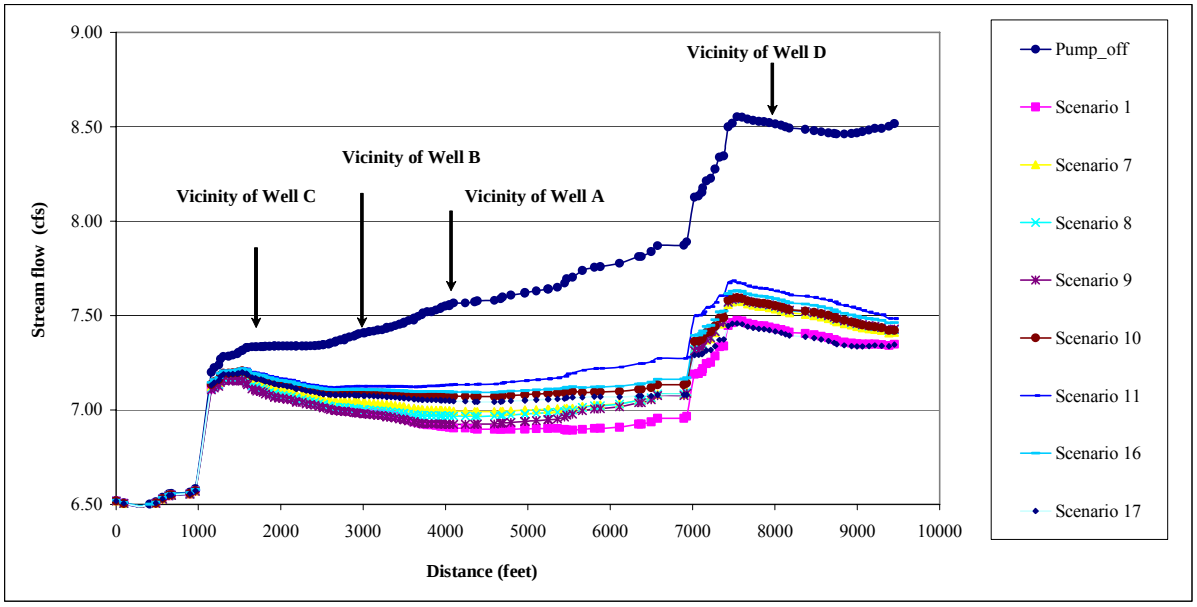

Figure 9.4: Stream flow in the vicinity of pumping wells (day 140 of 1966).

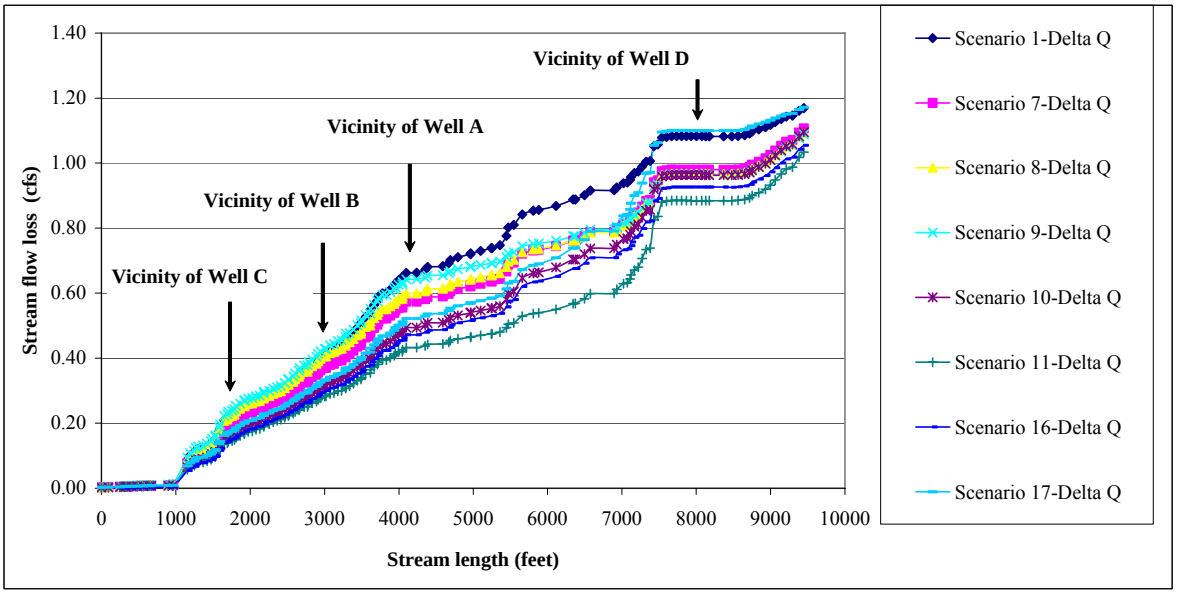

Figure 9.5: Stream flow loss in the vicinity of pumping wells (day 140 of 1966).

9.3 Comparison of Scenarios and Discussion

A summary of the maximal ΔQ index for the eleven primary scenarios is presented in Table 9.2. Several interesting observations can be made from this summary (emphasis is placed in the vicinity of Well A).

Table 9.2: Summary of ΔQ for selected pumping scenarios

Simulation Scenario	Meadows	Near Well-C	Near well-B	Near well-A	Near well-D	Near Gurleyville Rd.
Scenario-1	0.1	0.3	0.53	0.78	1.2	1.22
Scenario-2	0.1	0.3	0.53	0.76	1.16	1.19
Scenario-3	0.09	0.29	0.52	0.75	1.14	1.16
Scenario-4	0.07	0.21	0.38	0.56	0.86	0.88
Scenario-5	0.05	0.14	0.26	0.38	0.56	0.58
Scenario-6	0.02	0.07	0.13	0.19	0.28	0.29
Scenario-7	0.08	0.26	0.46	0.66	1.11	1.15
Scenario-8	0.09	0.28	0.5	0.68	1.11	1.15
Scenario-9	0.1	0.31	0.57	0.74	1.12	1.17
Scenario-10	0.07	0.22	0.4	0.58	1.08	1.13
Scenario-11	0.07	0.21	0.38	0.56	1.18	1.21

Scenario 10: Well A is moved to A' location (250 ft south of Well A)
Scenario 11: Well A is moved to A' location (approximately halfway between Wells A and D)

First, there exists an almost perfect linear dependence of ΔQ as a function of the total daily pumping (Scenario 6, 5, 4, and 1). This finding provides justification for the almost linear decrease of the total daily pumping as the stream flow in the Fenton River decreases (Section 9.1). Second, there exists very little difference between scenarios that spread the same total pumping over longer durations during the day (Scenarios 1, 2, and 3). Third, as more pumping is switched from Wells A and B to Wells D and C, which reach their registered capacity (Scenarios 1, 7, 8, and 9) the effects in the vicinity of Well A are reduced with minimal changes being effected due to re-distribution of pumping between Wells B and C. Fourth, it appears that the best management scenarios (Scenario 10 and 11) call for relocation of Well A by moving it either 250 feet in the South direction (i.e., without requiring a new permit) or approximately halfway between the original location of Well A and D (on university property).

It should be noted, however, that no formal optimization analysis has been conducted in regards to the placement of Well A as such an analysis was beyond the scope of this study. The new location of Well A was chosen under the premise that a well located in the parts of the aquifer where the Stratified Drift has greater thickness will have substantially reduced effects on the Fenton River stream flow. Based on this preliminary analysis and with the caveat emptor statement above, the cost of relocating Well A beyond the 250 feet distance may not be justified as the decrease in ΔQ is only minimal.

It should also be noted that the management scenarios discussed herein were implemented for the severe drought conditions of the mid-60s. According to a statistical analysis conducted for the Mount Hope River and employing correlations established between the stream flow in the Fenton and Mount Hope Rivers, the summer of 1966 was characterized by a prolonged drought that placed it approximately in the 95% of the

historical record thereby making it analogous and relevant to other drought conditions, such as the ones present in the summer of 2005.

10.0 BIBLIOGRAPHY AND GENERAL REFERENCES

Annear, T., I. Chisholm, H. Beecher, A. Locke, R. Jacobson, and 11 other authors. 2004. Instream flows for riverine resource stewardship, revised edition. Instream Flow Council, Cheyenne, WY.

Argus One Numerical Environment – A GIS Modeling System, 2001, Argus Interware, Inc. Jericho, NY, USA.

Austrian Standard Önorm 6232. 1995. Richtinien fuer die oekologische Untersuchung und Bewertung von Fleissgewaessern. Oesterreische Normungsinstitut, Vienna, Austria, 38 pp.

Bain, M.B., J.T. Finn and H.E. Booke. 1985. A quantitative method for sampling riverine microhabitats by electrofishing. North American Journal of Fisheries Management. Vol. 5:489-493.

Baker, E.A., T.G. Coon. 1997. Development and evaluation of alternative habitat suitability criteria for brook trout. Transactions of the American Fisheries Society. 126:65-76.

Benson, A. K., 1995, Applications of ground penetrating radar in assessing some geological hazards: examples of groundwater contamination, faults, cavities. Journal of Applied Geophysics, vol. 33(1-3), pp.177-193.

Beres, M., and Haeni, F. P., 1991. Application of ground-penetrating-radar methods in hydrogeologic studies. Ground water, vol. 29(3), pp. 375-386.

Bovee, K.D. 1986. Development and evaluation of habitat suitability criteria for use in the instream flow incremental methodology. Instream Flow Information Paper: No. 21. US Fish and Wildlife Service, Biological Report 86(7). 235 pp.

Bovee, K.D. 1994. Data collection procedures for the Physical Habitat Simulation System. NERC IF-305 course manual, Fort Collins, CO.

Bovee, K.D. 1982. A guide to stream habitat analysis using the instream flow incremental methodology. Instream Flow Information Paper No. 12. U.S. Fish and Wildlife Service, Office of Biological Services. FWS.OBS-82/26. 248 pp.

Boyd, T.M, 2003, Introduction to geophysical exploration, Seismic refraction, 15 Jul., 2004. < http://www.mines.edu/fs_home/tboyd/GP311>.

Bozek, M.A., and F.J. Rahel. 1992. Generality of microhabitat suitability models for young Colorado River cutthroat trout (*Oncorhynchus clarki pleuriticus*) across sites and among years in Wyoming streams. Canadian Journal of Fisheries and Aquatic Sciences. 49:552-564.

Burger, R.H., 1992, Exploration geophysics of the Shallow Subsurface, Prentice Hall, pp. 107- 113

Capra, H., S. Valentin and P. Briel. 1995. Habitat time series and trout population dynamics. Bulletin Fransais De La Peche Et De La Pisciculture. 337-344.

Constantz, J., Stewart, A.E., Niswonger, R., and L. Sarma, Analysis of temperature profiles for investigating stream losses beneath ephemeral channels, *Water Resour. Res., 38(12), 1316:* 52-13, 2002.

Constanz, J., Tyler, S.W., and E. Kwicklis, Temperature-profile methods for estimating percolation rates in arid environments, *Vadose Zone Journal, (2):* 12-24, 2003.

Cook, J.C., 1960, Proposed monocycle-pulse very-high-frequency radar for air-borne ie and snow measurement. AIEE Comm. Electron., 51, pp. 588-594.

Daniels, J.J., Veldl, M.A., and Stepp, T., 1988, The application of ground penetrating radar for locating surface spills: Soc. Expl. Geophys. Ann. Meeting, Anaheim.
Department of the Army, New England Division Corps of Engineers, Waltham, MA. (August 1982). "Mansfield Hollow Lake, Mansfield Center, Connecticut. Forest Management Plan and Fish and Wildlife Management Plan."
Dowman, C.E., Ferre, P.A., Hoffman, J.P., Rucker, D.F., and J.B. Callegary, Quantifying ephemeral streambed infiltration from downhole temperature measurements collected before and after streamflow, *Vadose Zone Journal, (2):* 595-601, 2003.
Environmental Simulations Inc. (ESI), 2003. Guide to Using Aquifer-Win32. www.groundwatermodels.com.
Fausch, K.D., and R.J. White. 1986. Competition among juveniles of coho salmon, brook trout, and brown trout in a laboratory stream, and implications for Great Lakes tributaries. Transactions of the American Fisheries Society. 115:363-381.
Ferris, J. G., D. B. Knowles, R. H. Brown, and R. W. Stollman, 1962. *Theory of Aquifer Tests*.: U. S. Geolog. Survey Water-Supply Paper 1536-E.
Freeman, M.C., Z.H. Bowen and K.D. Bovee. 1997. Transferability of habitat suitability criteria: response to comment. North American Journal of Fisheries Management. 19:626-628.
Galloway, D.L., and others, 2003, Evolving Issues and Practices in Managing Ground-Water Resources: U. S. Geological Survey Circular 1247, 73 p.
Giddings, Jr. M. T., Induced Infiltration at the University of Connecticut Well Field, Masters Thesis, 1966, University of Connecticut, Department of Geology and Hydrogeology, Storrs, Connecticut.
Glover, R. E., Balmer, G. G., 1954. River Depletion Resulting from Pumping a Well Near a River. Trans. Am. Geophys. Union. V 35, pp. 468-470.
GeoImage, LLC, 2003, Principle of tomography.
Glozier, N.E., J.M Culp and G.J. Scrimgeour. 1997. Transferability of habitat suitability curves for a benthic minnow, *Rhinichthys cataractae*. Journal of Freshwater Ecology. 12:379-393.
Groshens, T.P., and D.J. Orth. 1994. Transferability of habitat suitability criteria for smallmouth bass, *Micropterus dolomieu*.
Harbaugh, A.W., Banta, E.R., Hill, M.C., and McDonald, M.G., 2000, MODFLOW-2000, the U.S. Geological Survey modular ground water model -- User guide to modularization concepts and the Ground Water Flow Process: U.S.G.S. Open-File Report 00-92, 121 p.
Hasbrouck Geophysics, Inc., 2004, Rippability (Seismic refraction), Hobson-Overton, Dec., 2004 < http://www.hasgeo.com/refrac.htm>.
Haeni, F.P., 1988, Application of seismic refraction techniques to hydrologic studies, United States Government Printing office, Washington, pp. 1-44.
Haeni, F.P., McKeegan, D.K., Capron, D.R., 1987, Ground penetrating radar study of the thickness and extent of sediments beneath Silver Lake, Berlin and Meriden, Connecticut, Water-resources investigations report, 85-4108.
Hess, A.E., and Paillet, F.L., 1990, Applications of the thermal-pulse flowmeter in the hydraulic characterization of fractured rocks: West Conshohocken, Penn., American Society for Testing and Materials, Standard Technical Publications 1101, p. 99-112.

Hoag, G.E., Ogden, F., Neumann, R., Perkins, C., Starn, J., Warner, G., 2002. Long-term impact analysis of the University of Connecticut's Fenton River water supply wells on the habitat of the Fenton River, Proposal submitted to the University of Connecticut.

Jens, G. 1986. 'Tauchstäbe zur Messung der Strömungsgeschwindigkeit und des Abflusses.' Deutsche Gewässerkundliche Mitteilungen, 12. Jahrgang, 4, 90-95.

Kessel, Q., 1997. The Use of Fenton and Willimantic Rivers as a Water Source by the University of Connecticut (letter written to the Mansfield Conservation Commission).

Keys, W.S., 1990, Borehole geophysics applied to ground-water investigations: U. S. Geological Survey Techniques of Water-Resources Investigations, book 2, chap. E-2, 149 p.

Lankston, R.W., 1990, High-resolution refraction data acquisition and interpretation. In: Ward, S.H. (ed.), Geotechnical and Environmental Geophysics. Vol. I: Review and Tutorial. Tulsa: Society of Exploration Geophysicists, pp. 45-73.

Leggete, Brashears & Graham, Inc., 2002. Level A Mapping for Fenton River Field University of Connecticut, Final Report prepared for the University of Connecticut, LBG Trumbull, Connecticut.

Leggete, Brashears & Graham (LBG), Inc, Contour map of bedrock surface. Hartford: Ground water and environmental engineering services, 2001.

Meade, D.B, Ground-water availability in Connecticut, Hartford: The Survey, 1978.

Milhous, R.T., A.A. Updike and D.M. Schneider. 1989. Physical habitat simulation system reference manual – version II. Instream Flow Information Paper No. 26. U.S. Fish and Wildlife Service, Biological Report 89(16). v.p.

Miller, D.R., G. S. Warner, F.L. Ogden, and A.T. DeGaetano, Precipitation in Connecticut, Report No. 38, Institute of Water Resources, University of Connecticut, December, 2003.

Mooney, H.M., 1981, Handbook of engineering geophysics, v. 1: Seismic: Minneapolis, Bison Instruments, Inc., pp. 220

Morgan, N.A., 1967, The use of continuous seismic profiles to solve hidden-layer problems, Geophysical Prospecting, v. 15, no. 1, pp. 35-43.

Moyle, P.B., and D.M. Baltz. 1985. Microhabitat use by an assemblage of California stream fishes: developing criteria for instream flow determinations. Transactions of the American Fisheries Society. 114:695-704.

Nadim, F., Bagtzoglou, A.C., Starn, J.J., 2004, Ground water flow simulation of a glacial aquifer and its implication for the management of University of Connecticut water supply system during drought periods, pp. 863-865.

Newcomb, T.J., S.A. Perry and W.B. Perry. 1995. Comparison of habitat suitability criteria for smallmouth bass (*Miropterus dolomieu*) from three West Virginia rivers. Rivers. 5:170-183.

NOAA, National Climatic Data Center, Historical Climatological Network Data, Precipitation. URL: http://lwf.ncdc.noaa.gov/oa/climate/research/ushcn/ushcn.html, last accessed October 17, 2005.

Parasiewicz, P. (in print). Using a fish-habitat time-series analysis to define flow-augmentation strategy for the Quinebaug River, Connecticut and Massachusetts,

USA. Environmental Biology of Fishes Special Issue: MesoHABSIM and Target Fish Community: Methods and Approach.
Parasiewicz, P. 1996. Estimation of physical habitat characteristics using automation and geodesic-based sampling. Regulated Rivers: Research and Management. 12:575-583.
Rahn, P., Surficial Geology of the Spring Hill Quadrangle, [Hartford] State Geological and Natural History Survey of Connecticut, 1970.
Rahn, P., The Hydrogeology of an Induced Streambed Infiltration Area, Ground Water, 1971, 21-32.
Redpath, B.B, 1973, Seismic refraction exploration for engineering site investigation, National technical information service.
Reynolds, J.M., 2000, An introduction to applied and environmental geophysics, John Wiley & Sons Ltd., England, pp. 681-749.
Rodgers, J., Bedrock geological map of Connecticut, Connecticut Geological and Natural History Survey: Hartford, 1985.
Ronan, A.D., Prudic, D.E., and C.E. Thodal, Field study and simulation of diurnal temperature effects on infiltration and variably saturated flow beneath an ephemeral stream, *Water Resour. Res.,(34)*9: 2137-2153, 1998
Sheriff, R.E., 2002, Encyclopedic Dictionary of Applied Geophysics, 4th Ed., Society of Exploration Geophysicists.
Smemoe, C.M, 2000, Processing and visualization of ground penetrating radar for accessing natural hydrogeologic conditions, GPR Oct., 2004. <http://emrl.byu.edu/chris/gpr.htm>.
Smith, C. 1985. The inland fishes of New York state. New York State Department of Environmental Conservation, 50 Wolf Road, Albany, NY 12233.
Stallman, R.W., *Methods of collecting and interpreting ground-water data*, U. S. Geol. Surv. Water Supply Pap. 1544-H, 36-46., 1963.
Strakosh, T.R., R.M. Neumann, and R.A. Jacobson 2003. Development and assessment of habitat suitability criteria for adult brown trout in southern New England rivers. Ecology of Freshwater Fish. 12:265-274.
Stone, J.R., Schafer, J.P., London, E.H., Thompson, W.B., Surficial materials map of Connecticut. Reston, VA: The US Geological Survey; Denver, CO: For sale by Map Distribution, 1992.
Tabachnik, B.G., and L.S. Fidell. 2001. Using multivariate statistics. Allyn & Bacon, Needham Heights, MA 02494.
Theis, C. V., 1941. The Effect of a Well on the Flow of a Nearby Stream. Am. Geophys. Union Trans. Pt. #, pp. 734-738.
Thomas, J.A., and K.D. Bovee. 1993. Application and testing of a procedure to evaluate transferability of habitat suitability criteria. Regulated Rivers: Research and Management. 8:285-294.
United States. Agricultural Stabilization and Conservation Service. Aerial Photography Division, Spring Hill quadrangle, Connecticut, aerial photographs, Salt Lake City, 1963.
University of Connecticut, October 1999. Water Supply Plan.
Waddle, T. J., editor. 2001. PHABSIM for Windows: User's Manual and Exercises. USGS, Fort Collins, CO.

Williams, J.G. 1996. Lost in space: minimum confidence intervals for idealized PHABSIM studies. Transactions of the American Fisheries Society 125(3): 458-465.

Williams, J.H., and Conger, R.W., 1990, Preliminary delineation of contaminated water-bearing fractures intersected by open-hole bedrock wells: Ground Water Monitoring, v. 10, no. 3, p. 118-126.

Williams, J. H., and Johnson, C.D., 2000, Borehole-wall imaging with acoustic and optical televiewers for fractured-bedrock aquifer investigations: Proceedings of the 7th Minerals and Geotechnical Logging Symposium, Golden, Colo., October 24-26, 2000, p. 43-53, CD ROM.

Yilmaz, O., 2001, Seismic data analysis: processing, inversion, and interpretation of seismic data, Society of Exploration Geophysicists, pp. 920-938.

Appendix A. Fisheries Habitat

Appendix A.1: Photographic Examples of Hydromorphologic Units:
TO BE INCLUDED ON CD.

Contents:

Appendix A.2: Modeling subreach, site and transects.
Figures:

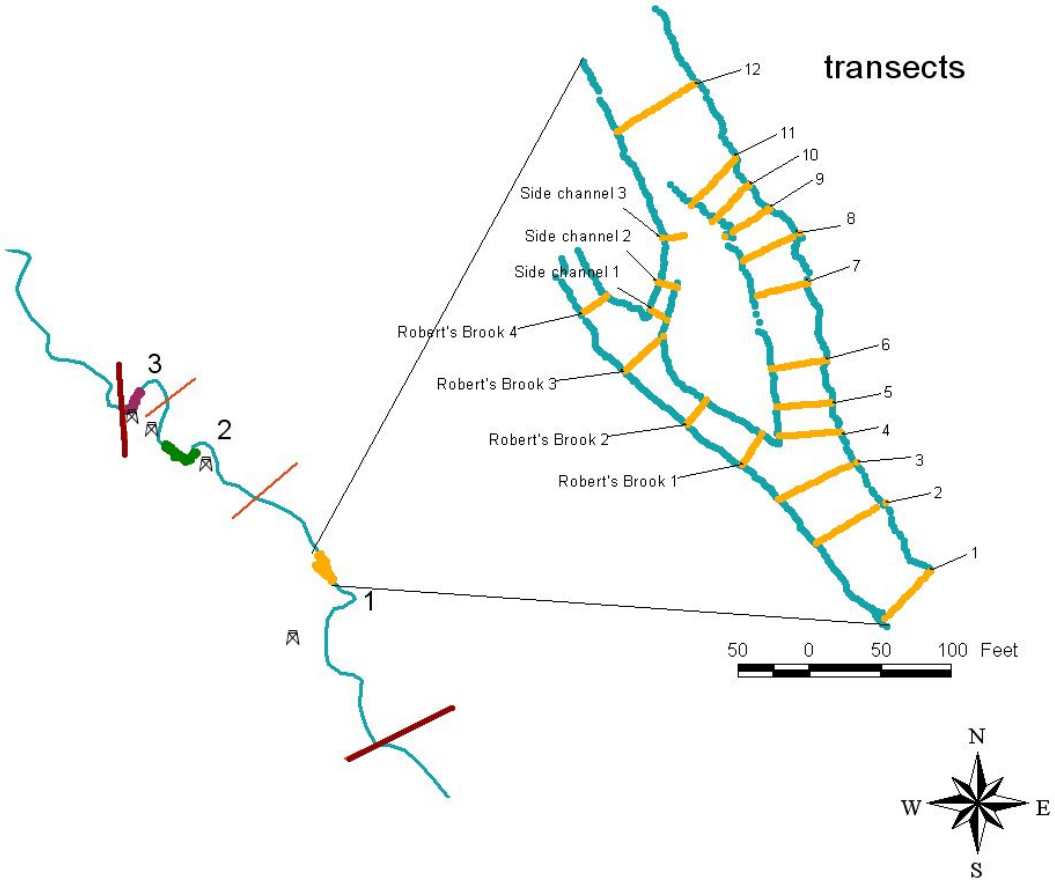

Figure A.2.1 - Modeling subreach, site and transects for Site 1.

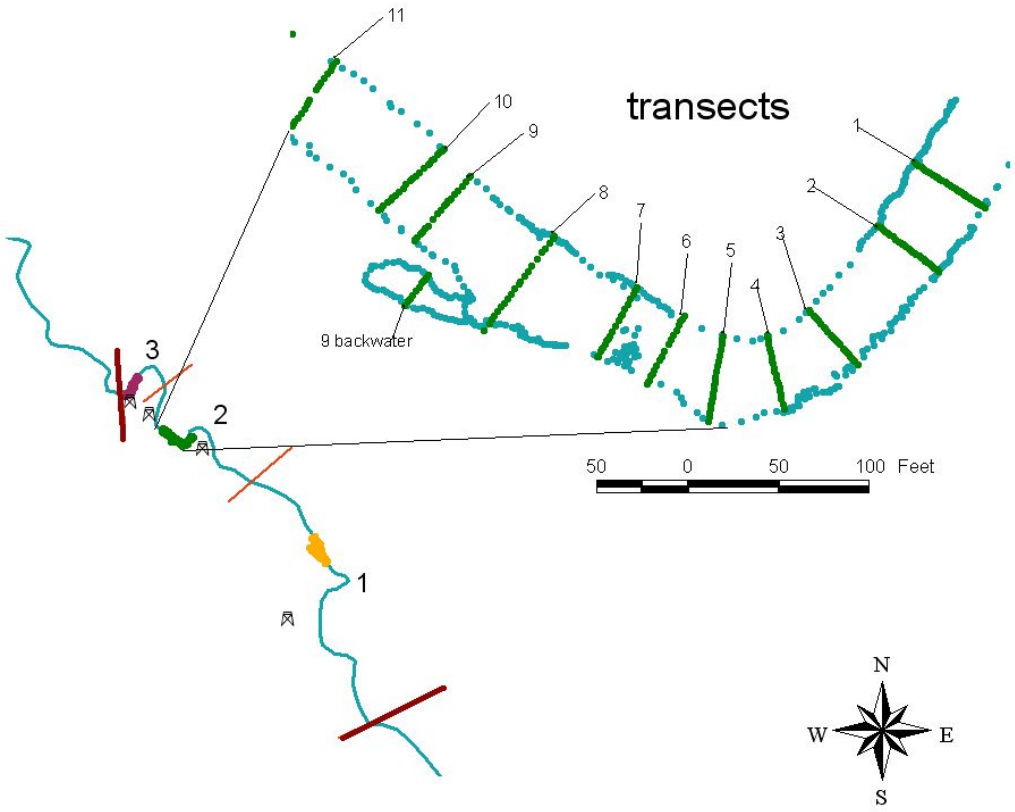

Figure A.2.2 - Modeling subreach, site and transects for Site 2.

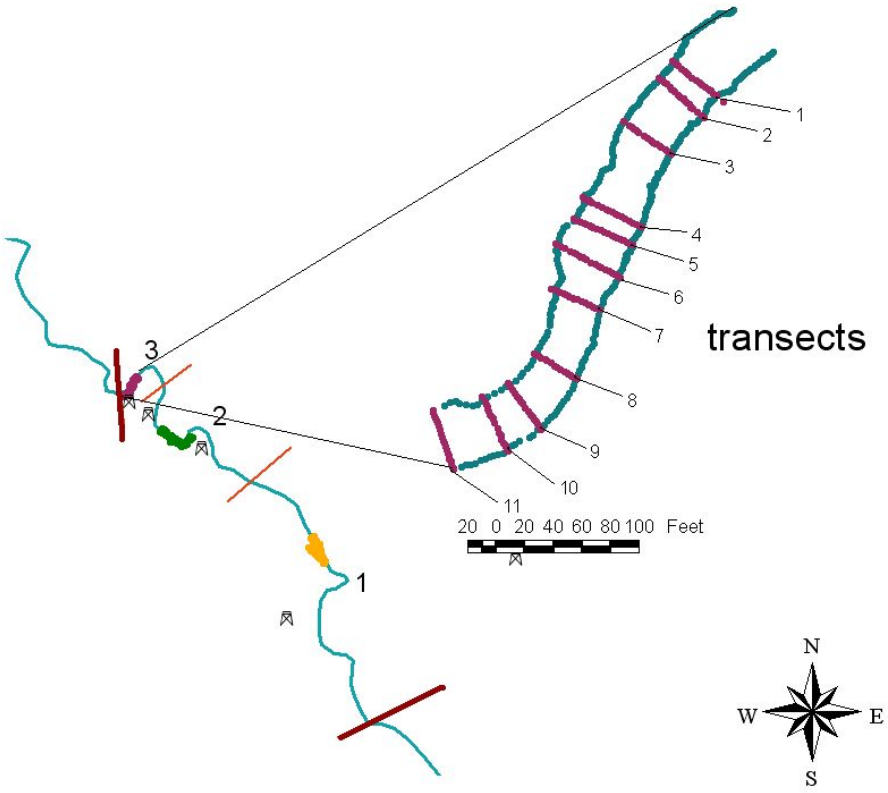

Figure A.2.3 - Modeling subreach, site and transects for Site 3.

Appendix A.3: Water Surface Elevation Calibration Longitudinal Profile Figures:

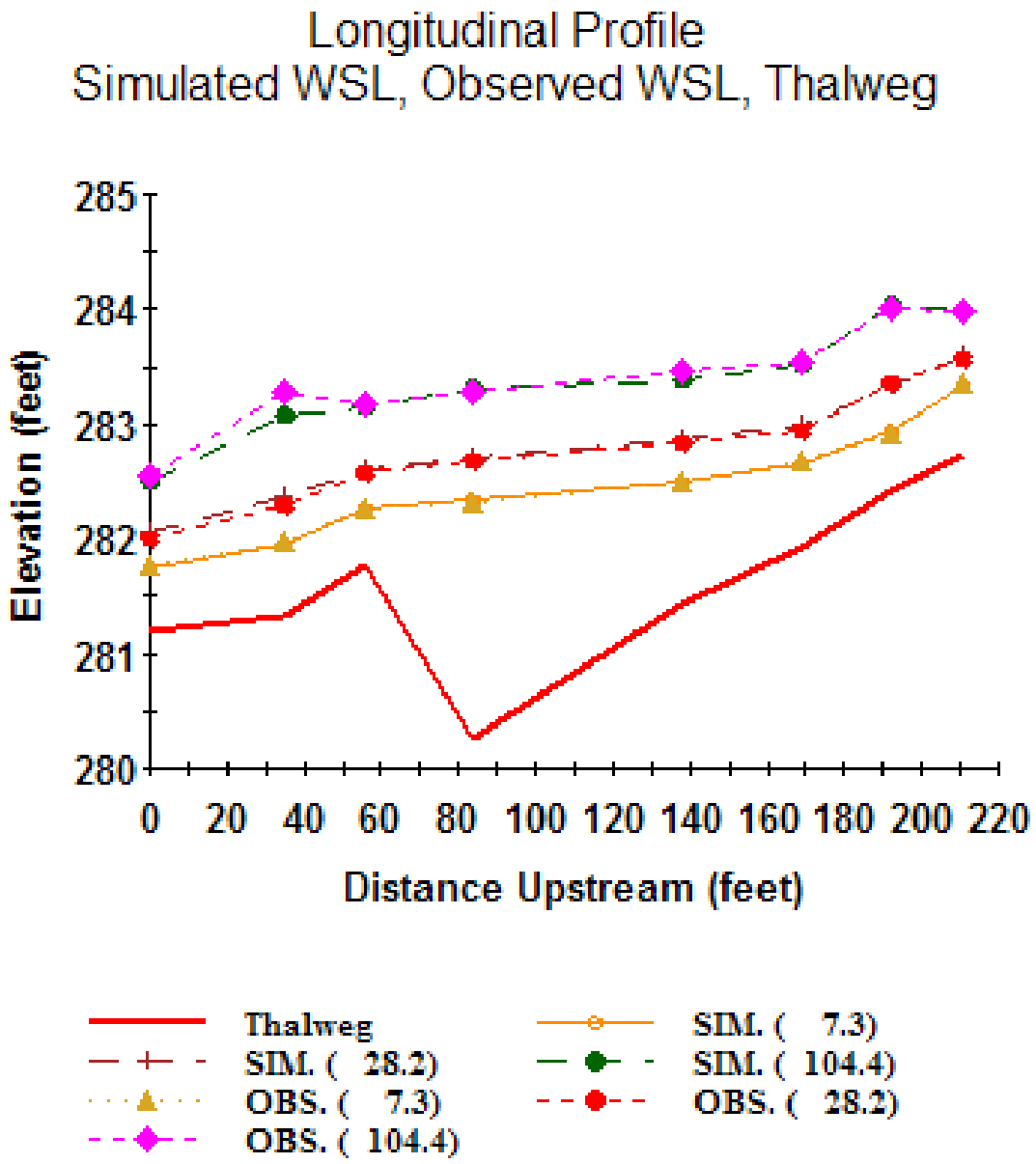

Figure A.3.1 - Water Surface Elevation Calibration Longitudinal Profile: Modeling Sub-Reach 1 at 6.4, 37.4 and 109.3 cfs

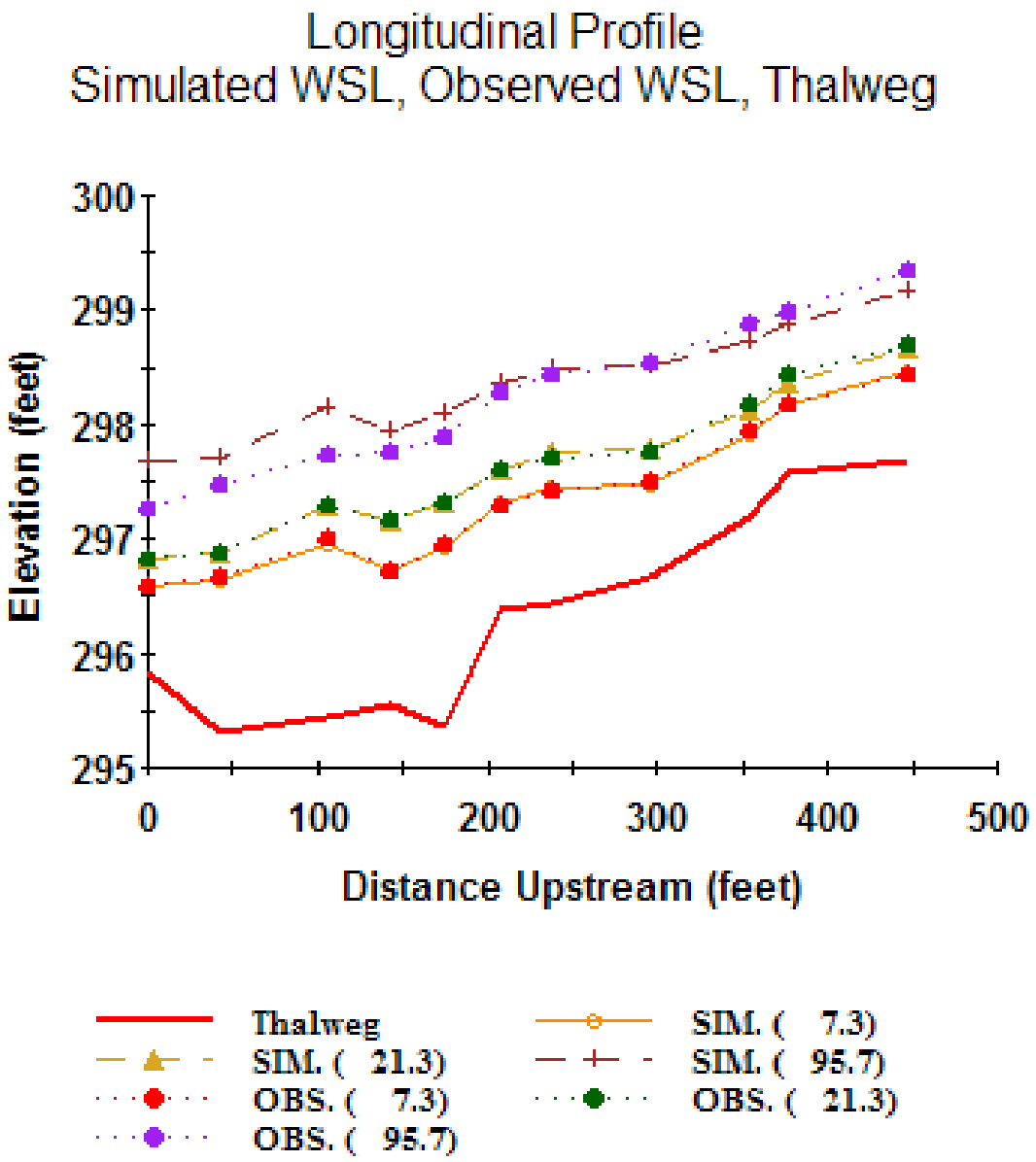

Figure A.3.2 - Water Surface Elevation Calibration Longitudinal Profile: Modeling Sub-Reach 2 at 6.4, 37.4 and 109.3 cfs

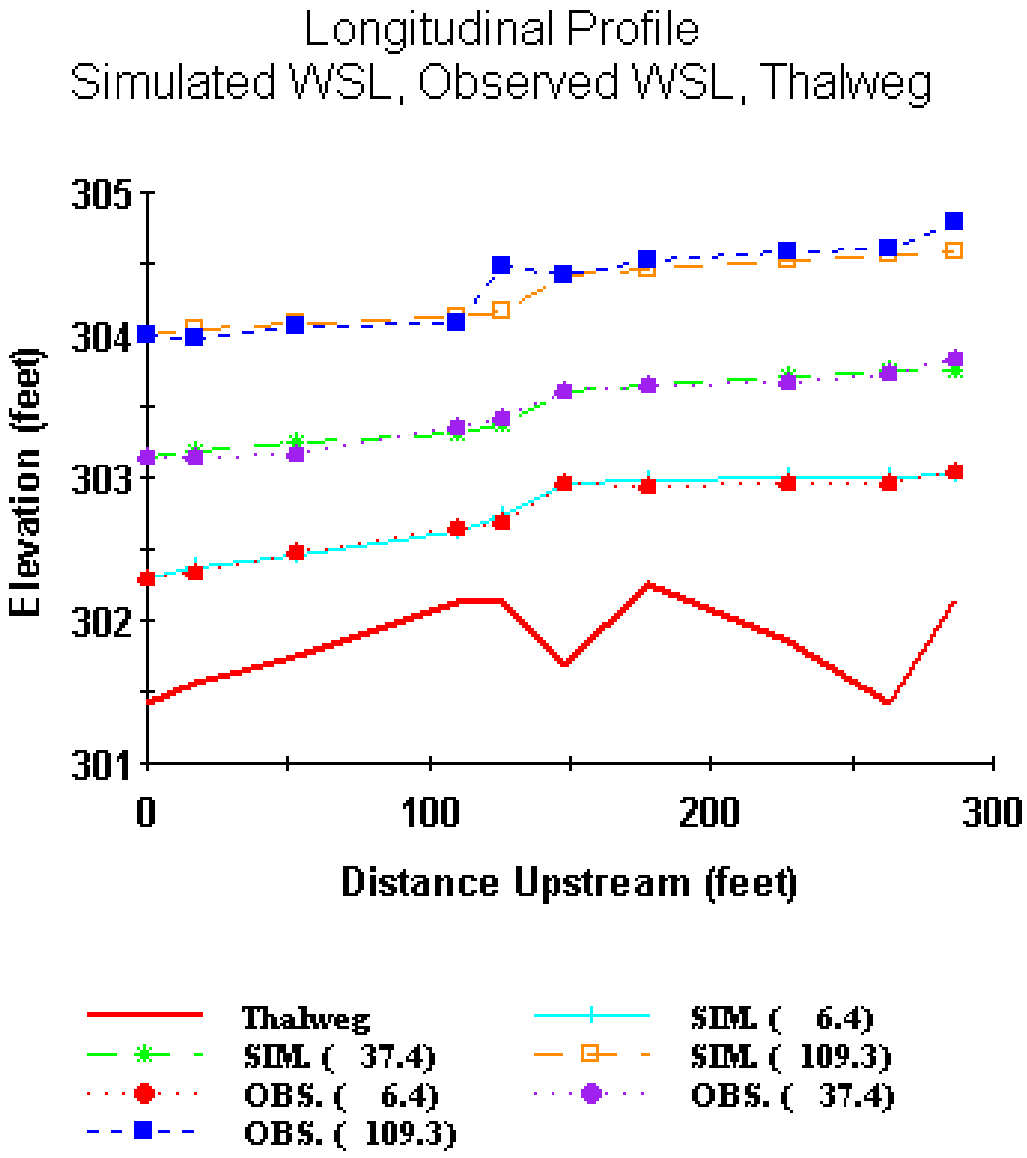

Figure A.3.3 - Water Surface Elevation Calibration Longitudinal Profile: Modeling Sub-Reach 3 at 6.4, 37.4 and 109.3 cfs

Appendix A.4: Modeling Sub-Reach 1, 2 and 3 - Bed Profile, and Simulated Water Surface Elevation and Velocity Distributions at a discharge of 2 cfs.

Figures:

Figure A.4.1. Modeling sub-reach 1 – bed profile, and simulated water surface elevation and velocity distributions (at 2 cfs) for cross-sections (transects) 0.0 through 209.2.

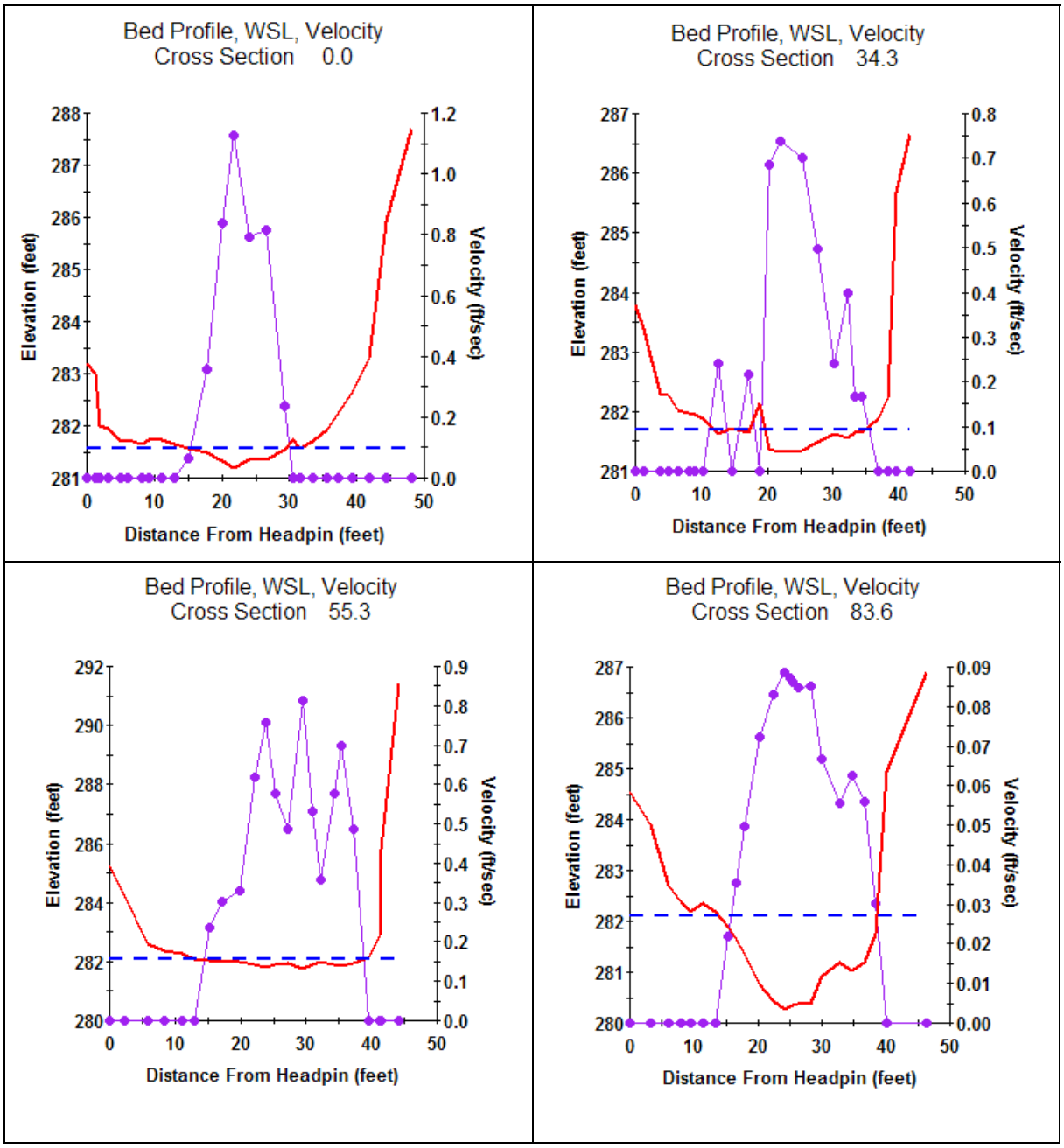

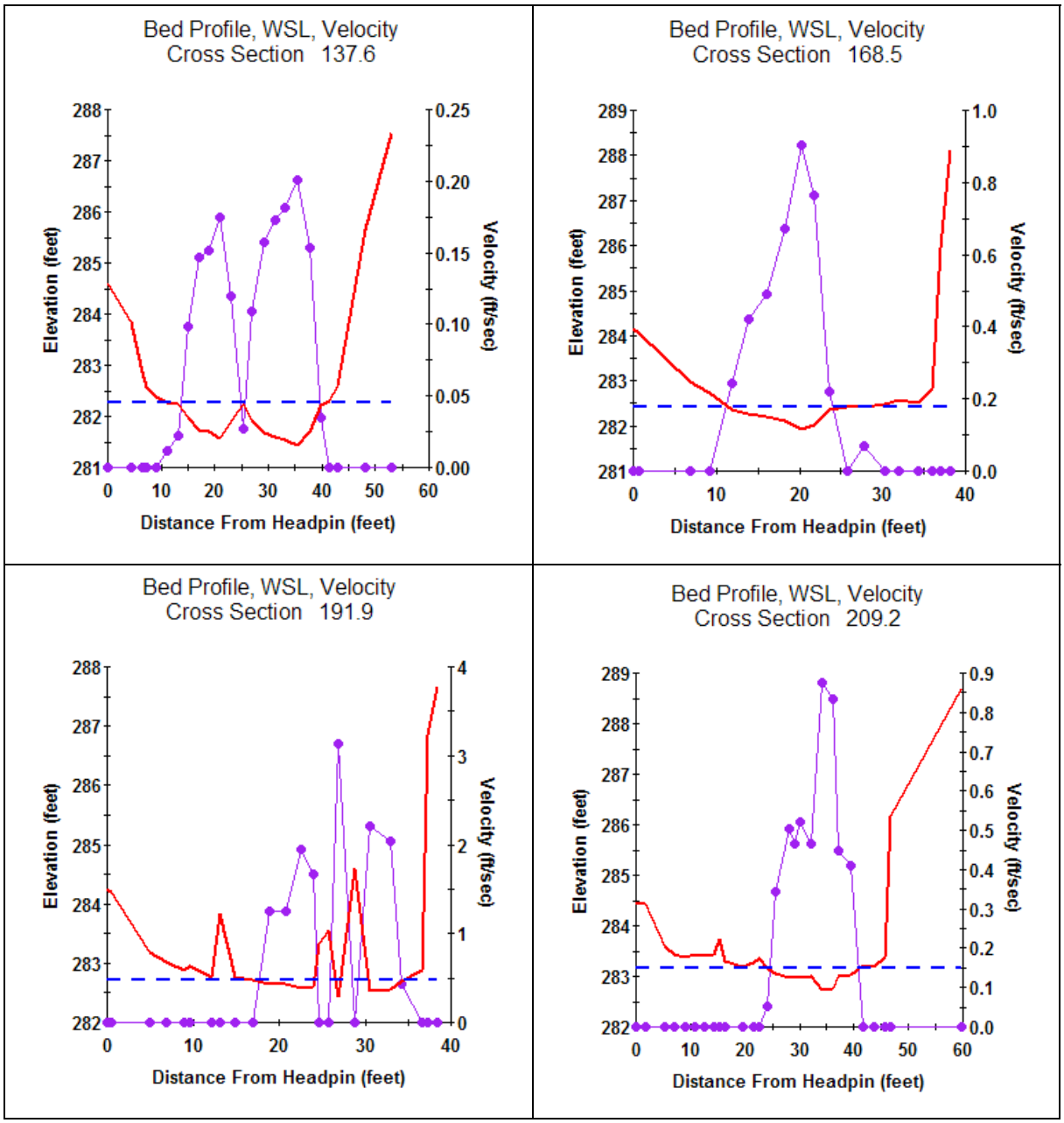
Bed Profile, WSL, Velocity
Cross Section 137.6
Elevation (feet)
Velocity (ft/sec)
Distance From Headpin (feet)
Bed Profile, WSL, Velocity
Cross Section 168.5
Elevation (feet)
Velocity (ft/sec)
Distance From Headpin (feet)
Bed Profile, WSL, Velocity
Cross Section 191.9
Elevation (feet)
Velocity (ft/sec)
Distance From Headpin (feet)
Bed Profile, WSL, Velocity
Cross Section 209.2
Elevation (feet)
Velocity (ft/sec)
Distance From Headpin (feet)

Figure A.4.2. Modeling sub-reach 2 – bed profile, and simulated water surface elevation and velocity distributions (at 2 cfs) for cross-sections (transects) 0.0 through 447.9.

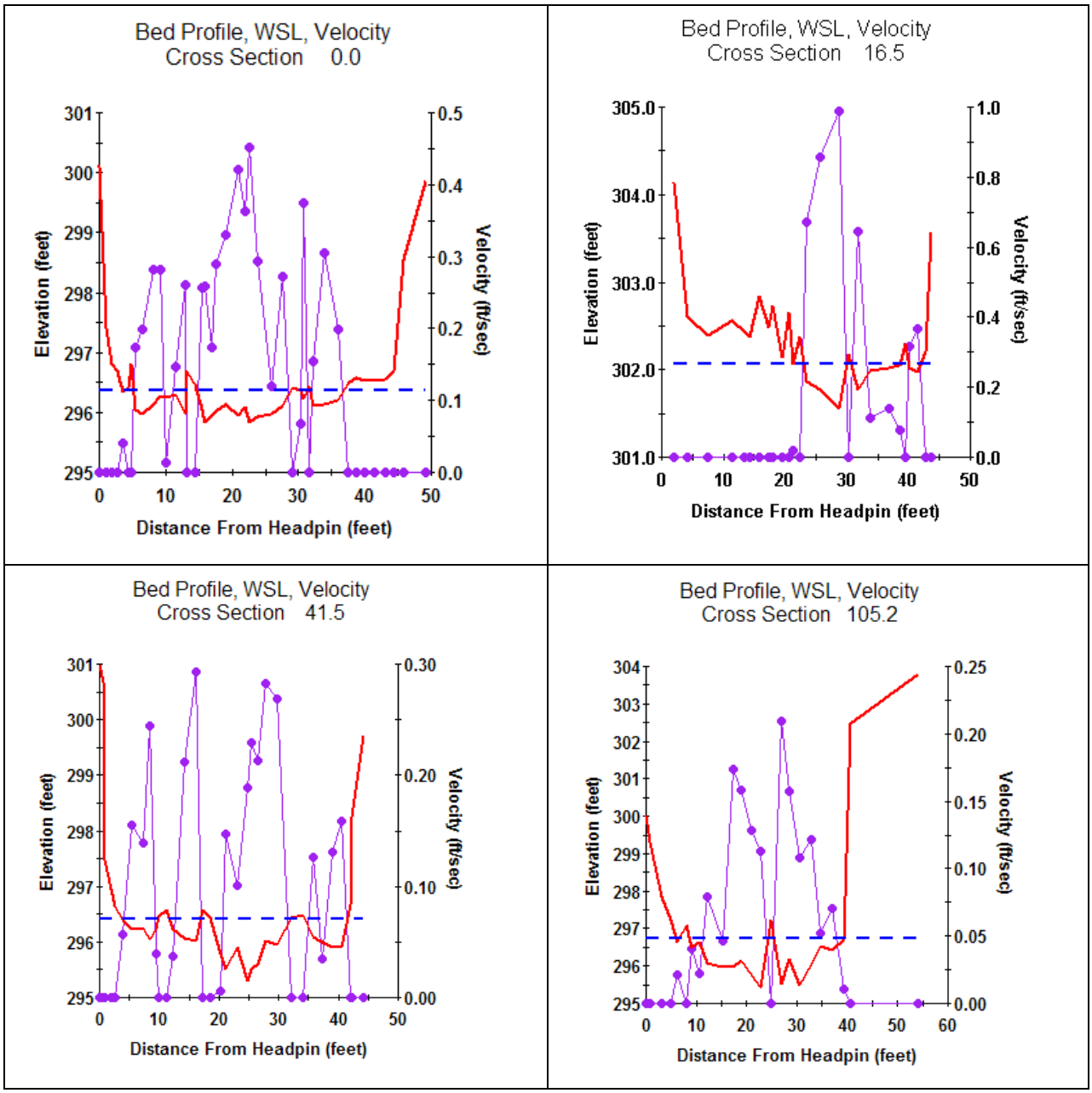

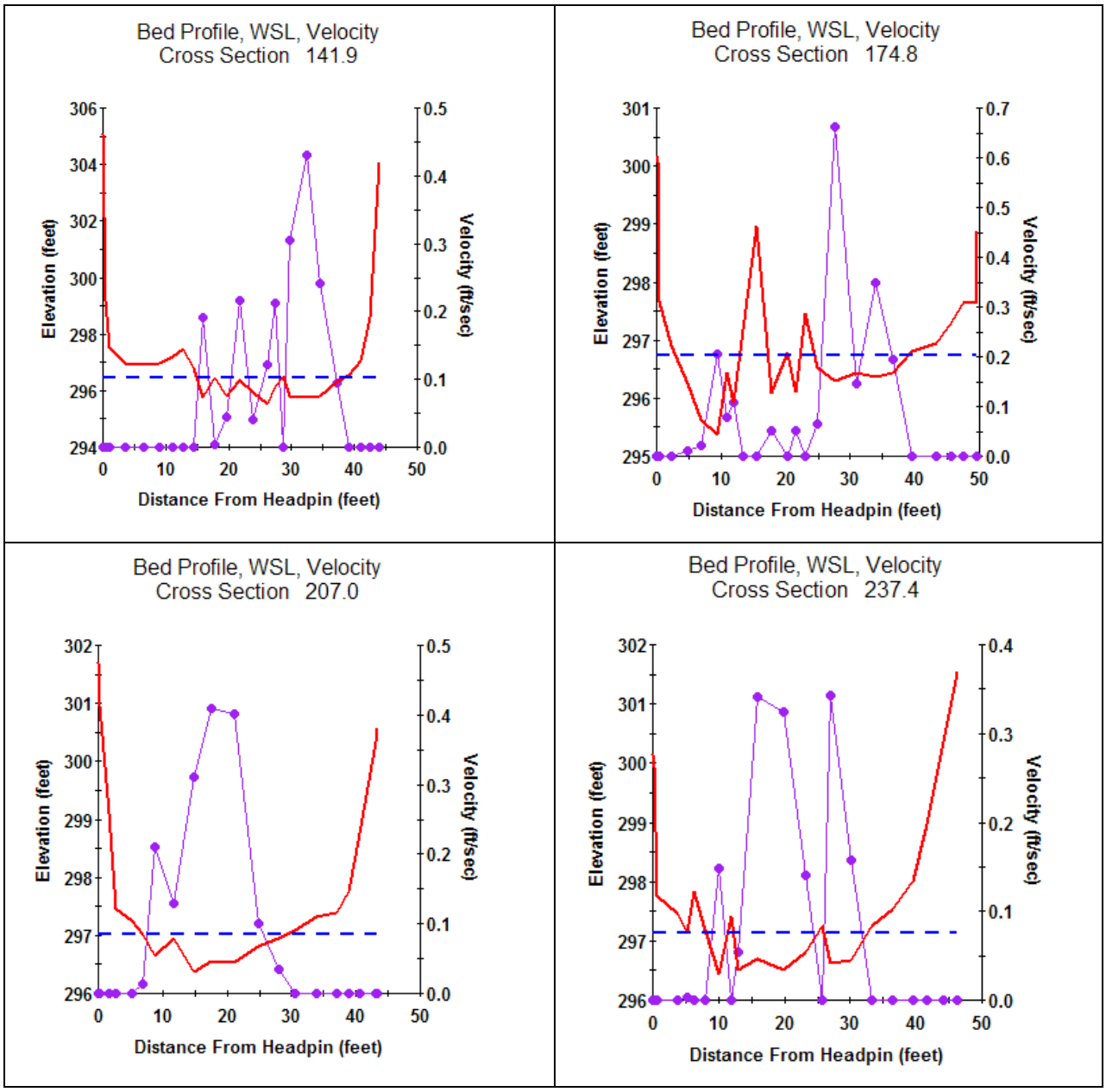
Bed Profile, WSL, Velocity
Cross Section 141.9
Elevation (feet)
Velocity (ft/sec)
Distance From Headpin (feet)
Bed Profile, WSL, Velocity
Cross Section 174.8
Elevation (feet)
Velocity (ft/sec)
Distance From Headpin (feet)
Bed Profile, WSL, Velocity
Cross Section 207.0
Elevation (feet)
Velocity (ft/sec)
Distance From Headpin (feet)
Bed Profile, WSL, Velocity
Cross Section 237.4
Elevation (feet)
Velocity (ft/sec)
Distance From Headpin (feet)

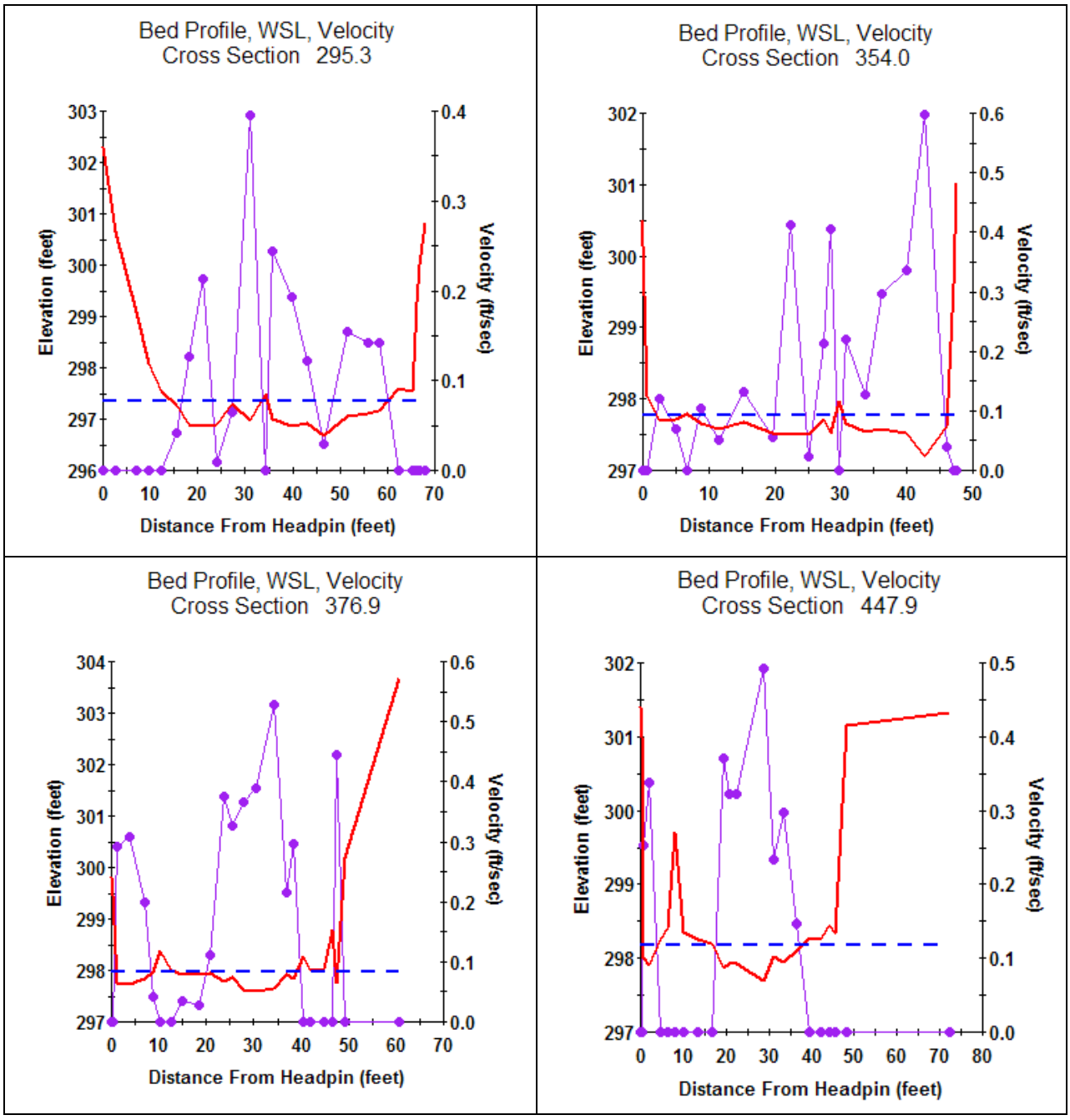
Bed Profile, WSL, Velocity
Cross Section 295.3
Elevation (feet)
Velocity (ft/sec)
Distance From Headpin (feet)
Bed Profile, WSL, Velocity
Cross Section 354.0
Elevation (feet)
Velocity (ft/sec)
Distance From Headpin (feet)
Bed Profile, WSL, Velocity
Cross Section 376.9
Elevation (feet)
Velocity (ft/sec)
Distance From Headpin (feet)
Bed Profile, WSL, Velocity
Cross Section 447.9
Elevation (feet)
Velocity (ft/sec)
Distance From Headpin (feet)

Figure A.4.3. Modeling sub-reach 3 – bed profile, and simulated water surface elevation and velocity distributions (at 2 cfs) for cross-sections (transects) 0.0 through 286.5.

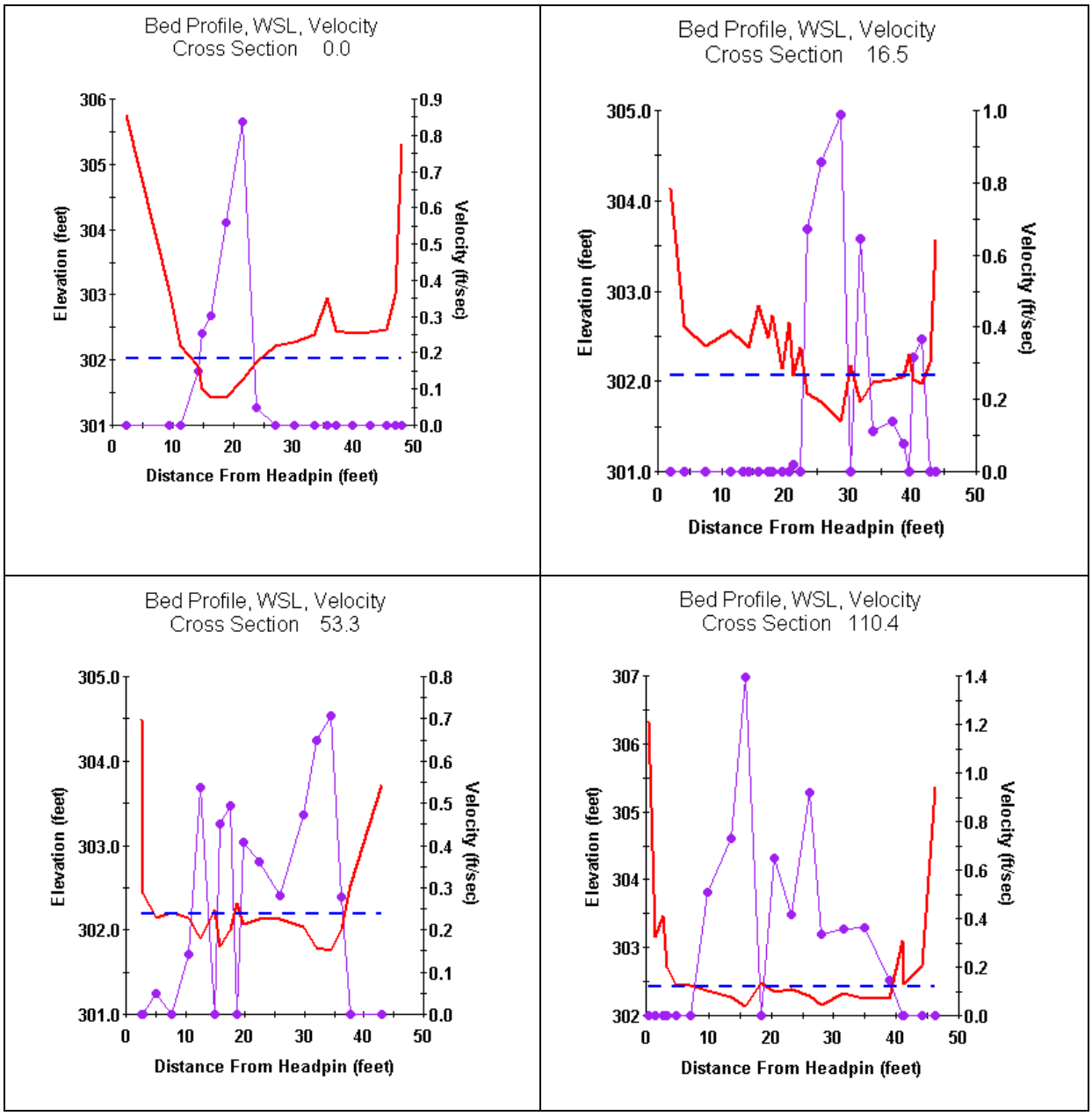

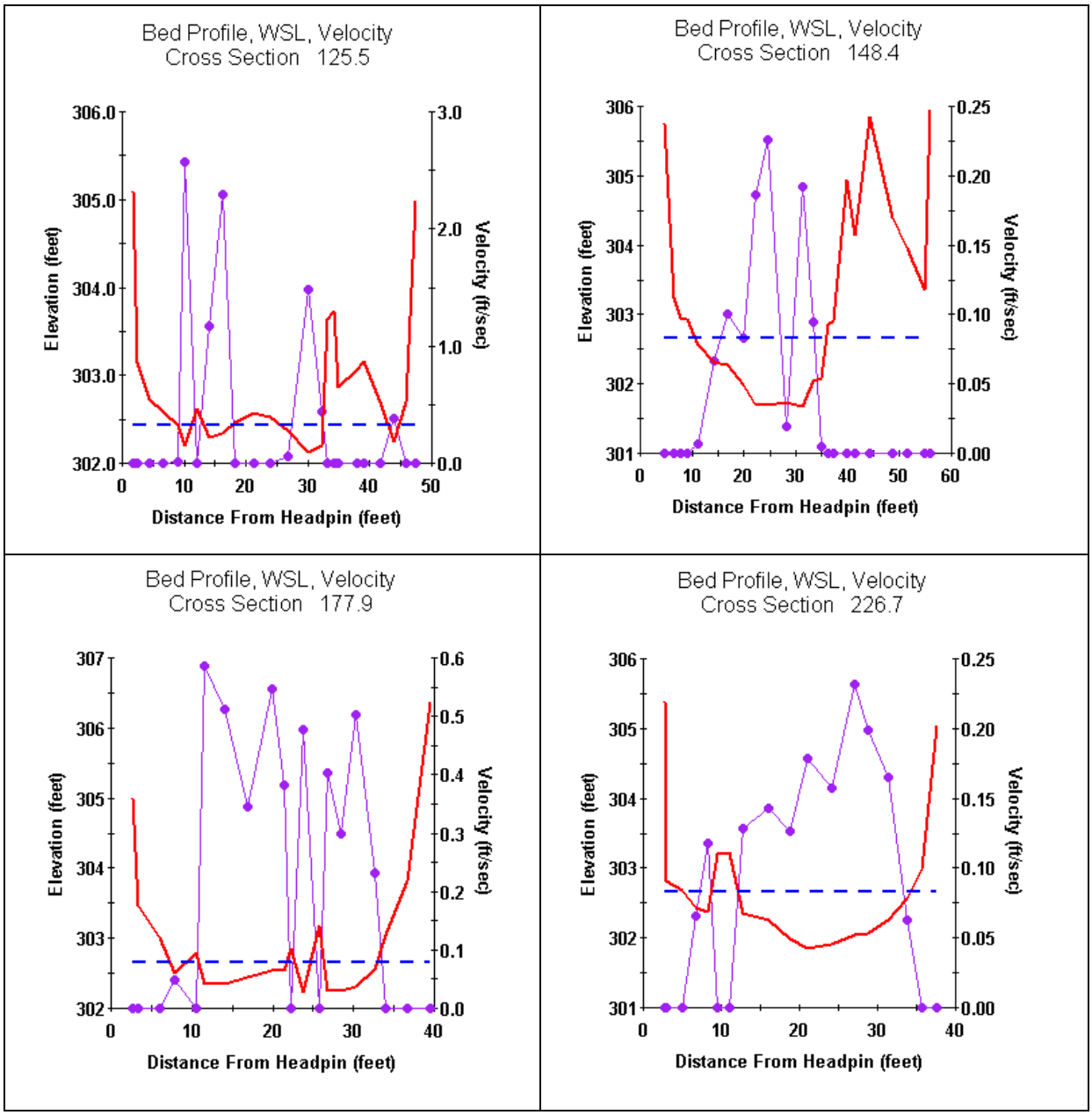
Bed Profile, WSL, Velocity
Cross Section 125.5
Elevation (feet)
Velocity (ft/sec)
Distance From Headpin (feet)
Bed Profile, WSL, Velocity
Cross Section 148.4
Elevation (feet)
Velocity (ft/sec)
Distance From Headpin (feet)
Bed Profile, WSL, Velocity
Cross Section 177.9
Elevation (feet)
Velocity (ft/sec)
Distance From Headpin (feet)
Bed Profile, WSL, Velocity
Cross Section 226.7
Elevation (feet)
Velocity (ft/sec)
Distance From Headpin (feet)

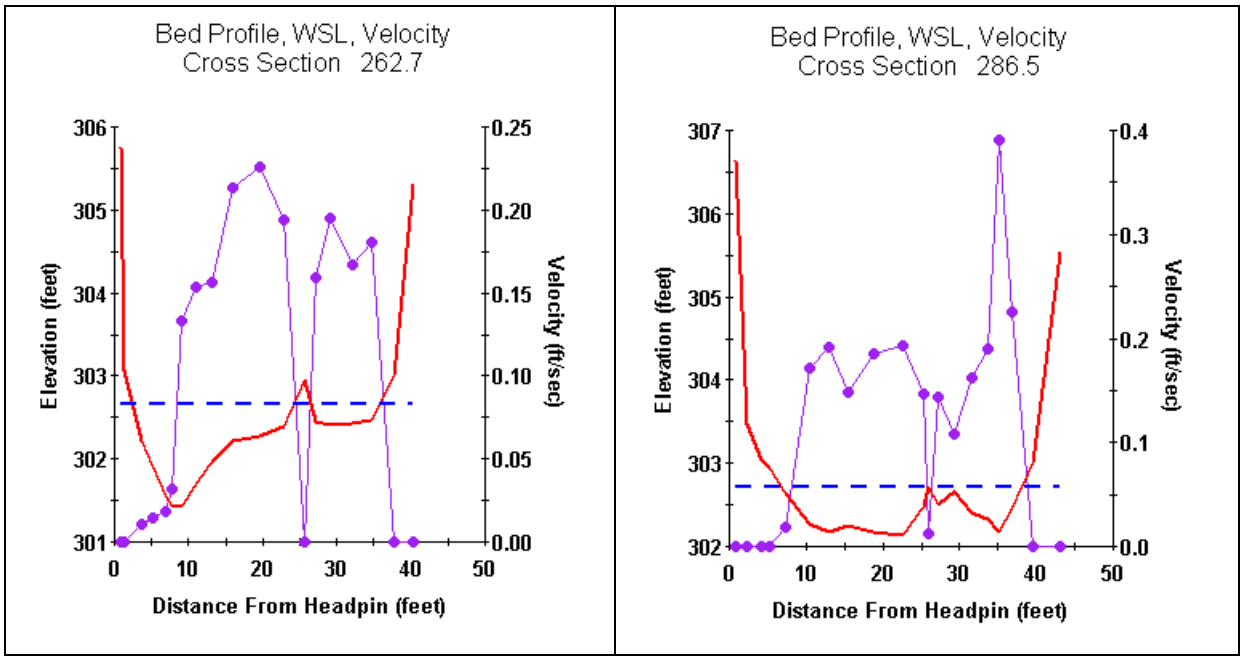
Bed Profile, WSL, Velocity
Cross Section 262.7
Elevation (feet)
306
305
304
303
302
301
0.25
0.20
0.15
0.10
0.05
0.00
Velocity (ft/sec)
0
10
20
30
40
50
Distance From Headpin (feet)
Bed Profile, WSL, Velocity
Cross Section 286.5
Elevation (feet)
307
306
305
304
303
302
0.4
0.3
0.2
0.1
0.0
Velocity (ft/sec)
0
10
20
30
40
50
Distance From Headpin (feet)

Appendix A.5: Modeling Sub-Reach 1, 2 and 3 Weighted Usable Area Projections Figures:

A.5.1 Modeling Sub-Reach 1

A.5.2 Modeling Sub-Reach 2

A.5.3 Modeling Sub-Reach 3

Figure A.5.1. Modeling sub-reach 1 – weighted usable area response curves for adult brook trout, brown trout, tessellated darter and fallfish.

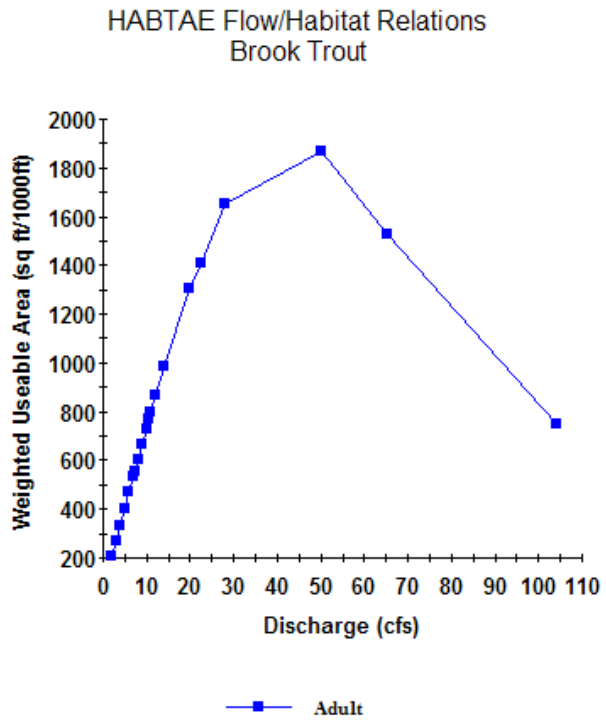

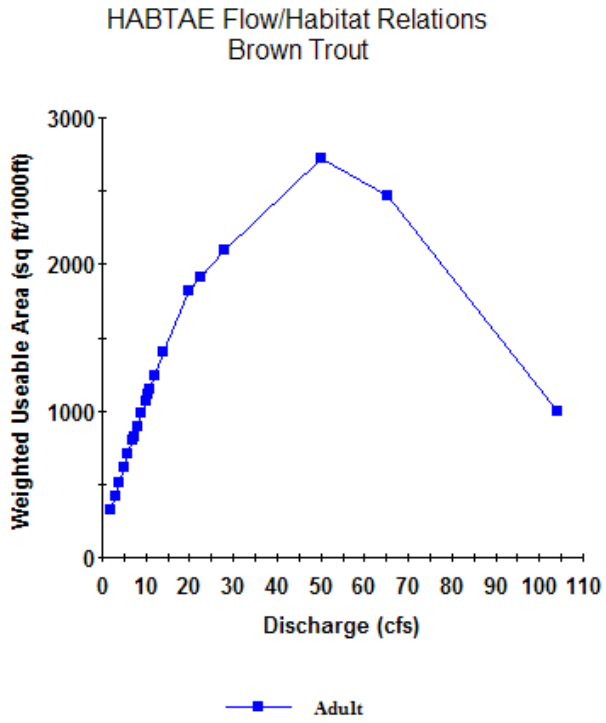

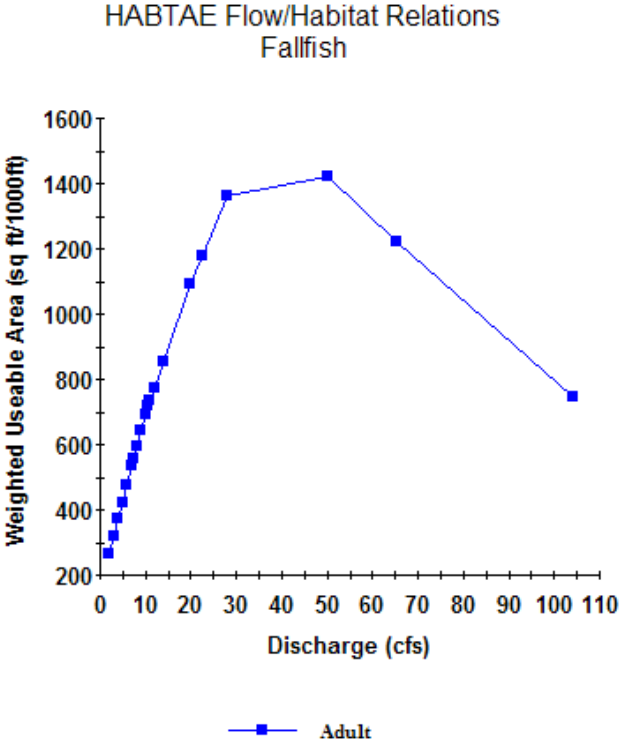

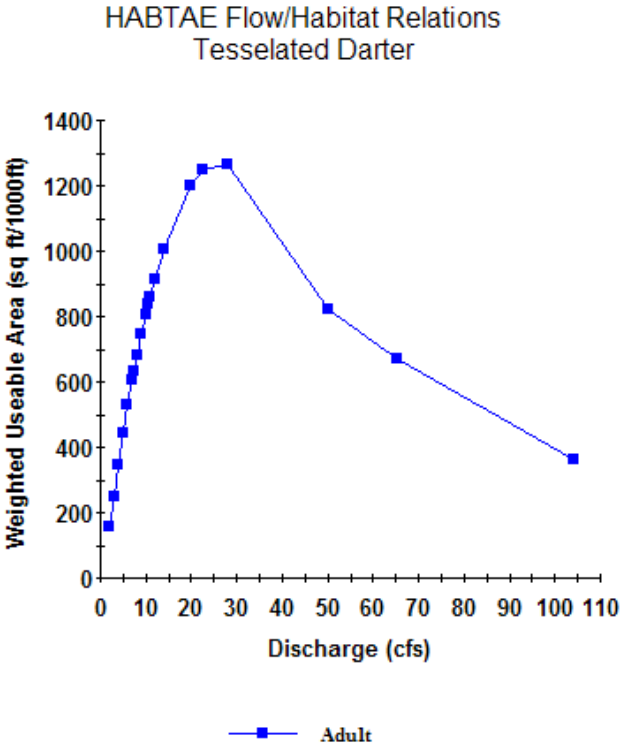

Figure A.5.2. Modeling sub-reach 2 – weighted usable area response curves for adult brook trout, brown trout, tessellated darter and fallfish.

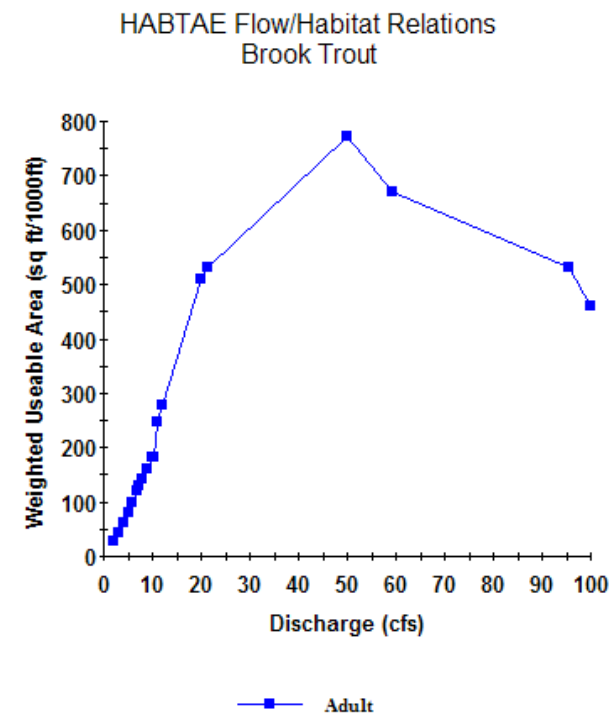

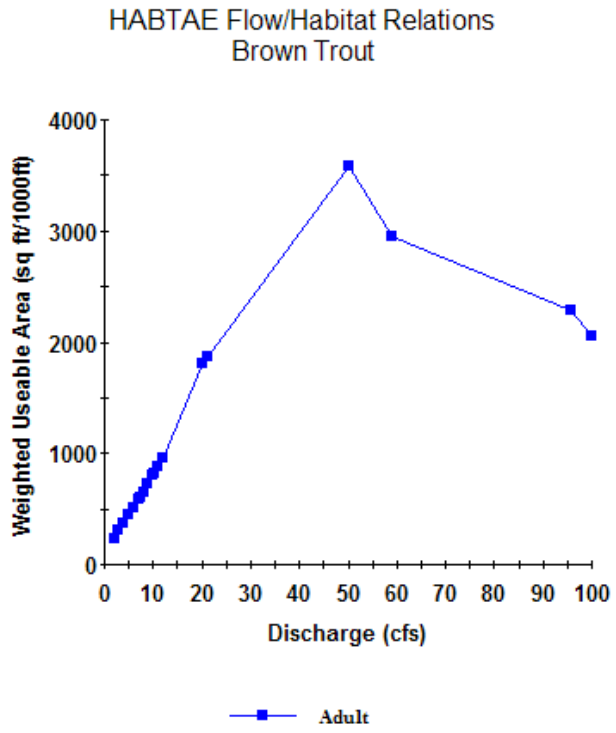

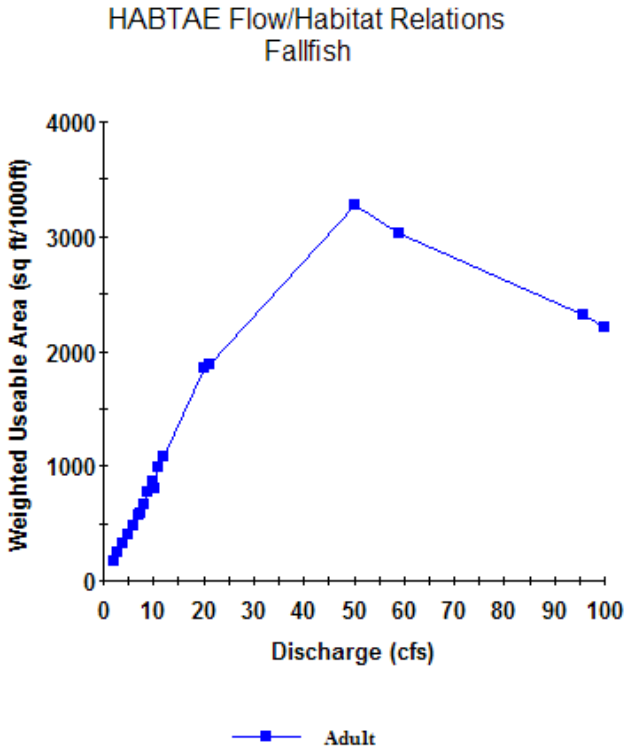

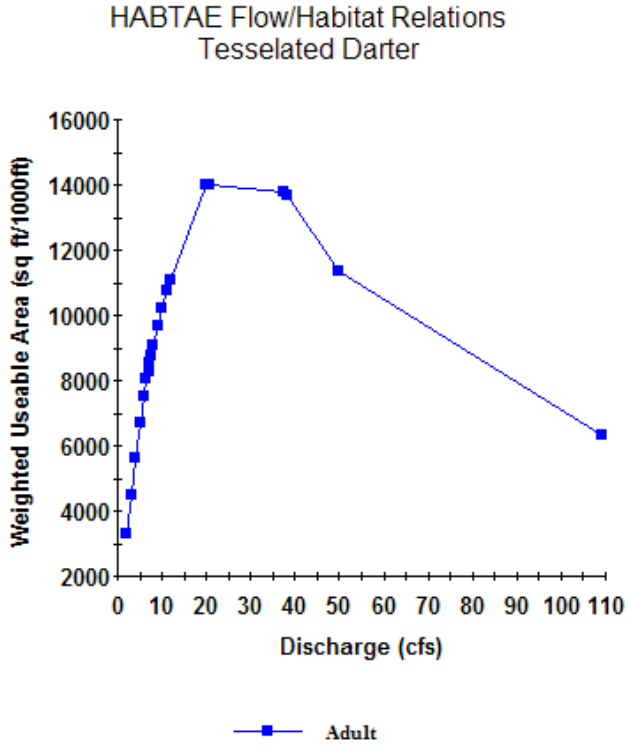

Figure A.5.3. Modeling sub-reach 3 – weighted usable area response curves for adult brook trout, brown trout, tessellated darter and fallfish.

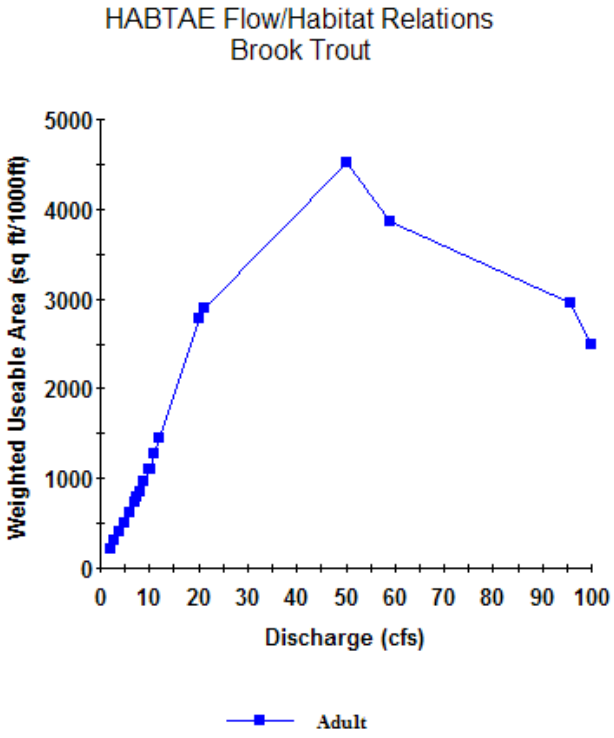

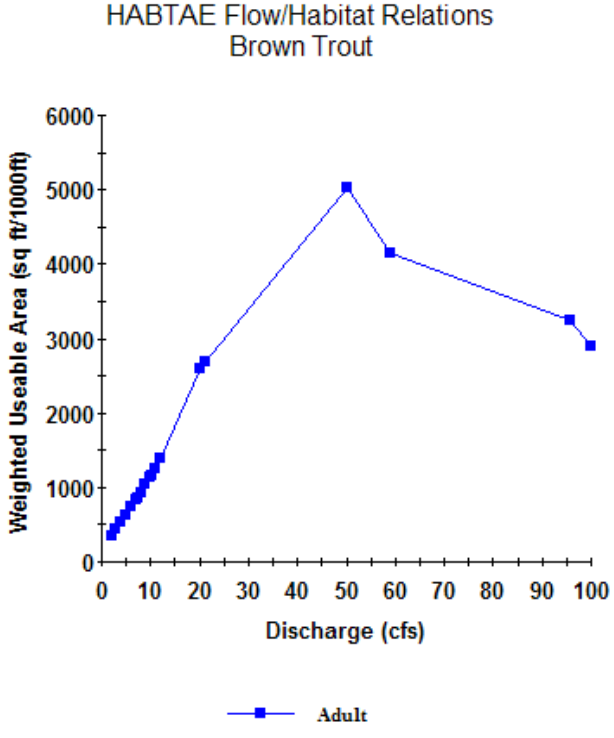

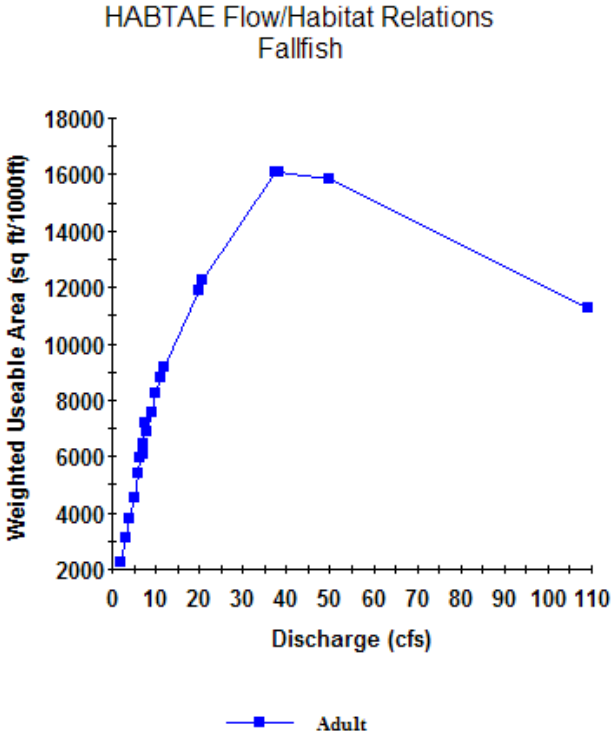

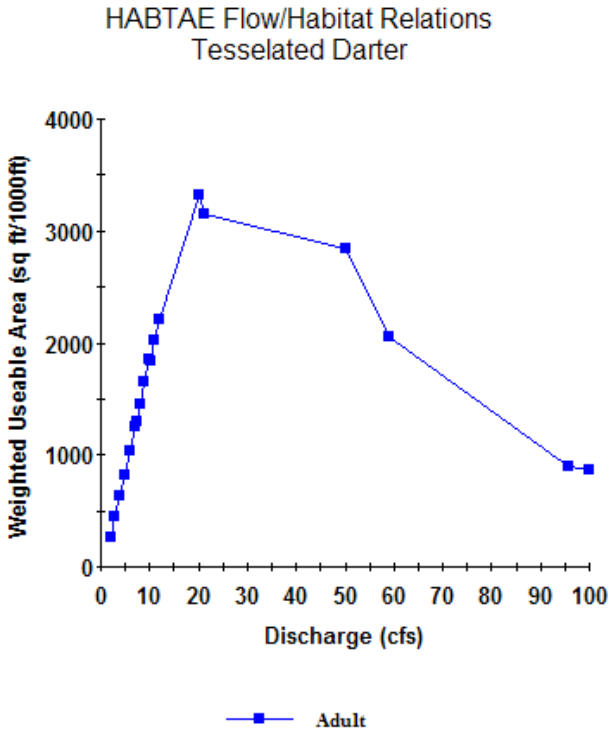

APPENDIX B. Surface Water Measurements

Discharge measurements were taken at various points along the Fenton River during the study period. Techniques of measurement included the Price or pygmy current meters, the Marsh-McBirney velocity meter, an Acoustic Doppler Current Profiler (ADCP), and weirs built in the stream bed. The Price and pygmy (much smaller version) current meters are mechanical devices that measure the velocity based on a calibrated rotating cups. The March-McBirney velocity meter is based on changes in the magnetic field at different water velocities. The Price, pygmy and Marsh-McBirney are all point measurement devices. The ADCP instrument, the StreamPro™ by RD Instruments, measures both the depth and velocities using sound waves that are reflected off of the bed of the stream and particles in the flow, respectively. The instrument is pulled across the stream and provides a two-dimensional distribution of velocity with depth and distance from the bank. It automatically determines a discharge for each transect taken. A picture of the StreamPro™ is shown in Fig. B.1, and an example graph of velocity distribution in a stream cross section is shown in Fig. B.2.

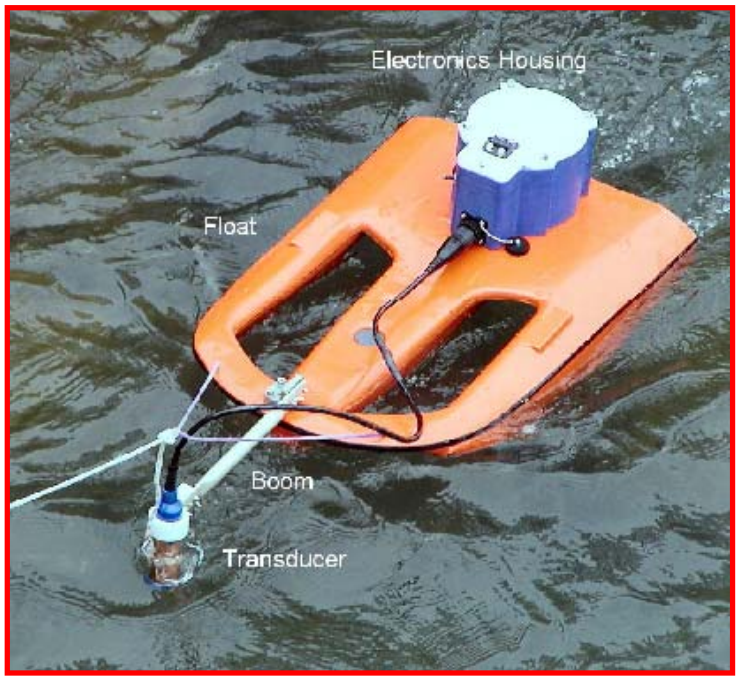

Figure B.1: Picture of StreamPro™ ADCP used in Fenton Study for discharge measurements. Courtesy of RD Instruments.

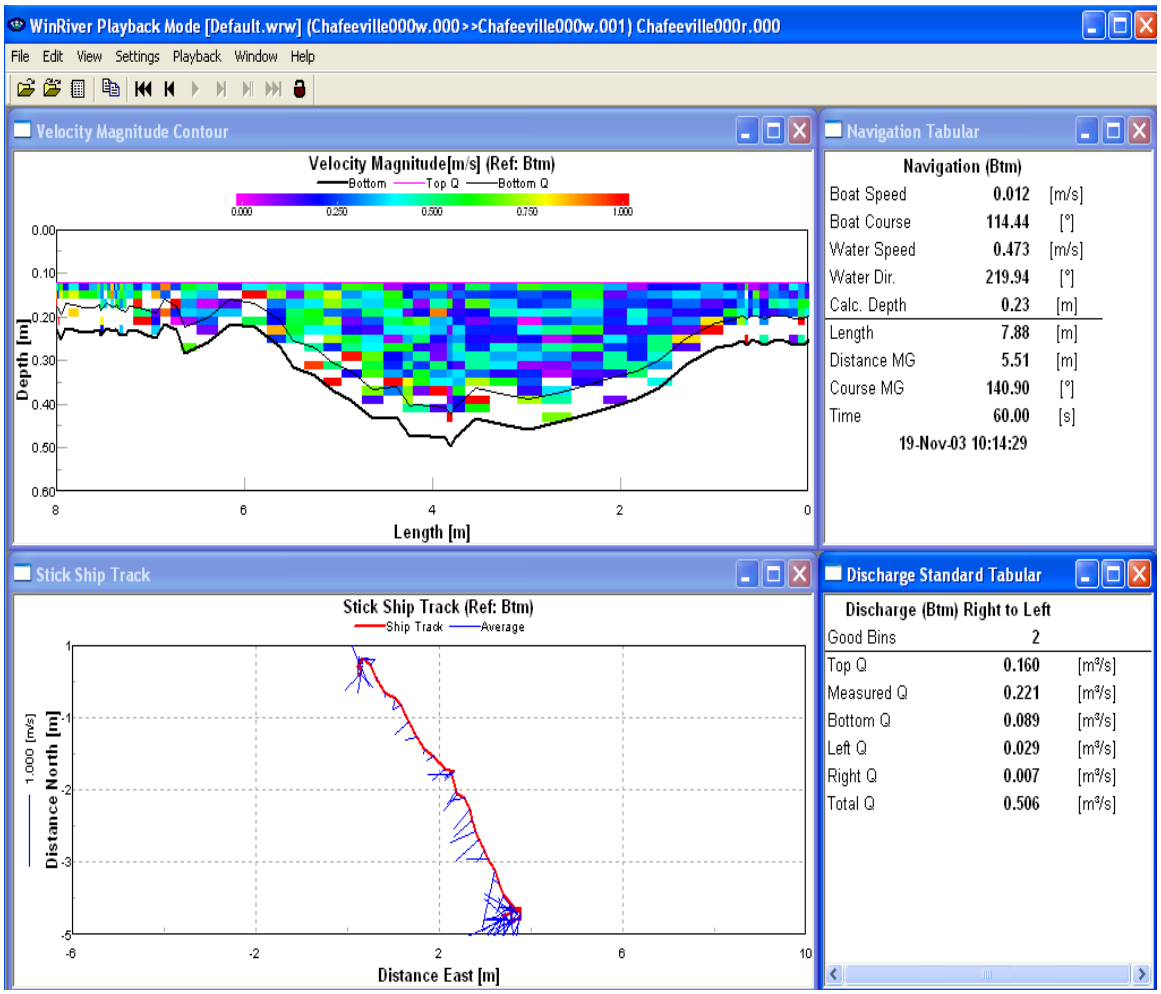

Figure B.2: Graphs of example outputs for StreamPro™ ADCP. Courtesy of RD Instruments.

The primary measurement points using ADCP were: Old Turnpike Road, 'Above Meadow', 'Below Meadow', at Gurleyville Road and at Chaffeeville Road. Measurements were taken on a frequent basis throughout the summer and fall 2004 at these points. Fig. B.3 shows the locations of these points. Additional measurements were taken at selected points of interest on an occasional basis, especially during the pumping tests. Stage levels (local water surface elevations) were measured both manually and with pressure transducers connected to automated data recorders. Data from the discharge measurements and stage recorders were used to determine rating curves that can be used to estimate additional discharges at times when only stage is known. Two different automated stage recorders were used: the LevelLogger by Solinst™ and Minitroll™ by Insitu, Inc. Both devices record the depth using pressure transducers at selected intervals

of time. These devices can be left in the field for long periods, and the data downloaded to computers when needed.

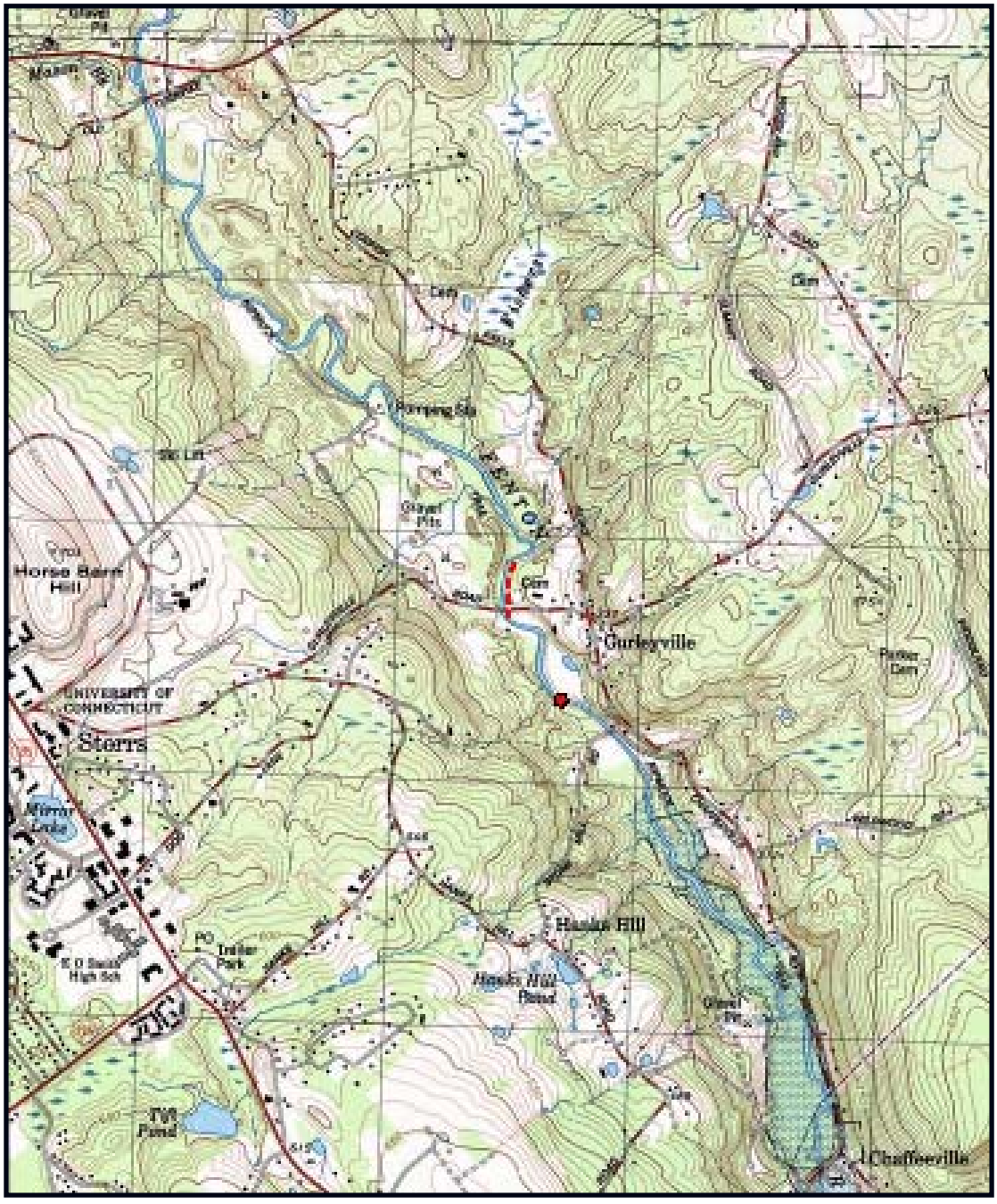

Figure B.3: Primary measurement points using ADCP

Weirs (or flumes) were built in two places in the Fenton River and in three tributaries (Fishers Brook, Roberts Brook and an unnamed intermittent stream) to the Fenton. The discharges were used to perform mass balances and to assess impacts of pumping on stream flow. The two weirs on the Fenton bracketed Well A. The weirs/flumes were built under the permit issued by the CT DEP. The two weirs in the Fenton and the flume in Roberts Brook were either completely or partial destroyed by the high flows that occurred in September, 2004 from hurricanes/tropical storms that moved through the area. The weirs/flumes were removed at the end of the project.

Appendix C. Pumping Test Methodology

In the spring and summer of 2004, the University of Connecticut conducted a series of pumping tests to perform a detailed hydrogeologic assessment of the Fenton River aquifer. A total of 17 monitoring wells were available during the pumping tests (Figure C.1). Eleven of these monitoring wells (MW-##-99) were installed by Leggette, Brashears, and Graham, Inc. for their Level A Mapping Study in 1999. The six additional monitoring wells (UC-##-03) were installed by the University of Connecticut.

Four pumping tests were conducted for each of the production wells (A, B, C, and D). For each pumping test, the pumping well was off for at least 24 hours prior to the test. Static water levels were recorded in designated monitoring wells using pressure transducers (MiniTROLLs) at a 10 minute interval to the nearest 0.01 ft (Refer to Tables C.1 and C.3 for pumping test configurations of gauged monitoring wells). During the test, water levels in monitoring wells were measured every minute. For all pumping tests, the pumping phase of the test lasted more than 72 hours (Refer to Tables C.2 and C.4 for a summary of the pumping phase from each test). The recovery phase lasted as long if not longer than the pumping phase for each test. Locations and elevations of wells can be found in Table C.5.

Table C.1: Configurations of gauged monitoring wells for the August 2004 pumping test.

	Pump A	**Pump B**	**Pump C**	**Pump D**
MW-1-99	X	X	X	
MW-3-99	X	X	X	
MW-4D-99	X	X	X	
MW-4S-99	X	X	X	
MW-5-99		X	X	
MW-6-99		X	X	
MW-7-99	X	X	X	
MW-8-99	X			
MW-9-99	X	X	X	X
MW-10-99	X	X	X	X
MW-11-99				X
UC-1D-03				X
UC-1S-03				X
UC-4-03	X			X
UC-5-03	X			X
UC-6-03		X	X	
UC-K-03	X	X	X	X

Table C.2: Pumping phase summary for the August 2004 pumping test.

	Pump A	Pump B	Pump C	Pump D
Pump Start (GMT)	8/2/04 14:07	7/26/04 16:38	8/9/04 12:18	8/30/04 15:02
Pump End (GMT)	8/6/04 17:41	7/30/04 18:17	8/13/04 17:11	9/2/04 19:50
Avg. Pumping Rate (GPM)	270	560	375	346

Table C.3: Configurations of gauged monitoring wells for the March 2004 pumping test.

Monitoring Well	Pump A	Pump B	Pump C	Pump D
MW-1-99				
MW-3-99				
MW-4D-99		×		
MW-4S-99		×		
MW-5-99		×		
MW-6-99		×		
MW-7-99				
MW-8-99				
MW-9-99				
MW-10-99				
MW-11-99				
UC-1D-03				
UC-4-03				
UC-5-03				
UC-6-03				
UC-K-03				
USGS-Bedrock1		×		
USGS-Bedrock2		×		

Table C.4: Pumping phase summary for the March 2004 pumping test.

Pump B (Average Pumping Rate Throughout the Pump Test was 560 GPM).

Pump Start (GMT)	03/04/04	22:04
Pump End (GMT)	03/30/04	12:04

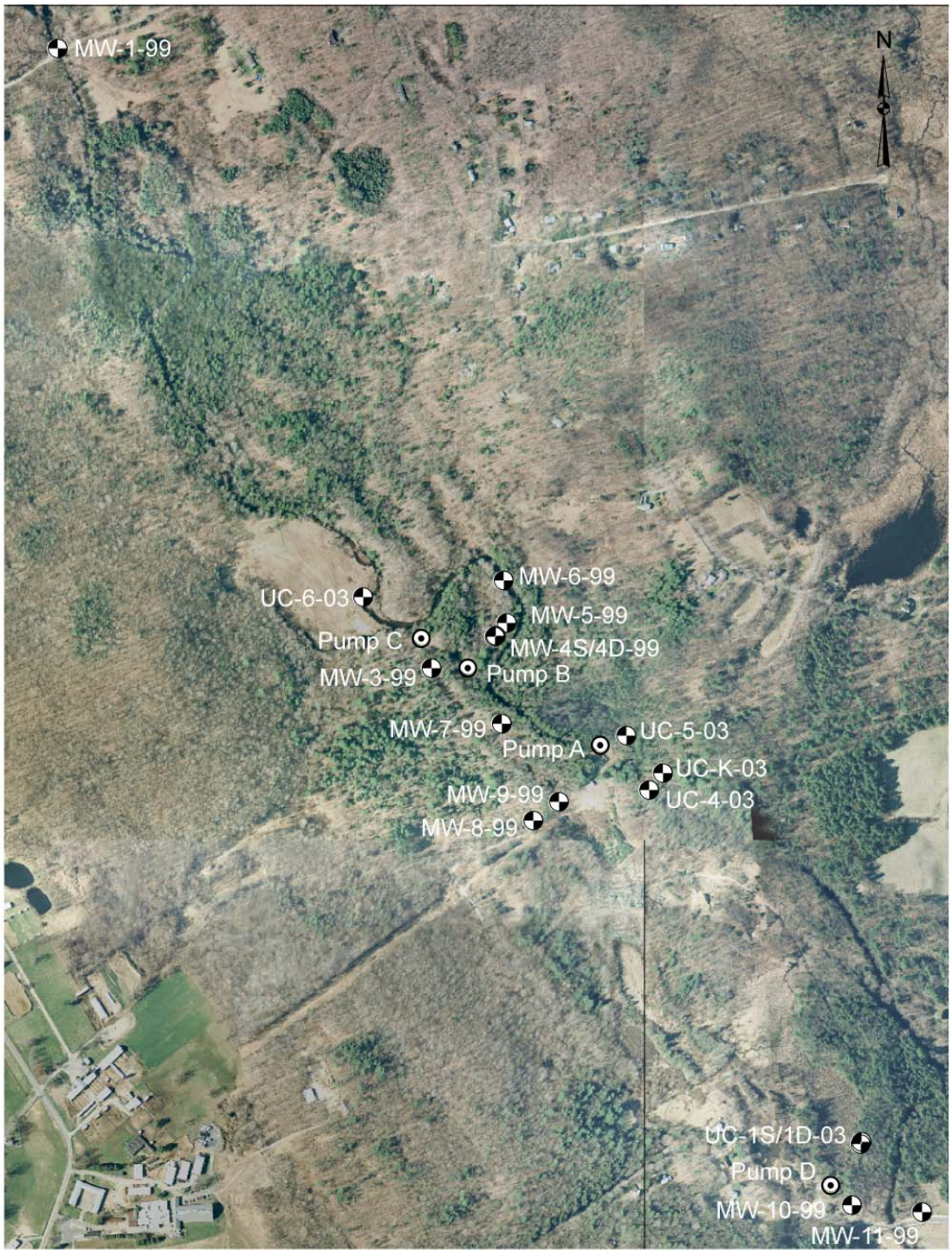

Figure C.1: Map of monitoring and production well locations along the Fenton River.

Table C.5: Locations and elevations of wells

Wells	Northing (ft)	Easting (ft)	Ground Elevation (ft)
MW-1-99	364657.43	738045.84	329.16
MW-3-99	361085.53	740198.45	313.48
MW-4D-99	361270.06	740569.94	304.66
MW-4S-99	361264.26	740568.75	304.81
MW-5-99	361344.17	740632.59	304.82
MW-6-99	361590.08	740615.50	306.30
MW-7-99	360764.58	740605.25	311.00
MW-8-99	360206.17	740788.75	312.31
MW-9-99	360316.37	740939.47	306.33
MW-10-99	357989.52	742623.94	291.35
MW-11-99	357945.08	743026.74	285.79
UC-1D-03	358340.81	742677.82	290.31
UC-1S-03	358350.64	742679.66	290.53
UC-4-03	360379.48	741457.14	297.38
UC-5-03	360693.64	741326.29	297.30
UC-6-03	361492.97	739806.21	308.78
UC-K-03	360481.21	741537.70	296.30
Pump A	360703.47	741203.94	305.24
Pump B	361144.63	740438.00	308.53
Pump C	361315.79	740173.30	310.99
Pump D	358166.37	742531.59	292.26
USGS-BR1 (HB)	-72.23959 (long)	41.82039 (lat)	471.863
USGS-BR2 (FR)	-72.23539 (long)	41.82391 (lat)	316.850

APPENDIX D. Temperature Monitoring in the Fenton River

Results of Temperature monitoring

Temperature loggers were placed along the Fenton River and the major tributaries of Fishers brook, Roberts brook and a small unnamed brook above the meadow to assess temperature changes in the river. These measurements indicate the influence of tributaries as well as the possible exchange between surface water in the Fenton River and ground water. The instrument used was the HOBO Temperature Pro by Onset Computer Corporation, Bourne, MA, USA as shown in the Figure D.1. The map shows the positions of the temperature loggers. The following figures show some of the results.

Figure D.1 HOBO Submersible Temperature Logger

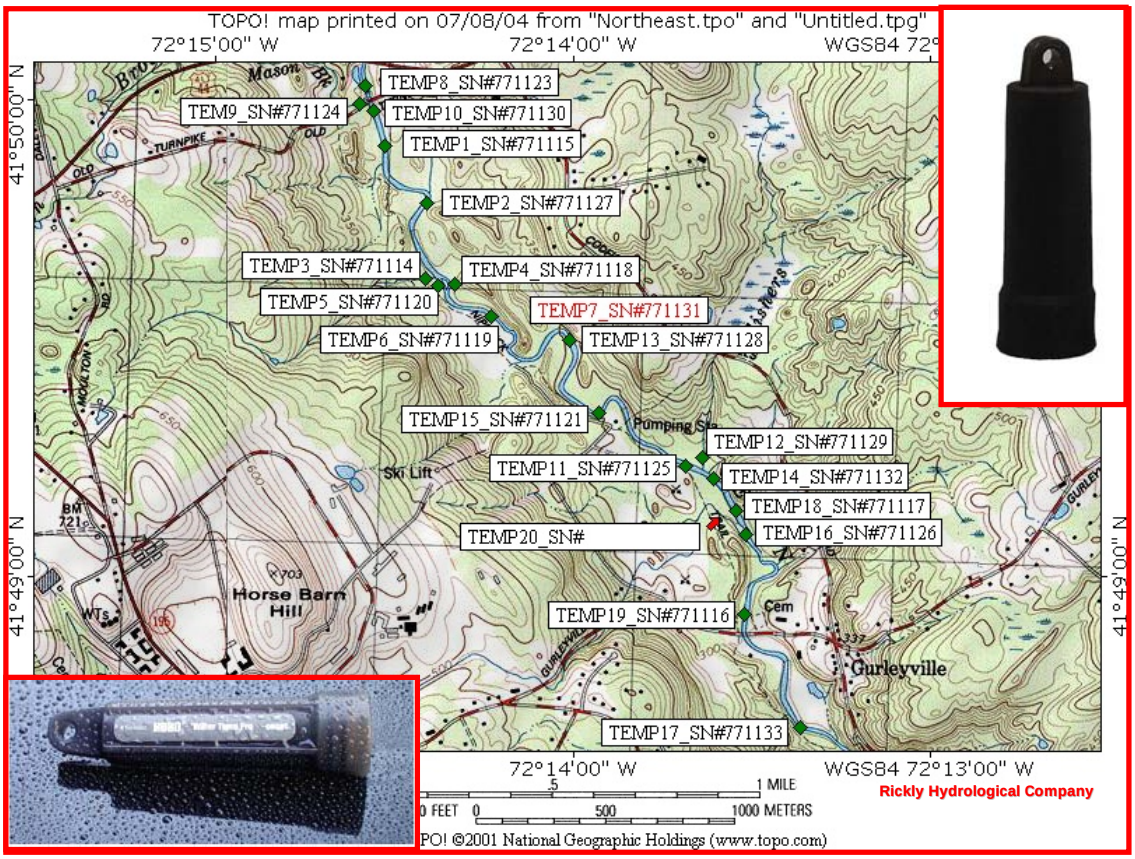

Figure D.2 Temperature monitoring sites

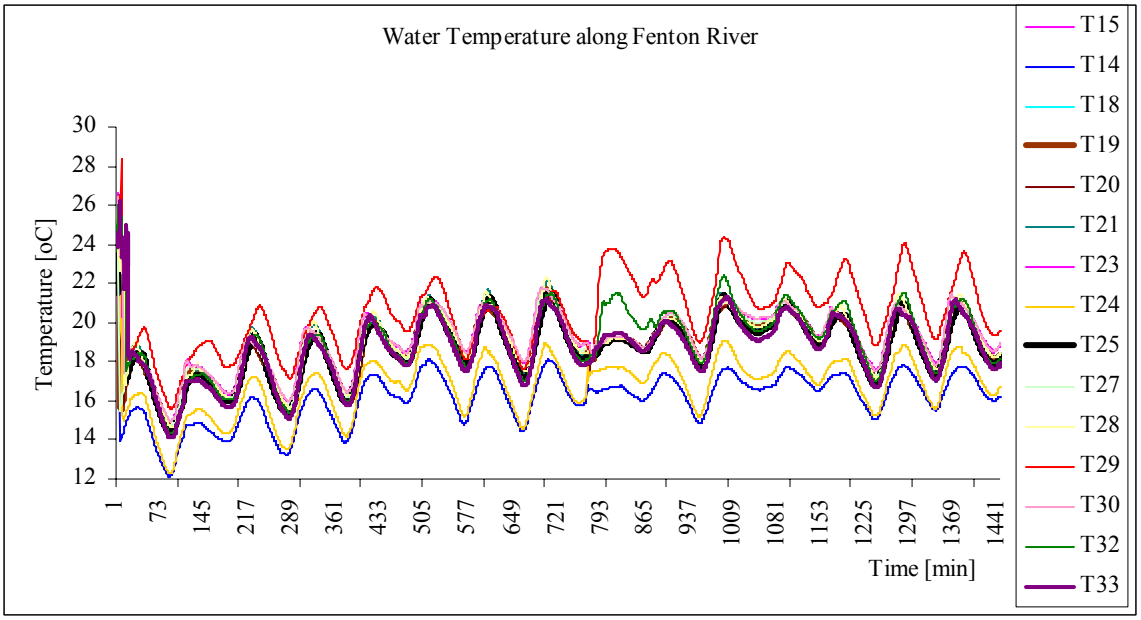

Fig. D.3 Water Temperature in different places along the Fenton River during the summer of 2004

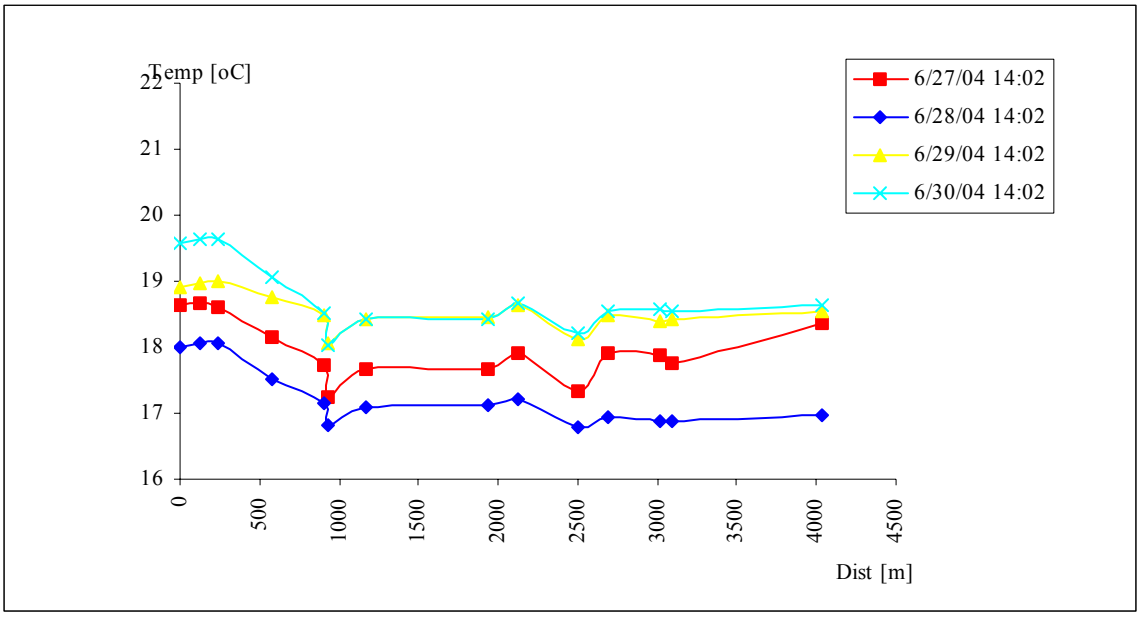

Figure D.4 Longitudinal Profile of River Water Temperature on Different Dates Temperature as Function of the Distance in Fenton River during the spring of 2004. Reference Points: 0 m: OldTurnpike; 1000 m: Noname Brook; 1000-2000 m: Meadow, 4000 m: Gurleyville

APPENDIX E. Core Sample Logs and Photographs Produced by USGS

Depth interval	Thickness recovered	Material description	Materials Unit
	UCSB - 1		
0 - 4 ft	2.9 ft	soil	**alluvium**
	0.46 ft	f-vcs sand	
4 - 8 ft	0.29 ft	f-vcs sand	**sand**
	1.2 ft	sandy gravel	**&**
	0.83 ft	f-vcs sand	**gravel**
	0.5 ft	pebbly sand	
8 - 12 ft	2.5 ft	m-cs, few pebbles	
			sand
12 - 16 ft	0.67 ft	m-cs sand	
	1.4 ft	sandy gravel	
			sand
16 - 20 ft	0.33 ft	cs-vcs sand	**&**
	0.7 ft	sandy gravel	**gravel**
	0.17 ft	m-cs sand	

Core number UCSB-1

0-35" soil, one stone (1.5"x1.5"x1") at 25.5"

30.5 - 40.5" fine-very coarse sand (sub-rounded - rounded)

48 - 51.5" tan ms (fine - very coarse sand)

51.5 - 66" dirty gravel (angular - sub angular)

66 - 76" ms (fine - very coarse brown sand), iron staining, heavy at 71 - 76"

76 - 82" pebbly sand (sub-rounded rounded)

moist 8 - 12'

96 - 100" gray, shattered stone

100 - 126.5" medium sand, grading down to coarse sand (sub-rounded-rounded),

few pebbles, stone at 108-109" and 116-117"

147 -151" black zone, medium - coarse sand

144 -154.5" medium - coarse sand

154.5 - 171.5 sandy gravel (sub-rounded rounded stones)

192 - 196" coarse to very coarse sand

196 - 204.5" sandy gravel (sub-rounded - rounded stones)

204 - 206.25" medium to course sand

Depth interval	Thickness recovered	Material description	Materials Unit
	UCSB - 2		
0 - 4 ft	0.92 ft	pebbly sand	
	0.63 ft	shattered stones	
	0.38 ft	pebbly sand	
	0.21 ft	f-m sand (laminated)	
	0.75 ft	shattered stones	**sand**
			&
4 - 8 ft	0.63 ft	gravel	**gravel**
	1.33 ft	f-m sand (laminated) few stones	
8 - 12 ft	3.1 ft	sandy gravel	

Core number UCSB-2

0-11 "
pebbly sand

11-19"
shattered
stones

19-24"
pebbly sand

24-27" f-m
sand
(laminated)

27-36"
shattered
stones

0-8" gravel

8-24" f-m
sand
(laminated)
few stones

0-37" sandy
gravel

Depth interval	Thickness recovered	Material description	Materials Unit
	UCSB - 3		
0 - 4 ft	2.4 ft	soil	
			alluvium
4 - 8 ft	0.25 ft	soil	
	2.8 ft	sandy gravel	**sand**
			&
8 - 12 ft	1.5 ft	sandy gravel	**gravel**
	0.54 ft	m-cs sand (laminated)	
	0.38 ft	cs-vcs pebbly sand	
			sand
12 - 16 ft	2.96 ft	m-vcs pebbly sand	

Core number UCSB-3

0-29" soil

0-3" soil

3-34" sandy gravel

0-18" sandy gravel

18-25" m-cs sand (laminated)

25-30" cs-vcs pebbly sand

0-35.5" m-vcs pebbly sand

Depth interval	Thickness recovered	Material description	Materials unit
	UCSB - 4		
0 - 4 ft	1.1 ft	soil	**alluvium**
	1.6 ft	sandy gravel	
4 - 8 ft	3.5 ft	f-vcs sandy gravel	
8 - 12 ft	2.3 ft	cs-vcs sandy gravel	**sand**
			&
12 - 16 ft	2.2 ft	vcs sandy gravel	**gravel**
16 - 20 ft	1.8 ft	m-cs sandy gravel	
20 - 24 ft	2.3 ft	m-cs sandy gravel	

Core number UCSB-4

0-13" soil

13-32" sandy gravel

shattered stones

0-42" f-vcs sandy gravel

0-28" cs-vcs sandy gravel

0-26" vcs sandy gravel

0-22" m-cs sandy gravel

0-28 " m-cs sandy gravel

Depth interval	Thickness recovered	Material description	Materials Unit
	UCSB - 5		
0 - 4 ft	1.7 ft	soil	**alluvium**
	1.0 ft	f-vcs sandy gravel	**sand**
			&
4 - 8 ft	1.9 ft	m-cs sandy gravel	**gravel**
	1.2 ft	m-cs sand, few pebbles	
8 - 12 ft	3.0 ft	m-cs sand	**sand**
12 - 16 ft	2.8 ft	m-cs pebbly sand	
16 - 20 ft	1.75 ft	silt & cs sand	
	1.4 ft	silt & vfs, (laminated)	**fines**
	0.2 ft	sandy gravel	**sand**
			&
20 - 24 ft	0.9 ft	m-vcs sandy gravel	**gravel**
	1.5 ft	f-vfs, silt (laminated)	**fines**
24 - 28 ft	2.3 ft	silty, sandy gravel	**sand**
			&
28 - 31 ft	2 ft	sandy gravel	**gravel**

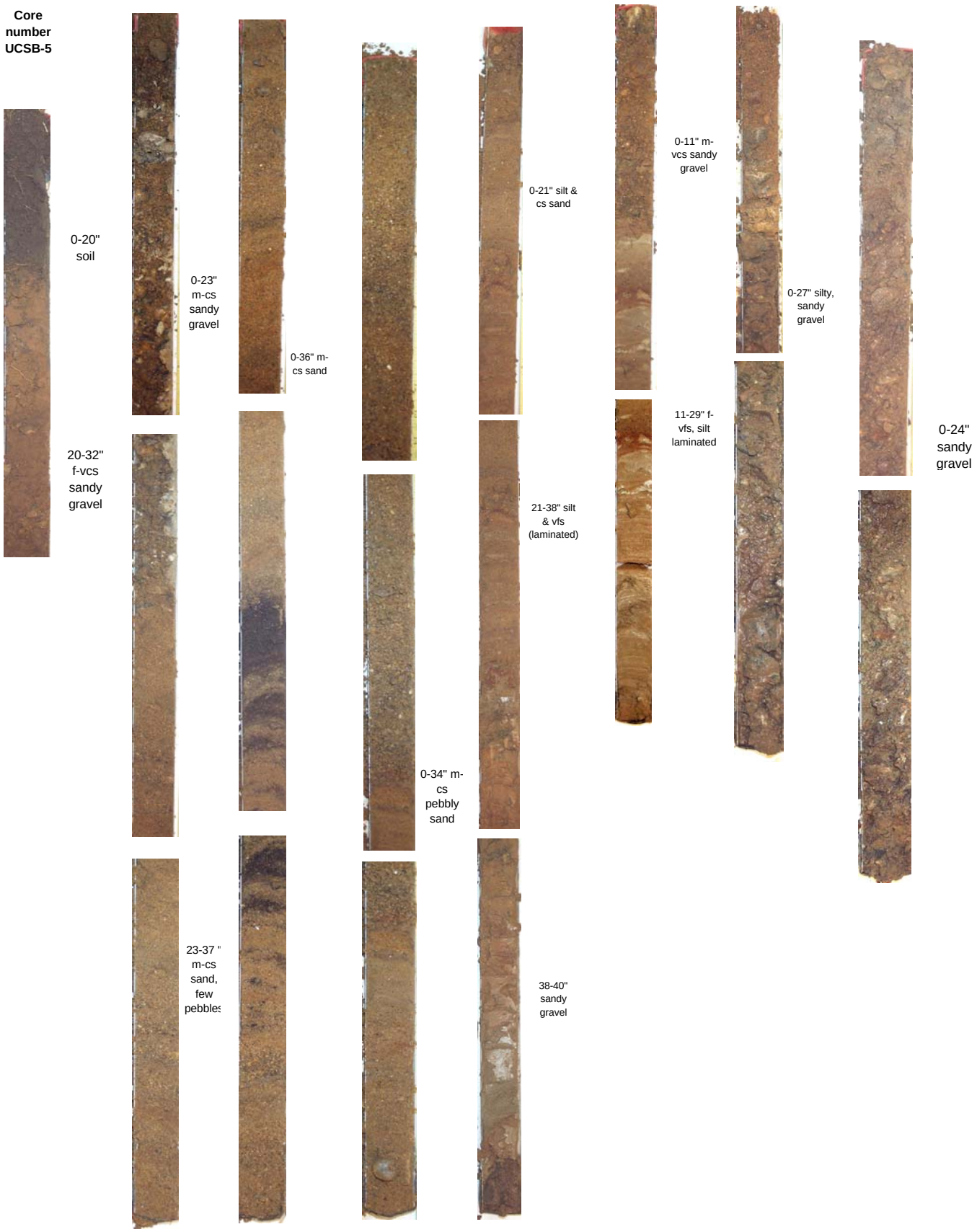
Core number UCSB-5
0-20" soil
20-32" f-vcs sandy gravel
0-23" m-cs sandy gravel
23-37 " m-cs sand, few pebbles
0-36" m-cs sand
0-34" m-cs pebbly sand
0-21" silt & cs sand
21-38" silt & vfs (laminated)
38-40" sandy gravel
0-11" m-vcs sandy gravel
11-29" f-vfs, silt laminated
0-27" silty, sandy gravel
0-24" sandy gravel

Depth interval	Thickness recovered	Material description	Materials unit
	UCSB - 6		
0 - 4 ft	2.7 ft	soil	**alluvium**
4 - 8 ft	1.4 ft	f sand (laminated)	**sand**
	1.6 ft	m-cs sandy gravel	
8 - 12 ft	2.1 ft	m-cs sandy gravel	
12 - 16 ft	2.2 ft	m-vcs pebbly sand	
			sand
16 - 20 ft	2.2 ft	m-vcs pebbly sand	**&**
			gravel
20 - 24 ft	1.9 ft	cs-vcs sandy gravel	
24 - 28 ft	2.2 ft	sandy gravel	
28 - 32 ft	2.3 ft	m-vcs sandy gravel	

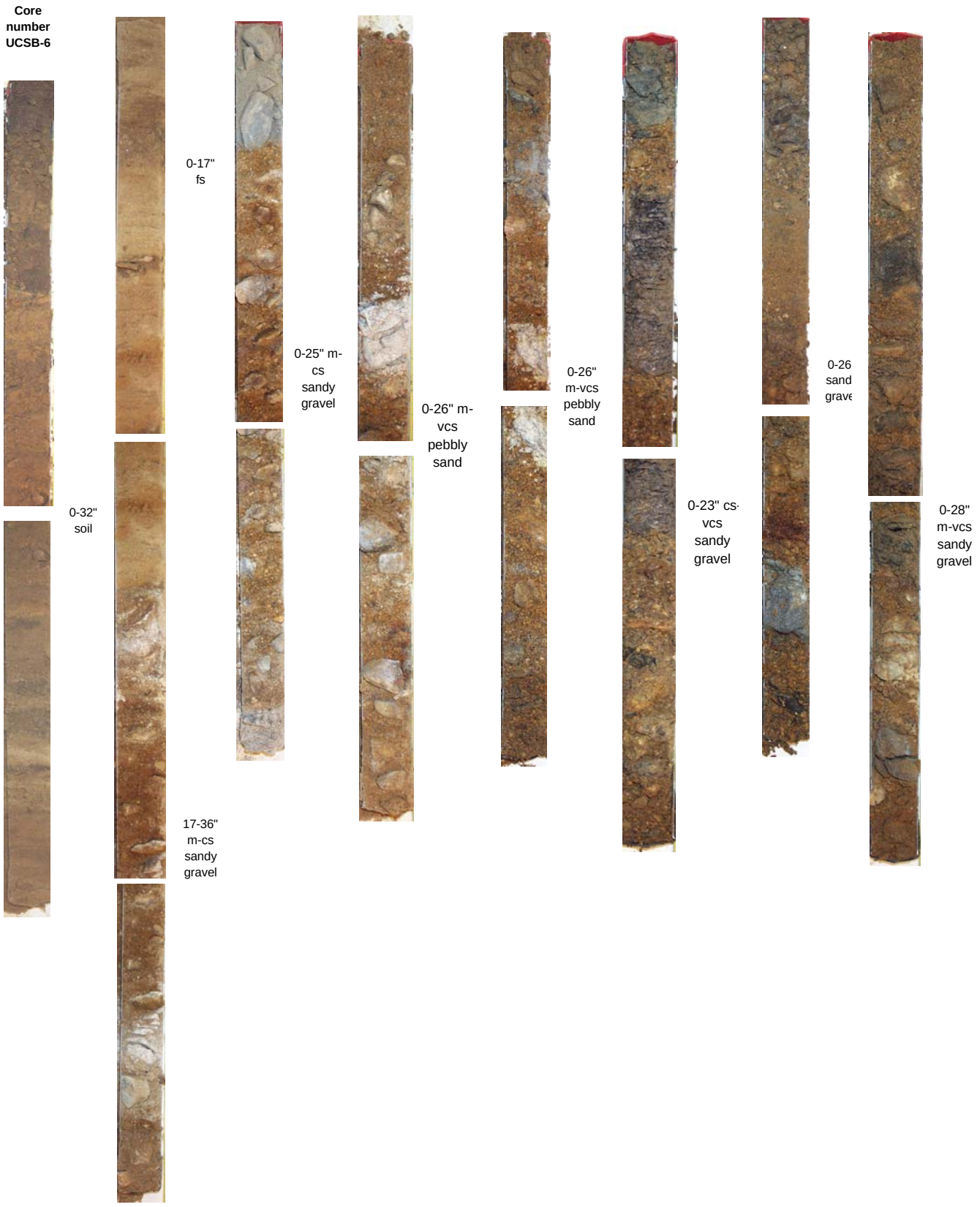
Core number UCSB-6
0-32" soil
0-17" fs
17-36" m-cs sandy gravel
0-25" m-cs sandy gravel
0-26" m-vcs pebbly sand
0-26" m-vcs pebbly sand
0-23" cs-vcs sandy gravel
0-26 sand grave
0-28" m-vcs sandy gravel

Depth interval	Thickness recovered	Material description	Materials unit
	UCSB - 7		
0 - 4 ft	2.5 ft	soil	
			alluvium
4 - 8 ft	1.2 ft	soil	
	0.5 ft	silt & vfs, trace clay (laminated)	
8 - 12 ft	2.8 ft	silt & vfs, trace clay (laminated)	
			fines
12 - 16 ft	3.1 ft	silt & vfs, trace clay (laminated)	**(dark organic bands)**
16 - 20 ft	3.4 ft	silt & vfs, trace clay (laminated)	
20 - 24 ft	0.25 ft	gravel	
	0.33 ft	silt & clay	
	1.1 ft	sandy gravel	**sand**
			&
24 - 28 ft	2.8 ft	sandy gravel	**gravel**
28 - 32 ft	1.9 ft	vcs sandy gravel	
	0.54 ft	silt & vfs (laminated)	**fines**

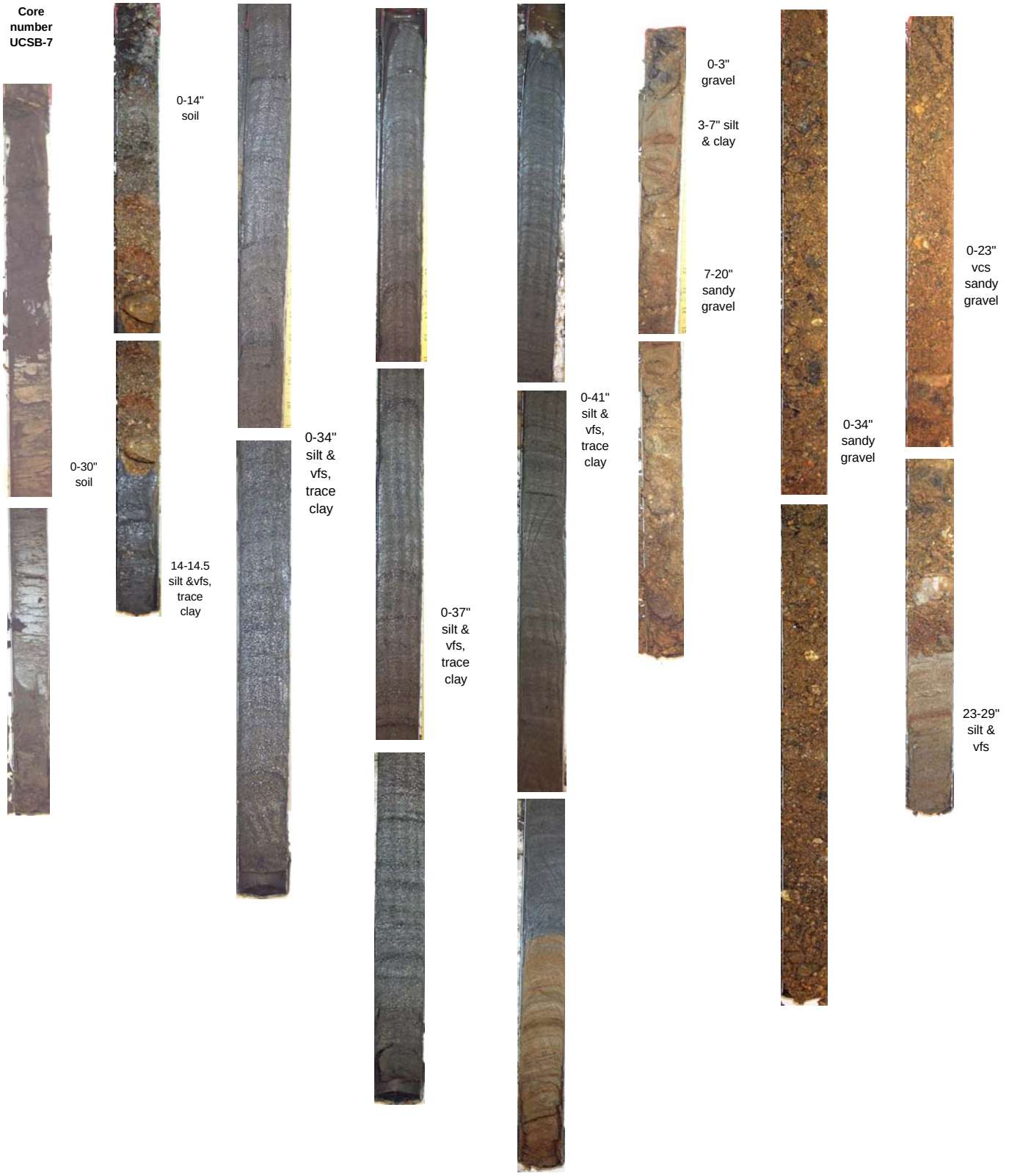
Core number UCSB-7
0-30" soil
0-14" soil
14-14.5 silt &vfs, trace clay
0-34" silt & vfs, trace clay
0-37" silt & vfs, trace clay
0-41" silt & vfs, trace clay
0-3" gravel
3-7" silt & clay
7-20" sandy gravel
0-34" sandy gravel
0-23" vcs sandy gravel
23-29" silt & vfs

Depth interval	Thickness recovered	Material description	Materials unit
	UCSB - 7B		
0 - 4 ft	1.5 ft	soil	**alluvium**
	1.5 ft	f-cs	
			sand
4 - 8 ft	0.25 ft	m-cs	
	1.6 ft	sandy gravel	**sand & gravel**
8 - 12 ft	0.67 ft	m-cs	
	2.1 ft	f-vf silty sand (laminated)	**sand**
12 - 16 ft	2.4 ft	sandy gravel	
			sand
16 - 20 ft	2.5 ft	sandy gravel	**&**
			gravel
20 - 24 ft	1.4 ft	sandy gravel	

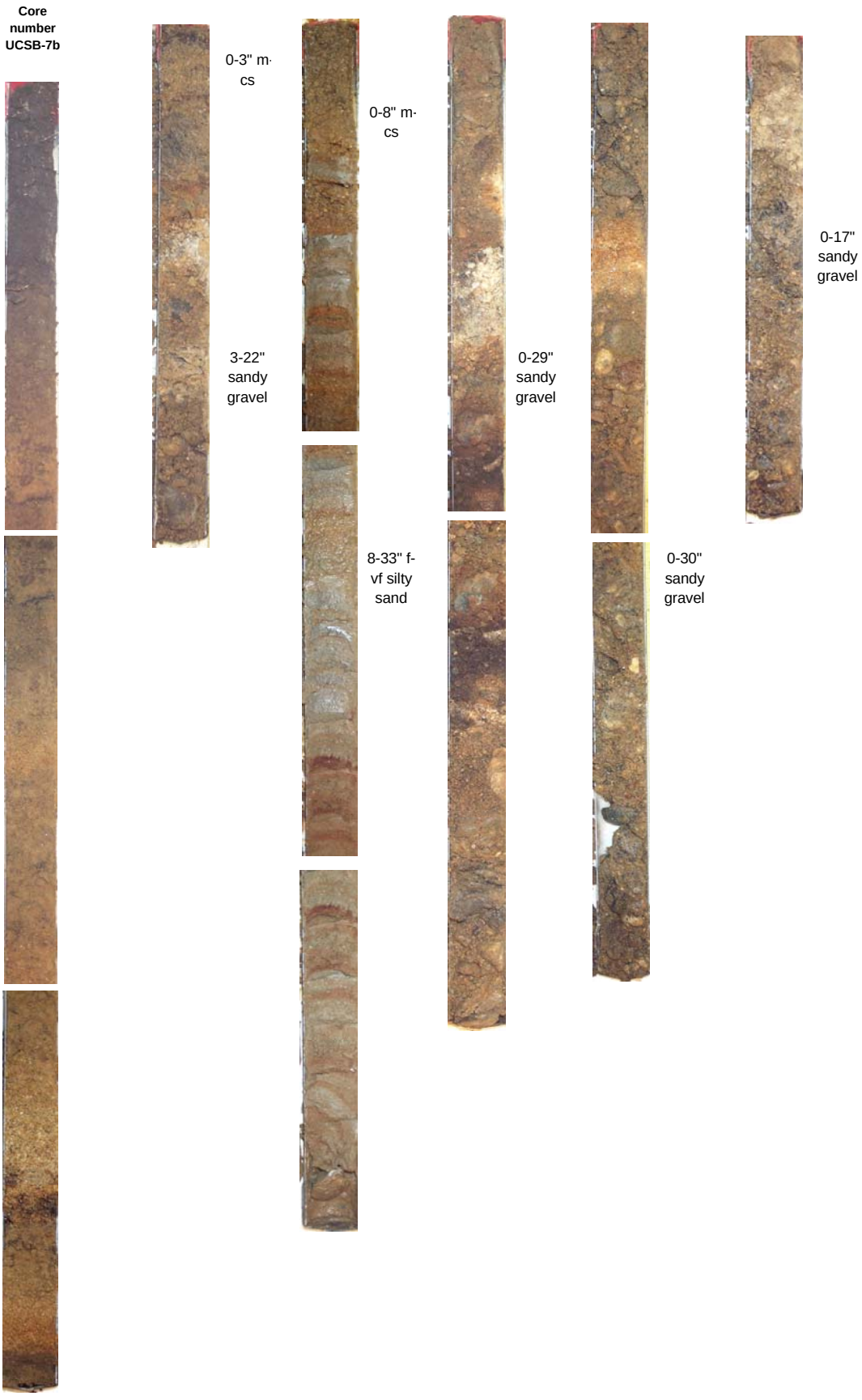
Core number UCSB-7b
0-3" m-cs
3-22" sandy gravel
0-8" m-cs
8-33" f-vf silty sand
0-29" sandy gravel
0-30" sandy gravel
0-17" sandy gravel

Depth interval	Thickness recovered	Material description	Materials Unit
	UCSB - 8		
0 - 4 ft	3.5 ft	soil	
			alluvium
4 - 8 ft	1.0 ft	soil	
	1.1 ft	m- vcs sandy gravel	**sand**
			&
8 - 12 ft	0.8 ft	m- cs pebbly sand	**gravel**
12 - 16 ft	2.9 ft	silt & vfs, trace clay (laminated)	
16 - 20 ft	3.6 ft	silt & vfs, trace clay (laminated)	
20 - 24 ft	1.5 ft	silt & vfs, trace clay (laminated)	
24 - 28 ft	3.75 ft	silt & vfs, trace clay (laminated)	**fines**
			(dark organic bands)
28 - 32 ft	3.7 ft	silt & vfs, trace clay (laminated)	
32 - 36 ft	3.75 ft	silt & vfs, trace clay (laminated)	
37 - 41 ft	0.8 ft	f-cs sand, vertical clay lens	
	1.9 ft	sandy gravel	**sand**
			&
41 - 45 ft	2.8 ft	sandy gravel	**gravel**

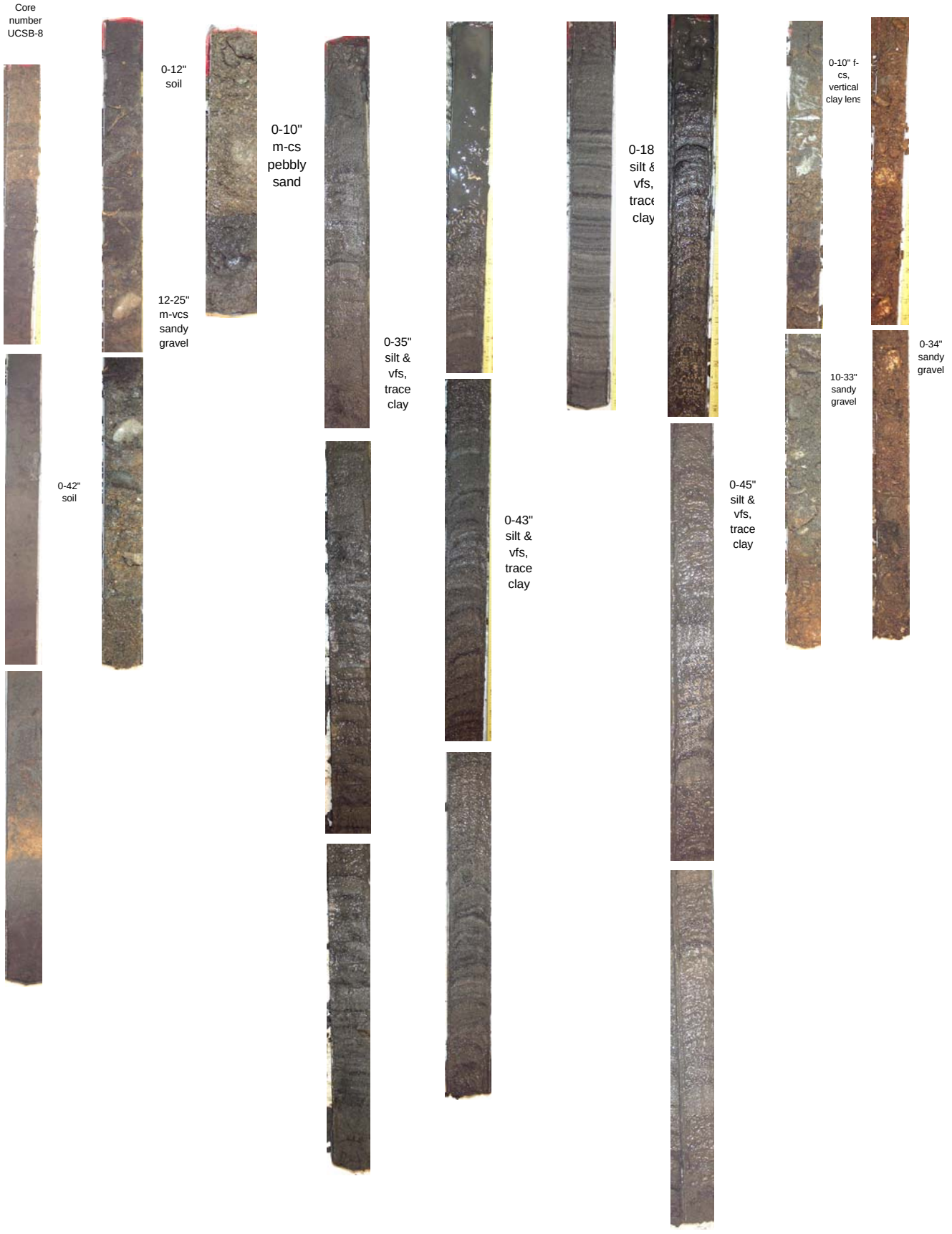
Core number UCSB-8
0-42" soil
0-12" soil
12-25" m-vcs sandy gravel
0-10" m-cs pebbly sand
0-35" silt & vfs, trace clay
0-43" silt & vfs, trace clay
0-18 silt & vfs, trace clay
0-45" silt & vfs, trace clay
0-10" f-cs, vertical clay lens
10-33" sandy gravel
0-34" sandy gravel

Bedrock Well MS 84 near Well B
Conventional Logs

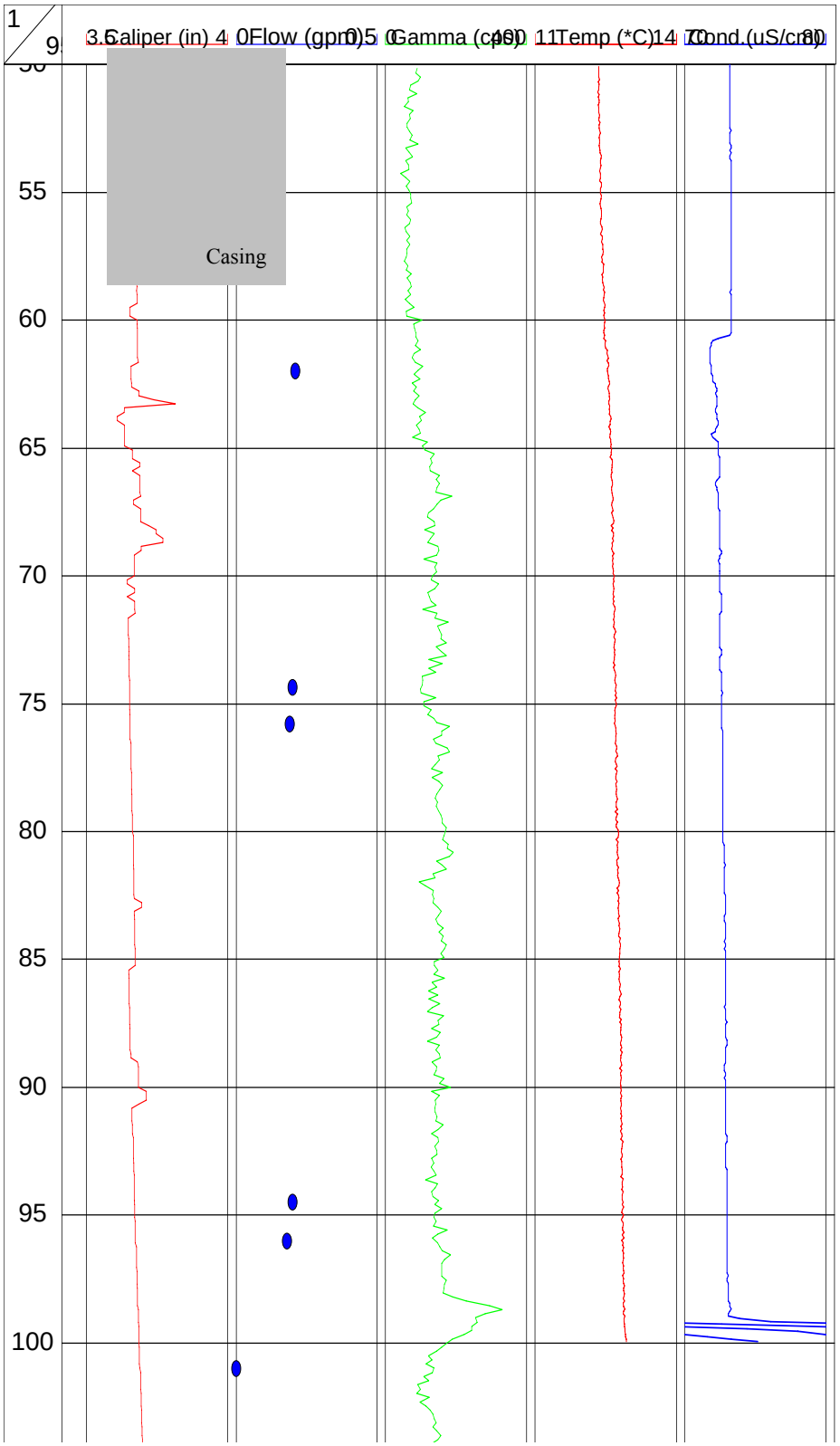
1
9
3.6
Caliper (in) 4
0
Flow (gpm)
0.5
0
Gamma (cps)
400
11
Temp (*C)
14
70
Cond.(uS/cm)
80
Casing
55
60
65
70
75
80
85
90
95
100

Bedrock Well MS 84 near Well B
Conventional Logs

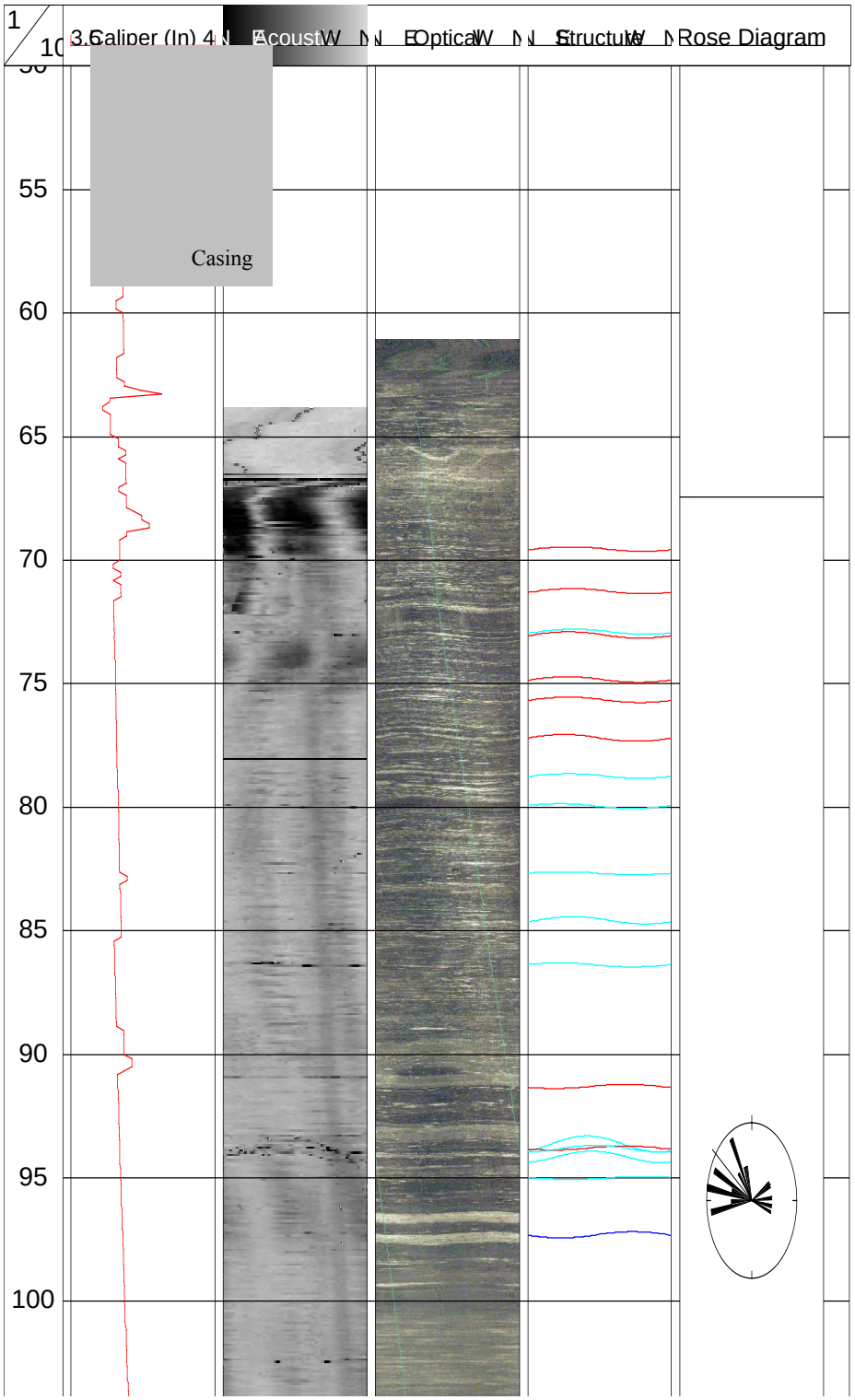

Bedrock Well MS 84 near Well C
Conventional Logs

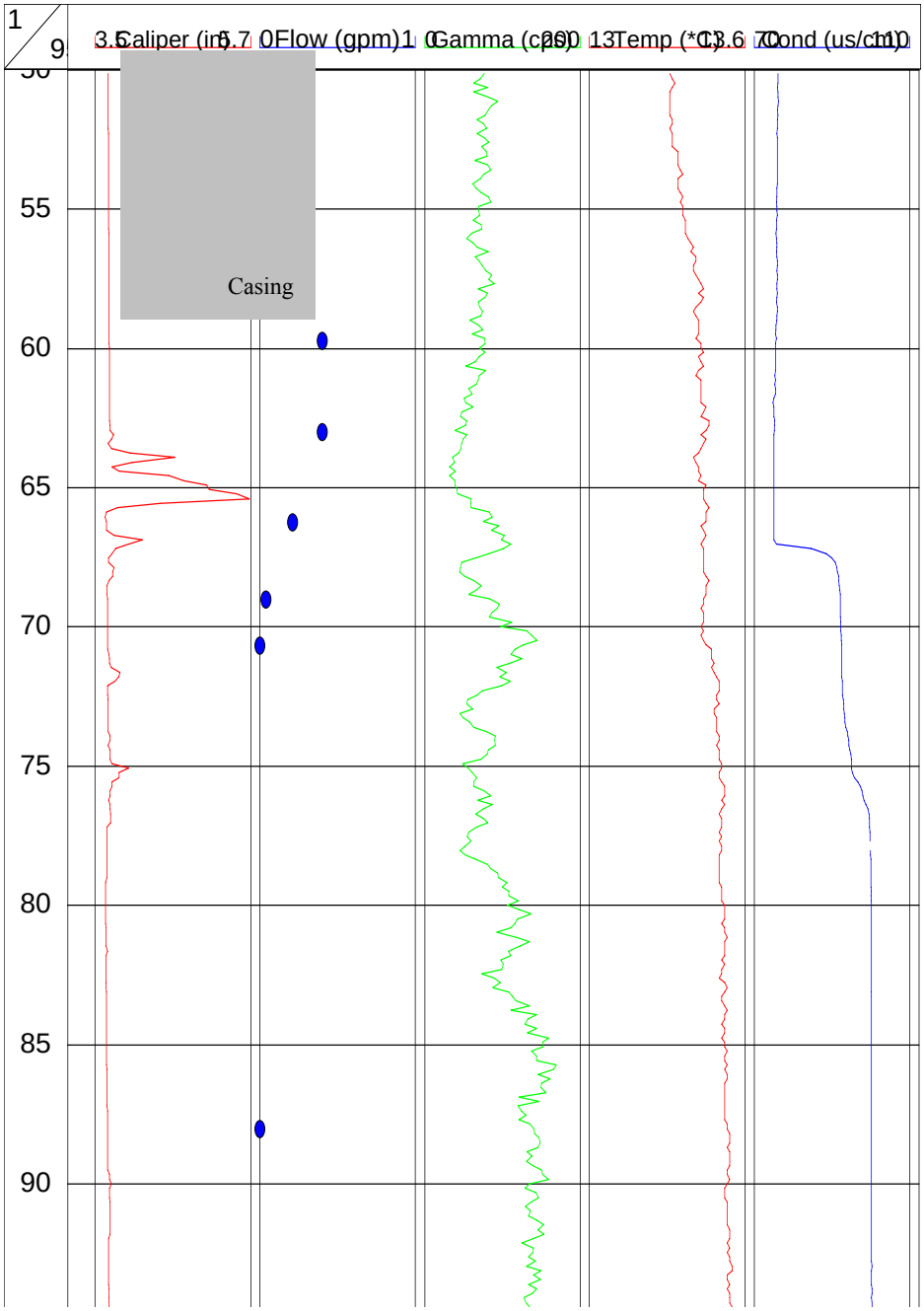

Bedrock Well MS 84 near Well C
Image Logs

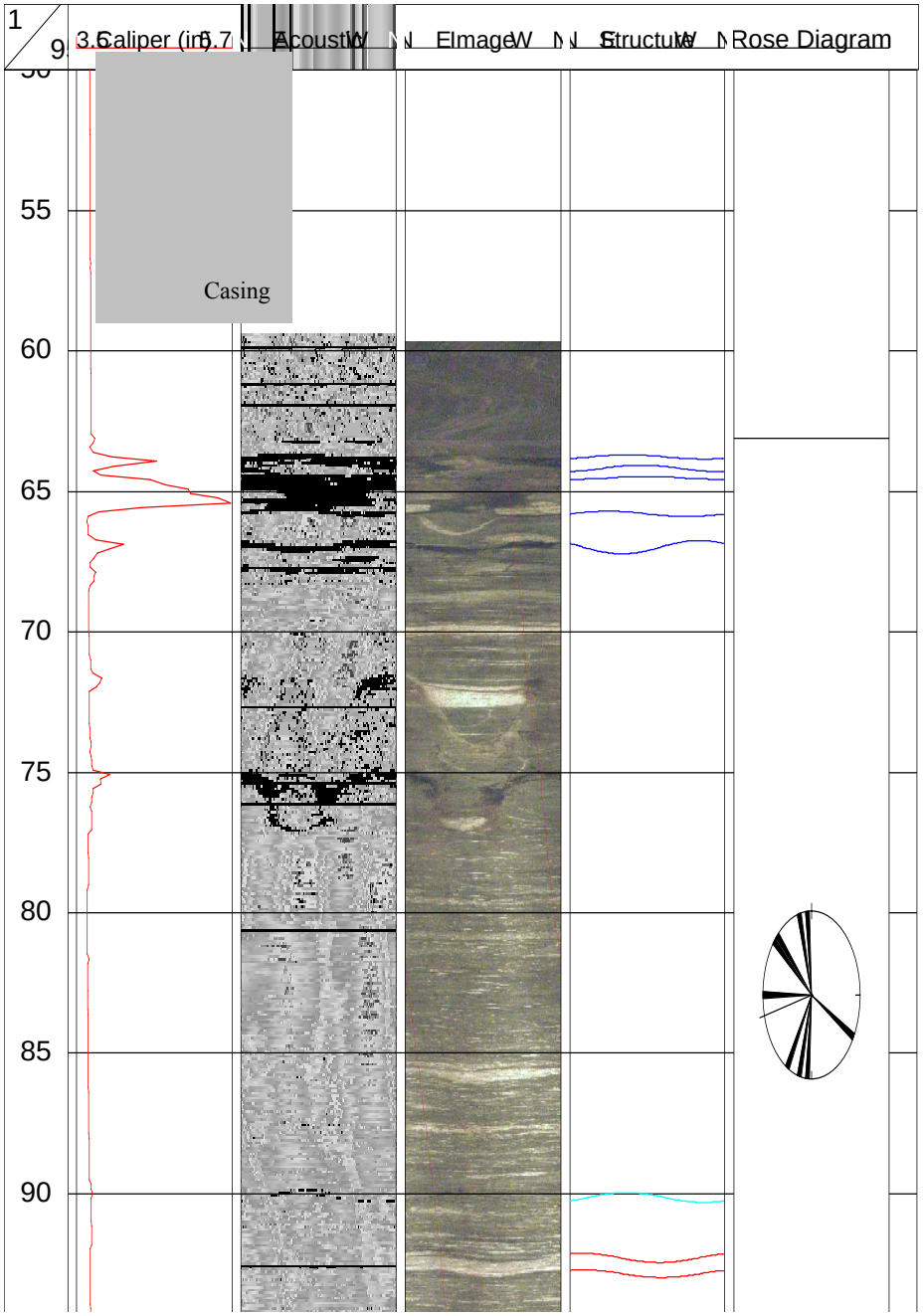

APPENDIX F. Estimating Recharge to Groundwater for 1966

Storrs, Connecticut, Estimated groundwater recharge at UConn Fenton River well field. Rainfall and snowfall data from NCDC, Historical Climate Data Network, Daily Values, Station 068138, Storrs, Connecticut.

A water balance model was created to calculate recharge as a flux to/from the groundwater table. This water balance model was based on daily data, and consisted of recharge which was assumed equal to rainfall minus available interception storage, minus potential evapotranspiration, plus snow melt. The assumptions used in the model are listed below:

1. Growing season maximum interception storage 0.118 in (3 mm)

2. Non-Growing season interception storage is 0.02 in (0.5 mm)

3. Growing season is assumed to start May 20 and end November 1. At the start of the growing season it takes 30 days for interception to increase to its' maximum amount. Interception storage stays at this value until Sep. 16, when it decreases linearly to the winter value on Nov. 1.

4. Monthly potential ET values taken from (2005) Utah Climate Center / Utah State University. Use of data must credit the Utah Climate Center.

5. Monthly PET values were distributed to daily values using wieghting factors that were calculated as the maximum vapor pressure deficit per day divided by the sum of all the vapor pressure deficits for the particular month that the day occurs in. The vapor pressure deficit calculation assumed that the
nightly low temperature is a good approximation of the daily dew point temperature.

6. Potential ET during the non-growing season is not always satisfied unless it is raining.

7. Sublimation of snow is neglected.

8. Snow liquid water equivalents are calculated using empirical data published by NOAA relating the SNOW/WATER ratio to the dew point when the snow fell. The nightly low temperature was assumed to be an estimate of the dew point temperature on days that it snowed. The relationship used is:
SNOW/WATER=20-0.51*Td, with Td in degrees F.

9. Snow melt was estimated using a degree-day approach: melt=alpha*T where alpha is a melt factor assumed equal to 0.45, and T is the average daily temperature calculated as (Tmax-Tmin)/2.0

10. Negative values of recharge are the result of PET demand that is not satisfied by rainfall or interception storage. Some of this PET demand comes from soil moisture,

some of it comes from groundwater. It is assumed that ½ of PET demand comes from soil moisture and 1/2 from groundwater. With this assumption, the sum of the estimated actual recharge column below is 21.36 inches, which is 48% of the 44.4 inches of total precipitation (rain+snow) received during 1966.

YEAR	MONTH	DAY	RAINFALL (inches)	SNOWFALL LIQUID EQUIV. (inches)	POTENTIAL ET (inches)	ESTIMATED ACTUAL RECHARGE (inches)
1966	1	1	0.00	0.00	0.034	0.0000
1966	1	2	0.00	0.00	0.047	0.0000
1966	1	3	0.79	0.00	0.022	0.7678
1966	1	4	0.00	0.00	0.017	0.0000
1966	1	5	0.00	0.00	0.029	0.0000
1966	1	6	0.18	0.00	0.023	0.1565
1966	1	7	0.02	0.00	0.008	0.0115
1966	1	8	0.37	0.46	0.023	0.3273
1966	1	9	0.00	0.00	0.009	0.0000
1966	1	10	0.00	0.00	0.045	0.0000
1966	1	11	0.00	0.00	0.029	0.0000
1966	1	12	0.00	0.00	0.015	0.0000
1966	1	13	0.00	0.00	0.017	0.0000
1966	1	14	0.02	0.05	0.016	0.0000
1966	1	15	0.00	0.00	0.020	0.0000
1966	1	16	0.00	0.00	0.023	0.0000
1966	1	17	0.00	0.00	0.028	0.0000
1966	1	18	0.00	0.00	0.016	0.0000
1966	1	19	0.00	0.00	0.018	0.0000
1966	1	20	0.00	0.08	0.016	0.0000
1966	1	21	0.04	0.00	0.010	0.0104
1966	1	22	0.00	0.00	0.022	0.0000
1966	1	23	0.60	0.00	0.007	0.5727
1966	1	24	0.10	0.13	0.009	0.0710
1966	1	25	0.00	0.00	0.019	0.0000
1966	1	26	0.00	0.00	0.017	0.0000
1966	1	27	0.00	0.04	0.016	0.0000
1966	1	28	0.00	0.00	0.018	0.0000
1966	1	29	0.00	0.00	0.011	0.0000
1966	1	30	0.68	0.48	0.027	0.6328
1966	1	31	0.00	0.00	0.012	0.0000
1966	2	1	0.00	0.00	0.027	0.0000
1966	2	2	0.00	0.00	0.024	0.0000
1966	2	3	0.09	0.15	0.014	0.0555
1966	2	4	0.13	0.38	0.013	0.0966
1966	2	5	0.03	0.10	0.018	0.0000
1966	2	6	0.00	0.00	0.039	0.0000
1966	2	7	0.00	0.00	0.027	0.0000
1966	2	8	0.00	0.00	0.039	0.0000
1966	2	9	0.00	0.00	0.032	0.0000
1966	2	10	0.00	0.00	0.058	0.0000
1966	2	11	0.05	0.08	0.042	0.1401
1966	2	12	0.00	0.00	0.047	0.0858

1966	2	13	1.23	0.19	0.034	1.2354
1966	2	14	0.98	0.00	0.052	1.0067
1966	2	15	0.00	0.00	0.044	0.0057
1966	2	16	0.00	0.00	0.023	0.0000
1966	2	17	0.20	0.00	0.019	0.1614
1966	2	18	0.00	0.00	0.031	0.0000
1966	2	19	0.00	0.00	0.027	0.0000
1966	2	20	0.02	0.05	0.023	0.0000
1966	2	21	0.00	0.00	0.022	0.0000
1966	2	22	0.00	0.00	0.036	0.0000
1966	2	23	0.00	0.00	0.037	0.0000
1966	2	24	0.00	0.00	0.025	0.0000
1966	2	25	0.91	1.18	0.033	0.8572
1966	2	26	0.00	0.13	0.031	0.0000
1966	2	27	0.00	0.00	0.060	0.0000
1966	2	28	0.00	0.00	0.044	0.0057
1966	3	1	0.95	0.00	0.056	0.9721
1966	3	2	0.00	0.00	0.050	0.0340
1966	3	3	0.00	0.00	0.099	0.0289
1966	3	4	0.00	0.00	0.080	0.0475
1966	3	5	0.27	0.00	0.023	0.2711
1966	3	6	0.09	0.00	0.021	0.0639
1966	3	7	0.00	0.00	0.040	0.0000
1966	3	8	0.00	0.00	0.059	0.0000
1966	3	9	0.00	0.00	0.100	0.0000
1966	3	10	0.00	0.00	0.072	0.0410
1966	3	11	0.00	0.00	0.057	0.0000
1966	3	12	0.19	0.52	0.040	0.1543
1966	3	13	0.53	0.69	0.016	0.4937
1966	3	14	0.00	0.00	0.051	0.0000
1966	3	15	0.00	0.00	0.034	0.0000
1966	3	16	0.00	0.00	0.065	0.0000
1966	3	17	0.00	0.00	0.082	0.0000
1966	3	18	0.00	0.00	0.115	0.0000
1966	3	19	0.07	0.00	0.126	0.0717
1966	3	20	0.00	0.00	0.048	0.0750
1966	3	21	0.00	0.00	0.073	0.0000
1966	3	22	0.00	0.00	0.064	0.0000
1966	3	23	0.00	0.00	0.064	0.0734
1966	3	24	0.00	0.00	0.102	0.0354
1966	3	25	1.20	0.00	0.093	1.1957
1966	3	26	0.00	0.00	0.035	0.0000
1966	3	27	0.00	0.00	0.013	0.0000
1966	3	28	0.00	0.00	0.037	0.0000
1966	3	29	0.00	0.00	0.056	0.0000
1966	3	30	0.00	0.00	0.064	0.0000
1966	3	31	0.08	0.00	0.043	0.0854
1966	4	1	0.00	0.00	0.067	0.0000
1966	4	2	0.00	0.00	0.057	0.0000
1966	4	3	0.00	0.00	0.066	0.0000
1966	4	4	0.00	0.00	0.064	0.0293
1966	4	5	0.00	0.00	0.082	0.0000
1966	4	6	0.00	0.00	0.090	0.0000
1966	4	7	0.00	0.00	0.103	0.0000
1966	4	8	0.00	0.00	0.052	0.0463
1966	4	9	0.00	0.00	0.079	0.0000
1966	4	10	0.00	0.00	0.076	0.0000

1966	4	11	0.00	0.00	0.091	0.0000
1966	4	12	0.00	0.00	0.110	0.0127
1966	4	13	0.00	0.00	0.071	0.0131
1966	4	14	0.00	0.00	0.106	0.0000
1966	4	15	0.00	0.00	0.151	0.0000
1966	4	16	0.03	0.00	0.135	0.0079
1966	4	17	0.05	0.00	0.164	0.0000
1966	4	18	0.00	0.00	0.185	0.0000
1966	4	19	0.00	0.00	0.152	0.0052
1966	4	20	0.03	0.00	0.057	0.0559
1966	4	21	0.00	0.00	0.114	0.0332
1966	4	22	0.15	0.00	0.114	0.2620
1966	4	23	0.00	0.00	0.177	0.0000
1966	4	24	0.55	0.00	0.060	0.4704
1966	4	25	0.10	0.00	0.175	0.0000
1966	4	26	0.00	0.00	0.148	0.0000
1966	4	27	0.00	0.00	0.128	0.0000
1966	4	28	0.02	0.00	0.076	0.0000
1966	4	29	0.19	0.00	0.119	0.0507
1966	4	30	0.01	0.00	0.128	0.0000
1966	5	1	0.60	0.00	0.120	0.4602
1966	5	2	0.00	0.00	0.082	0.0000
1966	5	3	0.00	0.00	0.134	0.0000
1966	5	4	0.08	0.00	0.108	0.0000
1966	5	5	0.00	0.00	0.126	0.0000
1966	5	6	0.00	0.00	0.126	0.0000
1966	5	7	0.00	0.00	0.105	0.0000
1966	5	8	0.15	0.00	0.083	0.0465
1966	5	9	0.44	0.00	0.064	0.3557
1966	5	10	0.05	0.00	0.064	0.0000
1966	5	11	0.00	0.00	0.118	0.0000
1966	5	12	0.00	0.00	0.064	0.0000
1966	5	13	0.33	0.00	0.093	0.2167
1966	5	14	0.00	0.00	0.166	0.0000
1966	5	15	0.00	0.00	0.218	0.0000
1966	5	16	0.00	0.00	0.221	0.0000
1966	5	17	0.00	0.00	0.164	0.0000
1966	5	18	0.00	0.00	0.159	0.0000
1966	5	19	0.95	0.00	0.162	0.7684
1966	5	20	0.02	0.00	0.217	-0.0035
1966	5	21	0.00	0.00	0.186	-0.0060
1966	5	22	0.35	0.00	0.243	0.2970
1966	5	23	0.00	0.00	0.211	-0.0136
1966	5	24	0.00	0.00	0.181	-0.0146
1966	5	25	0.00	0.00	0.179	-0.0173
1966	5	26	0.00	0.00	0.175	-0.0198
1966	5	27	0.00	0.00	0.259	-0.0334
1966	5	28	0.46	0.00	0.175	0.3608
1966	5	29	0.03	0.00	0.172	-0.0277
1966	5	30	0.00	0.00	0.241	-0.0428
1966	5	31	0.00	0.00	0.164	-0.0318
1966	6	1	0.00	0.00	0.132	-0.0277
1966	6	2	0.35	0.00	0.145	0.2201
1966	6	3	0.05	0.00	0.196	-0.0474
1966	6	4	0.00	0.00	0.223	-0.0575
1966	6	5	0.00	0.00	0.235	-0.0644
1966	6	6	0.00	0.00	0.271	-0.0787

1966	6	7	0.00	0.00	0.228	-0.0699
1966	6	8	0.00	0.00	0.234	-0.0754
1966	6	9	0.00	0.00	0.225	-0.0763
1966	6	10	1.27	0.00	0.143	1.0793
1966	6	11	0.00	0.00	0.128	-0.0476
1966	6	12	0.00	0.00	0.145	-0.0561
1966	6	13	0.00	0.00	0.131	-0.0529
1966	6	14	0.20	0.00	0.223	-0.0446
1966	6	15	0.05	0.00	0.191	-0.0833
1966	6	16	0.08	0.00	0.128	-0.0577
1966	6	17	0.00	0.00	0.139	-0.0648
1966	6	18	0.00	0.00	0.270	-0.1304
1966	6	19	0.00	0.00	0.164	-0.0819
1966	6	20	0.70	0.00	0.241	0.3411
1966	6	21	0.00	0.00	0.223	-0.1115
1966	6	22	0.00	0.00	0.228	-0.1141
1966	6	23	0.00	0.00	0.279	-0.1393
1966	6	24	0.00	0.00	0.225	-0.1124
1966	6	25	0.00	0.00	0.292	-0.1461
1966	6	26	0.04	0.00	0.143	-0.0713
1966	6	27	0.00	0.00	0.305	-0.1523
1966	6	28	0.00	0.00	0.220	-0.1102
1966	6	29	0.00	0.00	0.206	-0.1030
1966	6	30	0.00	0.00	0.223	-0.1115
1966	7	1	0.00	0.00	0.205	-0.1026
1966	7	2	0.00	0.00	0.324	-0.1620
1966	7	3	0.00	0.00	0.307	-0.1533
1966	7	4	0.00	0.00	0.145	-0.0724
1966	7	5	0.00	0.00	0.218	-0.1088
1966	7	6	0.00	0.00	0.155	-0.0775
1966	7	7	0.42	0.00	0.185	0.1174
1966	7	8	0.00	0.00	0.205	-0.1026
1966	7	9	0.00	0.00	0.211	-0.1054
1966	7	10	0.00	0.00	0.192	-0.0962
1966	7	11	1.36	0.00	0.243	0.9985
1966	7	12	0.00	0.00	0.221	-0.1105
1966	7	13	0.00	0.00	0.213	-0.1064
1966	7	14	0.15	0.00	0.229	-0.0985
1966	7	15	0.00	0.00	0.199	-0.0996
1966	7	16	0.00	0.00	0.193	-0.0966
1966	7	17	0.00	0.00	0.210	-0.1049
1966	7	18	0.00	0.00	0.254	-0.1268
1966	7	19	0.00	0.00	0.153	-0.0767
1966	7	20	1.50	0.00	0.150	1.2324
1966	7	21	0.00	0.00	0.156	-0.0782
1966	7	22	0.00	0.00	0.239	-0.1194
1966	7	23	0.00	0.00	0.188	-0.0938
1966	7	24	0.00	0.00	0.211	-0.1054
1966	7	25	0.00	0.00	0.246	-0.1231
1966	7	26	0.35	0.00	0.167	0.0652
1966	7	27	0.03	0.00	0.176	-0.0880
1966	7	28	0.67	0.00	0.133	0.4195
1966	7	29	0.05	0.00	0.109	-0.0545
1966	7	30	0.00	0.00	0.148	-0.0740
1966	7	31	0.00	0.00	0.187	-0.0937
1966	8	1	0.00	0.00	0.214	-0.1072
1966	8	2	0.00	0.00	0.178	-0.0890

1966	8	3	0.15	0.00	0.169	-0.0687
1966	8	4	0.00	0.00	0.201	-0.1005
1966	8	5	0.00	0.00	0.185	-0.0926
1966	8	6	0.00	0.00	0.202	-0.1011
1966	8	7	0.00	0.00	0.221	-0.1106
1966	8	8	0.00	0.00	0.203	-0.1013
1966	8	9	0.00	0.00	0.146	-0.0731
1966	8	10	0.28	0.00	0.190	-0.0140
1966	8	11	0.00	0.00	0.139	-0.0694
1966	8	12	0.10	0.00	0.101	-0.0507
1966	8	13	0.00	0.00	0.219	-0.1095
1966	8	14	0.00	0.00	0.194	-0.0971
1966	8	15	0.97	0.00	0.119	0.7334
1966	8	16	0.00	0.00	0.067	-0.0337
1966	8	17	0.78	0.00	0.090	0.5718
1966	8	18	0.00	0.00	0.197	-0.0983
1966	8	19	0.00	0.00	0.261	-0.1306
1966	8	20	0.00	0.00	0.246	-0.1232
1966	8	21	0.00	0.00	0.189	-0.0947
1966	8	22	0.13	0.00	0.128	-0.0580
1966	8	23	0.10	0.00	0.083	-0.0416
1966	8	24	0.00	0.00	0.158	-0.0791
1966	8	25	0.00	0.00	0.130	-0.0648
1966	8	26	0.00	0.00	0.169	-0.0847
1966	8	27	0.00	0.00	0.205	-0.1024
1966	8	28	0.00	0.00	0.152	-0.0762
1966	8	29	0.00	0.00	0.207	-0.1037
1966	8	30	0.00	0.00	0.187	-0.0936
1966	8	31	0.00	0.00	0.207	-0.1037
1966	9	1	0.00	0.00	0.192	-0.0962
1966	9	2	0.00	0.00	0.210	-0.1050
1966	9	3	0.00	0.00	0.215	-0.1076
1966	9	4	0.89	0.00	0.181	0.5907
1966	9	5	0.29	0.00	0.156	0.0160
1966	9	6	0.00	0.00	0.131	-0.0655
1966	9	7	0.00	0.00	0.129	-0.0646
1966	9	8	0.00	0.00	0.125	-0.0627
1966	9	9	0.00	0.00	0.116	-0.0580
1966	9	10	0.00	0.00	0.147	-0.0733
1966	9	11	0.00	0.00	0.179	-0.0895
1966	9	12	0.00	0.00	0.134	-0.0668
1966	9	13	0.00	0.00	0.126	-0.0630
1966	9	14	0.10	0.00	0.079	-0.0394
1966	9	15	1.00	0.00	0.087	0.7947
1966	9	16	0.00	0.00	0.152	-0.0743
1966	9	17	0.00	0.00	0.134	-0.0639
1966	9	18	0.00	0.00	0.138	-0.0646
1966	9	19	0.00	0.00	0.138	-0.0631
1966	9	20	0.00	0.00	0.100	-0.0447
1966	9	21	0.70	0.00	0.034	0.5653
1966	9	22	1.11	0.00	0.099	0.9226
1966	9	23	0.05	0.00	0.072	-0.0299
1966	9	24	0.00	0.00	0.095	-0.0380
1966	9	25	0.00	0.00	0.089	-0.0347
1966	9	26	0.00	0.00	0.086	-0.0327
1966	9	27	0.00	0.00	0.089	-0.0328
1966	9	28	0.00	0.00	0.070	-0.0251

1966	9	29	0.27	0.00	0.046	0.1501
1966	9	30	0.11	0.00	0.081	-0.0154
1966	10	1	0.52	0.00	0.071	0.3900
1966	10	2	0.63	0.00	0.050	0.5167
1966	10	3	0.00	0.00	0.082	-0.0250
1966	10	4	0.00	0.00	0.078	-0.0229
1966	10	5	0.00	0.00	0.037	-0.0106
1966	10	6	0.00	0.00	0.073	-0.0199
1966	10	7	0.00	0.00	0.097	-0.0253
1966	10	8	0.00	0.00	0.128	-0.0319
1966	10	9	0.00	0.00	0.149	-0.0355
1966	10	10	0.00	0.00	0.096	-0.0219
1966	10	11	0.00	0.00	0.125	-0.0273
1966	10	12	0.00	0.00	0.064	-0.0132
1966	10	13	0.00	0.00	0.087	-0.0170
1966	10	14	0.00	0.00	0.080	-0.0147
1966	10	15	0.00	0.00	0.085	-0.0148
1966	10	16	0.40	0.00	0.063	0.3276
1966	10	17	0.00	0.00	0.086	-0.0130
1966	10	18	0.00	0.00	0.045	-0.0064
1966	10	19	0.99	0.00	0.020	0.9391
1966	10	20	0.75	0.00	0.071	0.6896
1966	10	21	0.00	0.00	0.062	-0.0068
1966	10	22	0.00	0.00	0.073	-0.0071
1966	10	23	0.00	0.00	0.086	-0.0075
1966	10	24	0.00	0.00	0.059	-0.0045
1966	10	25	0.00	0.00	0.070	-0.0046
1966	10	26	0.00	0.00	0.082	-0.0045
1966	10	27	0.00	0.00	0.083	-0.0036
1966	10	28	0.00	0.00	0.121	-0.0040
1966	10	29	0.00	0.00	0.100	-0.0022
1966	10	30	0.00	0.00	0.086	-0.0009
1966	10	31	0.00	0.00	0.052	0.0000
1966	11	1	0.00	0.00	0.064	0.0000
1966	11	2	0.20	0.00	0.052	0.1281
1966	11	3	1.96	0.00	0.042	1.8979
1966	11	4	0.00	0.00	0.048	0.0000
1966	11	5	0.00	0.00	0.043	0.0000
1966	11	6	0.72	0.00	0.025	0.6752
1966	11	7	0.00	0.00	0.033	0.0000
1966	11	8	0.04	0.00	0.052	0.0000
1966	11	9	0.05	0.00	0.025	0.0054
1966	11	10	0.00	0.00	0.049	0.0000
1966	11	11	0.30	0.00	0.036	0.2444
1966	11	12	0.12	0.00	0.040	0.0600
1966	11	13	0.00	0.00	0.033	0.0000
1966	11	14	0.00	0.00	0.031	0.0000
1966	11	15	0.00	0.00	0.014	0.0000
1966	11	16	0.00	0.00	0.030	0.0000
1966	11	17	0.00	0.00	0.060	0.0000
1966	11	18	0.05	0.00	0.039	0.0000
1966	11	19	0.00	0.00	0.046	0.0000
1966	11	20	0.00	0.00	0.027	0.0000
1966	11	21	0.00	0.00	0.032	0.0000
1966	11	22	0.00	0.00	0.037	0.0000
1966	11	23	0.00	0.00	0.055	0.0000
1966	11	24	0.00	0.00	0.084	0.0000

1966	11	25	0.00	0.00	0.051	0.0000
1966	11	26	0.07	0.00	0.027	0.0229
1966	11	27	0.00	0.00	0.060	0.0000
1966	11	28	0.03	0.00	0.013	0.0000
1966	11	29	0.16	0.00	0.034	0.1055
1966	11	30	0.17	0.00	0.024	0.1259
1966	12	1	0.00	0.00	0.023	0.0000
1966	12	2	0.13	0.00	0.025	0.0850
1966	12	3	0.00	0.00	0.012	0.0000
1966	12	4	0.00	0.00	0.013	0.0000
1966	12	5	0.00	0.00	0.024	0.0000
1966	12	6	0.00	0.00	0.021	0.0000
1966	12	7	0.00	0.00	0.020	0.0000
1966	12	8	0.00	0.00	0.066	0.0000
1966	12	9	0.08	0.00	0.055	0.0052
1966	12	10	0.00	0.00	0.036	0.0000
1966	12	11	0.17	0.00	0.047	0.1033
1966	12	12	0.00	0.00	0.020	0.0000
1966	12	13	0.00	0.00	0.014	0.0000
1966	12	14	0.49	0.42	0.007	0.4677
1966	12	15	0.00	0.00	0.009	0.0000
1966	12	16	0.00	0.00	0.023	0.0000
1966	12	17	0.00	0.00	0.032	0.0122
1966	12	18	0.00	0.00	0.030	0.0878
1966	12	19	0.00	0.00	0.042	0.0000
1966	12	20	0.00	0.00	0.018	0.0000
1966	12	21	0.11	0.14	0.008	0.0821
1966	12	22	0.00	0.00	0.014	0.0000
1966	12	23	0.00	0.00	0.011	0.0000
1966	12	24	0.10	0.16	0.008	0.0719
1966	12	25	0.42	0.34	0.008	0.3916
1966	12	26	0.00	0.00	0.009	0.0000
1966	12	27	0.00	0.00	0.010	0.0000
1966	12	28	0.00	0.00	0.010	0.0000
1966	12	29	1.20	0.09	0.042	1.1381
1966	12	30	0.00	0.00	0.013	0.0000
1966	12	31	0.00	0.00	0.016	0.0000